

**VARIOUS DURABILITY ASPECTS OF
SLURRY INFILTRATED FIBER CONCRETE**

**A THESIS SUBMITTED TO
THE GRADUATE SCHOOL OF NATURAL AND APPLIED SCIENCES
OF
MIDDLE EAST TECHNICAL UNIVERSITY**

BY

ADEL MOHAMED GILANI

**IN PARTIAL FULFILLMENT OF THE REQUIREMENTS
FOR
THE DEGREE OF DOCTOR OF PHILOSOPHY
IN
CIVIL ENGINEERING**

SEPTEMBER 2007

Approval of the thesis:

**VARIOUS DURABILITY ASPECTS OF
SLURRY INFILTRATED FIBER CONCRETE**

Submitted by **ADEL MOHAMED GILANI** in partial fulfillment of the requirements for the degree of **Doctor of Philosophy in Civil Engineering, Middle East Technical University**, by

Prof. Dr. Canan Özgen
Dean, Graduate School of **Natural and Applied Sciences**

Prof. Dr. Güney Özcebe
Head of Department, **Civil Engineering, METU**

Prof. Dr. Mustafa Tokyay
Supervisor, **Civil Engineering, METU**

Assoc. Prof. Dr. İ. Özgür Yaman
Co-Supervisor, **Civil Engineering, METU**

Examining Committee Members

Prof. Dr. Turhan Y. Erdoğan
Civil Engineering, METU

Prof. Dr. Mustafa Tokyay
Civil Engineering, METU

Prof. Dr. Kambiz Ramyar
Civil Engineering, Ege University

Assoc. Prof. Dr. Uğurhan Akyüz
Civil Engineering, METU

Dr. Mustafa Şahmaran
Civil Engineering, Gaziantep University

Date: September 7, 2007

I hereby declare that all information in this document has been obtained and presented in accordance with academic rules and ethical conduct. I also declare that, as required by these rules and conduct, I have fully cited and referenced all material and results that are not original to this work.

Name, Last Name: **Adel M. Gilani**

Signature :

ABSTRACT

VARIOUS DURABILITY ASPECTS OF SLURRY INFILTRATED FIBER CONCRETE

Gilani, Adel Mohamed

**Ph.D., Department of Civil Engineering
Supervisor: Prof. Dr. Mustafa Tokyay
Co-Supervisor: Assoc. Prof. Dr. İ. Özgür Yaman**

September 2007, 212 pages

Slurry infiltrated fiber concrete (SIFCON) was first produced in 1979 in the USA, by incorporating large amounts of steel fiber in molds to form very dense network of fibers. The network is then infiltrated by a fine liquid cement-based slurry or mortar. The steel fiber content can be as high as 30 % by volume. This percentage usually does not exceed 2 % in normal fiber reinforced concrete (FRC) for reasons related to mixing and workability. Due to its high fiber content, SIFCON demonstrates unique and superior mechanical properties in the areas of both strength and ductility.

Most of previous research work on SIFCON has focused mainly on investigating the mechanical properties of this material. On the other hand, the studies carried out in the field of durability of SIFCON are quite limited.

Therefore, it seemed that it would be worth to study the various durability aspects of SIFCON.

In view of the above, the objectives of this study are to investigate and provide information about durability of SIFCON, mainly permeability, resistance to chloride penetration, freezing and thawing and drying shrinkage. This information will help in providing the necessary database and knowledge about the ability of SIFCON to withstand the conditions for which it has been designed without deterioration, especially when it is intended to be used in aggressive environments

The investigations included studying the effects of the following on durability of SIFCON: (i) matrix type (slurry or mortar), (ii) fiber contents (7%, 9.5%, and 12% by volume), and (iii) steel fiber geometry (hooked or crimped).

The results obtained indicated that SIFCON, especially when prepared using mortar not slurry, has shown good durability characteristics in spite of its apparent high water absorption. The SIFCON made with the highest possible fiber volume fractions showed the best results. However, it was concluded that SIFCON needs to be protected with suitable low permeability overlays to ensure ideal improved performance by protecting the steel fibers exposed on the surfaces especially against chloride attack.

Keywords: Slurry Infiltrated Fiber Concrete (SIFCON), Drying Shrinkage, Water Absorption, Chloride Penetration, Freezing and Thawing.

ÖZ

YÜKSEK PERFORMANSLI LİF DONATILI ÇİMENTO ESASLI KOMPOZİTİN (SIFCON) ÇEŞİTLİ DURABİLİTE ÖZELLİKLERİNİN ARAŞTIRILMASI

Gilani, Adel Mohamed

**Doktora, İnşaat Mühendisliği Bölümü
Tez Yöneticisi: Prof. Dr. Mustafa Tokyay
Yardımcı Tez Yöneticisi: Doç. Dr. İ. Özgür Yaman**

Eylül 2007, 212 sayfa

Yüksek performanslı lif donatılı çimento esaslı kompozit (SIFCON) ilk kez 1979 yılında Amerika Birleşik Devletleri'nde çok yoğun lif sistemi oluşturmak amacı ile kalıba yüksek oranda çelik lifler yerleştirilerek üretilmiştir. Daha sonra elde edilen bu yoğun lif sistemine çimento bazlı şerbet veya harç enjekte edilmektedir. SIFCON'da kullanılan çelik lif oranları % 30 mertebelerine kadar olabilmektedir. Bu oran geleneksel normal lifli betonlarda olası karışım ve işlenebilirlik sorunları nedenlerinden dolayı % 2 mertebesini aşmamaktadır. Yüksek oranda çelik lif içermesinden dolayı, SIFCON, normal lifli betonlara kıyasla, çok üstün dayanım ve süneklilik özellikler göstermektedir.

Daha önceleri yapılan çalışmalar genellikle SIFCON malzemesinin mekanik özellikleri üzerine yapılmış olmasına rağmen bu malzemenin durabilitesi üzerine literatürde çok sınırlı çalışma bulunmaktadır. Bu nedenle, SIFCON malzemesinin çeşitli durabilite özellikleri üzerine çalışma yapmak önem arz etmektedir. Yukarıda yapılan açıklamaların ışığında, bu çalışmanın amacı SIFCON malzemesinin geçirimsizlik, klor iyonu geçirimsizliğine dayanımı, donma-çözünme ve kuruma büzülmesi gibi önemli durabilite özelliklerinin incelenmesi ve literatürde eksik olan bu bilgilerin kazandırılmasıdır. Bu tür çalışma sonucunda elde edilecek olan bilgi birikimi, SIFCON malzemesinin herhangi bir bozulmaya maruz kalmadan farklı şartlar altında tasarlanabilmesi için gerekli olan bilgi ve veritabanını sağlamakta yardımcı olacaktır.

Bu çalışma kapsamında, SIFCON'un çeşitli durabilite özellikleri ve üretiminde etkisi incelenen değişkenler: (i) matris çeşidi (şerbet veya harç), (ii) lif oranı (% 7, % 9.5 ve % 12), ve (iii) çelik lif geometrisi (kancalı veya kıvrımlı). Elde edilen sonuçlar ışığında, özellikle harç kullanılarak elde edilen SIFCON malzemesinin yüksek oranda görel su emme kapasitesine rağmen iyi durabilite özellikleri gösterdiği görülmüştür. Ayrıca, olası en yüksek lif oranı ile üretilen SIFCON karışımının en iyi sonuç verdiği gözlemlenmiştir. Fakat, özellikle klor hücumuna karşı, SIFCON malzemesinin yapımında kullanılan çelik liflerin herhangi bir aşınmaya maruz kalmaması için uygun düşük geçirimli kaplamalar ile korunması gerekmektedir.

Anahtar Kelimeler: Yüksek Performanslı Lif Donatılı Çimento Esaslı Kompozit (SIFCON), Kuruma Büzülmesi, Su Emme, Klor Geçirgenliği, Donma ve Çözünme.

*TO
NAHLA AND ZEYNEDDIN,*

*AND TO
THE MEMORY OF THE LATE PROFESSORS
JUMA LABIB AND AHMED BEN ZETUN*

ACKNOWLEDGEMENTS

First of all, I am deeply grateful to my supervisor, Prof. Dr. Mustafa Tokyay, for giving me the great opportunity to join the Ph.D. program in METU under his supervision, and for his outstanding guidance and dedication throughout the years of my Ph.D. study. I am also grateful to the co-supervisor, Assoc. Prof. Dr. İsmail Özgür Yaman, for his support and attention to details which proved invaluable in producing quality research.

Sincere appreciation and thanks are due to Prof. Dr. Turhan Y. Erdoğan and Prof. Dr. Kambiz Ramyar for their comments and constructive contributions during their serving in the thesis progress committee.

Thanks are extended, as well, to Mehmet Yerlikaya of Beksa Co. and Cem Ayhan of Polyfibers Co. for providing the steel fibers used in the research. Dr. Cevdet Öztin and Selahattin Uysal of the Department of Chemical Engineering, METU, are highly appreciated for their help in the part of chloride chemical analysis.

A special, sincere thanks goes to my fellow graduate student Barış Erdil. His kind assistance in the experimental work will never be forgotten. In addition, the support and kindness received from many others is highly acknowledged. Those include my father-in-law Prof. Dr. Adel Elwefati, my brother Muhaned, Dr. Mustafa Şahmaran, Dr. T. Kemal Erdem, the teaching assistants İ. Raci Bayer, Burak Uzal, Dilek Okuyucu, Bora Acun, Semih Erhan, and to my colleagues M. Salih Ölmez, Özlem Kasap, and Tuğçe Sevil.

The devoted friendship of Abdulghani M. Ramadan, Hazem Zubi, Masoud Alrmah, Salah Ageil, Annour Al-Alem, and Wael Albawwab will be always profoundly appreciated.

Many thanks go, also, to Cuma Yıldırım, Necdet Aydoğan, and Ali Sünbüle of the technical staff of the civil engineering department, METU, for their assistance with the laboratory work.

The financial support provided by the General People's Committee of Higher Education in Libya throughout most of my Ph.D. study period must be acknowledged.

I can not end without thanking all the nice people of Turkey who made me feel at home throughout the years I spent among them.

Finally, I am very grateful to my family for the continuous support and love. My wife, Nahla, deserves special and sincere thanks for her endless encouragement and patience in the hard times, and for her help in typing the manuscript. Moreover, the presence of the joy of my life, my child Zeyneddin, was always a great source of motivation.

Thank you all, from the bottom of my heart, for making my life much happier and easier!

TABLE OF CONTENTS

ABSTRACT	iv
ÖZ	vi
DEDICATION	viii
ACKNOWLEDGEMENTS	ix
LIST OF TABLES	xiii
LIST OF FIGURES	xiv

CHAPTERS

1. INTRODUCTION	1
1.1 General	1
1.2 Objective and Scope	3
2. LITERATURE REVIEW AND BACKGROUND	5
2.1 Introduction	5
2.2 Preparation	5
2.3 Materials and mix proportions	9
2.3.1 Steel fibers	10
2.3.2 Matrix	12
2.3.3 Mix proportions	12
2.4 Engineering properties of SIFCON	14
2.4.1 Unit weight	14
2.4.2 Behavior in compression	15
2.4.3 Behavior in tension	22
2.4.4 Behavior under flexural loading	26
2.4.5 Behavior in shear	31

2.4.6 Bond of bars embedded in SIFCON	34
2.5 Durability of SIFCON	35
2.5.1 Drying shrinkage strain	35
2.5.2 Resistance to freezing and thawing	37
2.6 Applications of SIFCON	38
2.6.1 Earthquake resistant structures	38
2.6.2 Repair and retrofit of structural components	39
2.6.3 Bridge deck and pavement overlay	40
2.6.4 Precast concrete products	41
2.6.5 Explosive-resistant structures	41
2.6.6 Refractory applications	43
2.6.7 Security applications	44
3. EXPERIMENTAL STUDY	45
3.1 Introduction	45
3.2 Materials	46
3.2.1 Cement	46
3.2.2 Aggregate	47
3.2.3 Mixing water	50
3.2.4 Chemical admixture	50
3.2.5 Steel Fibers	50
3.3 Experimental program	52
3.3.1 Mix proportions	52
3.3.2 Preparation and casting of test specimens	55
3.4 Experimental tests	56
3.4.1 Stress-strain relationships	57
3.4.2 Drying shrinkage test	62
3.4.3 Water absorption test	64
3.4.4 Chloride penetration test	66
3.4.5 Freeze-thaw resistance test	71

4. TEST RESULTS AND DISCUSSIONS	79
4.1 Stress-strain properties	79
4.1.1 Effects of fiber content on stress-strain relationship	81
4.1.2 Effect of matrix type on stress-strain relationship	89
4.1.3 Effect of fiber type on stress-strain relationship	91
4.1.4 Summary of stress-strain tests	91
4.2 Drying shrinkage test	95
4.2.1 SIFCON vs. plain mixes	95
4.2.2 Effect of fiber volume fraction	95
4.2.3 Effect of matrix type	98
4.2.4 Effect of fiber type	105
4.3 Water absorption test	108
4.3.1 Absorption of plain mixes	109
4.3.2 Absorption of SIFCON	112
4.3.3 Summary of water absorption results	122
4.4 Chloride penetration test	128
4.4.1 Analysis of total chloride contents by weight of cement	130
4.4.2 Total chloride contents by total weight	139
4.4.3 Chloride diffusion coefficients (D_a)	139
4.5 Freezing and thawing test	144
4.5.1 Change in dynamic modulus of elasticity	144
4.5.2 Weight loss	152
4.5.3 Summary of the results of freezing and thawing tests ...	161
5. CONCLUSIONS AND RECOMMENDATIONS	162
5.1 Conclusions	162
5.2 Recommendations	165
5.2.1 Recommendations for practice	165
5.2.2 Recommendations for future research	166
REFERENCES	168

APPENDICES

A. RESULTS OF STRESS-STRAIN TEST IN UNIAXIAL COMPRESSION	179
B. RESULTS OF WATER ABSORPTION TEST	194
C. RESULTS OF CHLORIDE PENETRATION TEST	201
CURRICULUM VITAE	210

LIST OF TABLES

TABLES

Table	2.1	Some SIFCON slurry mix designs from the literature (by weight of cement)	13
Table	2.2	Reported slurry mix designs and strength values	16
Table	2.3	Reported fiber properties	17
Table	2.4	Tensile strengths of SIFCON	24
Table	2.5	Flexural strength of SIFCON	27
Table	3.1	Physical and mechanical properties of the cement used in the study	46
Table	3.2	Chemical analysis of the cement used in the study ..	47
Table	3.3	Results of SSD specific gravity and absorption of aggregates	47
Table	3.4	Aggregate grading	49
Table	3.5	Specifications of steel fibers used in the experimental work (as provided by the manufactures)	51
Table	3.6	Mixture proportions, by weight	53
Table	3.7	Mixture proportions per kg/m ³	53
Table	3.8	The mixtures and tests performed in the experimental study	58
Table	3.9	Shrinkage grades for conventional concrete	64
Table	3.10	Depths of dust samples collected for chloride analysis	68
Table	3.11	The details of a typical freezing/thawing cycle	76
Table	4.1	Summary of peak strength and toughness results	82
Table	4.2	Summary of crack mapping	104
Table	4.3	Typical ranges of coefficient of thermal expansion ...	104

Table 4.4	Absorption of SIFCON mixes by weight of slurry or mortar	117
Table 4.5	Summary of water absorption results	127
Table 4.6	Cement contents by total weight in mixtures under study	129
Table 4.7	Effect of depth from surface on reduction of chloride ions ingress	133
Table 4.8	The influence of edge effect on density of SIFCON	134
Table 4.9	Best-fit diffusion coefficients for SIFCON and concrete	143
Table A.1	A part of the data of a typical stress-strain test	179
Table A.2	An example of toughness calculations	180

LIST OF FIGURES

FIGURES		
Figure	2.1	Placement of steel fibers in a mold 6
Figure	2.2	Fiber orientation and edge effect in a molded SIFCON cylinder specimen 8
Figure	2.3	Orientation of fiber in cored SIFCON as influenced by the coring direction with respect to fiber placement direction 8
Figure	2.4	Slurry infiltration aided with external vibration 9
Figure	2.5	An example of failed preparation because of lack of fluidity in slurry 10
Figure	2.6	Typical profiles of steel fibers commonly used in SIFCON 11
Figure	2.7	Effect of steel fiber content on the unit weight of SIFCON 14
Figure	2.8	Compressive strength vs. water/ binder ratios 18
Figure	2.9	Tested SIFCON compression specimens showing consistent shear failure 18
Figure	2.10	Typical load-deformation behavior for 10.2×17.8 cm cylindrical SIFCON specimens 19
Figure	2.11	Typical effects of stress-strain curve of SIFCON in specimens 20
Figure	2.12	Typical stress-strain curves of SIFCON in compression for different mix designs 21
Figure	2.13	Typical stress-strain curves of molded and cored SIFCON specimens in compression 21
Figure	2.14	Tension dog bone specimens 22
Figure	2.15	Stress-strain behavior in axial tension 25

Figure	2.16	Tensile stress- displacement curves of various fiber types and contents in a mix of W/C of 0.45	25
Figure	2.17	Load-deflection curves in flexure for hooked-end fibers with l=30mm and d=0.5mm	26
Figure	2.18	Flexural strengths versus fiber contents	28
Figure	2.19	Comparison of load-deflection curves for SIFCON, ordinary FRC with 2% steel fibers, and plain matrix ...	29
Figure	2.20	Effect of fiber content in SIFCON on the flexural load-deflection curve	30
Figure	2.21	Comparison of load-deflection behavior of beams with and without silica fume	30
Figure	2.22	Direct shear test specimen	32
Figure	2.23	Geometry of double shear SIFCON specimen and fixture used to attach to load cell and actuator	32
Figure	2.24	Load-deformation behavior of shear specimens, fiber content = 6 %	33
Figure	2.25	Shear stress versus	33
Figure	2.26	Drying shrinkage of SIFCON and plain unreinforced slurry	36
Figure	2.27	Schematic representation of SIFCON joints in the structural system	39
Figure	2.28	Infiltration of the steel fiber bed with the slurry in pavement overlay application	40
Figure	2.29	Installation of a precast SIFCON slab at a commercial airport	42
Figure	2.30	Schematic diagram of a hardened silo structure containing SIFCON	43
Figure	3.1	Gradings of 1.0 mm and 0.6 mm sand	49
Figure	3.2	Fibers used in the experimental study	52

Figure	3.3	The testing system of stress-strain behavior	60
Figure	3.4	The data acquisition system used in compression stress-strain test	60
Figure	3.5	Typical plot of strain versus time	61
Figure	3.6	Influence of strain rate on the compressive strength of concrete	62
Figure	3.7	The drying shrinkage specimens and the length measurement device	64
Figure	3.8	A mold for chloride penetration test specimens	68
Figure	3.9	AASHTO T 259 test setup	68
Figure	3.10	Setup of extracting dust samples of chloride penetration test	70
Figure	3.11	Collecting dust samples in sealed bags for chloride chemical analysis	70
Figure	3.12	A typical example of deterioration in concrete due to freezing and thawing	71
Figure	3.13	Specimens subjected to freezing-thawing cycles in the climate chamber	75
Figure	3.14	Freezing and thawing cycles in a typical day	76
Figure	3.15	The climate room used for freeze-thaw test and its control panel	77
Figure	3.16	UPV testing of freeze-thaw specimens	78
Figure	4.1	Typical stress-strain behavior of SIFCON	80
Figure	4.2	Toughness of slurry SIFCON vs. reference concrete (M3)	83
Figure	4.3	Shear Failure and high deformation in a tested SIFCON specimen	85
Figure	4.4	SIFCON in different stages of stress-strain test	87

Figure	4.5	Toughness of mortar SIFCON vs. reference concrete (M3)	89
Figure	4.6	Effect of SIFCON mix type on toughness	90
Figure	4.7	Effect of fiber type on toughness of SIFCON	92
Figure	4.8	Cross sections in SIFCON samples	94
Figure	4.9	Drying Shrinkage of slurry SIFCON vs. M1 & M3	96
Figure	4.10	Drying Shrinkage of mortar SIFCON vs. M2 & M3	97
Figure	4.11	The Influence of mix type on shrinkage of SIFCON after 224 days of drying	99
Figure	4.12	Crack microscope used in crack mapping of SIFCON	100
Figure	4.13	Drying shrinkage cracks in slurry SIFCON specimens	101
Figure	4.14	Drying shrinkage cracks in slurry SIFCON and the plain matrix	102
Figure	4.15	The effect of fiber type on the drying shrinkage of SIFCON after 224 days of drying	107
Figure	4.16	The effect of fiber type on cracking of slurry SIFCON	108
Figure	4.17	Absorption vs. time during 48 hrs for M1, M2 and M3	111
Figure	4.18	Absorption vs. time during the first 2 hrs for M1, M2 and M3	111
Figure	4.19	Absorption indices for M1, M2 and M3	112
Figure	4.20	Absorption vs. time in 48 hrs for slurry SIFCON, M1 and M3	115
Figure	4.21	Absorption vs. time in 48 hrs for mortar SIFCON with 1.0 mm sand, M2 and M3	116
Figure	4.22	Effect of SIFCON mix type on total water absorption	119

Figure	4.23	Absorption vs. time in 48 hrs for mortar SIFCON with 0.6 mm sand, M2(F) and M3	124
Figure	4.24	Effect of sand size on total absorption of mortar SIFCON	125
Figure	4.25	Effect of fiber type on the absorption of several SIFCON mixes	126
Figure	4.26	Chloride ingress profiles for slurry SIFCON vs. control concrete (Based on chloride content by mass of cement)	131
Figure	4.27	Chloride ingress profiles for mortar SIFCON vs. control concrete (Based on chloride content by mass of cement)	132
Figure	4.28	Effect of mix type on chloride penetration when hooked fibers (F1) are used (Based on chloride content by mass of cement)	137
Figure	4.29	Effect of mix type on chloride penetration when crimped fibers (F2) are used (Based on chloride content by mass of cement)	138
Figure	4.30	Effect of fiber type on chloride penetration of slurry SIFCON (Based on chloride content by mass of cement)	140
Figure	4.31	Effect of fiber type on chloride penetration of mortar SIFCON (Based on chloride content by mass of cement)	141
Figure	4.32	Drop in RDME for plain mixes	146
Figure	4.33	Drop in RDME for slurry SIFCON vs. plain slurry	148
Figure	4.34	Drop in RDME for mortar SIFCON vs. plain mortar	149
Figure	4.35	Effect of mix type on drop in RDME after 300 freeze-thaw cycles	150

Figure	4.36	Effect of fiber type on RDME drop after 300 freeze-thaw cycles	151
Figure	4.37	Weight loss of plain mixes due to freeze-thaw	153
Figure	4.38	Plain specimens after 300 cycles of freezing and thawing	153
Figure	4.39	Weight loss in slurry SIFCON due to freeze-thaw cycles	154
Figure	4.40	The surface scaling in slurry SIFCON made using hooked fibers	156
Figure	4.41	Weight loss in mortar SIFCON due to freeze-thaw cycles	157
Figure	4.42	Representative samples of mortar SIFCON after 300 cycles of freezing and thawing	158
Figure	4.43	Effect of mix type on weight loss of SIFCON due to 300 freeze-thaw cycles	159
Figure	4.44	Effect of fiber type on weight loss after 300 freeze-thaw cycles	160
Figure	A.1	Stress-strain results of M1F1-7	181
Figure	A.2	Toughness-strain results of M1F1-7	181
Figure	A.3	Stress-strain results of M1F1-9.5	182
Figure	A.4	Toughness-strain results of M1F1-9.5	182
Figure	A.5	Stress-strain results of M1F1-12	183
Figure	A.6	Toughness-strain results of M1F1-12	183
Figure	A.7	Stress-strain results of M1F2-7	184
Figure	A.8	Toughness-strain results of M1F2-7	184
Figure	A.9	Stress-strain results of M1F2-9.5	185
Figure	A.10	Toughness-strain results of M1F2-9.5	185
Figure	A.11	Stress-strain results of M1F2-12	186
Figure	A.12	Toughness-strain results of M1F2-12	186

Figure	A.13	Stress-strain results of M2F1-7 (three specimens)	187
Figure	A.14	Toughness-strain results of M2F1-7	187
Figure	A.15	Stress-strain results of M2F1-9.5	188
Figure	A.16	Toughness-strain results of M2F1-9.5	188
Figure	A.17	Stress-strain results of M2F1-12	189
Figure	A.18	Toughness-strain results of M2F1-12	189
Figure	A.19	Stress-strain results of M2F2-7	190
Figure	A.20	Toughness-strain results of M2F2-7	190
Figure	A.21	Stress-strain results of M2F2-9.5	191
Figure	A.22	Toughness-strain results of M2F2-9.5	191
Figure	A.23	Stress-strain results of M2F2-12	192
Figure	A.24	Toughness-strain results of M2F2-12	192
Figure	A.25	Stress-strain results of M3	193
Figure	A.26	Toughness-strain results of M3	193
Figure	B.1	Absorption vs. time during the first 2 hrs for M1F1	194
Figure	B.2	Absorption indices for M1F1	194
Figure	B.3	Absorption vs. time during the first 2 hrs for M1F2	195
Figure	B.4	Absorption indices for M1F2	195
Figure	B.5	Absorption vs. time during the first 2 hrs for M2F1	196
Figure	B.6	Absorption indices for M2F1	196
Figure	B.7	Absorption vs. time during the first 2 hrs for M2F2	197
Figure	B.8	Absorption indices for M2F2	197
Figure	B.9	Absorption vs. time during the first 2 hrs for M2(F)	198
Figure	B.10	Absorption index for M2(F)	198
Figure	B.11	Absorption vs. time during the first 2 hrs for M2F1(F)	199
Figure	B.12	Absorption indices for M2F1(F)	199
Figure	B.13	Absorption vs. time during the first 2 hrs for M2F2(F)	200

Figure	B.14	Absorption indices for M2F2(F)	200
Figure	C.1	Chloride ingress profiles for slurry SIFCON vs. control concrete (Based on chloride content by total weight)	201
Figure	C.2	Chloride ingress profiles for mortar SIFCON vs. control concrete (Based on chloride content by total weight)	202
Figure	C.3	Effect of mix type on chloride penetration when hooked fibers (F1) are used (Based on chloride content by total weight)	203
Figure	C.4	Effect of mix type on chloride penetration when crimped fibers (F2) are used (Based on chloride content by total weight)	204
Figure	C.5	Effect of fiber type on chloride penetration of slurry SIFCON (Based on chloride content by total weight)	205
Figure	C.6	Effect of fiber type on chloride penetration of slurry SIFCON (Based on chloride content by total weight)	206
Figure	C.7	Comparison of model and experimental data for slurry SIFCON	207
Figure	C.8	Comparison of model and experimental data for mortar SIFCON	208
Figure	C.9	Comparison of model and experimental data for control concrete	209

CHAPTER 1

INTRODUCTION

1.1 General

Slurry infiltrated fiber concrete (SIFCON) is a relatively new special type of high performance (steel) fiber-reinforced concrete (HPFRC). SIFCON is made by preplacing short discrete fibers in the molds to its full capacity or to the desired volume fraction, thus forming a network. The fiber network is then infiltrated by a fine liquid cement-based slurry or mortar. The fibers can be sprinkled by hand or by using fiber-dispensing units for large sections. Vibration is imposed if necessary during placing the fibers and pouring the slurry. The steel fiber content can be as much as 30 % by volume [1]. In conventional fiber reinforced concrete (FRC), where fibers are mixed together with other ingredients of concrete, this percentage is limited to only about 2 % for practical workability reasons.

Because of its high fiber content, SIFCON has unique and superior mechanical properties in the areas of both strength and ductility [1]. The main differences between FRC and SIFCON, in addition to the clear difference in fiber volume fraction, lie in the absence of coarse aggregates in SIFCON which, if used, will hinder the infiltration of the slurry through the dense fiber network. Furthermore, SIFCON contains relatively high cement and water contents when compared to conventional concrete.

Although it is still a relatively new construction product, SIFCON has been used successfully in a number of areas since the early 1980's. Some of those applications are explosive-resistant containers, security blast-resistance vaults, and repair of structural components, bridge decks, airfield pavements and abrasive-resistance surfaces [2].

Most of previous research work on SIFCON found by literature survey has focused mainly upon studying the mechanical properties of this unique material. The research work in this area included, for example, behavior under different loading conditions, crack propagation, toughness, ductility or energy absorption, elasticity in tension and compression.

On the other hand, the research work undertaken in the field of durability of High Performance Fiber Reinforced Concrete Composites (HPFRCC) in general is quite limited, and covers only few types not including SIFCON. Those types are normal fiber reinforced concrete (FRC), silica fume blended cements and reactive powder concrete (RPC) [3]. Actually, very few researches dealt with some durability aspects of SIFCON but without reporting clear enough details and information [1, 2, 4].

However, the failure of concrete structures normally arises due to problems with the durability of concrete elements rather than strength related issues. Therefore, the durability, of HPFRCC in general and SIFCON in particular, seems to be an under-emphasized area of research.

In fact, HPFRCC generally employ a dense matrix and an appreciable amount of fibers, thus there would be increased load carrying capacity, toughness and ductility. Therefore, the main point here will not be the strength criterion, but the durability.

1.2 Objective and Scope

As stated above, being a relatively new construction material, very little information on SIFCON durability characteristics is known from published previous researches. In light of this, the objectives of this study are to investigate and provide information about various aspects of SIFCON durability, mainly permeability, resistance to chloride penetration, freezing and thawing and drying shrinkage. This information will help in providing the necessary database and knowledge about the ability of SIFCON to withstand the conditions for which it has been designed without deterioration, especially when it is intended to be used in aggressive environments like the cases of marine structures or bridges subjected to freeze-thaw damage and de-icing salts in cold regions. The understanding of SIFCON behavior related to durability will help in achieving a rational design of structure using SIFCON where corrosive or an aggressive environment prevails.

The scope of the study was designed in a way to serve the planned objectives. It involved conducting a number of tests related to durability, and for every one of these tests the following parameters were studied:

- (a) Investigation of the effects of SIFCON matrix type, slurry or mortar, on durability, to define the most appropriate mix design when high durability is required.
- (b) Studying the effects of using different volume fraction (contents) of steel fibers, to decide on the most desirable fiber content. Three different volume fractions were used, 7 %, 9.5 % and 12 %.
- (c) Investigating the effects of steel fiber type, *i.e.* its geometrical shape. The comparison was made between the most widely used steel fiber shapes, which are hooked and crimped fibers.

For every test and every investigation, in addition to the inter-comparisons between SIFCON specimens themselves, the results were compared to reference conventional concrete specimens which designed to be a low permeability concrete of good quality as a control mix.

Furthermore, a complete set of SIFCON and control concrete specimens were mechanically tested to confirm the stress-strain behavior of SIFCON used in the research. The aim of this was to make sure that trends found in literature can be achieved using SIFCON made in this study. In addition, stress-strain investigations provided some useful information which could not be found in previous studies.

In Chapter 2, a literature survey is made on SIFCON, concentrating on preparation, mix proportions, mechanical properties and applications. Experimental program is discussed in Chapter 3, including materials properties and details of tests conducted on SIFCON and control concrete. The results of the experimental studies are presented and discussed in Chapter 4. Finally, the conclusions and recommendations of the research are stated in Chapter 5.

CHAPTER 2

LITERATURE REVIEW AND BACKGROUND

2.1 Introduction

SIFCON was first developed in 1979 by Lankard Materials Laboratory, Columbus, Ohio, USA, by incorporating large amounts of steel fibers in steel fiber reinforced cement-based composites [4].

SIFCON is similar to fiber reinforced concrete in that it has a discrete fiber matrix that lends significant tensile properties to the composite matrix. The fiber volume fraction, V_f (volumetric percent of fibers), of traditional fiber reinforced concrete is limited by the ability to effectively mix the fibers into the fresh concrete. This limits the fiber volume V_f to between 1 % and 2 %, depending upon the type of fiber used and the required workability of the mix. On the other hand, SIFCON specimens are produced with V_f between 5 % and 30 % [4, 5].

The fiber volume depends upon the fiber type, *i.e.* length and diameter, and the vibration effort utilized to fill the form. Smaller or shorter fibers will pack denser than longer fibers, and higher fiber volumes can be achieved with added vibration time.

2.2 Preparation

Analogous to prepalced aggregate concrete, SIFCON is prepalced fiber concrete with the placement of steel fibers in a mold or form, or on a

substrate, as the initial construction step. Fiber placement is accomplished by hand, Figure 2.1, or through the use of commercial fiber dispersing units. As stated before, the amount of fibers that can be incorporated depends on fiber dimensions, especially aspect ratio (l/d), fiber geometry, and placement technique. External vibration can be applied during the fiber placement operation. The stronger the vibration, the higher achievable V_f .



Figure 2.1: Placement of steel fibers in a mold
The first step in the preparation of SIFCON

One of the important aspects in the fabrication of SIFCON is fiber orientation. As might be expected, when steel fibers are placed onto a substrate or into a mold, a preferred fiber orientation occurs. The orientation is essentially two-dimensional, perpendicular to the gravity vector. The orientation effect is more exaggerated with some fibers than with others. In

general, there is a trend toward a three-dimensional fiber orientation that accompanies reduction in fiber diameter and aspect ratio [1].

The fiber orientation phenomenon must be considered when designing field installations of SIFCON or in preparing laboratory specimens. The preparation of test specimens of SIFCON requires special considerations relating mainly to the need of avoiding non-uniform fiber distributions and of avoiding unfavorable fiber orientation. The fiber density at the edges of the mold can be much less, compared to the interior. Additionally, a number of fibers may align vertically (parallel to the long cylinder axis) along the outer surface. Figure 2.2 depicts the edge effects in molded SIFCON.

One way to avoid the fiber orientation and edge effect problems is to cast a slab and obtain the test specimens by coring. Here again, attention should be paid to the orientation of fibers. If fibers are aligned along the diameter of the cylinder, a much higher compressive strength can be expected compared to a cylinder in which fibers are aligned along the axis of the cylinder. Actually, it is reported that specimens with fibers perpendicular to loading axis may exhibit twice the strength of specimens with fibers placed parallel to load direction, Figure 2.3 [1]. Cylinders shown in the Figure 2.3 are cored vertically and horizontally from a slab with horizontally placed steel fibers.

Once the steel fibers have been placed on a substrate or in a mold, then they are infiltrated with a fine-grained cement-based slurry. The slurry must be flowable and liquid enough and have sufficient fineness to infiltrate thoroughly the dense matrix in the fiber-filled forms. The infiltration step is accomplished by simple gravity-induced flow or gravity flow aided by external vibration or pressure grouting from the bottom of the bed [4]. Slurry infiltration by gravity flow aided by a vibrating table is shown in Figure 2.4.

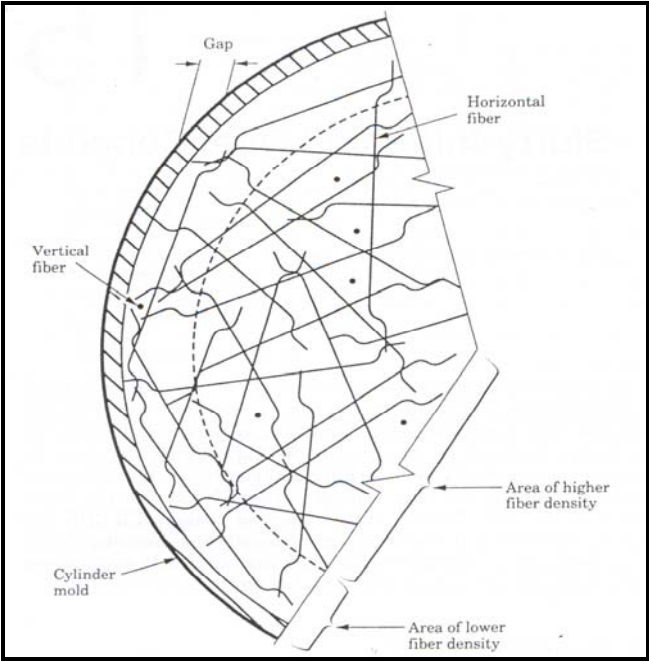


Figure 2.2: Fiber orientation and edge effect in a molded SIFCON cylinder specimen [1]

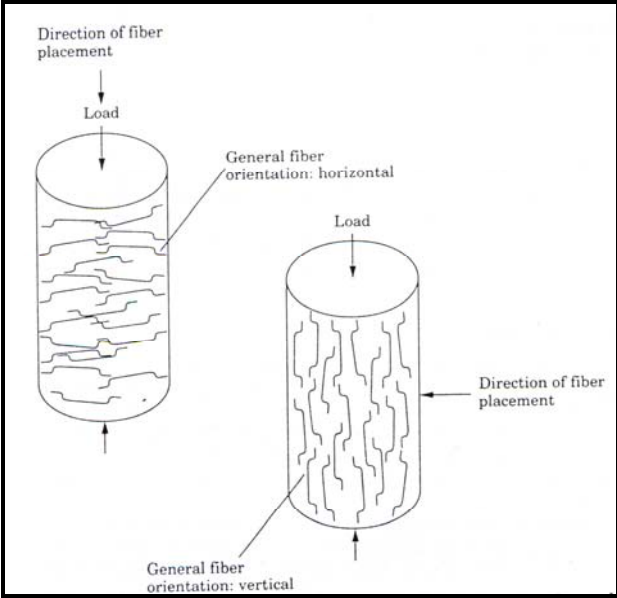


Figure 2.3: Orientation of fiber in cored SIFCON as influenced by the coring direction with respect to fiber placement direction [1]



Figure 2.4: Slurry infiltration aided with external vibration

The choice of infiltration technique is dictated largely by the ease with which the slurry moves through the packed fiber bed. Figure 2.5 shows an example of what happens if the slurry is not flowable enough, or if the vibration is not intense enough. The degree of voids or honey combing extent depends on how flowable is the slurry, and how strong is the vibration.

2.3 Materials and mix proportions

The primary constituent materials of SIFCON are steel fibers and cement-based slurry. The matrix can contain:

- (a) Only cement (slurry or cement paste).
- (b) Cement and sand (mortar).
- (c) Cement and other additives (mainly fly ash or silica fume).

In most cases, high-range water-reducing admixtures (superplasticizers) are used in order to improve the flowability of the slurry to ensure complete infiltration without increasing the water-cement ratio (W/C). The dosage of

superplasticizers has the greatest effect on fluidity, cohesiveness and penetrability of cement slurries.



Figure 2.5: An example of failed preparation because of the lack of fluidity of slurry

The dense fiber network is also clear in the figure

2.3.1 Steel fibers

A large variety of steel fibers have been investigated for use in SIFCON. To develop better mechanical anchorage and bond between the fibers and the matrix, the fibers can be modified along its length by inducing mechanical deformations or by roughening its surface. The most widely used types are hooked and crimped fibers. Surface deformed and straight fibers are used also, but they are less popular [5-8].

In most cases, the cross section of steel fibers is circular. It can be also rectangular, square, triangular or flat [10]. Typical examples of steel fibers used for SIFCON are shown in Figure 2.6. In most applications in the USA and Europe, steel fibers with hooked-ends have been used [2]. Most common steel fibers have a length from 25 to 60mm, and a diameter ranging from 0.4 to 1 mm. Their aspects ratio (l/d), that is, the ratio of length over diameter or equivalent diameter, is generally less than 100, with a common range from 40 to 80 [9].

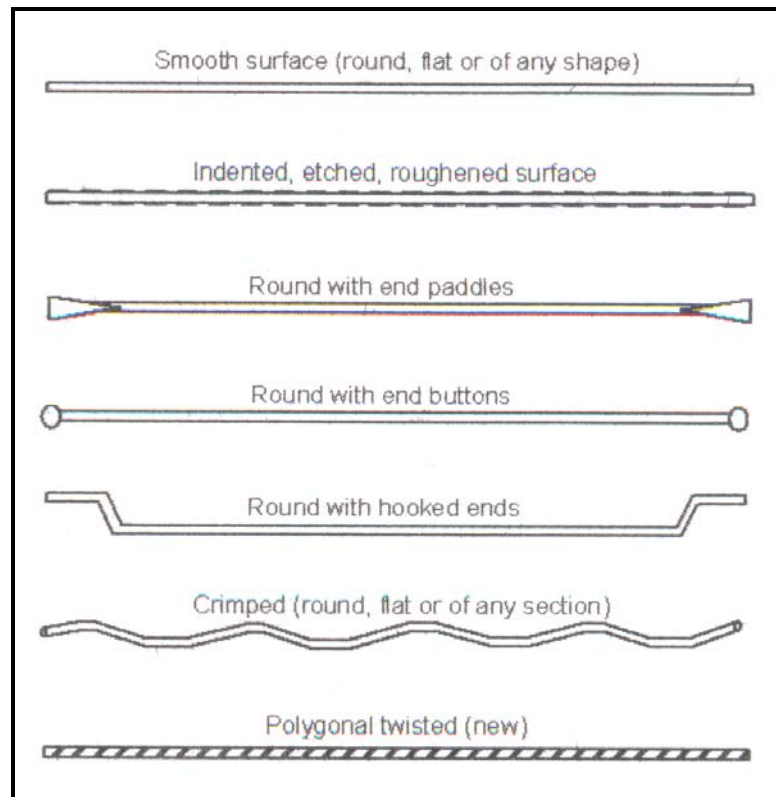


Figure 2.6: Typical profiles of steel fibers commonly used in SIFCON [9]

2.3.2 Matrix

The matrix of SIFCON does not contain coarse aggregate which, of course, cannot infiltrate through the tiny spaces between the steel fibers. The matrix compositions investigated in literature include cement, cement-sand, cement-fly ash, cement- silica fume, cement-sand-fly ash and cement-sand-silica fume [5, 6, 11-19]. Matrices containing mineral additives such as fly ash or silica fume were found to have better shrinkage characteristics [2]. Typically, silica fume addition is reported to increase the strength, where as the addition of fly ash results in some reduction in strength [7]. Moreover, an increase in the proportion of sand is reported to increase the compressive strength [10].

2.3.3 Mix proportions

The primary variables in the mix proportioning are fiber content and matrix composition. The fiber volume fraction is commonly controlled by the placement technique and the fiber geometry. The recommended water-cement ratio for the slurry (matrix) is 0.4 or less. Superplasticizers (SP) can be used, if necessary, to improve the flowability of the slurry, which should be liquid enough to flow through the dense fiber bed without leaving honeycombs. Only fine sand should be used. Very fine sand of less than 0.5 mm in size is reported to use in preparing mortar SIFCON [1, 4, 5].

If fly ash is used as a cement replacement additive, about 20 % of the cement could be replaced with fly ash. If silica fume is used, the recommended dosage is 10 % by weight of cement. Both Type I and Type III (ASTM) cements can be used [2]. Table 2.1 shows some slurry mix designs by relative weight of constituents as taken from 11 different studies dealt with SIFCON.

Table 2.1: Some SIFCON slurry mix designs from the literature (by weight of cement) [5, 6, 11-19]

Reference No.	SIFCON Composition				
	Cement ⁽¹⁾	Fine Sand	Water	Fly Ash or ⁽²⁾ Silica Fume	SP
5	1	0.2	0.355	0.2	0.02
	1	0.3	0.255	0.2	0.04
6	1	-	0.3	0.1	0.048
11	1	2	0.6	-	Not reported
12	1	-	0.36	-	0.03
	1	-	0.5	-	-
13	1	1	0.6	0.2	Not reported
	1	0.8	0.53	0.2	Not reported
	1	0.6	0.45	0.2	Not reported
	1	-	0.36	0.2	Not reported
14	1	1	0.4	-	0.013
	1	1	0.32	-	0.035
15	1	1	0.48	0.2	0.02
16	1	-	0.36	0.2	0.03
	1	-	0.325	0.25	0.04
17	1	1.5	0.4	0.2	0.01
	1	1	0.32	0.2	0.02
	1	0.5	0.24	0.2	0.03
18	1	1	0.45	-	0.032
19	1	0.9	0.5	0.3	0.024

⁽¹⁾ In all references, Type I Portland cement was used, except for references 6 and 11 where Type III was used.

⁽²⁾ In all references Fly ash was used, except for reference 6 where silica fume is used.

As can be seen from Table 2.1, using mortar is more popular than slurry for making SIFCON. The sand proportion to cement by weight ranges from 0.2 to 2, and it is equal to 1 in most cases. Adding fly ash is popular as well to

improve the mix properties. In most cases, using superplasticizers is inevitable because of the relatively low W/C ratio, and the need to produce a highly flowable mix.

2.4 Engineering properties of SIFCON

2.4.1 Unit weight

The unit weight of SIFCON is typically higher than concrete and normal FRC because of the relatively heavy weight of the high fiber content. For a slurry unit weight of 1920 kg/m^3 , the addition of steel fibers results in an increase in density varying from 2160 to 3130 kg/m^3 , for steel volume fraction ranging from 5 to 20 volume percent. The unit weight increase is almost linearly proportional to the fiber content, as shown in Figure 2.7 [1].

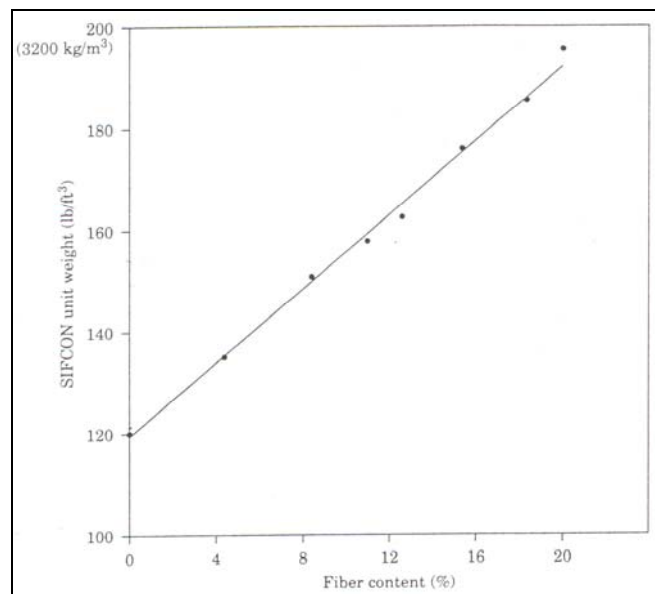


Figure 2.7: Effect of steel fiber content on the unit weight of SIFCON [1]

2.4.2 Behavior in compression

SIFCON is known for its high compressive strength. The highest compressive strength reported for SIFCON is 210 MPa [1]. The composite is also very ductile as compared to a plain matrix. The compressive behavior of SIFCON was investigated using both cast and cored cylinders, and the variables investigated included [1, 5, 7]:

- (a) Fiber orientation effect - parallel and perpendicular to the loading axis.
- (b) Fiber geometry - hooked ends, crimped and deformed.
- (c) Matrix composition - plain cement matrix, matrix containing sand or fly ash, silica fume, or their combinations.

The following is a summary of the results of various investigations.

i) **Compressive Strength:**

Compressive strength of SIFCON depends on mix design, matrix strength, fiber orientation, fiber volume fraction, and fiber geometry. Since fibers themselves do not break, the tensile strength of fibers does not influence the compressive strength of SIFCON. Table 2.2 presents the range of compressive strengths obtained from various fiber types and matrix mix proportions, while Table 2.3 shows the properties of steel fibers used in the investigation [5]. For every mixture, the resulted compressive strength value depends on fiber orientation, content, type, and dimensions.

Strength of SIFCON may be 2 times the strength of the plain matrix. An increase in matrix strength results in an increase of SIFCON compressive strength. Fiber geometries showed less influence than matrix strength. The SIFCON strength is higher when fibers are oriented perpendicular to loading axis, but it should be noted that even if dominant alignment was perpendicular to loading axis, some fibers are still aligned in other directions.

Table 2.2: Reported slurry mix designs and strength values [5]

Mix No.	Mix Constituents	Relative Weight of Constituents	W/C ⁽¹⁾	Strength Range (MPa)
1	Type I cement	1	0.30	52 to 117
	Fly ash	0.20		
	Water	0.36		
	SP	0.03		
2	Type I cement	1	0.35	41 to 93
	Fly ash	0.20		
	Silica slurry ⁽²⁾	0.20		
	Water	0.355		
	SP	0.02		
3	Type I cement	1	0.30	41 to 86
	Fly ash	0.20		
	Silica slurry ⁽²⁾	0.30		
	Water	0.255		
	SP	0.04		
4	Type I cement	1	0.26	69 to 121
	Fly ash	0.25		
	Water	0.325		
	SP	0.04		

⁽¹⁾ W/C is water/cementitious materials ratio including fly ash and silica.

⁽²⁾ A slurry of approximately 50 % water and 50 % amorphous silica particles by weight.

The effect of the water/cementitious ratio on the compressive strength of SIFCON is shown in Figure 2.8 [8]. In that study, all mixes had an 11.6 % volume fraction of steel fibers with hooked ends. The fibers were 30 mm long and had a diameter of 0.5 mm, which makes the reinforcing index equals to about 700.

From Figure 2.8, it can be noticed that the matrix strength is influencing the composite compressive strength significantly. A higher matrix strength could be obtained by using a lower w/c ratio or lower fly ash content. The strength of SIFCON also increases with age as the matrix matures to attain higher strengths.

Table 2.3: Reported fiber properties [5]

Fiber Type	Length (mm)	Diameter (mm)	Aspect Ratio, (l/d)	Volume Fraction, V_f (%)	Reinforcing Index ($V_f \cdot l/d$)
Crimped	25	0.9	28	20 to 23	560 to 644
Hooked	30	0.5	60	10 to 12	600 to 720
Deformed	30	0.5	60	10 to 12	600 to 720

Typical failure mode of SIFCON in compression seems to be shear failure, Figure 2.9. The size of cylindrical specimens shown in this Figure is 3×6 in (7.62×15.24 cm), with $l/d = 2$. Even longer specimens with an l/d ratio of 4 are reported to have shear failure as well [5].

Cored specimens sustain 15 % to 30 % more failure load than cast specimens [5]. The difference could be the result of better fiber packing in the cored specimens as discussed earlier.

ii) Stress-strain behavior in compression:

Even though SIFCON has typically higher compressive strength than normal concrete, its uniqueness is much more important in the area of energy absorption, ductility and toughness. A great energy absorbing capacity and a ductile mode of failure, make SIFCON suitable and perfect for applications involving impact, blast, and earthquake loading.

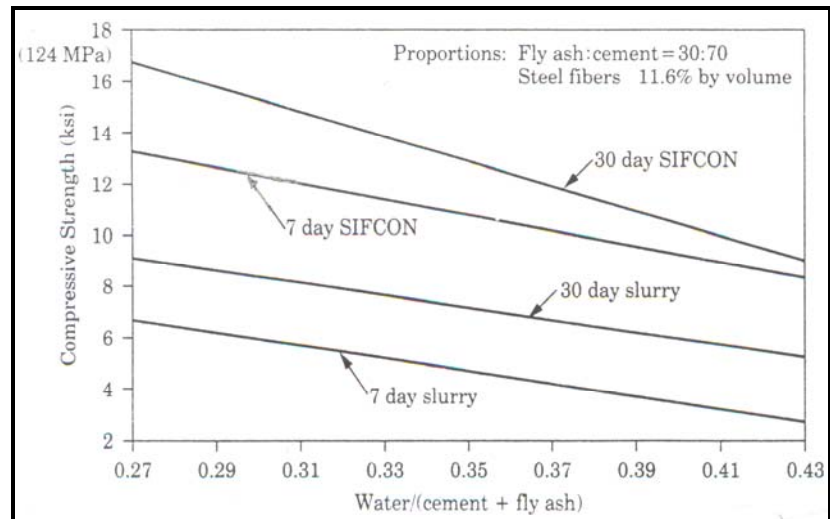


Figure 2.8: Compressive strength vs. water/ binder ratios [5]

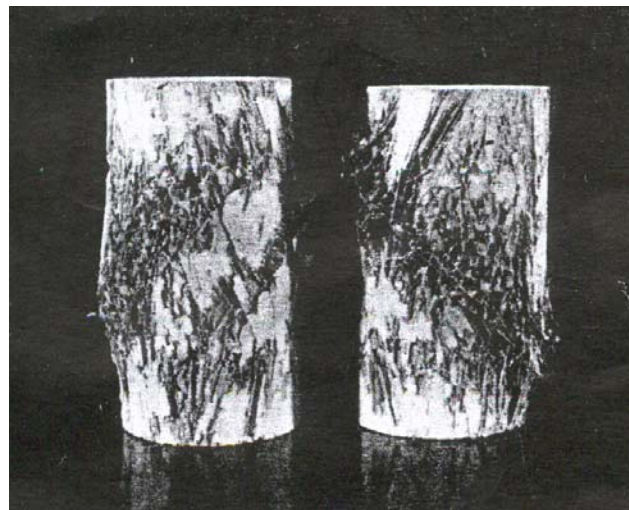


Figure 2.9: Tested SIFCON compression specimens showing consistent shear failure [5]

Typical stress-strain (load-deformation) relationships of SIFCON in compression are presented in Figures 2.10 to 2.13 [1, 5]. The study of those figures leads to the following observations:

- (a) SIFCON has a quite large strain capacity.

- (b) The energy absorption could be 1 to 2 orders of magnitude higher than that of a plain matrix.
- (c) Fiber orientation that is perpendicular (normal) to the loading axis results in not only higher strength but also higher ductility. This should be expected because, as the concrete cracks and expands along the diameter, the fibers provide confining effect, improving both load capacity and ductility. Fibers with better bonding capacity provide better results because they can transfer more loads across the cracks.

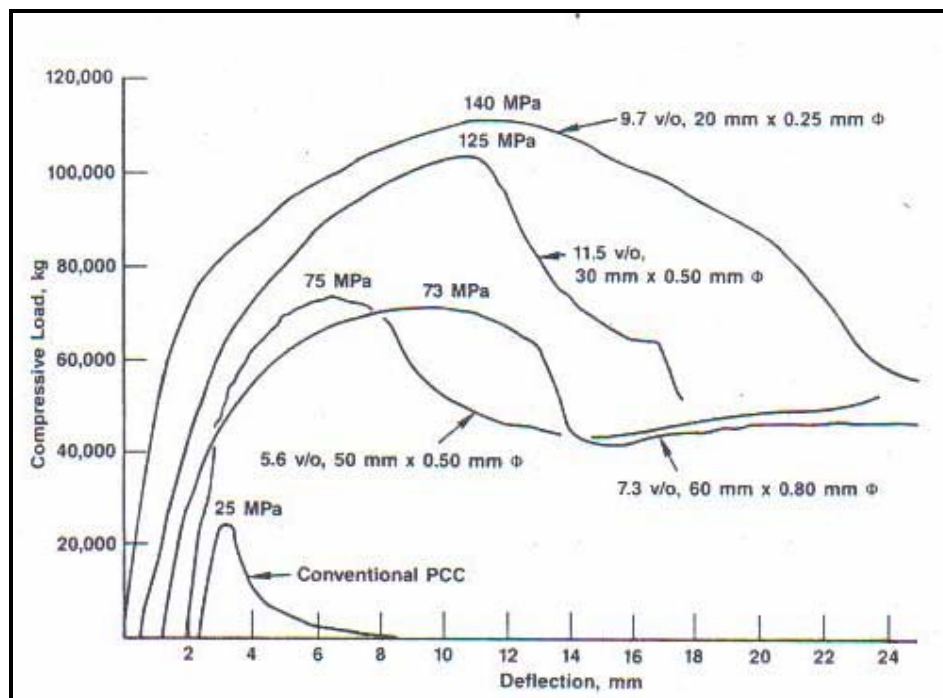
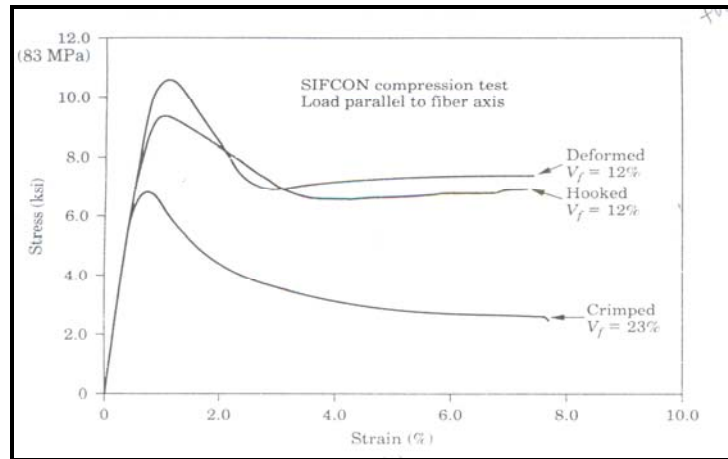


Figure 2.10: Typical load-deformation behavior for 10.2×17.8 cm cylindrical SIFCON specimens [1]

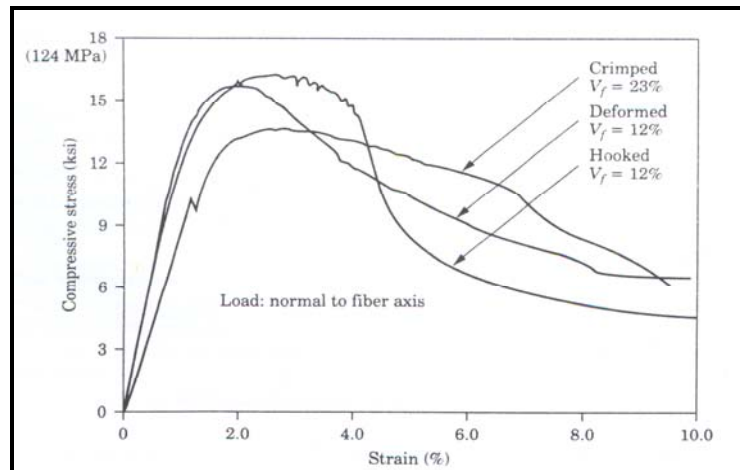
Here a deformation of 24 mm corresponds to a strain of 0.135

Attempts have been made to measure the elastic modulus of SIFCON composites. For these measurements, the compressive strength-strain relationship between zero stress and 20 % of the ultimate stress was used. Values obtained have typically ranged from 14 to 24.5 GPa. [5]. Another

study reported almost the same range (14.7 to 24.5 GPa) [13]. Comparing this range to report typical values of elastic moduli for normal-strength concrete (20 to 40 MPa) which ranges from 21 to 34 GPa [20], leads to the conclusion that modulus of elasticity of SIFCON is slightly lower than the normal concrete modulus. This is a result of the absence of coarse aggregate and the high cement contents in SIFCON matrices.



(a) Loading parallel to fiber axis, mix no. 2 (Table 2.2), cored specimens



(b) Loading normal to fiber axis, mix no. 1 (Table 2.2), cored specimens

Figure 2.11: Typical effects of stress-strain curve of SIFCON in specimens [5]

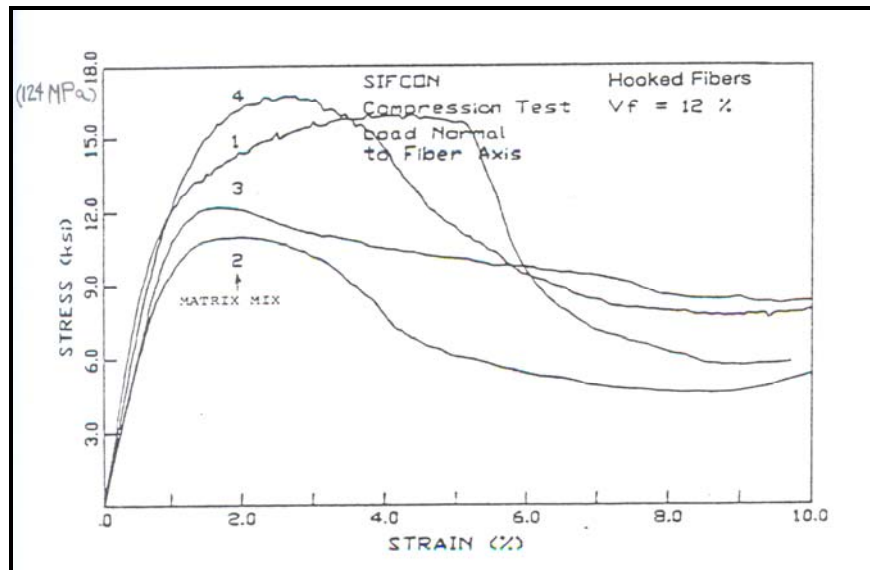


Figure 2.12: Typical stress-strain curves of SIFCON in compression for different mix designs [5]
Mix details are presented in Table 2.2

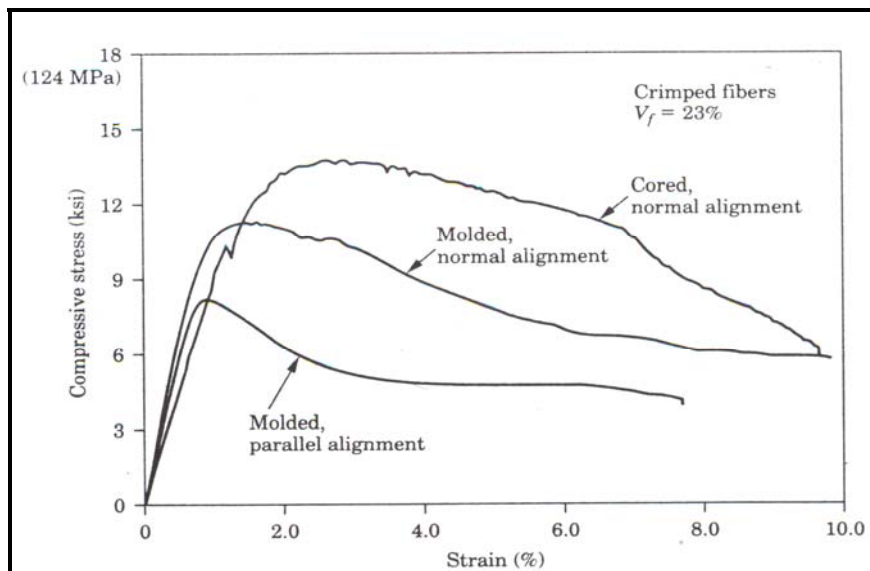


Figure 2.13: Typical stress-strain curves of molded and cored SIFCON specimens in compression (Mix 1, Table 2.2) [5]

2.4.3 Behavior in tension

The tensile strength of SIFCON can exceed 20 MPa, compared to the plain matrix of 7 MPa [6,16]. Tension tests consisted of uniaxial tensile tests on dog bone-shaped prism specimens, Figure 2.14.

The investigated variables included [6, 8, 16]:

- (a) Fiber type and geometry consisting of straight, hooked and surface deformed fibers.
- (b) Fiber volume fraction ranging from 5 % to 13.8 %.
- (c) Matrix composition using admixtures and W/C ratio ranging from 0.26 to 0.45.

The fibers were manually distributed into the molds and oriented as much as practicable in a direction parallel to the loading axis of the test specimens. The molds were placed on vibrating tables and subjected to vibration during fiber placement to obtain compaction of fibers. Alignment was more effective in the narrow testing region of the molds.

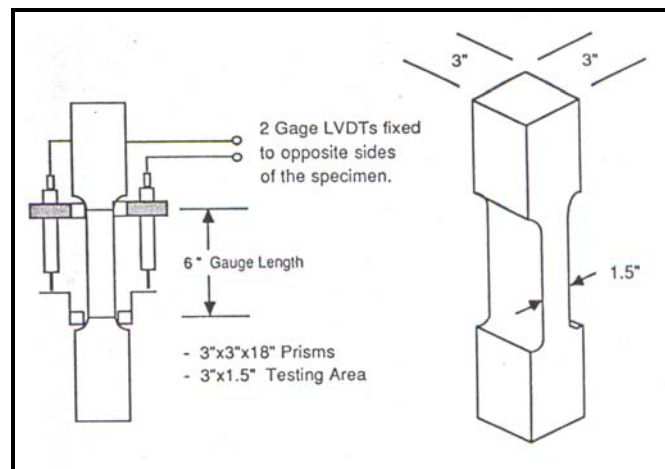


Figure 2.14: Tension dog bone specimens [16]

The following sections provide a brief review of SIFCON behavior under tension.

i) Tensile strength:

As mentioned previously, the tensile strength of SIFCON is about three times the strength of the plain matrix. Table 2.4 presents the tensile strengths for various combinations of SIFCON matrix compositions, fiber types and fiber volume fractions. The results indicate the following trends:

- (a) A matrix containing either fly ash or silica fume provides higher strength than a plain matrix, and matrix containing silica fume provides the highest strength. Since failure occurs by the debonding of fibers and spalling of the matrix, a denser matrix can be expected to provide a better strength.
- (b) Lower water-cement ratio results in better matrix bonding and hence provides higher tensile strengths. The differences are higher for fibers with relatively weak bond strength. For example, in the case of hooked fibers that have good mechanical bond, lower water-cement ratios do not improve the tensile strength significantly.
- (c) Tensile strengths are greater for fiber volume fractions higher than 10 % compared to volume fractions lower than 10 %.
- (d) Overall, tensile strengths higher than 14 MPa can be expected for matrices containing silica fume and a fiber content of about 8 %, or matrices containing fly ash and a fiber content of about 12 %.

ii) Stress-strain behavior in tension

As in the case of compression, SIFCON exhibits high ductility in the tension mode. Typical stress-strain curves obtained using different fiber types and

volume fractions are presented in Figures 2.15 and 2.16. Figure 2.15 shows the stress-strain curves for specimens containing hooked-end fibers and a matrix made with silica fume. Figure 2.16 presents results for specimens made by using a plain cement slurry and three different types of fibers.

Table 2.4 Tensile strengths of SIFCON [6, 8, 16]

Sample no.	Matrix constituents	Water-cement ratio*	Fiber type, l/d	Volume fraction %	Tensile strength (MPa)	Remarks
1	C+10% SF	0.3	HE, 50/5	5	13.6	} 19mm thick specimen
2	C+10% SF	0.3	HE, 50/5	8	15.7	
3	C only	0.45	DF, 30/5	8.5	7.0	} 35mm thick specimen
4	C only	0.45	ST, 25/4	8.5	4.0	
5	C only	0.45	HE, 30/5	8.5	9.2	
6	C only	0.45	HE, 30/5	13.5	14.1	
7	C only	0.35	HE, 60/8	7.4	6.7	
8	C only	0.35	EE, 25/5	9.9	7.8	
9	C only	0.35	HE, 50/8 + EE	6.5 + 4.0	6.9	
10	C only	0.45	HE, 60/8 + EE	6.1 + 4.2	10.7	
11	C+20% FA	0.35	HE, 30/5	11.7	15.6	} 37mm thick specimen
12	C+20% FA	0.35	DF, 30/5	12.6	10.9	
13	C+25% FA	0.26	HE, 30/5	12.1	15.7	
14	C+25% FA	0.26	DF, 30/5	13.8	16.1	

* Weight of fly ash was included with the weight of cement for water-cement ratio.

C = cement
SF = silica fume
FA = fly ash
HE = hooked ends
DF = deformed
ST = straight

l = length of fiber (mm)
 d = diameter of fiber (mm)
1 in. = 25.4 mm
1 ksi = 6.89 MPa
EE = deformed

In all cases, the stress-strain (load-deformation) curves have three distinct regions. The first part, which is primarily elastic, is very steep. After the initiation of micro cracks, the curve becomes nonlinear, representing post crack behavior. A well-defined descending branch exists for all the fiber and matrix combinations investigated.

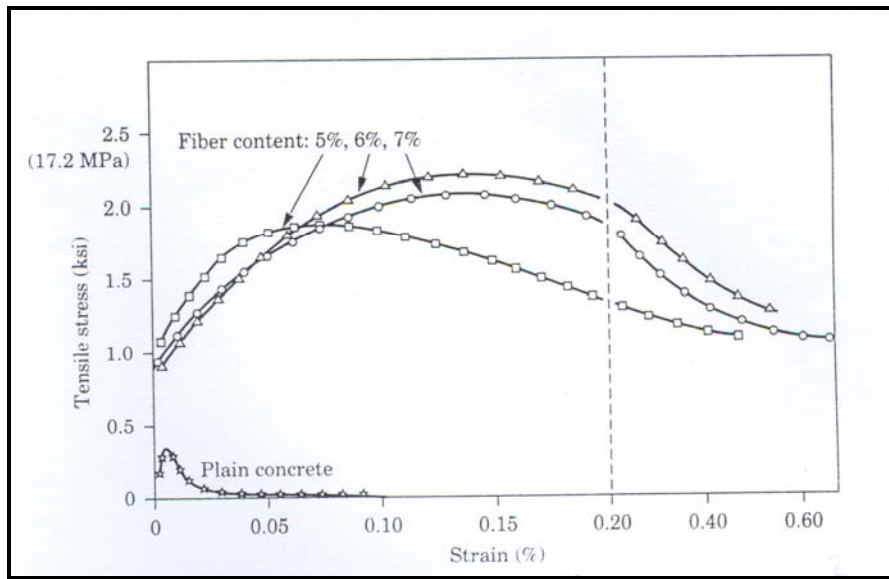


Figure 2.15: Stress-strain behavior in axial tension [6]

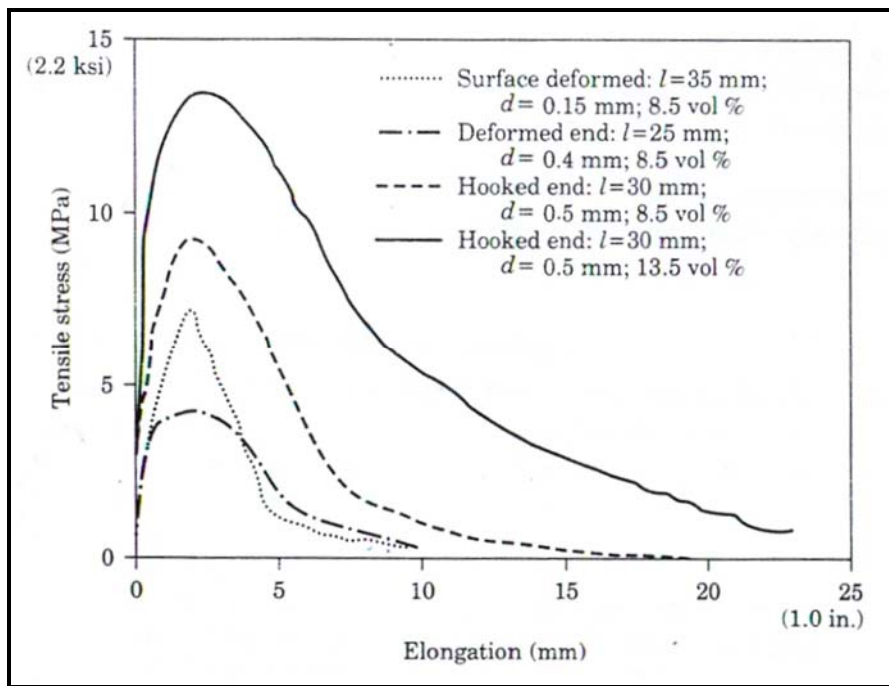


Figure 2.16: Tensile stress-displacement curves of various fiber types and contents in a mix of W/C of 0.45 [8]

Specimens with fibers oriented parallel to the loading direction and specimens containing a cement silica-fume matrix exhibit a longer plateau near the peak load. The descending parts of the stress-strain curves are also less steep for these specimens. The specimens could sustain peak load at strains as great as 20 %. Compared to plain slurry, the toughness index of SIFCON in tension evaluated at 0.02 strain can reach 1000 [16].

2.4.4 Behavior under flexural loading

In most field applications, SIFCON is subjected to bending stress, at least partially. Hence, the behavior under flexural loading plays an important role in field applications. Flexural tests have been conducted using SIFCON beams both under static and cyclic loading [4, 6, 21, 22]. The investigations were designed to evaluate the various fiber lengths, types, contents, and matrix compositions. The typical load-deflection response is shown in Figure 2.17. That study dealt with 19 mm thick SIFCON beam specimens cut from a slab with a 76 mm width and 356 mm length.

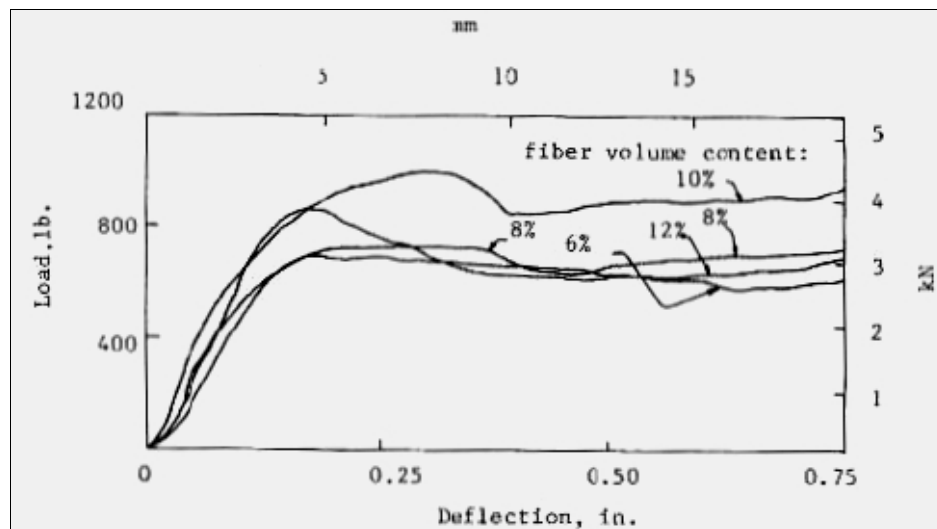


Figure 2.17: Load-deflection curves in flexure for hooked-end fibers with $l = 30$ mm and $d = 0.5$ mm [21]

For mix design, see Table 2.1 [Ref.6]

i) Flexural strengths:

Table 2.5 presents the flexural strength of four fiber lengths and various fiber contents. In all cases the slurry was made of cement +10% silica fume with a W/C ratio of 0.3. Amount of super plasticizer was 4.8 % by weight of cement. The flexural strength was computed using the average maximum load of three specimens, and the classical bending theory equation [21].

Figure 2.18 presents the variation of flexural strength for different fiber contents and lengths. The study of Table 2.5 and Figure 2.18 leads to the following observations [21]:

Table 2.5: Flexural strength of SIFCON [21]

Fiber (length/dia.) (mm)	Fiber Volume (%)	Maximum Flexural Strength (MPa)
30/0.5	6	55.2
	8	61.8
	10	91.9
	12	62.7
40/0.5	4	46.9
	6	67.7
	8	75.4
	10	76.5
50/0.5	4	36.5
	5	58.8
	6	78.6
	8	73.7
60/0.5	5	49.6
	6	53.7
	8	72.1
	10	63.4

(a) The flexural strength of SIFCON is an order of magnitude greater than the flexural strength of normal fiber-reinforced concrete.

- (b) For a constant fiber length, the flexural strength increases with the volume fraction of fiber only up to a certain limit. After certain fiber content, the bond strength decreases because of the lack of matrix in between the fibers, thus reducing the flexural strength. The optimum fiber content seems to be in the range of 8 % to 10 %.
- (c) The optimum fiber volume seems to decrease with an increase in fiber length. For the same fiber volume, longer fibers provide a slight increase in flexural strength.

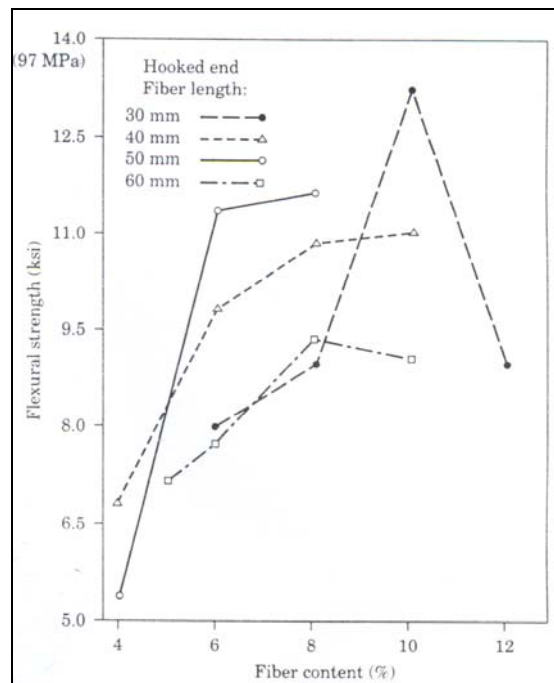


Figure 2.18: Flexural strengths versus fiber contents [21]

ii) Load-deflection behavior in flexure:

The load-deflection behavior of a SIFCON shown in Figure 2.19 is quite different from the load-deflection behavior of typical FRC beams. The curves

have a relatively short linear elastic response and a considerable plateau at the peak. The beams can also sustain a high percentage of peak loads (more than 80 % of peak load) even at large deflections. Figure 2.19 shows a comparison of the load deflection curves for a SIFCON specimen, a fiber reinforced concrete specimen, and a plain concrete specimen. While fiber length and fiber volume fraction influence strength, Figure 2.18, the ductility is not affected by either of the variables, as shown in Figure 2.20.

Figure 2.21 presents the comparison of load-deflection behavior for specimens made with and without silica fume. All the specimens had 8 % fiber content. As can be seen from this figure, the use of silica fume increases the flexural strength, and hence the toughness substantially. This increase can be explained by the fact that the silica fume results in a much denser matrix. The increase in the matrix density possibly provides as much improvement in bond between the matrix and the fiber as in the compressive strength. The predominant failure pattern is by the pulling out of the fibers [21].

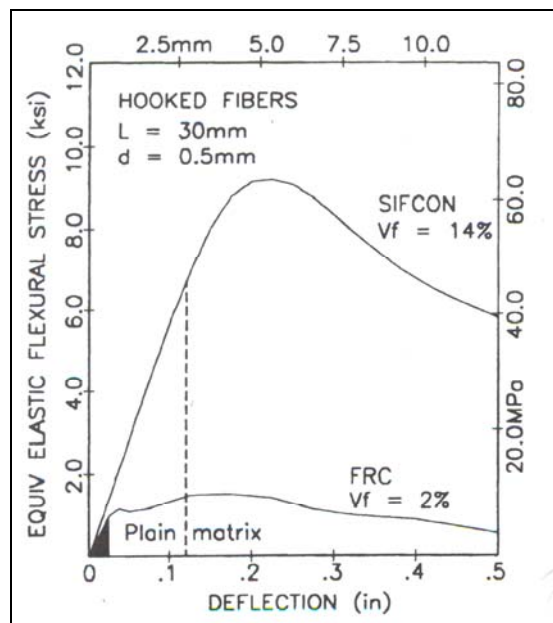


Figure 2.19: Comparison of load-deflection curves for SIFCON, ordinary FRC with 2% steel fibers, and plain matrix [22]

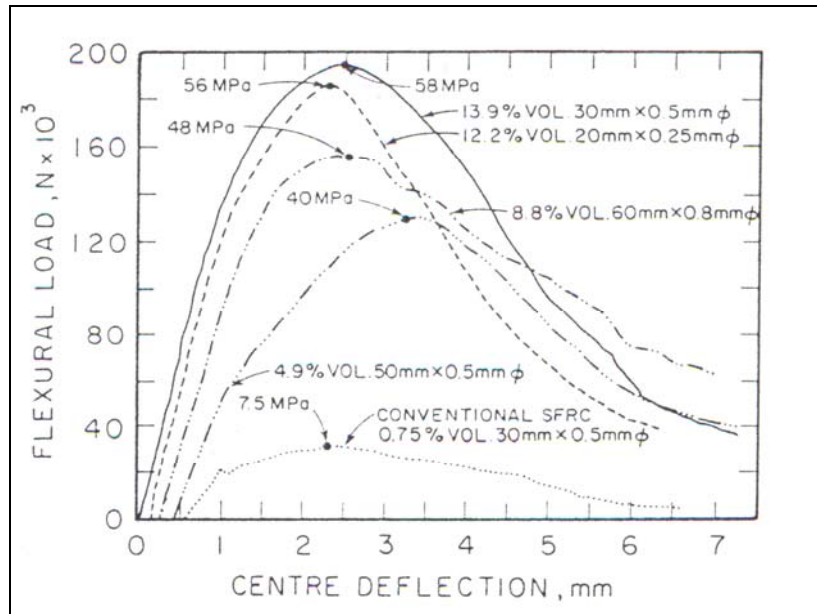


Figure 2.20: Effect of fiber content in SIFCON on the flexural load-deflection curve [1]

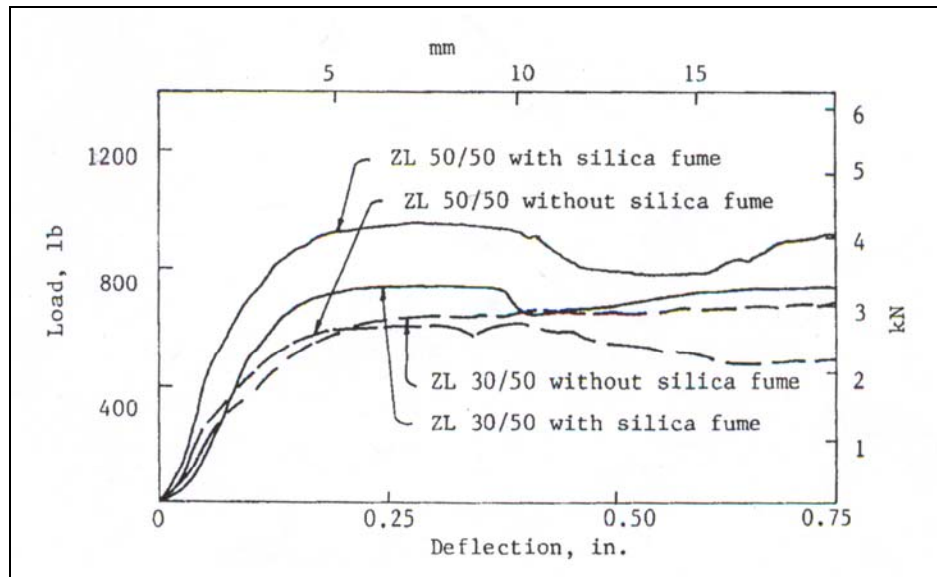


Figure 2.21: Comparison of load-deflection behavior of beams with and without silica fume [21]

The addition of sand beyond a cement-to-sand ratio of 1:1 decreases the compressive strength, whereas the flexural strength reduction starts when the

cement-to-sand ratio exceeds 1:1.5. The decrease in compressive strength is more rapid than flexural strength, the limited available results indicate that sand can be added to cement up to a ratio of 1:1.5 (cement: sand) without adversely affecting the flexural strength. These results are consistent with the results reported for compressive strength [2, 21].

2.4.5 Behavior in shear

The shear strength of FRC has been extensively studied [6, 14, 23, 24]. However, the equation for the shear strength predictions in FRC does not give accurate results for shear strength prediction in SIFCON [23,24]. Shear tests on SIFCON have been performed with direct shear specimens [6], torsion specimens [23], direct, double shear specimens [14], and specimens under combined tension and shear [24]. Figures 2.22 and 2.23 show two examples of shear specimens used in the investigations.

Each of these tests was performed with various slurry strengths, fiber reinforcement indexes ($V_f l/d$), and fiber types. Figure 2.24 shows the variation of load with respect to slip at shear plane [6]. The shear strength was computed by dividing the max load by the area of the shear plane. The average shear strength in this study [6] was 30.9 MPa, compared to about 5.5 MPa for plain concrete.

The results of another study are shown in Figure 2.25. In this study, the shear strength at maximum load was 2.8 MPa for the plain slurry and 2.9 MPa for the plain concrete. The addition of 6 % steel fibers by volume to the slurry matrix increased the shear strength about 10 times to 4 ksi (28 MPa) [14].

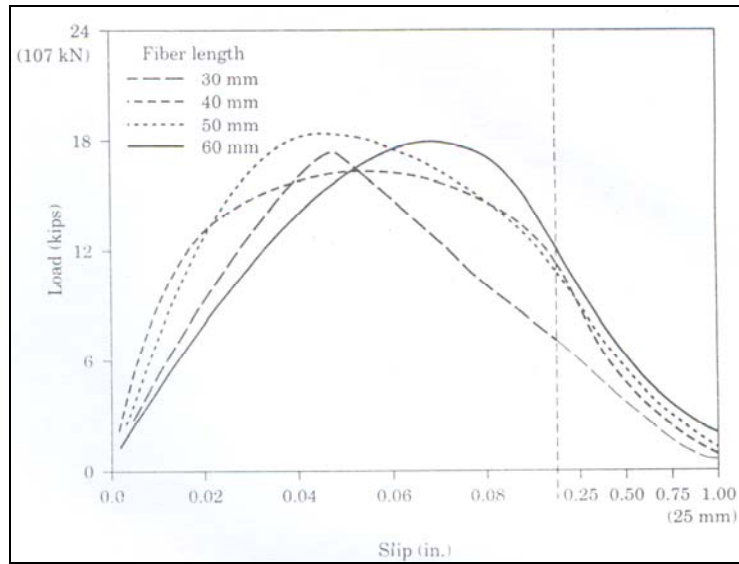


Figure 2.24: Load-deformation behavior of shear specimens, fiber content = 6 % [6]

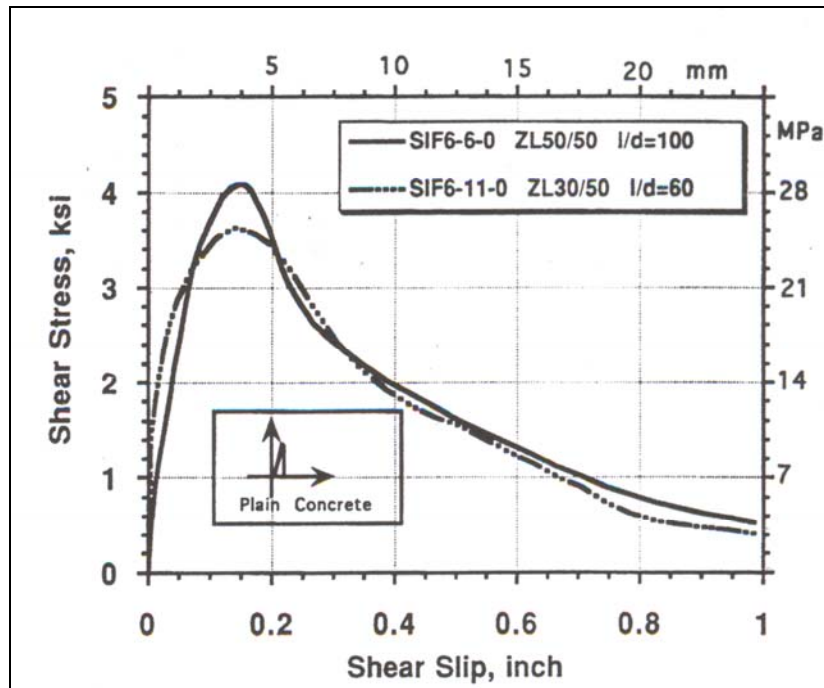


Figure 2.25: Shear stress versus slip response of SICON [14]

It is generally agreed that fiber orientation is the most important factor affecting SIFCON shear strength and behavior [23, 24]. Specimens with fibers oriented normal to the shearing plane (fibers bridging the shear plane) generally could not be failed. Regarding fiber type, hooked fibers performed substantially better than straight fibers. Dowel reinforcement across the shear plane increased the shear strength by only 12%. The major advantage of dowel reinforcement was to improve the post peak behavior of the specimens. Dowel reinforced SIFCON specimens exhibited energy absorption values 1000 times greater than unreinforced concrete [14].

2.4.6 Bond of bars embedded in SIFCON

The bond characteristics of reinforcing bars embedded in SIFCON have also been investigated [17, 25]. The SIFCON was prepared with 5 % of hooked steel fibers of 50 mm long and 0.5 mm diameter. The compressive strength of SIFCON was 61.4 MPa. Based on the test results conducted in those studies, the following conclusions were drawn:

- (a) SIFCON led to a significant increase in the bond strength of deformed reinforcing steel bars. Average bond stresses ranging from 14 to 28 MPa were observed. This range was between 2 and 4 times that of bars embedded in plain concrete.
- (b) The initial bond stiffness was at least 5 times higher than that observed for plain concrete.
- (c) Pullout work, or dissipated bond energy, was over 20 times greater than that for plain concrete.
- (d) Reinforcing bars embedded in SIFCON can resist slip up to 10 times more than when embedded in plain concrete and still maintain the peak load.

(e) No cracking was observed up to 70% of the peak load.

(f) Cover as small as 13 mm resulted in better performance than plain concrete.

In brief, reinforcing bars embedded in SIFCON exhibit higher bond strength, energy absorption, and load levels at larger slips than bars embedded in plain concrete or FRC.

2.5 Durability of SIFCON

As mentioned earlier, very little information is available in literature about durability aspects of SIFCON. The only available information was solely about drying shrinkage and resistance to freezing and thawing. The following sections present the available results of those two aspects of SIFCON durability.

2.5.1 Drying shrinkage strain

The drying shrinkage behavior of SIFCON is illustrated in Figure 2.26 along with that of unreinforced slurry. The data shown in the figure were obtained from $7.6 \times 7.6 \times 28.6$ cm beam specimens that were cured for 28 days before placing in a room at 23 °C and 50 % relative humidity [1].

The unreinforced slurry has exhibited a continual and large drying shrinkage strain over the 180 days exposure period. As can be seen from the figure, plain slurry can exhibit shrinkage strain up to 1500 micro-strains (0.15 %) in 28 days, and grow to 2500 micro-strains (0.25 %) in 100 days. However, SIFCON with 5 % to 18 % fiber volume fraction exhibits relatively low shrinkage strain between 200 and 500 micro-strains, in spite of the high cement content of the matrix. SIFCON strains peaked somewhere between 7

and 28 days. For exposure periods beyond 28 days, the SIFCON specimens have shown no significant further shrinkage despite continued shrinkage strain in the plain concrete. The magnitude of drying shrinkage strain for SIFCON in Figure 2.26 is within the range exhibited by conventional Portland cement concrete [1].

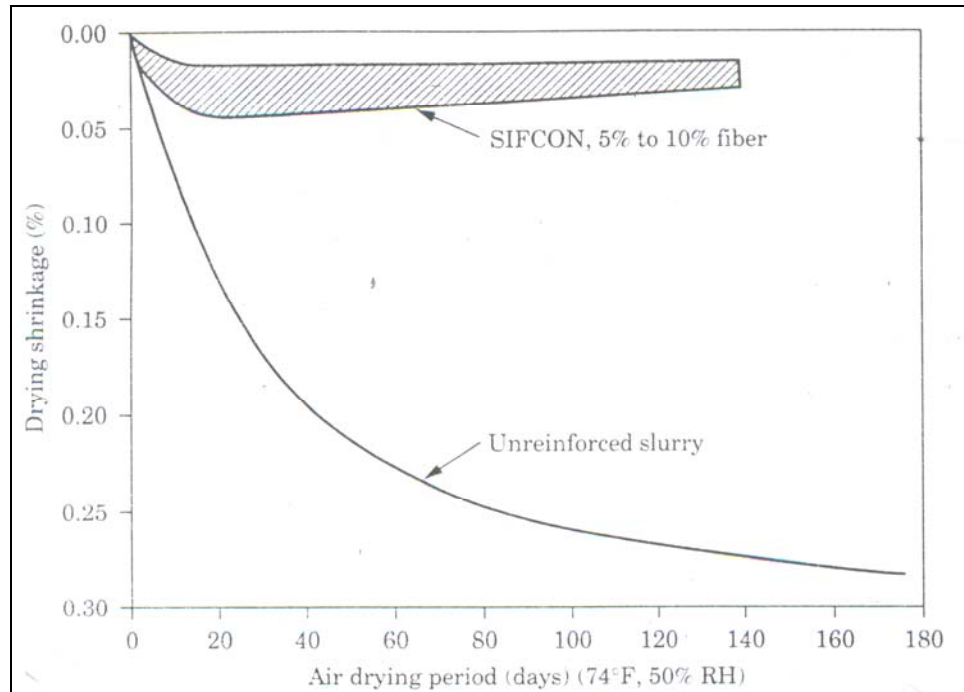


Figure 2.26: Drying shrinkage of SIFCON and plain unreinforced slurry [1]

The low shrinkage of SIFCON compared to plain slurry is probably due to the high fiber content, as well as to the nature of the reinforcing bed, in which the fibers form contact with each other, generating a fiber interlock effect [26]. Generally, the addition of sand reduces the shrinkage of the matrix considerably. Hence, SIFCON made with cement-sand mortar can be expected to have much less shrinkage strain than that shown in Figure 2.26, in which the slurry was made using only cement [2].

Actually, on this only available study on drying shrinkage of SIFCON, the author did not give the details of mix design, or explanations for the reason of exhibiting some increase in specimens lengths after the peak strain value, as can be seen in Figure 2.26.

2.5.2 Resistance to freezing and thawing

The durability SIFCON under freezing and thawing was evaluated previously in only one study [27]. The investigation was conducted using the rapid freeze-thaw procedure similar to the one recommended in ASTM C 666, Procedure A. Essentially, 4 sets of specimens containing 4 different fiber length (30, 40, 50 and 60 mm) subjected to 300 cycles of freezing and thawing. The temperature range was -17.8 °C to 4.4 °C approximately, and each cycle had a period of 4.5 hours. SIFCON prismatic specimens were made of cement + 10 % silica fume with a W/C ratio of 0.3. Fiber volume fraction was kept constant at 8 %. The size of prism specimens used in the test was 19 mm thick, 76 mm width, and 356 mm length. 50 mm slurry cubes were also subjected to the freeze-thaw cycles.

Half of the slurry cubes disintegrated in the freeze-thaw chamber where none of the SIFCON prism specimens disintegrated. However, there was considerable scaling on the SIFCON surfaces. After the freeze-thaw cycles, the specimens were tested in flexure. Because of the scaling, the flexural strength reduced considerably. The reduction in strength ranged from 26 % to 43 % compared to virgin specimens. The strength reduction could have been high because the specimens were relatively thin. There was no difference in the ductility of the specimens. Based on those results, the author recommended that thin SIFCON section exposed the freezing and thawing should be protected by some kind of overlay or coating [27].

2.6 Applications of SIFCON

Although SIFCON is still a relatively new material, the composite has been used successfully in a number of areas, especially for applications where high strength or high ductility or both are needed. These include a large variety of earthquake-resistant structures, military installations, explosive and penetration-resistant structures. In addition to many other uses such as airport pavements, parking lots and bridge decks. The following are some of the successful applications of SIFCON reported in the literature. Most of them have been applied in the USA since the early 1980's.

2.6.1 Earthquake resistant structures

Use of SIFCON in hinge regions of earthquake resistant structures was investigated [19]. The research studied the use of precast SIFCON flexural hinges to increase the seismic resistance of reinforced concrete frames. It was found that reinforced SIFCON hinges can exhibit superior performance as compared to reinforced concrete hinges. Many problems encountered with reinforced concrete hinges do not occur when using SIFCON hinges. For example, greater shear strength and toughness prevent shear sliding on through-depth flexural cracks in reinforced SIFCON. In contrast, reinforced concrete hinges develop a through-depth flexural crack. As loading progresses, sliding occurs on this plane, quickly degrading the structural integrity.

Another study proved also that using SIFCON in cast-in-place connections in framing systems permits much greater toughness and ductility than conventional fiber concrete [11]. Figure 2.27 illustrates the application of SIFCON joints in seismic resistant frames.

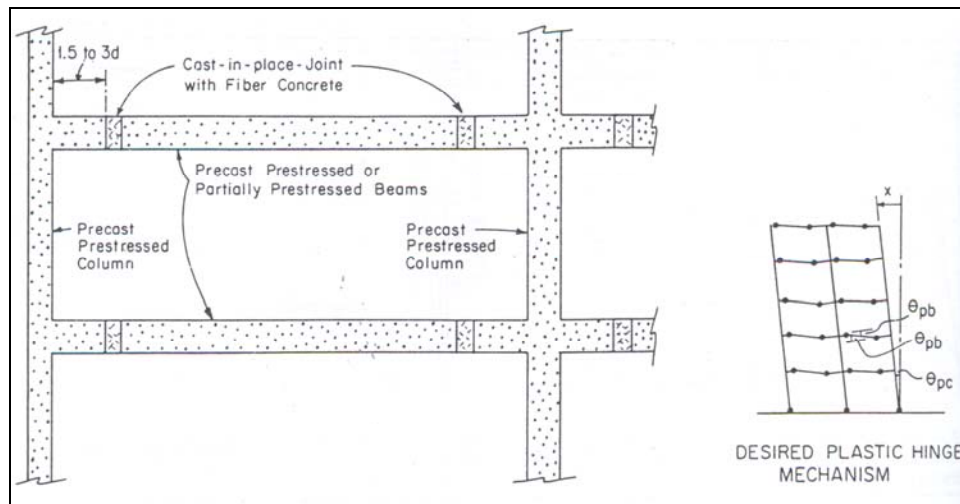


Figure 2.27: Schematic representation of SIFCON joints in the structural system [11]

2.6.2 Repair and retrofit of structural components

SIFCON serves as an excellent repair material because it is compatible with reinforced concrete in terms of stiffness and dimensional changes caused by temperature. It can be placed in hard-to-reach places and provides good bonding to the parent concrete because of the presence of fibers. The matrix can be modified to suit the particular repair. For example, rapid strength gain can be obtained using accelerators [2].

SIFCON was used to repair prestressed concrete beams spanning a highway in New Mexico, USA. The beams had been damaged by vehicle passing under the bridge. Some of the pretensioned tendons had been exposed by the damage. The beams were restored, using SIFCON, without removing them. Restoration in-place not only resulted in a large cost saving but also reduced the time of repair by a few months. The results have been satisfactory up to reporting date (8 years after repair) [1]. In addition, SIFCON can be effectively used along with slurry infiltrated mat concrete (SIMCON) for retrofit of non-ductile reinforced concrete frames [18].

2.6.3 Bridge deck and pavement overlay

SIFCON has been used for a number of bridge rehabilitation projects [28-30]. Typically, the area to be repaired is chipped off and cleaned thoroughly. The fibers are placed in position and infiltrated with slurry. In most cases, the infiltration is achieved by gravity alone. In certain applications, a thin layer of coarse aggregate were placed on the surface of the still fresh SIFCON and troweled into place to form a wearing surface. The repaired sections were functioning well after more than 6 years of repair work.

Pavement rehabilitation is similar to bridge deck rehabilitation except that the repair surfaces are normally large and the loading pattern is primary compressive. The construction sequence is the same as in bridge deck repairs. Figure 2.28 shows infiltration step in pavement rehabilitation. SIFCON was successfully used for overlays ranging in thickness from 20 to 50 mm [31].



2.28: Infiltration of the steel fiber bed with the slurry in pavement overlay application [31]

The best overlay performance was achieved when SIFCON overlays were used. SIFCON overlays require minimum thickness (13 to 50 mm), and should be used whenever an increase in the deck dead load is a limiting factor. SIFCON overlays are also highly recommended whenever a high early strength, a high level of impermeability, or high fatigue resistance is required [32].

2.6.4 Precast concrete products

A number of precast concrete products have been produced from SIFCON including precast slabs, small vaults, and cast pipe sections [2, 4, 31, 33]. For example, thin precast slabs that are 25 to 50 mm thick have been constructed and used as an impact and wear-resistant surfacing over conventional concrete. Slabs of dimensions 2.4m × 3.0m × 5cm were prepared with anchors cast into the bottom surface. Figure 2.29 shows the placement of a SIFCON slab into an excavated area containing fresh concrete at an airport. The slabs, which provided good impact resistance, have been used in airport taxiways. Precast SIFCON slabs, which supported the wheel loads of Boeing 767 aircrafts, showed no cracking through a one year service period [1].

2.6.5 Explosive-resistant structures

Because of its high flexural and compressive strength, combined with high ductility, SIFCON is being considered for use in structures to resist the effect of explosive loading [1, 34]. For instance, SIFCON has been used for making containers to store various kinds of ammunition. The primary concern in this application is to limit the spread of explosions from container to container. SIFCON provided good resistance in terms of containing the exploded materials in one chamber.

SIFCON was also evaluated for missile silo structures [34]. A model of hardened missile silo structure was constructed of SIFCON by the New Mexico Research Institute, Figure 2.30. The silo was 6 m height, having 15 cm thick SIFCON walls sandwiched between two 6 mm thick steel plates. First, the inner and outer steel liner sections were completely erected in 1.5 m long sections. Afterwards, the steel fibers were placed between the liners and then the slurry was infiltrated with the aid of external vibration in 1.5 m lifts to obtain properly compacted composite.

Following construction, the fully instrumented silo structure was subjected to explosive loading. The performance of the SIFCON structure in this test was found to be excellent and even exceeded expectations [34]. SIFCON has also demonstrated excellent resistance to the penetration of projectiles.

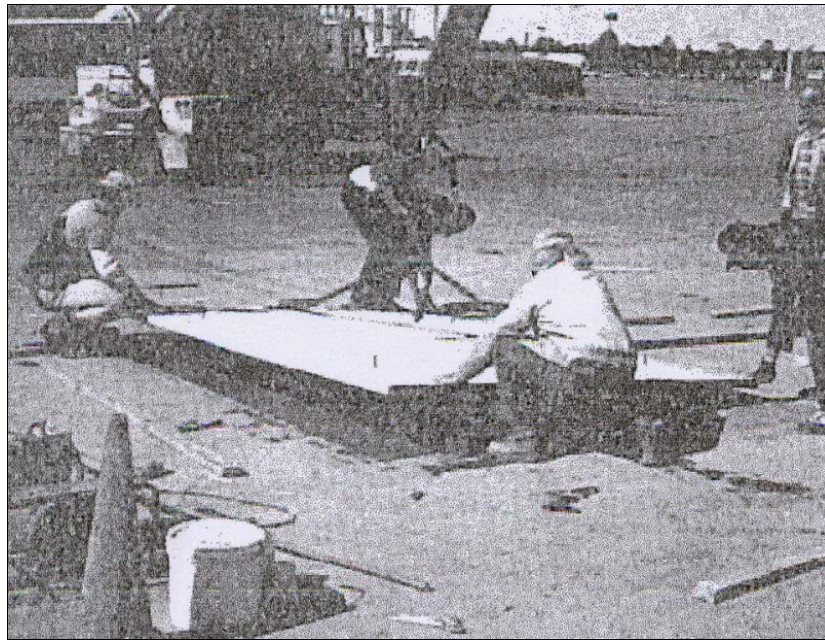


Figure 2.29: Installation of a precast SIFCON slab at a commercial airport [1]

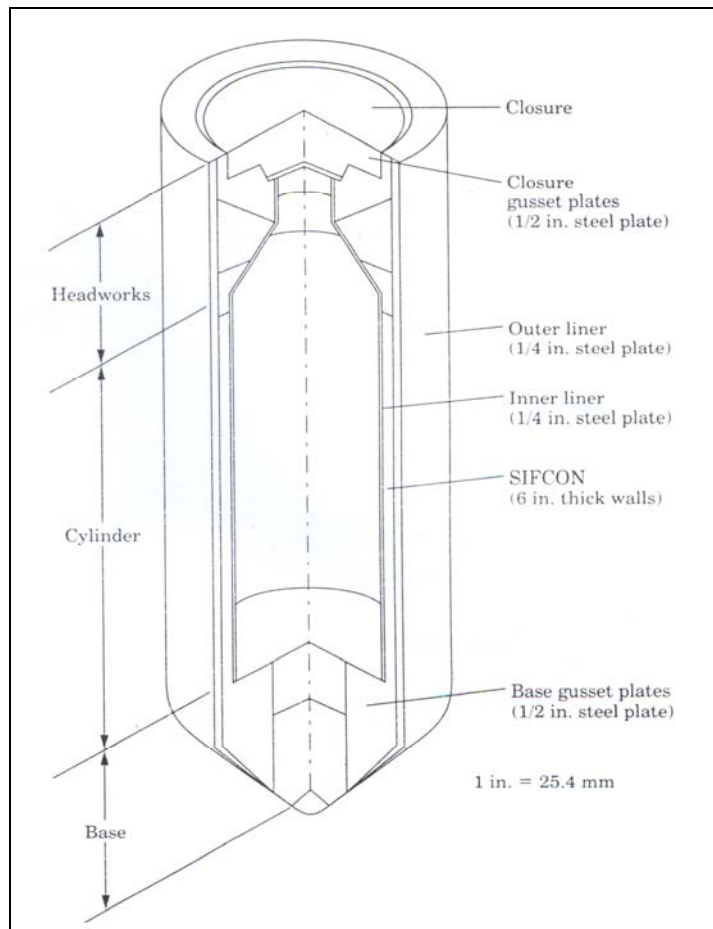


Figure 2.30 Schematic diagram of a hardened silo structure containing SIFCON [1]

2.6.6 Refractory applications

The concept of SIFCON has been also successfully used for refractory applications [31, 35, 36]. Precast SIFCON elements were used in these high temperature applications using stainless steel fibers and slurries based on calcium aluminate cement matrix. The applications included: seal plates, tubes used in the pressure casting of metals, plunging bells and lances for steel desulfurizing, furnace lintels and saddle piers.

SIFCON composites provide excellent resistance to spalling under high temperature, thermal shock conditions and under conditions of high mechanical abuse. Refractory SIFCON has worked far better than any other material for this application such as steel plates and conventional refractories. The reported performance of SIFCON in elevated temperatures application indicates that its improved performance easily justifies its increased cost relative to the conventional products [31].

2.6.7 Security applications

In this application, such as vault doors and safes, the product must have excellent resistance against blasting, torching, drilling, and chipping. Both reinforced concrete and steel have certain weaknesses. For example, steel walls can be torched, whereas the concrete walls can be drilled or blasted to gain entry.

Using SIFCON in this application has demonstrated its advantages over both concrete and steel. SIFCON walls cannot be torched because concrete will resist deterioration by heat and will also slow down heat conduction. The composite resisted the blast loading because of its high ductility. Chipping and drilling is very difficult because of the fiber intrusions. Hence, SIFCON is being used successfully for various types of safe vault doors. The mix composition used is a modified version of SIFCON. The preplaced fibers were mixed with clean coarse aggregates before infiltration with cement-based slurry [2].

CHAPTER 3

EXPERIMENTAL STUDY

3.1 Introduction

The main objective of this study was to investigate various characteristics related to the durability of SIFCON. The investigated durability characteristics were water absorption, chloride penetration, drying shrinkage and freezing-thawing resistance. Stress-strain behavior of SIFCON mixes under compression was also determined.

The experimental program involved conducting tests relevant with the durability aspects stated above on both slurry or paste SIFCON and mortar SIFCON mixtures. Each SIFCON mix was prepared using two types of steel fibers, hooked and crimped, and with three fiber volume fractions, 7 %, 9.5 %, and 12 %. The dimensions of steel fibers were the same. For all the tests, comparative interpretations were made within each slurry or mortar SIFCON, between the two types of SIFCONs used, as well as with a control conventional concrete designed to be a low permeability, high strength concrete. Hence, the effects of the following parameters on SIFCON durability were investigated:

- (a) SIFCON matrix types.
- (b) Fiber contents.
- (c) Fiber types.

3.2 Materials

The materials used in this study included ordinary portland cement, fine aggregate (crushed sand), mixing water, superplasticizers, and steel fibers. The properties of these materials are presented in the following sections.

3.2.1 Cement

The cement used in all mixtures of the study was an ordinary portland cement CEM I 42.5 R, which corresponds to ASTM C 150 Type I cement. The cement was obtained from SET Cement Plant in Ankara. The physical and mechanical properties of the cement used are listed in Table 3.1, and its chemical composition is presented in Table 3.2. All the results meet the requirements of ASTM C150 specification [37].

Table 3.1: Physical and mechanical properties of the cement used in the study

Test	Results	Related standard
Density	3.12 g/cm ³	ASTM C 188 [38]
Fineness	2982 cm ² /g	ASTM C 204 [39]
Normal consistency	27%	ASTM C 187 [40]
Soundness	0.7 mm	BS EN 196-3 [41]
Setting time:		
Initial	158 min	ASTM C 191 [42]
Final	225 min	
Compressive strength:		
3 days	23.1 MPa	ASTM C 109 [43]
7 days	32.6 MPa	

Table 3.2: Chemical analysis of the cement used in the study (*)

Oxide	CaO	SiO ₂	Al ₂ O ₃	Fe ₂ O ₃	MgO	K ₂ O	Na ₂ O
Content (%)	67.01	18.90	4.74	3.03	1.76	0.70	0.51

(*) The analysis was determined in accordance with ASTM C 114 [44]

3.2.2 Aggregate

The main aggregate type used in the study was crushed limestone fine sand with a maximum nominal size of 1.0 mm. In spite of being relatively coarse compared to the sand sizes usually used for SIFCON, using this size of sand proved to be successful in all the SIFCON mixes of the experimental program. A smaller size of the same crushed stone sand, maximum nominal size of 0.6 mm, was also used in a limited part of the investigation for comparative purposes.

For the control concrete mix, crushed limestone with a maximum nominal size of 20 mm was used as coarse aggregate, in addition to sand of 4.76 mm maximum size. All the aggregates used were from the same source. Specific gravity, absorption and sieve analysis tests were carried out for the fine and coarse aggregates in accordance with the standard test methods ASTM C 127, ASTM C 128, and ASTM C 136 [45-47]. Table 3.3 presents the bulk specific gravity and absorption capacity of the fine and coarse aggregates.

Table 3.3: Results of SSD specific gravity and absorption of aggregates

Property	Aggregate Type	
	Fine	Coarse
Bulk specific gravity (SSD)	2.60	2.69
Absorption capacity (%)	2.51	0.36

As mentioned above, three gradings of fine aggregate have been used in the mixes. For the control plain concrete, the sand has been used as it is from the source. It is designated as FA1. Sand FA1 was too coarse to be used successfully in making SIFCON specimens. Therefore, the sand used for all mortar SIFCON mixes, FA2, was screened on a sieve with opening smaller than 1mm. A third smaller size of sand, FA3, was obtained by sieving the original sand on 0.6 mm sieve. This size was used only in water absorption test for comparative purposes.

The coarse sand was sieved to obtain the required sizes for SIFCON. The sieve analysis results of the three sizes of fine aggregate, in addition to the coarse aggregate that was used only in making the control conventional concrete are given in Table 3.4. Each data value given in the table represents the average of three samples.

The grading of the coarse and fine aggregate (FA1) used for the control conventional concrete, conforms to the requirements of ASTM C 33 [48]. There are not any standard specifications for SIFCON constituents yet. The most important requirement of fine aggregate used in SIFCON is its size. It has to be sufficiently small to ensure ease of complete infiltration through steel fibers network without clogging or honeycombing.

Figure 3.1 illustrates the grading curves for the two types of sand used for making mortar SIFCON mixes in this study. The figure shows clearly the difference in grain size distribution between the two types. However, both types are well-graded.

Table 3.4: Aggregate grading

Sieve Size (mm)	Passing (%)			
	Coarse (20 mm)	Fine (FA1) (4.76 mm)	Fine (FA2) (1.0 mm)	Fine (FA3) (0.6 mm)
25.4	100	100	100	100
19.1	100	100	100	100
12.7	49.7	100	100	100
9.5	11.2	100	100	100
4.76	0.3	100	100	100
2.38	0	89.4	100	100
1.18	0	59.1	100	100
1.00	0	47.4	99.5	100
0.60	0	37.6	71.5	99.8
0.30	0	25.2	36.7	54.2
0.15	0	9.6	31.3	45.4

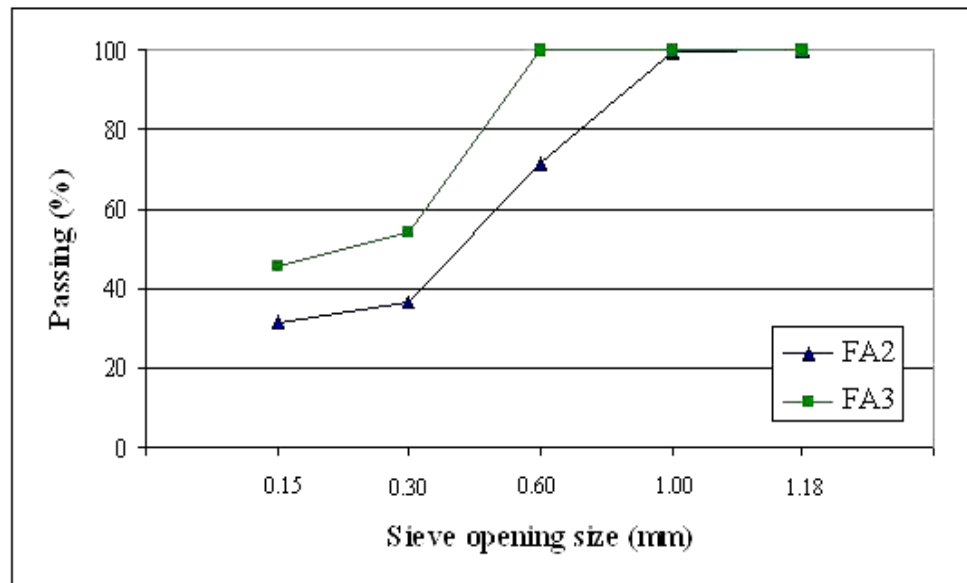


Figure 3.1: Gradings of 1.0 mm and 0.6 mm sand

3.2.3 Mixing water

The METU Campus tap water was used as the mixing water. It is drinkable, clear and apparently clean, and does not contain any substances at excessive amounts that can be harmful for making concrete. However, distilled water was used in preparing sodium chloride solution for chloride penetration and freeze-thaw resistance tests.

3.2.4 Chemical admixture

Only one type of superplasticizers (SP) was used in the study. It is a high range water reducing superplasticizing admixture named Rheobuild 1000 and produced by Degussa Construction Chemicals Ltd. Rheobuild 1000 is a ready-to-use, chloride free, liquid admixture which meets ASTM C 494 requirements for type A and F admixtures [49, 50]. This superplasticizer was used for mortar SIFCON mixes where flowing properties were required, and for the control concrete mix because of the low W/C ratio. On the other hand, there was no need to use any superplasticizer in slurry SIFCON mixes.

3.2.5 Steel Fibers

Numerous trials were made in the preliminary stages of the research in order to choose the appropriate fiber types. For example, it was found that using fibers glued in bundles is not applicable for SIFCON. Fibers used in making SIFCON have to be in a loose state (single or discrete) in order for the mixture to infiltrate the fiber bed without clogging or honeycombing. Therefore, glued fibers had to be dissolved and separated from each other before placing them into the molds. The dissolving process by water was time consuming and impractical, and still did not produce completely separated fibers.

In addition, it was necessary to choose fibers with equal, or at least close, aspect ratio values, so the same fiber volume fraction can be applied with the different types. Finally, the decision was taken to work on two different types of steel fibers of individual form that differ only in geometric shape, and have similar dimensions, as shown in Table 3.5. The two types are hooked and crimped fibers (Figure 3.2), which are the most common used types in SIFCON as mentioned previously in Chapter 2. The hooked fibers were produced by BEKSA Çelik Kord Sanayi ve Ticaret A.Ş., which is a branch of the world wide known company Bekaert. The crimped fibers have been manufactured by Polyfibers Elyaf Sanayi ve Dış Ticaret Ltd. Şti.

The hooked fibers and crimped fibers were designated as (F1) and (F2), respectively. The volume fractions of fibers are calculated based on the density of steel fibers which is taken as 7800 kg/m^3 [51].

Table 3.5: Specifications of steel fibers used in the experimental work (as provided by the manufactures)

Fiber brand name	Shape	Length, l (mm)	Diameter, d (mm)	Aspect ratio, l/d	Tensile strength (MPa)
RL 45/50 BN	Hooked	50	1.05	48	1050
S 50	Crimped (waved)	50	1.00	50	1200

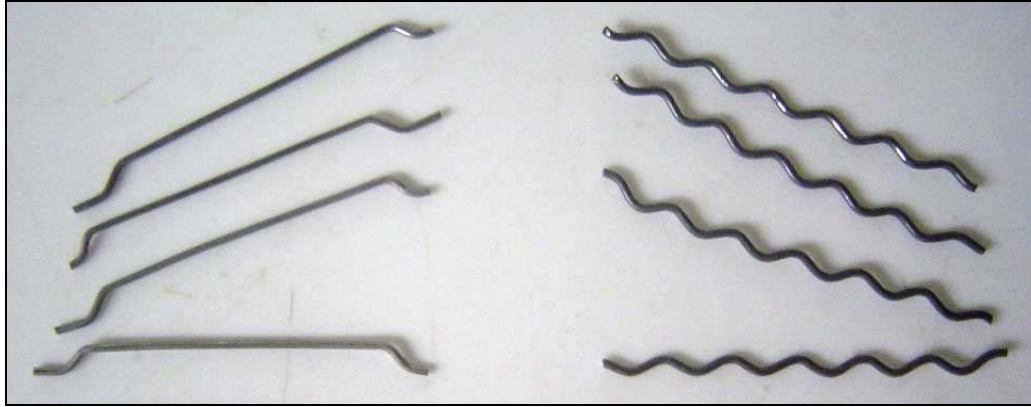


Figure 3.2: Fibers used in the experimental study

3.3 Experimental program

The first step in the experimental study was to prepare some trial mixes to reach final decisions on the details of mix proportions. Types and volume fractions of steel fibers to be used, the dimensions and types of molds, etc were also decided after the trial mixes. In the following, the details of the experimental program will be presented.

3.3.1 Mix proportions

The proportions of the three mixtures by weight are given in Table 3.6. Table 3.7 shows the quantities of constituents as per kg/m^3 . The three mixes represent the two common types of matrices used for SIFCON, slurry or paste (M1) and mortar (M2), in addition to a control mix of conventional plain concrete (M3). The literature review findings, as given in Table 2.1, helped in the design of SIFCON mixes. For the control concrete, it was designed to have good properties especially regarding impermeability and strength. W/C ratio was kept constant in all mixes.

It should be noted that SP was used in mixes (M2) and (M3) only, while it was not necessary to use it in (M1) because of its fluidity thanks to its high water content. SP dosages were chosen to be the minimum possible dosage giving the required workability (fluidity).

Table 3.6: Mixture proportions, by weight

Mix designation	Type	Cement	Water	Sand	Coarse aggregate	SP
M1	Slurry SIFCON	1	0.4	-	-	-
M2	Mortar SIFCON	1	0.4	1	-	0.012
M3	Control concrete	1	0.4	1.53	2.02	0.015

Table 3.7: Mixture proportions per kg/m³

Mix	Cement	Water	Sand	Coarse aggregate	SP
M1	1356.3	542.5	-	-	-
M2	885.1	354.1	885.1	-	10.6
M3	475.0	190.0	725.0	960.0	7.1

Each of the SIFCON mixes was prepared using two types of steel fibers, hooked (F1) and crimped (F2), with three volume fractions for every fiber type, $V_f = 7\%$, 9.5% , and 12% . These fiber contents were selected after many trials on the selected types of fibers, and the different sizes of molds used in the study.

It was found that the minimum practical limit that fills the molds without using vibration is about 7 %. On the other hand, 12 % volume fraction was approved as a maximum practical limit, even with intense vibration. In addition to these two extremes, 9.5 % was taken as an intermediate fiber content which can be achieved with light vibration during fiber placement into the molds.

For every test assigned in the experimental program, several specimens were prepared out of each batch to perform the required tests, according to the necessary number of specimens required for each test as specified in the related standard test methods. For most of the tests conducted in this study, plain slurry (M1) and plain mortar (M2) samples were prepared as well and tested, in addition to SIFCON and concrete specimens.

The above program led to six different batches that were prepared for every SIFCON mix as shown in the following example. Every batch represents a certain combination of mix type, fiber type and fiber content.

Example:

Mix 1 (M1) was composed of the following six batches:

M1F1-7 ^(*)	M1F1-9.5	M1F1-12
M1F2-7	M1F2-9.5	M1F2-12

(*) The batch designation is M1= Slurry, F1= Fiber type1 (hooked), 7= Volume fraction of fiber.

3.3.2 Preparation and casting of test specimens

i) SIFCON specimens

As mentioned previously in Chapter 2, the first step in preparing SIFCON is placing the fibers into the molds, up to the required volume fraction. No vibration was imposed during fiber placing for the specimens with a V_f of 7 % to insure filling the molds without large voids, while a light vibration was applied in the case of V_f of 9.5 %, and the vibration was relatively intense in the case of the maximum V_f (12 %) to ensure filling the mold with the required quality of fibers. The vibration was externally applied using a vibrating table.

The weight of steel fiber to be put in the mold depends on the required volume fraction, the dimensions of the mold, and, of course, on the specific gravity of the steel itself. The following example illustrates how to determine the fiber weight to be placed in the mold on the basis of volume fraction concept according to the required fiber content.

Mold: Cylinder

Dimensions: 68 mm diameter \times 135 mm height

$$\text{Volume of mold} = \pi \left(\frac{68}{2} \right)^2 \times 135 = 490 \text{ mm}^3 = 0.00049 \text{ m}^3$$

Specific gravity of steel fibers = 7.8

\therefore Density of steel fibers material = 7800 kg/m³

$$\begin{aligned} \text{For } V_f \text{ of } 7\% \Rightarrow \text{Weight of fibers in the mold} &= \frac{7}{100} \times 7800 \times 0.00049 \\ &= 0.2675 \text{ kg} \\ &= 267.5 \text{ g} \end{aligned}$$

After being filled with steel fibers up to the required volume fraction, the molds were filled with the slurry or mortar matrix which has to be flowable enough to ensure complete infiltration through the dense beds of fibers in the mold. Usually, vibration during matrix placing was necessary to avoid honeycombing or voids. Figure 2.4, shows the slurry infiltration process that was aided by external vibration by putting the mold on a vibrating table.

The mixing procedures for slurries (pastes) and mortars were in accordance with the requirements of ASTM C 305 [52]. For mortars, SP was added separately and gradually during the last minute of mixing period.

ii) Control concrete

Mixing of control concrete was done in a sequence that allows sufficient time for thorough mixing of all the constituents. The concrete mixture was prepared in about 5 minutes mixing time with a rotating planetary mixer of 150 kg capacity. The utilized mixing procedures were as follows:

- (a) The mixer internal surface was first dampened with water.
- (b) The sand and coarse aggregate were first mixed with 1/3 of mixing water for 1 minute.
- (c) The cement and 1/3 of the mixing water was then added, and mixed for an additional 1 minute.
- (d) Finally, the rest of the water and SP were pre-mixed and added to the mixer and mixed for 3 minutes.

3.4 Experimental tests

The experimental program consisted, first of all, of investigating stress-strain relationships of SIFCON to make sure that the material prepared and used in this study possesses similar engineering trends and properties to SIFCON known in the literature. Afterwards, a series of tests related to durability were

performed on SIFCON specimens, and the results were compared with each other, and with the reference concrete. This set of tests included:

- (a) Drying shrinkage.
- (b) Water absorption.
- (c) Resistance to chloride penetration.
- (d) Resistance to freeze-thaw damage.

The following sections discuss the details of the above mentioned tests. Table 3.8 presents the details of the experimental program. All mortar SIFCON mixes (M2) are made with a sand of 1 mm maximum size. In addition to the mixes shown in Table 3.8, a complete set of mortar SIFCON made with 0.6 mm size sand was tested for only water absorption.

3.4.1 Stress-strain relationships

As mentioned in Chapter 2, SIFCON is characterized generally with its high strength and very high strain capacity. Although stress-strain relationships are related to the mechanical properties of the materials, rather than their durability, the aim was only to ensure that the procedures followed in preparing SIFCON in this investigation would lead to a material with mechanical properties similar to what is known from the literature. Consequently, stress-strain properties of SIFCON in compression were studied.

A complete set of SIFCON and control concrete specimens was prepared for stress-strain test. The specimens were 100×200mm cylinders. Three specimens were made from every batch, thus the total number of tested specimen was 39.

Table 3.8: The mixtures and tests performed in the experimental study

Test	Specimen Designation												M1	M2	M3
	MIF1-7	MIF1-9.5	MIF1-12	MIF2-7	MIF2-9.5	MIF2-12	M2F1-7	M2F1-9.5	M2F1-12	M2F2-7	M2F2-9.5	M2F2-12			
Stress / Strain (cylinders)	✓	✓	✓	✓	✓	✓	✓	✓	✓	✓	✓	✓	-	-	✓
Drying shrinkage (prisms)	✓	✓	✓	✓	✓	✓	✓	✓	✓	✓	✓	✓	✓	✓	✓
Water Absorption (cylinders)	✓	✓	✓	✓	✓	✓	✓	✓	✓	✓	✓	✓	✓	✓	✓
Chloride penetration (slabs)	✓	✓	✓	✓	✓	✓	✓	✓	✓	✓	✓	✓	-	-	✓
Freezing / thawing (prisms)	✓	✓	✓	✓	✓	✓	✓	✓	✓	✓	✓	✓	✓	✓	✓

(✓) prepared and tested

(-) not prepared

The compression specimens were cast in cylindrical plastic molds. After infiltration, as discussed earlier, the specimens were covered with plastic sheets to aid in curing. The specimens were left to cure for 24 hours in the molds in the laboratory environment. The next day the specimens were demolded, labeled, and placed in lime-saturated water for 28 days until testing. Actually this procedure was the same for all the other tests, with the exception of the curing period in some cases. The specimens of chloride

penetration and freeze-thaw tests were cured for 14 days only, in response to the requirements of the related standard test methods.

After the curing period, all of the specimens were tested in uniaxial compression. Prior to testing, the top and bottom surfaces of all specimens were capped with gypsum to ensure true and parallel loading surfaces.

The testing system, Figure 3.3, consisted of a hydraulic universal testing machine connected to a data acquisition system adjusted to take one reading every 0.5 second. During the tests, load and deformation data were recorded and stored by the said system, Figure 3.4.

The deformation of specimens was measured by two linearly variable differential transformers (LVDT's) of 50 mm range placed so as to measure the actual specimen deformation between the upper and lower loading platens, Figure 3.3. The average of the two LVDT readings was considered in strain calculations. Strain was calculated by dividing the average platen displacement by the original specimen length. The load signal was taken directly from a 50 ton capacity load cell.

The load-deformation tests in compression were run at a strain rate ranging from 150 to 250 microstrains per second. For every specimen, the strain rate was almost constant. Figure 3.5 shows a typical relation between time and strain with almost constant strain rate. This rate can be considered as relatively high comparing to some previous studies on SIFCON behavior in compression. For example, strain rates of 100 and 166 microstrains per second were applied in two previous investigations [5, 19].



Figure 3.3: The testing system of stress-strain behavior
LVDT's are shown on two sides of the specimen, while the load cell is located under it

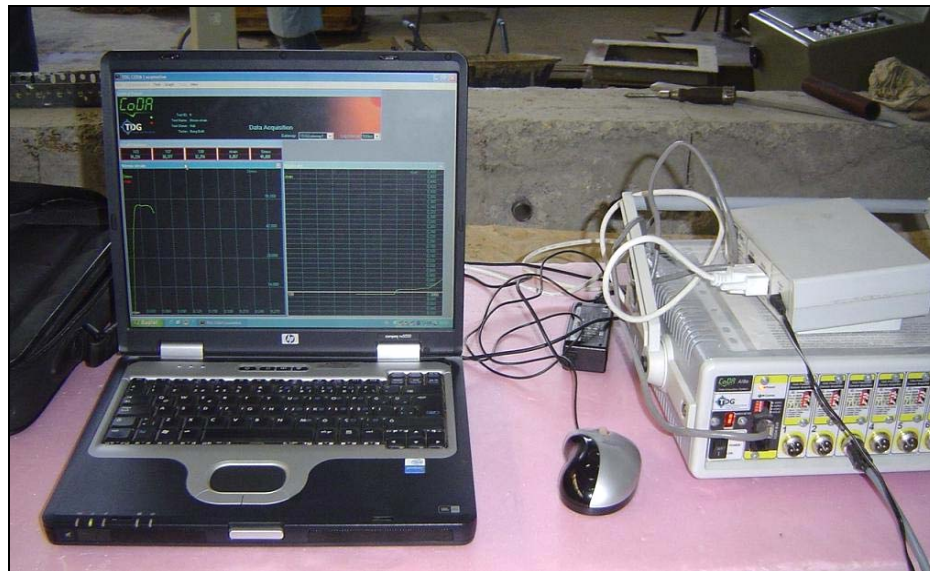


Figure 3.4: The data acquisition system used in compression stress-strain test

There are no specific requirements for strain rate in standard test methods, even for concrete. However, the range of strain rate recorded in the compression test in this study is still practically very small to affect the reliability of the results. It was reported in literature that significant changes in material response (for example, a 10 to 15 % change in compressive strength) occur only for differences in strain rate in the order of 10 times or more as demonstrated by the curve in Figure 3.6 [53].

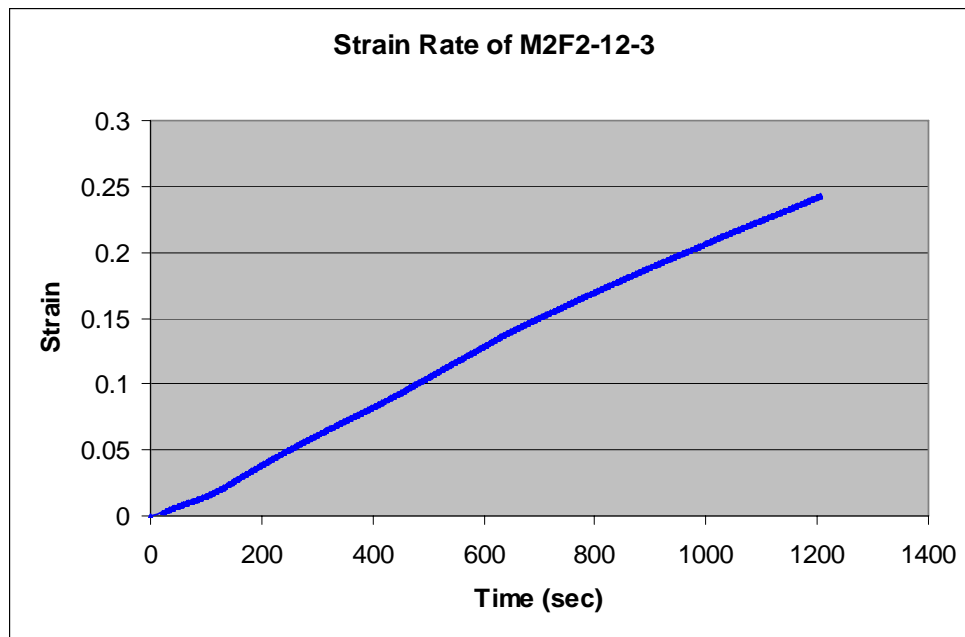


Figure 3.5: Typical plot of strain versus time

The figure shows a constant strain rate of 0.0002 strain/sec during the test

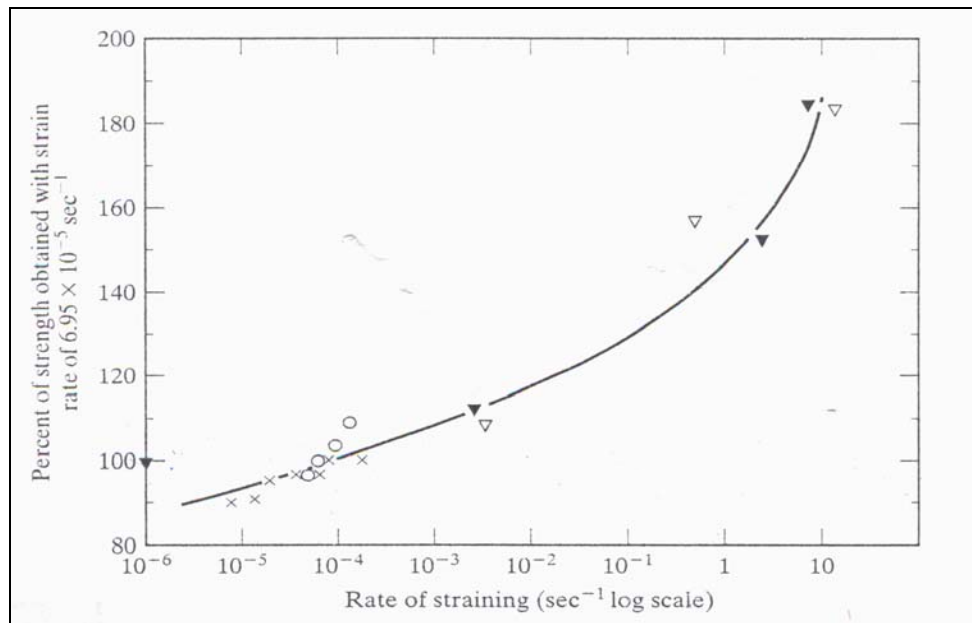


Figure 3.6: Influence of strain rate on the compressive strength of concrete [54]

3.4.2 Drying shrinkage test

In a dry environment, concrete may experience drying shrinkage. Drying shrinkage is essentially a volume change that takes place over time due to moisture loss from concrete. The rate of shrinkage decreases with time. Drying shrinkage is a major concern because excessive shrinkage can affect durability by causing cracking to concrete elements due to structural restraints on the concrete [53, 55].

Drying shrinkage is affected by a wide range of variables including the specimen geometry, mix proportions (mainly cement content, and W/C ratio), the chemical and physical properties of the raw materials, and the environment to which concrete is exposed to, especially temperature and relative humidity. Most of the drying shrinkage takes place in the first few

months. The tests indicate that about 70 % of 20-years shrinkage occurs in 3 months [56].

Measuring drying shrinkage of SIFCON and control specimens (M1, M2 and M3) was made with reference to ASTM C 157 [57]. Three $70 \times 70 \times 280$ mm prisms were used to determine the drying shrinkage, and the average of the three specimens was taken into consideration. After demolding, all of the specimens were cured in lime-saturated water for 28 days, and then sorted in the laboratory environment for the duration of the test at 23 ± 4 °C and 40 ± 5 % relative humidity.

The initial readings of specimens lengths were taken immediately after removing the samples from the curing tank, *i.e.* the moment of starting the duration of drying. This means that the 1-day reading, for example, refers to the length change of the specimen after 1 day of air drying after the 28 days wet curing period, *i.e.* the age of the specimen at that day is 29 days from casting.

The drying shrinkage for every specimen was measured up to $7\frac{1}{2}$ months. The results were recorded at 1, 3, 7, 14, 28, 56, 84, 112, 140, 168, 196 and 224 days of air drying which starts immediately after period of 28 days of wet curing. Figure 3.7 shows the test specimens and the length measurement device used for the determination of drying shrinkage.

The specimens length readings at each test age were compared with the initial length comparator reading to calculate the length change of specimens which was measured in micro-strains. The values shown in Table 3.9 can be used to evaluate shrinkage test results for concrete in general.



Figure 3.7: The drying shrinkage specimens and the length measurement device

Table 3.9: Shrinkage grades for conventional concrete [58]

Shrinkage (Microstrains)	Concrete class
< 400	Good
400 – 600	Moderate
600 – 800	Poor
> 800	Very poor

3.4.3 Water absorption test

The durability of concrete structures is of great concern, especially in aggressive environments. The major durability problems, such as the corrosion of steel reinforcement, damage by freezing and thawing of water in

pores, attack by chlorides and sulphates, were found to be controlled mainly by the penetrability or water permeability of concrete.

Therefore, it can be said that permeability of SIFCON is of an overriding importance with respect to durability concerns. It is believed that the major durability problems would be of no consequence to concrete that is relatively impermeable at the time of exposure to the environment and continues to remain impermeable throughout the expected service life [59]. Naturally, this applies to SIFCON as well.

In view of this, one of the major goals of the experimental program was to evaluate the permeability of SIFCON. It was intended to use testing for permeability as an indicator or measure of SIFCON durability. This was achieved by conducting water absorption test on SIFCON and control specimens in accordance with the requirements of the standard test method ASTM C 642 [60]. This test is an indirect, yet simple for testing permeability.

The specimens used for this test were 68×135 mm cylinders. The specimens were cured in lime-saturated water for 28 days, before conducting the test procedures specified in ASTM C 642. After the curing period, the specimens were dried completely then immersed in tap water. The specimens were weighed every 24 hours to check mass increases due to water absorption, until the difference in mass between the last two measurements was smaller than 0.5 % of the heavier mass which defines the saturation stage. The concrete specimens were found to reach this stage in a period of 48 hours while SIFCON specimens needed generally 3 to 4 days to reach the complete saturation.

For the first two hours, the test was modified to obtain also an immersed rate of absorption. The absorption of the specimens was recorded at fixed intervals of time during this period. These intervals were 2, 4, 9, 16, 25, 36, 49, 64, 81, 100 and 120 minutes after immersion in water. For every reading, the excess surface water was dried off with absorbent towels before weighing. Three specimens were tested for each case and the average result was recorded. This test measures water flow into unsaturated concrete through large pores, which can be considered as a measure of the relative permeability.

3.4.4 Chloride penetration test

The ability of concrete, and SIFCON, to resist the penetration of chloride ions is another critical parameter in defining durability, and determining the service life of steel-reinforced structures exposed to de-icing salts or marine environments. The resistance to chloride penetration is directly related to the material permeability. The deterioration of concrete usually involves movement of aggressive liquids from the surrounding environment into the concrete followed by physical damage and chemical reactions, possibly leading to irreversible damage. Therefore, the transport properties, rather than the mechanical properties, are the important factors for durability.

In view of this, the resistance of SIFCON to chloride penetration has been studied and compared with conventional concrete, to quantify durability characteristics of SIFCON. The steel fibers in SIFCON are very close to the exposed surface with almost no protecting cover if no overlay is used. This makes SIFCON, theoretically, more vulnerable to corrosion caused by chloride penetration than conventional reinforced concrete.

The SIFCON resistance to chloride penetration is investigated by the chloride penetration test which is described in the standard test method AASHTO T 259 [61]. This test is also referred to as the salt ponding test, and it is a long-term test for measuring the penetration of chloride into concrete. AASHTO T 259 reasonably simulates the actual chloride ingress. However, being a long-term test, it is not suitable for use as a quality control test during construction [62].

The specimens used in this test were 80 mm thick and 320×320 mm square slabs. A dam of 20 mm height and 20 mm width was cast as an integral part of the slabs around its perimeter to form a basin for the chloride solution. Figure 3.8 shows one of the plastic molds prepared especially for casting the slabs used in this test. The inner plate was used to form the required dam on four sides of the slab.

In accordance to AASHTO T 259 requirements, the slabs were moist cured for 14 days, then dried in laboratory environment at about 50 % relative humidity. After the drying period, a 3 % NaCl solution prepared with distilled water was ponded on the top surface for 90 days. The ponding surface area was 280×280 mm square. The other surfaces were left exposed to the drying environment including the lower surface which being put on steel bars during the test duration. Figure 3.9 schematically illustrates the test setup.

During the 90 days period, additional solution was added whenever necessary to maintain the 13 mm depth. The decrease in solution depth is a result of infiltration into the samples or evaporation. After the end of NaCl solution ponding time, the solution was removed from the slabs. Then, the slabs were allowed to dry and they were cleaned carefully from the salt crystals and corrosion products formed on the surface.



Figure 3.8: A mold for chloride penetration test specimens

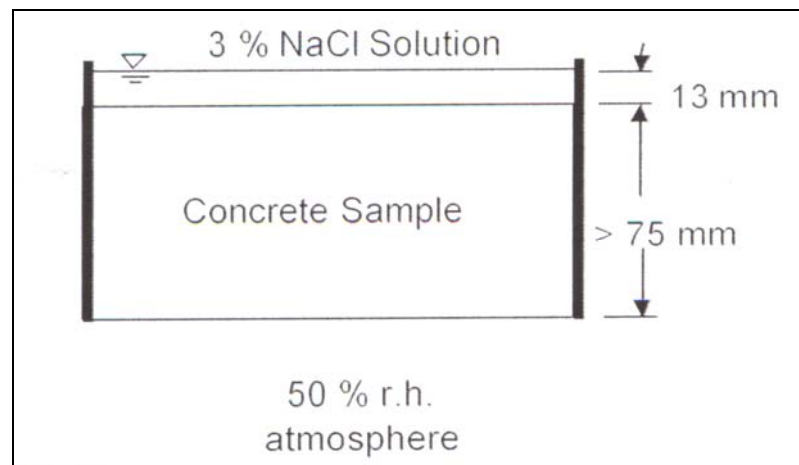


Figure 3.9: AASHTO T 259 test setup

Dust samples for chloride ion chemical analysis were taken from each slab using 12 mm pulverizing drilling bit in three specified locations in the surface subjected to NaCl solution ponding. From each one of the three points the dust samples were collected carefully from five different depths. The three samples corresponding to each depth were mixed up together to form one

representative sample. Table 3.9 shows the details of sample depths taken from each one of the three specified locations.

Table 3.10: Depths of dust samples collected for chloride analysis

Sample no.	1	2	3	4	5
Depth (mm)	0-15	15-30	30-45	45-60	60-75

The dust samples were sent in labeled sealed plastic bags to chemical analysis to find the chloride concentrations in the samples with respect to their total weight. The chemical analysis was performed in accordance with the directions of the standard test method AASHTO T 260 [63]. Figures 3.10 and 3.11 show the sampling procedures.

The average chloride concentration at each 15 mm depth is then determined. The net percent chloride by weight is obtained by subtracting the initial chloride content from the chloride content of the ponded specimen. Plain unponded samples were used to determine the initial chloride contents of the mixes. The results were used to construct chloride ingress profiles for all the specimens. Diffusion coefficients (D_a) were also found.



Figure 3.10: Setup of extracting dust samples of chloride penetration test

The extraction locations are marked with circles



Figure 3.11: Collecting dust samples in sealed bags for chloride chemical analysis

3.4.5 Freeze-thaw resistance test

One of the major factors affecting concrete durability is the ability of concrete to resist frost damage. Again, this property depends mainly on the material permeability. The basic mechanism of frost damage is well known. The formation of ice crystals can create pressure on the pore walls, and also a flow of water out of the pores through the paste to the nearest air void. In addition, unfrozen water is attached to the ice crystals during freezing. This cause the slow growth of the crystals, which in turn increases the internal stresses developed and leads to internal cracks and surface scaling [64]. Figure 3.12 is an example showing the effects of freezing and thawing on concrete.



Figure 3.12: A typical example of deterioration in concrete due to freezing and thawing

In addition to architectural damage, severe scaling can lead to progressive structural deterioration

Investigating the freeze-thaw resistance of SIFCON was a major part of the experimental study. The frost resistance of concrete is generally determined by subjecting specimens prepared in the laboratory to a number of cycles of freezing and thawing in water, or freezing in air and thawing in water, in temperature range from + 4 °C to – 18 °C.

In order to obtain results in a relatively short period, the specimens are generally subjected to five cycles or more per day; since, as in the ASTM C 666 standard procedure, the number of cycles is often fixed at 300 [65].

The outlines of the test method ASTM C 666 were adopted in studying the property of SIFCON resistance to freeze-thaw damage. Some changes in the details of the method were unavoidable for practical reasons. The changes were mainly in the temperature range and duration of cycles. The modification made on the ASTM C 666 standard procedures would not, anyway, affect the aim of the investigation, which was evaluating different SIFCON mixes, and comparing them with the control concrete, as long as all the specimens were being tested under the same conditions of temperature range, cycles duration, etc...

The specimens used in the test were 75 × 75 × 280 mm prisms of different SIFCON samples, and plain control mixes. Intentionally, no air-entraining admixtures were used in the mixes. The purpose was to investigate the behavior of SIFCON in the absence of air-entraining, and to accelerate the deterioration.

The durability of concrete involves resistance to frost, corrosion, penetration, carbonation, chemical attack and so on. Generally, properties of concrete have been well understood under the separate action of these deterioration mechanisms. However, the degradation of concrete is usually the result of

combined action of mechanical stress, physical and chemical attack. For example, in practice, de-icing process used for snow and ice removal in the cold regions of the world includes the effect of chloride salt attack in addition to freeze-thaw cycles in the same time.

Furthermore, deterioration can be accelerated by the combined action of several deterioration mechanisms. The conclusions obtained from separate tests are not always correct, and can have insufficient reliability. Test results found by some researchers showed that concrete tested for freeze-thaw cycles in chloride salt solution scaled much more severely than in fresh water [66-68].

The reason of why chloride solution is more harmful to concrete than fresh water is attributed mainly to osmotic and crystallization pressures that evolve when ice starts forming in the pores, and, less importantly, to the phenomena of temperature shock and displacement of the freezing front [69]. The important fact remains that the damage to concrete is greatly increased in the presence of de-icing salts.

Therefore, it is found necessary to study properties of SIFCON by subjecting it to the combined action of freeze-thaw cycles and chloride attack. The study aimed also to investigate the possible corrosion that may happen to steel fibers because of the chloride penetration. Accordingly, all freeze-thaw cycles were performed using a 3.5 % sodium chloride solution (NaCl), a concentration proven to be the most destructive comparing to weaker or stronger solutions [68]. Sodium chloride was chosen because it is one of the most widely used chemical de-icers. The test solution was prepared by completely dissolving 3.5 % mass of extra pure sodium chloride salt in 97 % mass of distilled water.

Specimens were kept in the NaCl solution for the whole duration of freezing and thawing cycles. The specimens were laid in one layer with enough spacing between them in wide open steel containers to ensure that they are completely surrounded by the solution except for the top surface which left exposed to air in order to provide the conditions necessary for corrosion to occur. Figure 3.13 shows the specimens in the climate chamber.

The exposed surfaces were changed at every 50 cycles to accelerate the degradation, and the containers were fed with solution whenever necessary to maintain its level. The range of temperature of cycles was selected to be -10 °C to 50 °C. This wide range (60 °C) is adopted intentionally to simulate the climatic conditions of Turkey where the average difference between the lowest and highest temperature throughout the year is about 60 °C according to a survey of recorded temperatures in large number of cities around the country in the period 1975 – 2005 [70].

In addition, it was assumed that this wide range of temperature applied in every single cycle could accelerate the deterioration. Anyway, this change in ASTM C 666 requirements will not affect the possibility of evaluating the behavior of SIFCON under freeze-thaw cycles due to the fact that all the specimens, including the control concrete, are being subjected to the same test conditions.

After a high number of trials made on the climate chamber to establish the most suitable duration of the freezing and thawing cycles it was decided that every cycle will be consisting of alternately setting the room temperature at -10 °C for about 6 hours (freezing period), followed by setting the temperature at 50 °C for about 3 hours (thawing period). Therefore, the duration of every cycle was approximately 9 hours. Table 3.11 shows the durations of a typical cycle.



Figure 3.13: Specimens subjected to freezing-thawing cycles in the climate chamber

The temperatures at the centers of the specimens have been checked regularly using thermocouples. It was found that the specimen temperature is around $-6\text{ }^{\circ}\text{C}$ at the end of freezing period and increases to approximately $16\text{ }^{\circ}\text{C}$ at the end of thawing period.

The cycles of climate room temperatures in a typical test day are shown in Figure 3.14. The climate room used in this test was automatically operated, and furnished with a control panel to monitor the variations in temperature and relative humidity and to make any necessary changes, Figure 3.15. The room was relatively big in size with internal volume of 15.4 m^3 , which can explain the relatively long time needed to reach the assigned temperatures.

Table 3.11: The details of a typical freezing/thawing cycle

Period	Setting temperature (°C)	Time to reach the required temperature (min)	Stoppage time (min)	Total period time (min)
Cooling from 50°C to -10°C	-10	339	30	369
Heating from -10°C to 50°C	50	162	30	192
Total cycle time (min)				561 (9hr 21min)

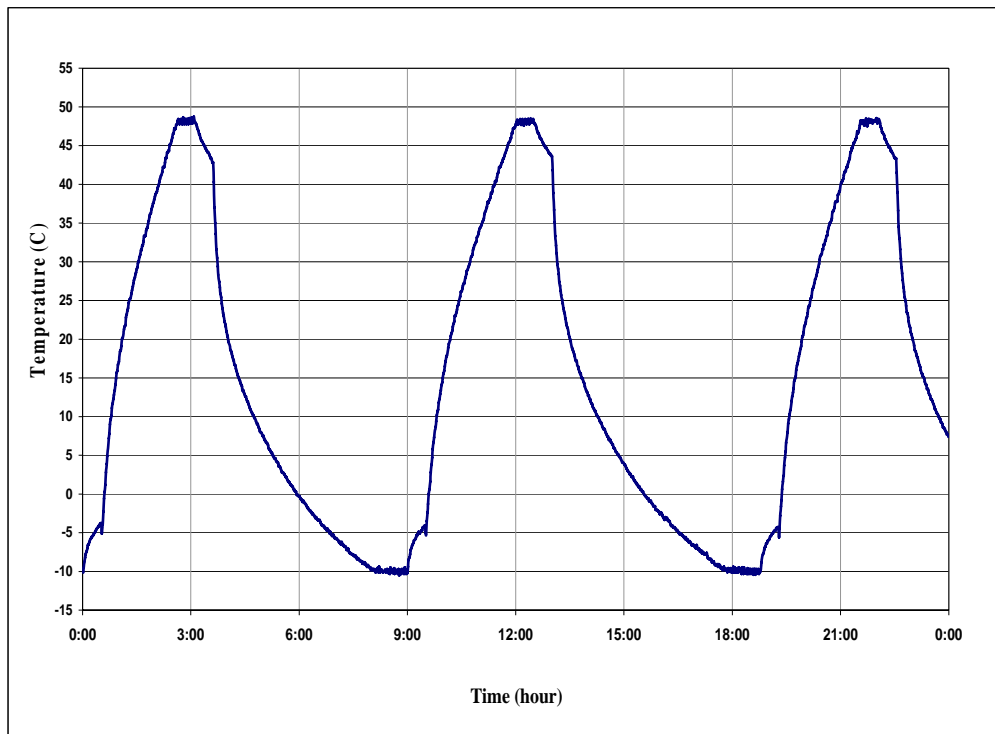


Figure 3.14: Freezing and thawing cycles in a typical day



Figure 3.15: The climate room used for freeze-thaw test and its control panel

The total number of cycles performed was 300. Before starting the test, initial readings of weight and ultrasonic pulse velocity (UPV) were taken for the specimens. The (UPV) measurement is described in ASTM C 597 [71]. The testing system consists of a pulser/receiver unit with a built-in data acquisition system and a pair of 50 KHz transducers, Figure 3.16.

UPV measurements were conducted by pressing the transducers firmly on the opposite ends of the specimens using petroleum jelly between the transducer and the specimen surface. UPV computation requires the acquisition of the pulse arrival time and specimen length. Pulse arrival time describes the elapsed time between the time of pulse application and arrival in the opposite face of the specimen. UPV was calculated by dividing the specimen length by the elapsed time of pulse travel. UPV measurements are usually affected by the internal structure of the concrete.

At intervals of 100 cycles, the specimens were again weighed and tested for UPV. All the readings were taken in a saturated surface dry condition (SSD).

The deterioration was evaluated by the weight loss that happens due to scaling, and the drop in the relative dynamic modulus of elasticity (RDME) calculated using UPV results. In addition, visual inspection and photographic documentation in different stages of the test were taken into consideration in investigating SIFCON resistance to rapid freezing and thawing.



Figure 3.16: UPV testing of freeze-thaw specimens

CHAPTER 4

TEST RESULTS AND DISCUSSIONS

The following tests were carried out within the scope of this thesis.

- a) Stress-strain behavior in compression.
- b) Drying shrinkage.
- c) Water absorption.
- d) Chloride penetration.
- e) Freezing and thawing.

In the following, the results of these tests are presented and discussed.

4.1 Stress-strain properties

As mentioned in Chapter 3, the properties of SIFCON specimens were tested under uniaxial, unconfined compression to demonstrate that SIFCON specimens prepared for durability tests in this study had generally similar behavior to that reported in the literature. Therefore, although the mechanical properties are not related directly to durability, conducting this test was the initial stage in the study.

Actually, investigating stress-strain relationships of SIFCON in this study had advantages over previous researches for providing clearer information on the effects of related parameters (mix type, fiber content, and fiber type) by concentrating on only one parameter in every investigation, while keeping the other parameters constant.

The details of conducting the test have been presented earlier in Section 3.4.1, while an example on part of the test raw data is shown in Appendix A (Table A.1). The results of the test will be presented and discussed based on toughness results. All the figures of stress-strain relationships are shown in Appendix A. Three specimens were tested from every SIFCON mix. Figure 4.1 shows typical stress-strain relationships of some SIFCON specimens along with the results of the reference concrete (M3).

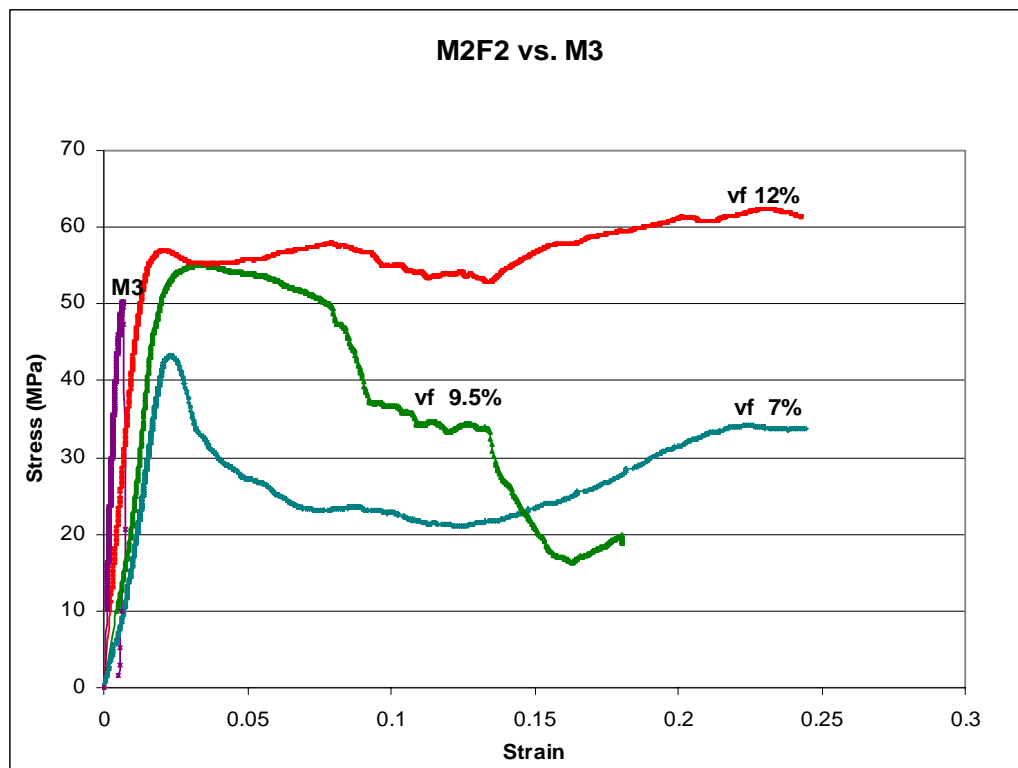


Figure 4.1: Typical stress-strain behavior of SIFCON
The results represent selected specimens of mortar SIFCON and control concrete

The toughness of every specimen was calculated. Toughness describes energy absorption which is given by the area below stress-strain curve. In practice, toughness is calculated based on the area up to a prescribed strain [72, 74].

The summary of the results of peak strength values and toughness calculations are presented in Table 4.1. The results represent the average of three specimens.

As mentioned above, the toughness is measured by the whole area under the stress-strain which shows the maximum amount of energy a unit volume of the material of SIFCON can absorb without failure. The toughness was measured for all SIFCON specimens up to 0.15 strains. All specimens experienced strains higher than this value. For control concrete, it is measured up to peak stress. In addition, toughness indices were measured as SIFCON toughness divided by concrete toughness. The index used to express toughness of SIFCON with respect to control concrete toughness.

The irregularly shaped areas under stress-strain curves were determined by using Simpson's rule in Microsoft Excel. An example of toughness calculations is given in Appendix A (Table A.2). In addition, complete toughness-strain relationships are presented in the Appendix A, along with stress-strain relations that are not presented in this chapter.

4.1.1 Effects of fiber content on stress-strain relationship

4.1.1.1 Slurry SIFCON

Figure 4.2 shows toughness values of slurry SIFCON specimens prepared with different steel fiber contents (7 %, 9.5 %, and 12 %). The figure includes also the results of control concrete (M3) for comparison.

Figure 4.2 shows also that slurry SIFCON specimens made with F1 and F2 demonstrate the general trends known about SIFCON in the literature. The followings can be observed in Figure 4.2 in addition to Figures A.1 to A.12 in Appendix A.

Table 4.1: Summary of peak strength and toughness results

Matrix type	Matrix ID	Peak compressive strength (MPa)	Toughness (KJ/m ³)	Toughness index
Control Concrete	M3	47.68 (3.3) ^(*)	205 (14.4)	1
Slurry SIFCON (Hooked fibers)	M1F1-7	36.30 (1.8)	1777 (36.8)	8.7
	M1F1-9.5	39.97 (5.0)	3677 (33.9)	17.9
	M1F1-12	53.52 (6.7)	5484 (39.0)	26.7
Slurry SIFCON (Crimped fibers)	M1F2-7	36.67 (2.5)	2903 (17.8)	14.1
	M1F2-9.5	39.50 (4.9)	4035 (11.4)	19.6
	M1F2-12	42.86 (2.3)	5048 (25.0)	24.6
Mortar SIFCON (Hooked fibers)	M2F1-7	45.12 (2.5)	2472 (14.3)	12.0
	M2F1-9.5	51.32 (2.1)	4398 (19.0)	12.4
	M2F1-12	56.93 (1.6)	6257 (23.9)	30.5
Mortar SIFCON (Crimped fibers)	M2F2-7	43.52 (1.1)	3500 (37.4)	17.0
	M2F2-9.5	55.10 ^(**)	6102	29.7
	M2F2-12	59.53 (3.9)	7076 (28.2)	34.5

^(*) Numbers in parentheses represent the coefficient of variation (%)

^(**) The results of only one specimen are available

(a) All specimens showed very high compression toughness (9 to 27 times greater than the toughness of normal concrete).

(b) All specimens showed very high strain capacity (ductility) of more than 0.2. In the literature, the maximum strains presented ranged from 0.1 to 0.14 [1, 5]. In this study, strains up to 0.245 have been reached in some specimens with still-increasing strength. It is most probable that the

recorded strain capacities could have been higher if LVDTs with ranges higher than 50 mm were used.

- (c) SIFCON made with 12 % V_f of hooked fibers showed relatively high strength (about 54 MPa). High strength also is one of the characteristics of SIFCON in general [1, 5, 7].
- (d) All specimens show that modulus of elasticity is slightly lower than that of plain concrete. Same finding was reported in several references [5, 14].
- (e) Figure 4.3 shows the failure mode of a SIFCON cylinder specimen with length-to-diameter ratio l/d of 2, tested under compression. It also shows how large is the deformation. It may be easily observed that failure occurs through the formation of a large diagonal shear crack, which is one of the characteristics of SIFCON [5]. The development of this shear crack was consistent. It occurred in almost every specimen. The shear crack usually developed near the end of the specimens in most of the cases.

Previous investigations made on specimens with l/d ratio higher than 2 showed also the development of major shear cracks. However, those cracks did not initiate near an end face [5]. This means that shear cracking represents the true failure mode of SIFCON, and it didn't develop as a result of the confining effects of the machine platens. In other words, shear failure did not happen because the restraining effects of platens and it can be considered as a property of SIFCON.

- (f) By examining the shape of the stress-strain curves shown in Appendix A, some regions may be identified:

Ascending Branch: This portion of the curve is very similar to that of conventional fiber reinforced concrete. It is initially linear with gradual

loss of linearity as the maximum load approaches and major cracks develop.

Descending Branch: After the peak load, the stress drops down gradually as a shearing crack develops.

Plateau: As the test progresses, the two specimen halves slide across one another along the shear crack. This results in an almost horizontal stress plateau.

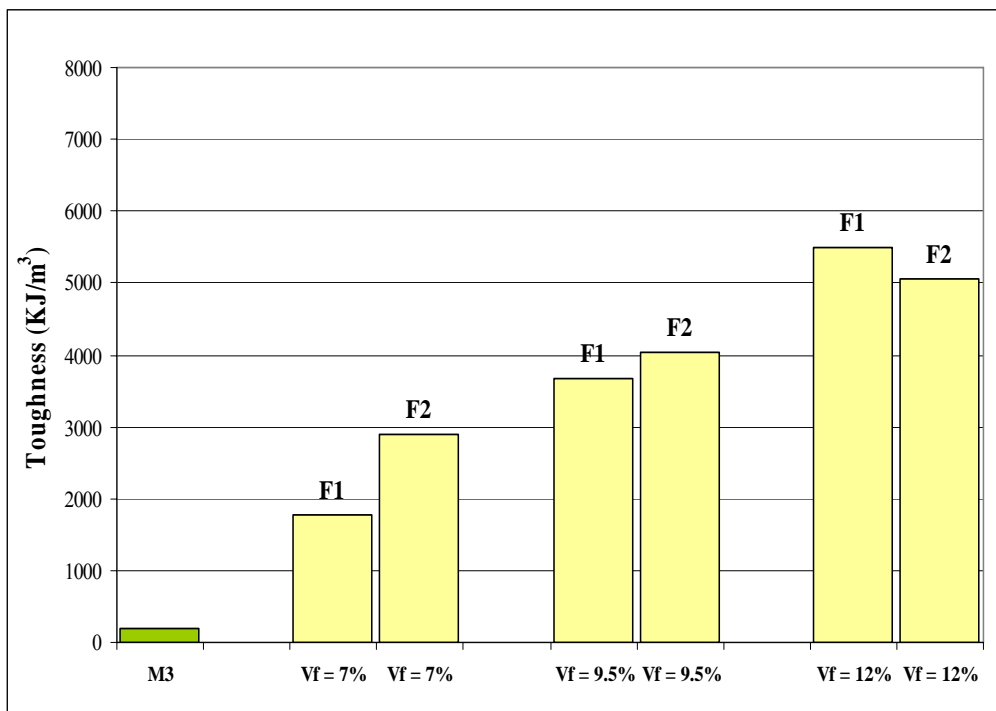


Figure 4.2: Toughness of slurry SIFCON vs. reference concrete (M3)



Figure 4.3: Shear Failure and high deformation in a tested SIFCON specimen

The above findings were also mentioned by other researchers [1, 5, 8]. In addition to these observations, the following points can be mentioned starting with additional regions in the stress-strain curve. The above mentioned parts of the stress-strain curves of SIFCON can be seen in the results of other studies as well [1, 5]. In this investigation, the strain values reached when the test was stopped were higher than those reported in the literature. This enabled to observe two additional trends or stages on the curves:

- (a) Sometimes a sudden drop in stress occurs. This is apparently because of the failure in the slurry itself until the steel fibers in the two specimen halves come in contact and the specimen start resisting the load again.

- (b) In almost all tests, the stress keeps decreasing until it reaches its minimal value during the test. Then, the sample starts to carry further loads gradually once again until it reaches a second peak. It is believed that this

phenomenon is a result of the fact that at some stage in the test, most of the slurry between the steel fibers will be crushed under the load, and the steel fibers in the failure plane become more closer to each other. The specimen, then, shows a new strength gain due to the interaction and friction between the fibers that become in direct contact with each other. In short, the strength gain is not attributed only to fiber-to-matrix bonding but also to fiber-to-fiber interlock and friction. This trend is seen clearly in all SIFCON specimens. Figure 4.4 shows different SIFCON specimens in different stages of the test.

- (c) It is clear from Table 4.1 and Figure 4.2 that the higher fiber content the higher the strength and absorbed energy (toughness). In general, in normal concrete there is a rapid propagation of microcracks under applied stress. On the other hand, the steel fibers included in SIFCON, would obstruct the propagation of microcracks, therefore increasing the strength of the material. Concerning toughness, plain concrete fails suddenly once the ultimate strength is exceeded. On the other hand, SIFCON continues to sustain loads even at deflections (strains) considerably in excess of the fracture deflection of the plain concrete.

Examination of fractured SIFCON specimens, Figure 4.4, shows that failure takes place primarily due to fiber pull-out or debonding, not fiber breaking. Thus, unlike plain concrete, SIFCON specimens do not break immediately after initiation of the first crack. This has the effect of increasing the work of fracture, which is referred to as toughness. Actually, after the first crack, the matrix itself does not resist any stress and the fibers carry the entire load taken by the SIFCON composite. The above findings, which agree with previous researches [1, 5, 7], were found also in the other SIFCON groups of specimens. Therefore, the results of the rest of specimens will be presented briefly in the following sections.



(a) Surface scaling starts after reaching the peak load



(b) Formation of diagonal shear crack



(c) The specimen shows high deformations but still resist the loading

Figure 4.4: SIFCON in different stages of stress-strain test

4.1.1.2 Mortar SIFCON

Figure 4.5 represents the toughness of mortar SIFCON made with hooked fibers (F1) and crimped fibers (F2).

Again, similar features to those already observed in slurry SIFCON, Figure 4.2, were obtained. The following remarks can be stated in short about mortar SIFCON mixes, Figure 4.5 and Figures A.13 to A.26 in Appendix A.

- (a) Similar characteristics of high ductility and toughness compared to plain concrete (M3) can be seen. Mortar SIFCON experienced toughness of 12 to 35 times higher than that of control concrete, depending on steel fiber content and type.
- (b) Sometimes, stress-strain relationships show some overlapping between the curves representing SIFCON specimens made with different fiber volume fractions. Indeed, this overlapping sometimes seems to be inevitable because of the difficulty to ensure the complete homogeneity of fiber distribution in the matrix practically. However, this observation was limited, and did not affect the general trends and the validity of findings.
- (c) The positive effect of increasing the fiber content on toughness and strength is clear here as well.
- (d) Similar to slurry SIFCON, the modulus of elasticity (E) of mortar SIFCON is smaller than that of plain concrete. In general, the higher the V_f the higher the value of E . A typical representation of this phenomenon can be found in Figure 4.1.

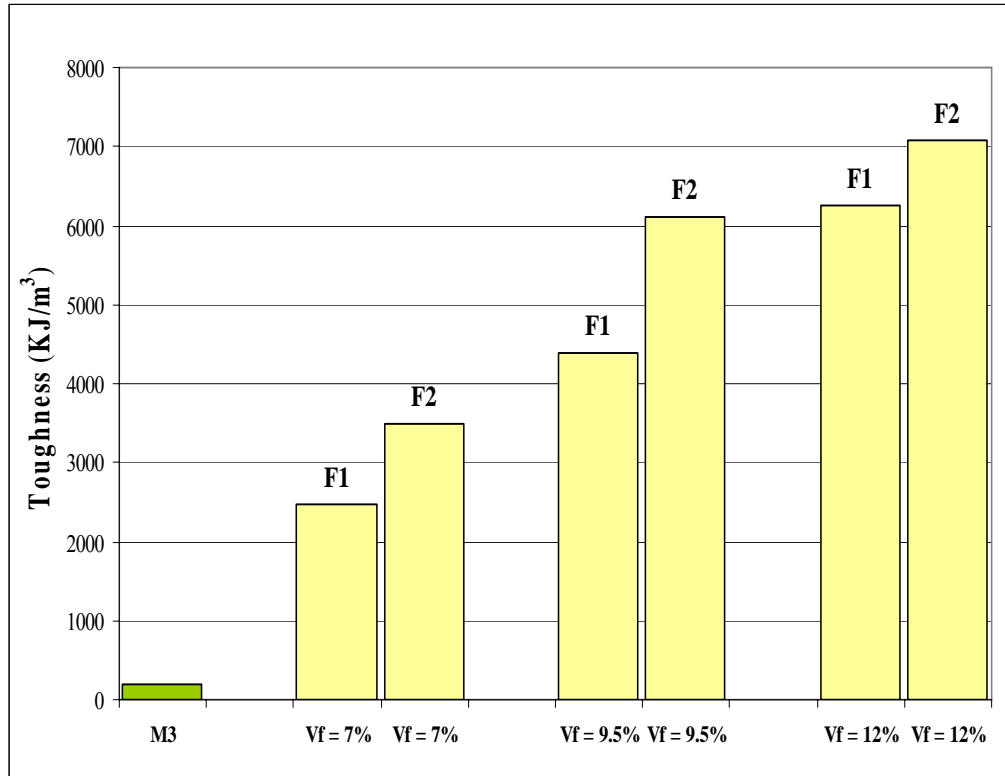
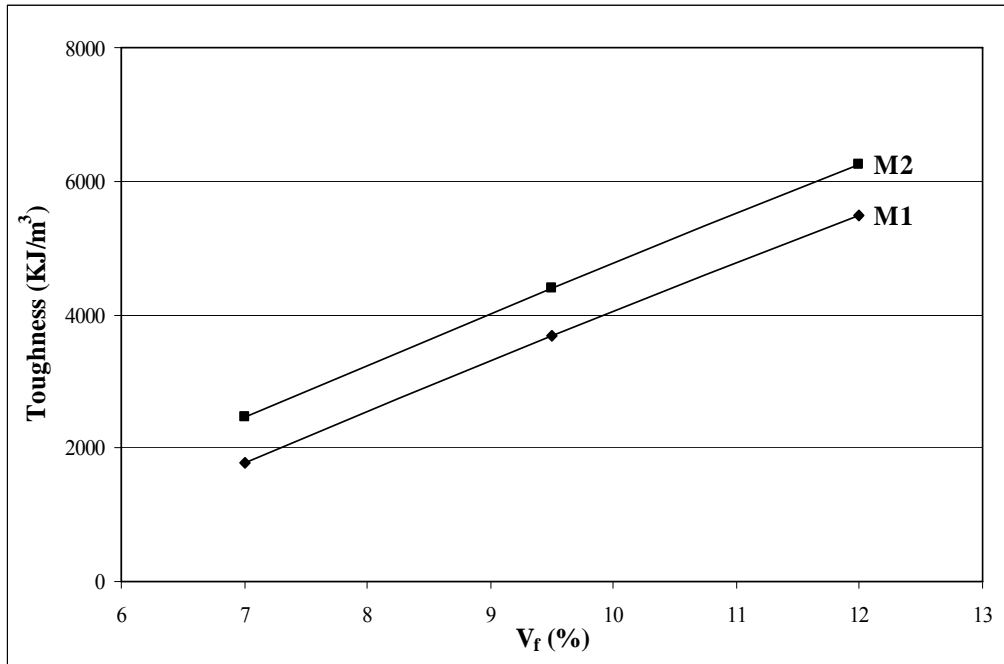


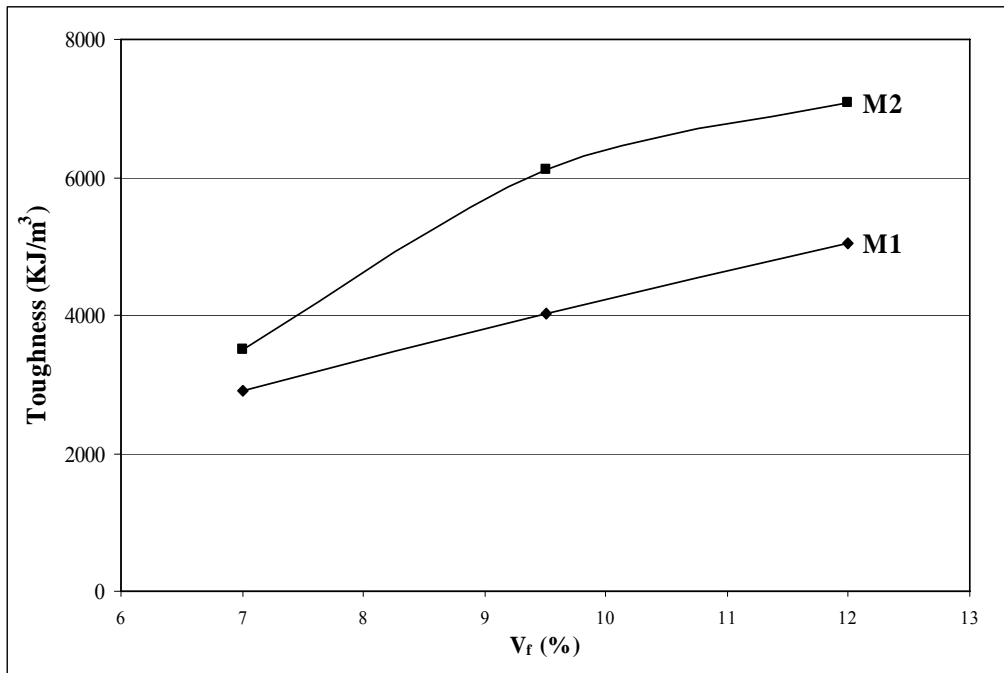
Figure 4.5: Toughness of mortar SIFCON vs. reference concrete (M3)

4.1.2 Effect of matrix type on stress-strain relationship

Figure 4.6 show the effect of SIFCON matrix type on toughness. The already-expected trends were recorded. Generally, including fine sand in SIFCON mixes will enhance the properties related to both strength and toughness compared to mixes made with cement only. This behavior can be attributed to the improvement in matrix phase, which also improves the volume stability and the bond strength between the fibers and matrix. The finding of the positive effect of the addition of sand on strength with a 1:1 ratio of sand to cement was reported also in a previous study [6]. Both mix types, M1 and M2, showed high ductility.



(a) SIFCON with hooked fibers



(b) SIFCON with crimped fibers

Figure 4.6: Effect of SIFCON mix type on toughness

4.1.3 Effect of fiber type on stress-strain relationship

The influence of steel fiber geometry on mechanical properties was also studied. The results of toughness are summarized in Figure 4.7. Figure 4.7(a) shows the effects of using the hooked and crimped fibers on slurry SIFCON specimens, while Figure 4.7(b) represents the effects of these steel fibers on mortar SIFCON.

The following observations can be mentioned:

Toughness: In most of the cases, SIFCON specimens made with crimped fibers showed higher toughness than that prepared with hooked fibers. This leads to the impression that the waved shape of crimped fibers results in a more fiber-to-fiber interlock and hence higher slip resistance.

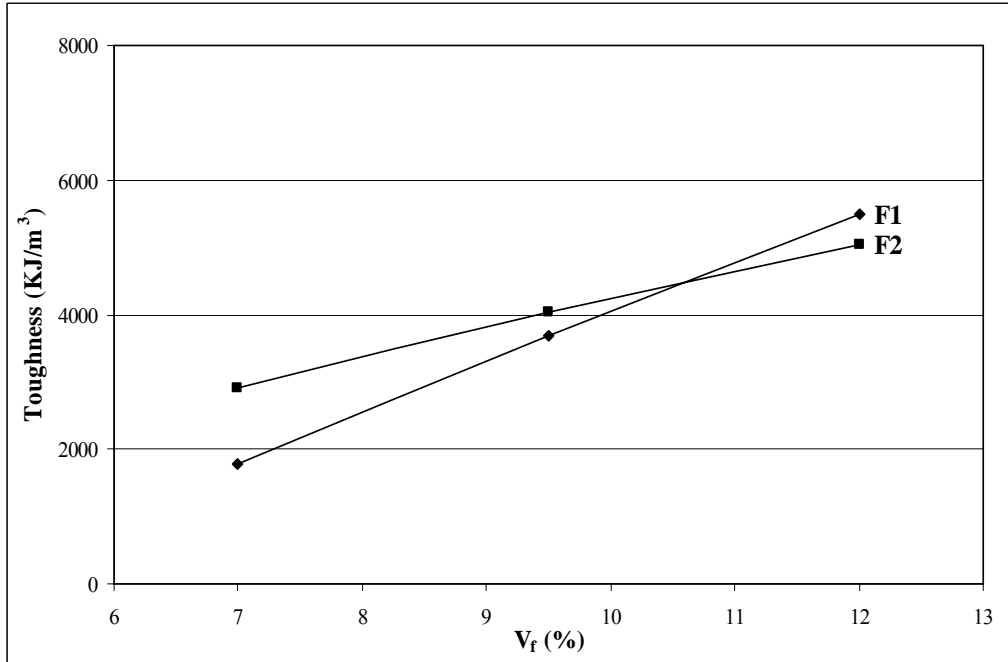
Compressive strength: The two fibers lead to almost the same peak strengths.

Ductility: Both hooked and crimped fibers lead to a very high strain capacity.

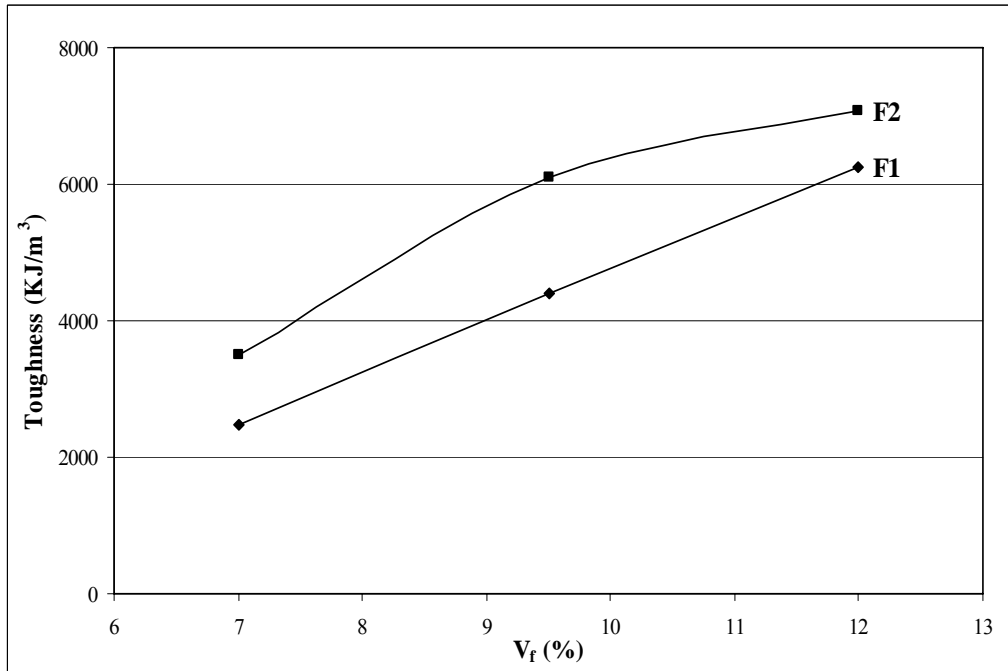
4.1.4 Summary of stress-strain tests

Comparing the results of this test with some related previous researches [1, 5-7] leads to the following points:

(a) SIFCON specimens made in this test have shown the same general characteristics reported about SIFCON in the literature which is the very high strain capacity and compression toughness when compared with the plain control concrete. Toughness indices ranged from 8.7 to 34.5 depending on SIFCON parameters, i.e. matrix type, fiber content, and fiber type. High toughness indices of SIFCON were reported also in some previous researches [1, 5].



(a) Slurry SIFCON



(b) Mortar SIFCON

Figure 4.7: Effect of fiber type on toughness of SIFCON

The findings of toughness investigation lead also to the following notes, which are valid in most of the cases:

- The toughness is directly proportional to fiber volume fraction (Figures 4.2 and 4.3).
- Mortar SIFCON showed higher toughness in all cases (Figure 4.6).
- Crimped fibers seemed to be more effective in increasing toughness due to their shape (Figure 4.7).

(b) The levels reached in peak compressive strength were not as high as the values reported generally in the literature. The main reasons for that can be summarized in:

- The reinforcing index $V_f \cdot l/d$ used in this thesis ranged from 350 in the case of 7 % V_f to 600 for 12 % V_f . The references that reported strengths higher than 80 MPa used reinforcing indices higher than 700. There is a direct relationship between the reinforcing index and the resulted peak strength.
- Higher strengths were achieved in the literature because of using W/C ratio lower than 0.4.
- The alignment of fibers was mainly vertical, Figure 4.8, *i.e.* parallel to loading axis.
- The specimens in this study were all molded, not cored. It is known that the edge effect plays an important role in strength results. As mentioned in Chapter 2, the fiber density at the edges of the molded specimens can be much lower than the interior.
- All the previous researches dealt only with the maximum possible V_f which is 12 % in the case of this study. So, it is logical to get lower strengths when fiber contents less than the maximum possible content are used.

However, even the SIFCON made with the mix proportions of this study, Table 3.6, showed relatively high compressive strengths which exceeded 50 MPa when V_f was 12 %. The highest strength recorded in the study was 62.4 MPa. The investigation, at the end, proved that SIFCON designed in this experimental program, mainly for durability testing, possess all the general features known about this composite.

Furthermore, the investigations made on the mechanical properties of SIFCON in this study provided clear comparisons between the parameters of mix type, fiber content and geometry. Such clear comparisons could not be found in the literature because of the simultaneous effects of several parameters. In this study, only one parameter was examined while keeping all the other parameters constant.

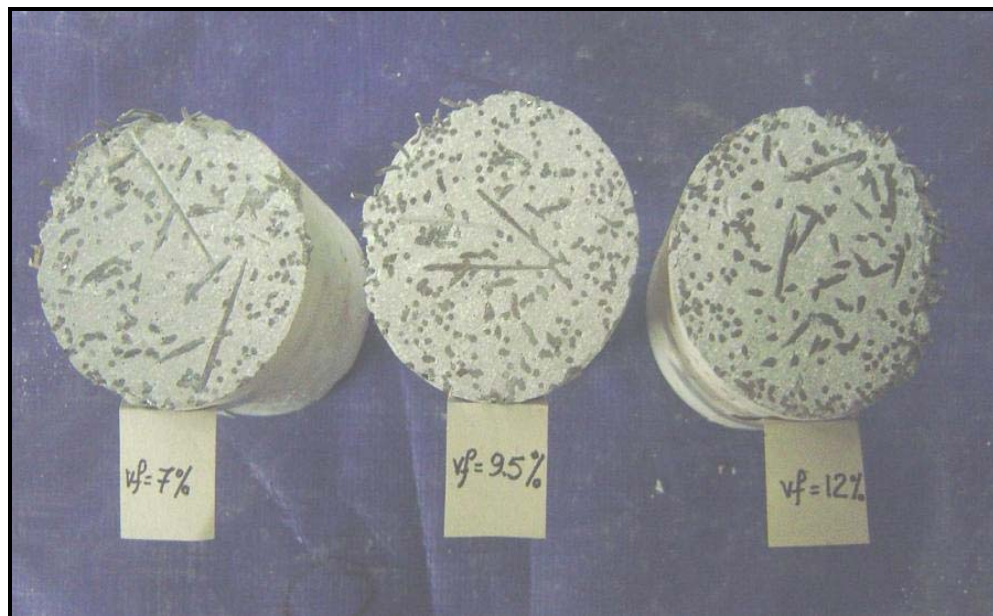


Figure 4.8: Cross sections in SIFCON specimens
The alignment of fibers is mainly vertical, parallel to the loading axis

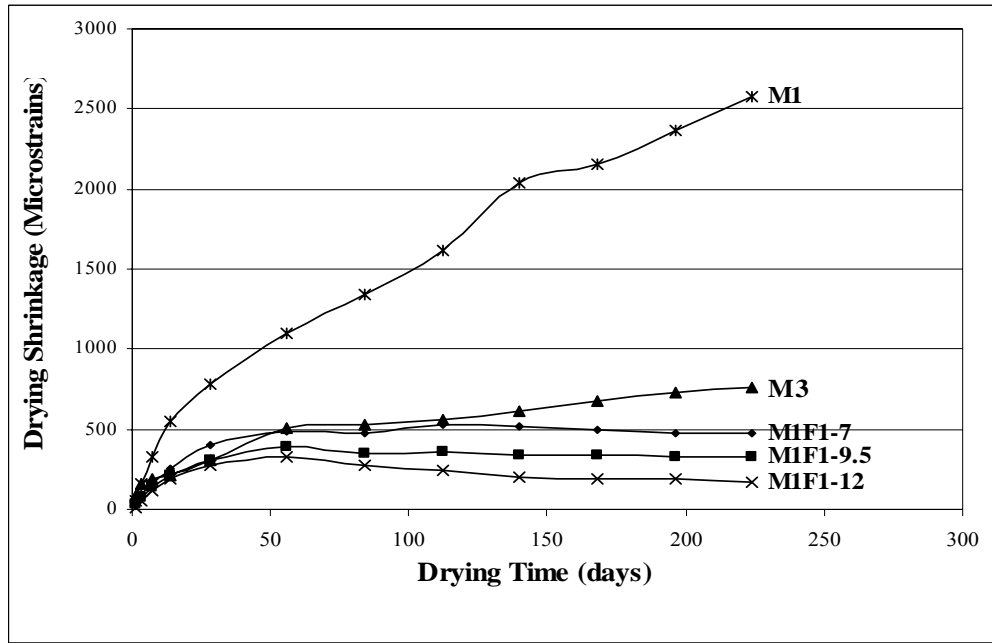
4.2 Drying shrinkage test

As mentioned in Chapter 3, drying shrinkage test of SIFCON and control concrete was conducted in accordance to ASTM C 157 [57]. The length change measurements of the prismatic specimens were taken up to 224 days of air drying. The details of the results are presented and discussed below.

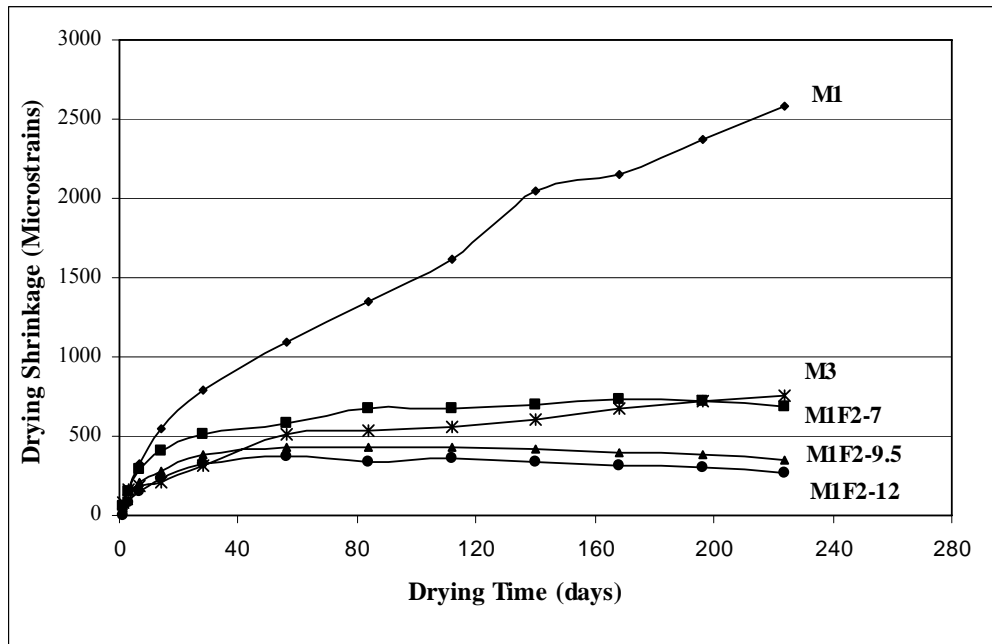
4.2.1 SIFCON vs. plain mixes

The unreinforced slurry (M1) has exhibited a continuously increasing large drying shrinkage over the 224 days of drying period. As can be seen from Figure 4.9, plain slurry (M1) exhibited high shrinkage strains that exceeded 2500 microstrains (0.25 %) in 224 days. On the other hand, slurry SIFCON prepared with 7 % to 12 % hooked fiber volume fraction exhibits low shrinkage strains ranging from 165 to 480 micro-strains (only 6 to 19 % of the shrinkage of the plain mix M1 depending on fiber content). Specimens with crimped fibers, as well, exhibited low drying shrinkage.

Similar findings were presented in the only available study dealt with drying shrinkage of SIFCON [1]. In that study, SIFCON made with fiber volume of 5 % to 18 % V_f exhibited 8 % to 20 % of the drying shrinkage of the plain matrix. The same trends were noticed in mortar SIFCON specimens, Figure 4.10. The shrinkage of SIFCON in this case represents 17 % to 50 % of the shrinkage of the plain mortar (M2). Comparing to slurry SIFCON, it seems that the inclusion of steel fibers in mortar SIFCON is less effective in reducing the shrinkage as can be investigated from Figures 4.9 and 4.10. The probable reasons will be discussed later.

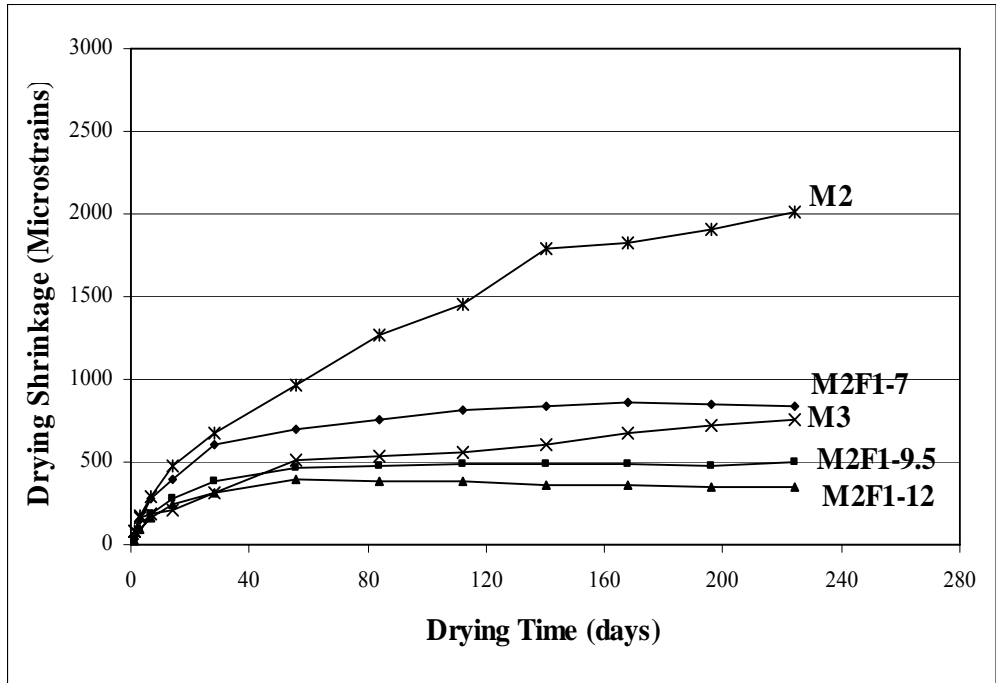


(a) With hooked fibers

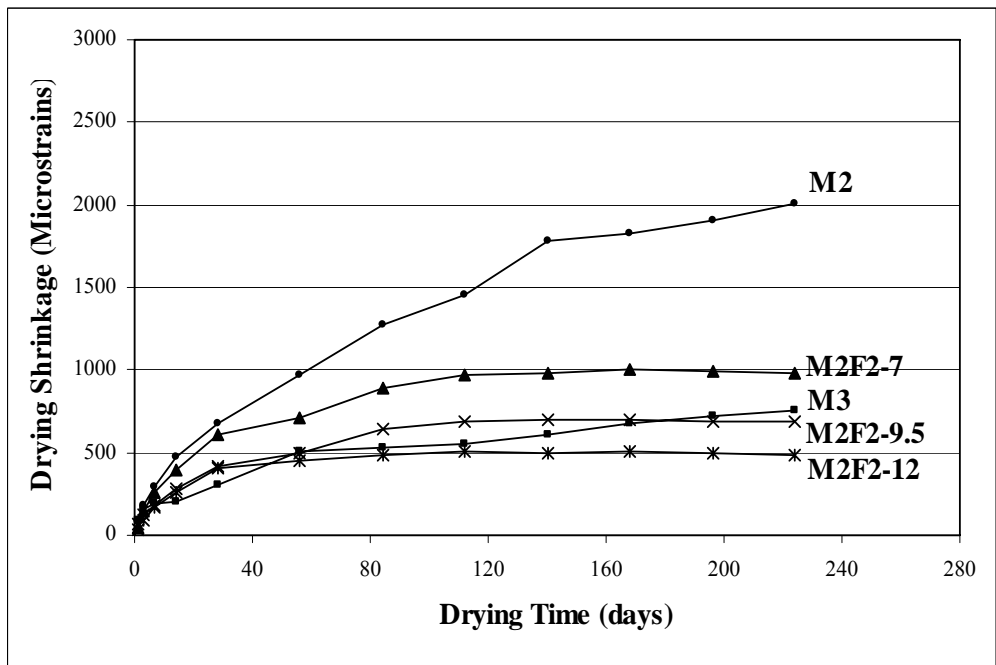


(b) With crimped fibers

Figure 4.9: Drying Shrinkage of slurry SIFCON vs. M1 & M3



(a) With hooked fibers



(b) With crimped fibers

Figure 4.10: Drying Shrinkage of mortar SIFCON vs. M2 & M3

4.2.2 Effect of fiber volume fraction

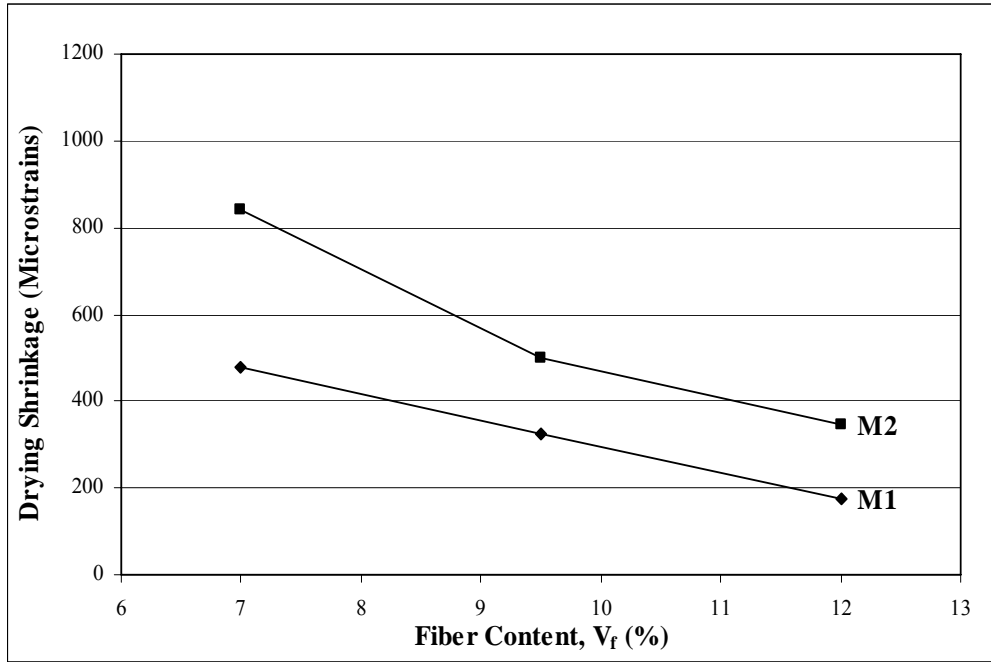
Figures 4.9 to 4.10 show the drying shrinkage results of SIFCON groups M1F1, M1F2, M2F1, and M2F2, respectively. The results of plain matrices, M1, M2, and M3 are shown in the figures also for comparative purposes.

In all the cases, it is clear that an increase in the fiber content results in a reduction in shrinkage. Other researchers observed also the same behavior in their work on normal fiber reinforced concrete [75, 76]. The fibers simply act as rigid inclusions in the SIFCON matrix, thereby reduce the shrinkage. Moreover, the higher is the fibers volume fraction, the higher will be the effect on the dimensional stability of the composite. The matrix will shrink less freely when it includes higher V_f . This conclusion was true for both slurry SIFCON, Figure 4.9, and mortar SIFCON, Figure 4.10.

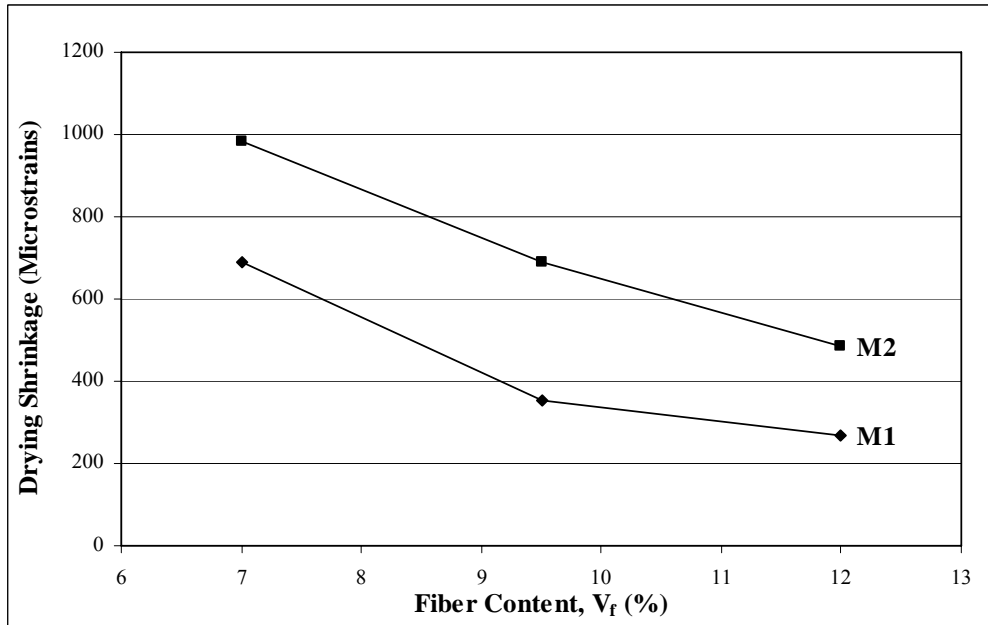
4.2.3 Effect of matrix type

It is generally known, in concrete technology, that inclusion of sand in the cement paste enhances volume stability, and therefore reduces the shrinkage of mortar comparing to the cement paste [55, 77]. The influence of grain size on drying shrinkage is known by the low shrinkage of the much more coarse-grained mixes and by the high shrinkage of fine-grained mixes. In brief, shrinkage is a paste property, and in concrete, the aggregate has a restraining influence on the volume changes that takes place within the paste [53, 55, 78].

Considering the generalization mentioned above, it was expected that slurry SIFCONs will show higher shrinkage than mortar SIFCONs. Surprisingly, this was true only in the case of plain mixes of M1 and M2, where the shrinkage of plain slurry after 224 days of drying was about 30 % higher than the plain mortar shrinkage. This was not the case in SIFCON in which both types of steel fibers are included in the plain mixes. This can be seen, clearly, in Figure 4.11.



(a) With hooked fibers



(b) With crimped fibers

Figure 4.11: The Influence of mix type on shrinkage of SIFCON after 224 days of drying

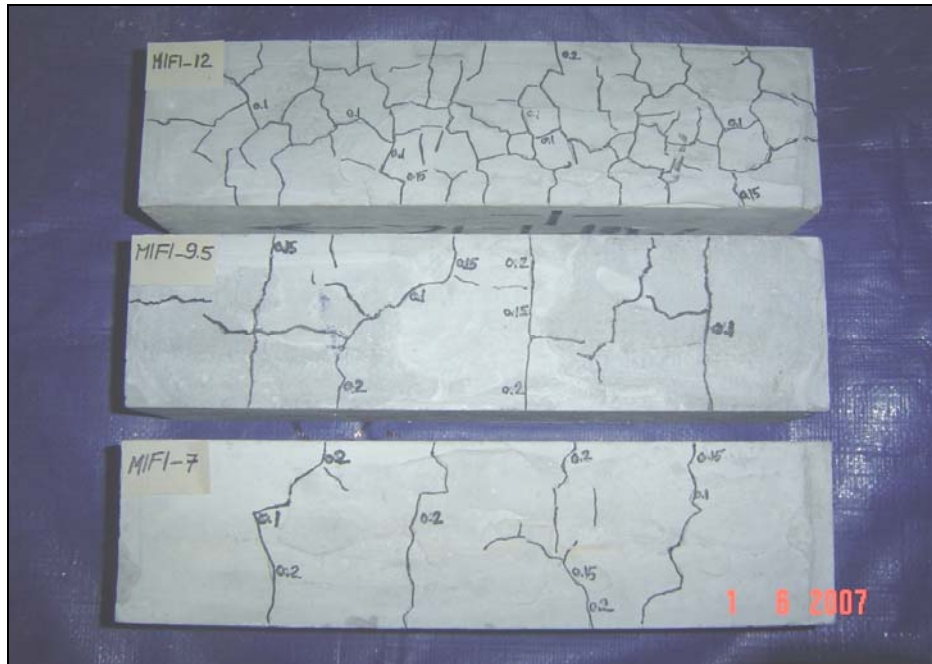
The 224 days shrinkage of mortar SIFCON specimens was 43 % to 100 % higher than the shrinkage of slurry SIFCON recorded at the same period. Mortar SIFCON specimens showed higher shrinkage starting from the beginning of the test until its end. The most possible reason of this unexpected behavior is the randomly distributed cracks observed on the surfaces of the slurry SIFCON specimens since the first days of air drying.

The surface cracks in SIFCON and plain specimens, if any, were mapped using a crack microscope of 10 × magnification level, presented in Figure 4.12. The following findings resulted from the crack mapping:

- (a) All slurry SIFCON specimens showed clear and many randomly distributed drying shrinkage cracks. The density of cracks was higher in the specimens containing higher fiber content. This can be attributed to the restraining effect of fibers which will be stronger as the fiber content increases. Figure 4.13 illustrates the cracking in representative samples of slurry SIFCON made with both types of steel fibers, hooked and crimped. The crack widths ranged from 0.05 mm to 0.2 mm as shown in Table 4.2.



Figure 4.12: Crack microscope used in crack mapping of SIFCON



(a) Representative samples of M1F1 group



(b) Representative samples of M1F2 group

Figure 4.13: Drying shrinkage cracks in slurry SIFCON specimens
The cracks are highlighted and thicknesses in mm are shown

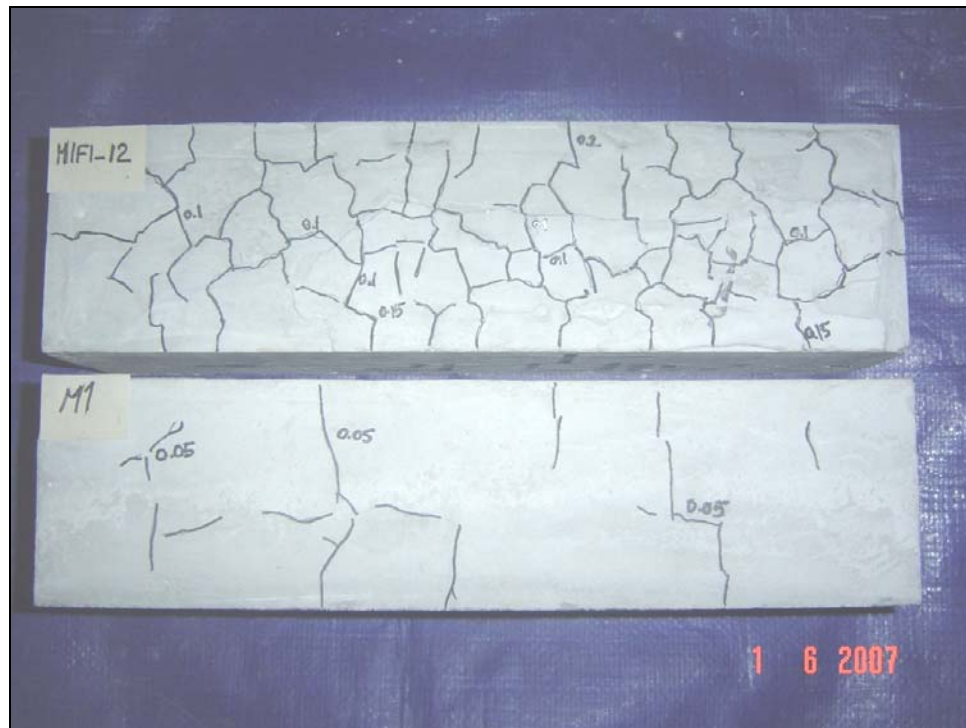


Figure 4.14: Drying shrinkage cracks in slurry SIFCON and the plain matrix

The plain matrix shows very few cracks compared with the fiber reinforced one

- (b) The plain slurry itself showed very few cracks when compared to slurry SIFCON specimens, Figure 4.14. This, again, proves that the cracks developed because of the inclusion of the restraining steel fibers.
- (c) Mortar SIFCON specimens showed very few cracks of negligible thicknesses (≤ 0.05 mm), while no cracks were noticed on the surfaces of the plain mortar and the control concrete.
- (d) Although increasing fiber volume fraction leads to increased cracking, it was noticed that the width of cracks is generally smaller in the specimens made with a higher fiber content.

The cracking of slurry SIFCON specimens can be attributed to the following:

(a) The higher cement content, Table 3.7, when compared to mortar SIFCON.

It is known that for a given W/C ratio, drying shrinkage increases with increasing cement content. This is expected due to the increase in the volume of the cement paste [20, 55, 56]. The presence of restraining steel fibers will resist the tendency of the specimens to shrink. The results will be in the form of spread cracks appear on the surfaces.

(b) The higher water content, Table 3.7, will cause the same problem because the withdrawal of water will be higher when compared to mortar SIFCON.

(c) The tensile strength of the plain slurry was 1.5 times lesser than that of plain mortar (3.0 MPa and 4.9 MPa, respectively). Therefore, slurry specimens showed more cracks responding to the tensile stresses.

(d) The differences in the coefficients of thermal expansion (CTE) of the constituents, Table 4.3. This table shows the big difference in CTE values between cement paste and steel fiber which compose slurry SIFCON. This difference is assumed to play some role in the cracking because of the different response to increases in temperature between the slurry and the fibers incorporated. The differences are generally less in the case of mortar SIFCON.

After all, it is believed that the high spread of open cracks in the specimens of slurry SIFCON has affected the recorded results of length change by increasing the specimen length, and making the shrinkage strain less than what was expected in the beginning. Unlike plain specimens, which are almost free of cracks, there are a lot of cracks in slurry SIFCON. These cracks will cause some increase in the specimen length which will be included in the

final result of the length change. However, the amount of shrinkage is, always, higher than the amount of expansion caused by the cracks.

Thus, every time the specimen shows some shrinkage with respect to the initial length before starting the test. In other words, the slurry SIFCON specimens will shrink, overall, but the net amount of this shrinkage is reduced by the assumed elongation that occurred as a result of the numerous cracks. Finally, the shrinkage of slurry SIFCON will be less than that of mortar SIFCON, in which the length change amount is not governed by the cracking as in the case of slurry SIFCON.

Table 4.2: Summary of crack mapping

	Specimens	Crack density	Crack thickness (mm)
Slurry SIFCON	M1F1-7	Low	0.1 – 0.2 (mostly 0.2)
	M1F1-9.5	Moderate	0.1 – 0.2 (mostly 0.2)
	M1F1-12	High	0.1 – 0.2 (mostly 0.1)
	M1F2-7	Low	0.05 – 0.2 (mostly 0.1)
	M1F2-9.5	Moderate	0.05 – 0.1
	M1F2-12	High	0.05 – 0.1
	Mortar SIFCON	Very low	≤ 0.05
	M1	Very low	≤ 0.05
	M2	No cracks	-
	M3	No cracks	-

Table 4.3: Typical ranges of coefficient of thermal expansion [20, 79]

Material	CTE (microstrains / °C)
Cement Paste	18 – 20
Mortar	9 – 12
Concrete	8.5 – 13
Steel	11 – 12

As explained before, mortar SIFCON shrinks, numerically, more than slurry SIFCON probably because of the strong effect of cracks on the length of the later. Therefore, the results of drying shrinkage test on SIFCON, in general, must be treated very carefully, especially when numerous cracks are developed as in the case of slurry SIFCON specimens tested in this study. Otherwise, the results of the test may lead to some misleading interpretations of SIFCON shrinkage behavior.

The cracking phenomenon in slurry SIFCON explains also its time-dependent nature. It can be seen in Figure 4.9 that, typically, the shrinkage reaches some peak and afterwards it decreases gradually. This is much clear in the specimens of the maximum fiber volume fraction (V_f of 12 %). It is expected that after this peak, more cracks will develop and the overall effect of cracking will be stronger than before. This trend was not experienced in mortar SIFCON samples, except for 12 % V_f case were very small drops in shrinkage strain occurred because of the existence of some few cracks in this group of specimens as well.

Actually, exhibiting some increase in specimen length after reaching the peak strain value was noticed also in the literature, Figure 2.26 [1]. However, no explanation for this behavior was available. Figure 4.10 shows also that for exposure periods beyond 112 days (about 4 months), the mortar SIFCON specimens have shown no significant further shrinkage despite continuous shrinkage strain in the plain mortar. For the slurry SIFCON specimens, the previously mentioned peaks have been reached in half that time (56 days).

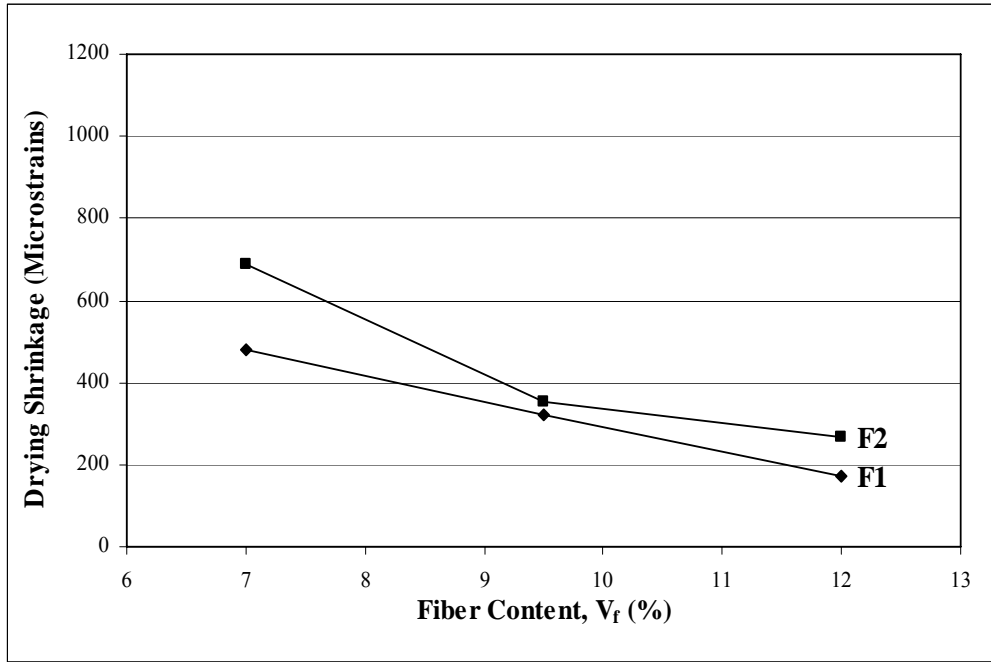
4.2.4 Effect of fiber type

The relation between drying shrinkage of SIFCON and geometrical shape of steel fibers used in making it can be examined in the Figures 4.15 and 4.16.

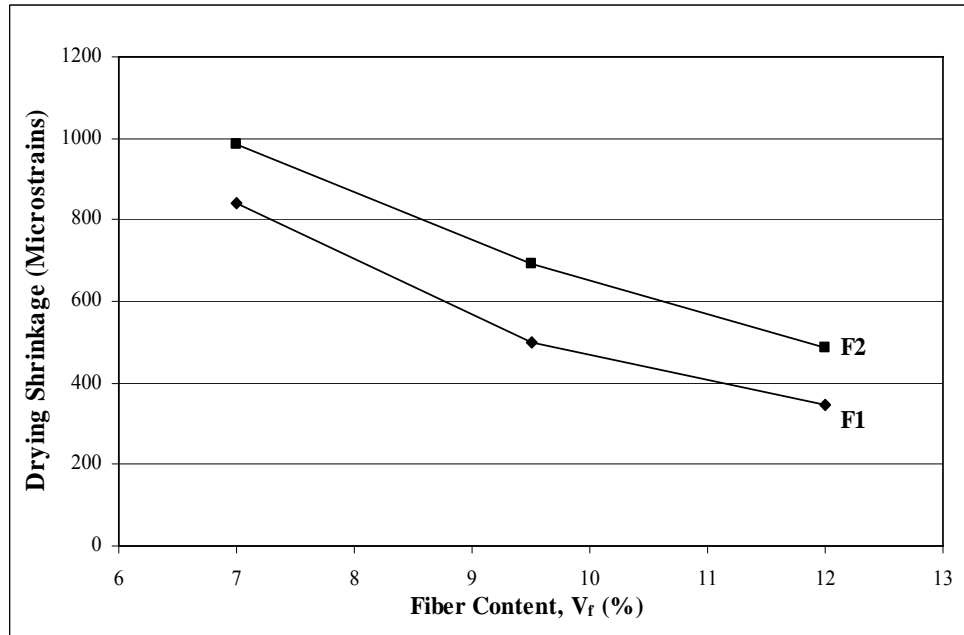
Figure 4.15 illustrates the drying shrinkage of slurry and mortar SIFCON made with hooked fibers (F1) and crimped fibers (F2) after 224 days exposure.

It is clear from the two figures that in both mix types and for all fiber contents, specimens made with hooked fibers show less shrinkage comparing to crimped fibers specimens. The increase in shrinkage of crimped fibers specimens compared to hooked ones ranges from 10 % to 50 % approximately. Most probably, the geometric shape of hooked ends plays an important role in enhancing the restraining effect of hooked fibers inside the matrix. The abrupt changes in the shape of hooked-end fibers may lead to more stress concentration at the ends and, then, more cracks. On the other hand, it seems that the wave shape of crimped fibers is less effective in preventing shrinkage movements in the mortar SIFCON specimens.

Concerning cracking in slurry SIFCON specimens, it seems that specimens made with hooked fibers crack slightly more than crimped fibers specimens. This can be observed in Figure 4.16. This again can be related to the shape of the fiber itself. Hooked fiber specimens crack more because the restraining effect on shrinkage movement of hooked ends is stronger than the waves of crimped fibers. The more restrained is the specimen, the more it cracks.



(a) Slurry SIFCON



(b) Mortar SIFCON

Figure 4.15: The effect of fiber type on the drying shrinkage of SIFCON after 224 days of drying

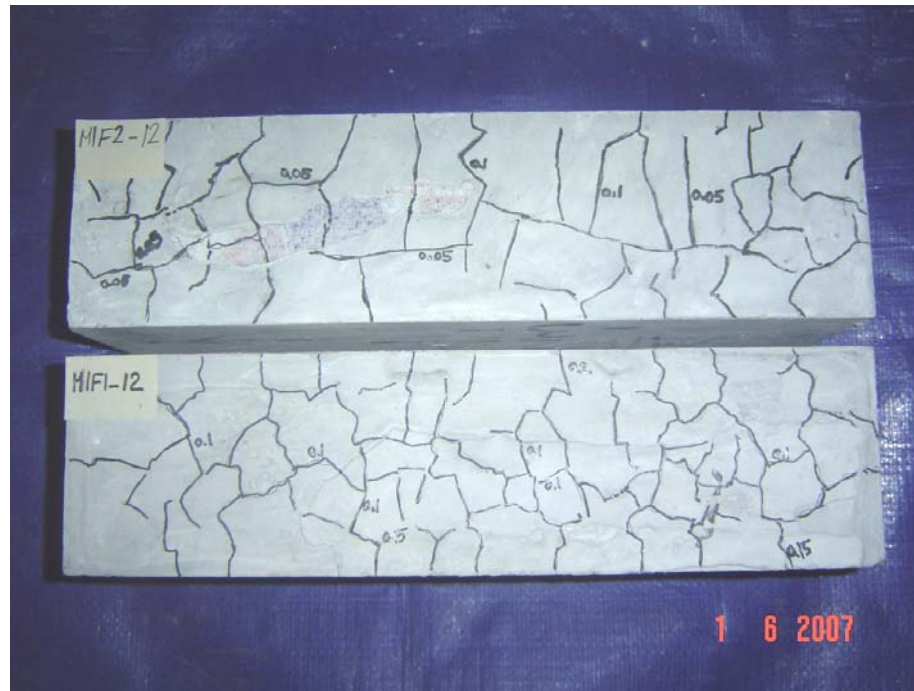


Figure 4.16: The effect of fiber type on cracking of slurry SIFCON
Using hooked fibers (MIF1-12) resulted in more cracks

4.3 Water absorption test

Deterioration of concrete structures is generally caused by penetration of aggressive agents (sulphates, chlorides, moisture, carbon dioxide ...) into concrete. Thus, concrete durability is strongly related to its permeability, which is a widely recognized durability index, since it quantifies the resistance of the material against penetrating agents [80].

Therefore, as one of its main objectives was to study the durability of SIFCON, this research intended to investigate the permeability of several SIFCON combinations. The permeability was evaluated through the results of water absorption test which was carried out according to the requirements of the standard test method ASTM C 642 [60]. The test details were discussed earlier in Section 3.4.3, and the results are presented and discussed below.

4.3.1 Absorption of plain mixes

Figure 4.17 shows the water absorption versus time of the 48 hour test period of the plain mixes used in SIFCON, slurry M1 and mortar M2; along with the control concrete M3. As can be seen clearly in this figure, plain slurry showed the highest absorption after 48 hours (20.35 %). The absorption capacities of plain mortar and control concrete were 9.03 % and 3.36 %, respectively at the same period. In other words, the absorption of plain slurry was 6 times the absorption of reference concrete, while plain mortar was less permeable (2.7 times the concrete absorption).

Such trends correspond to the expected behavior. The reasons of the very high absorption of plain matrices used for SIFCON, especially the slurry, with respect to concrete are discussed below:

- (a) It is assumed that the presence of aggregate reduces permeability. If the aggregate has a low permeability, which is the case in this study, its presence reduces the effective area over which the flow can take place. Furthermore, because the flow path has to circumvent the coarse and fine aggregate particles, the effective path becomes considerably longer. Thus, the effect of aggregate in reducing the permeability of concrete may be considerable. The interface zone does not seem to contribute to flow [55]. The same assumption explains why the absorption of slurry was two times more than that of the mortar absorption.
- (b) The high water content in slurry and mortar comparing to concrete will lead to more capillary pores, and more porous structure.
- (c) Cracks were observed even in the plain slurry and mortar specimens, because of the high drying temperature applied in the test. The drying

shrinkage cracking, mainly in slurry, increases the absorption capacity. Usually, concrete is free from such cracking because of the presence of coarse aggregate that improves the dimensional stability.

In this test, the weight of each specimen was recorded at fixed intervals of time for the first 2 hours in order to find the rate of absorption. Figure 4.18 shows the relation of absorption versus time during this period in the plain mixes.

By studying the rate of absorption with time in the first 2 hours, the relations were found to be nonlinear. By plotting the absorption versus $(t^{1/2})$, approximately linear relationships were found, Figure 4.20. The slope of the line, obtained from regression analysis, was used as an index to describe the water flow through connected capillary pores. The term Absorptivity index (A^*) was used for the slope of the line [81, 82]. The first 2 hours and absorptivity results of all SIFCON samples are given in Appendix B.

As shown in Figure 4.19, the value of the coefficient of correlation (R^2) for the linear regression between absorption and $(t^{1/2})$ is 0.935 or greater which indicates strong linear relationships. It is found, also, that absorptivity is related directly to absorption. Higher values of absorptivity indicate higher absorption, and hence higher permeability. Using this index (A^*) has the advantage of a reduced test time. Also, it reduces the experimental errors as the estimated slope is based on several measurements rather than a single measurement at the end of the test [82].

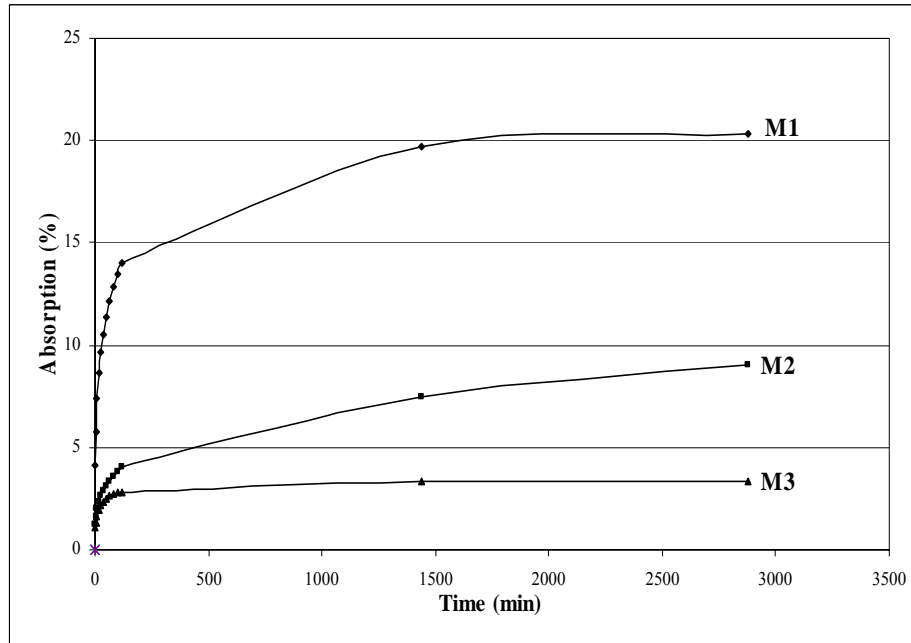


Figure 4.17: Absorption vs. time during 48 hrs for M1, M2 and M3

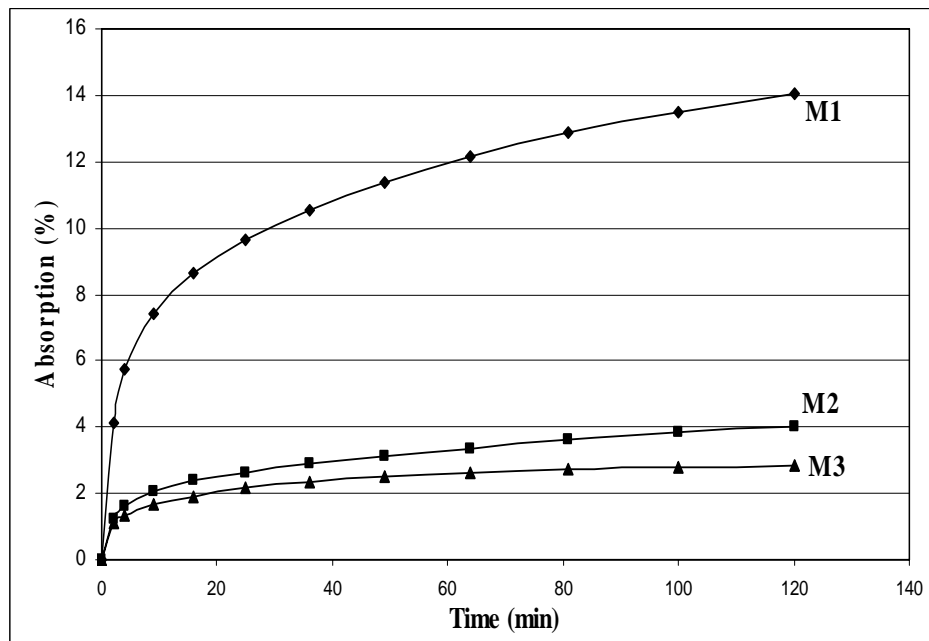


Figure 4.18: Absorption vs. time during the first 2 hrs for M1, M2 and M3

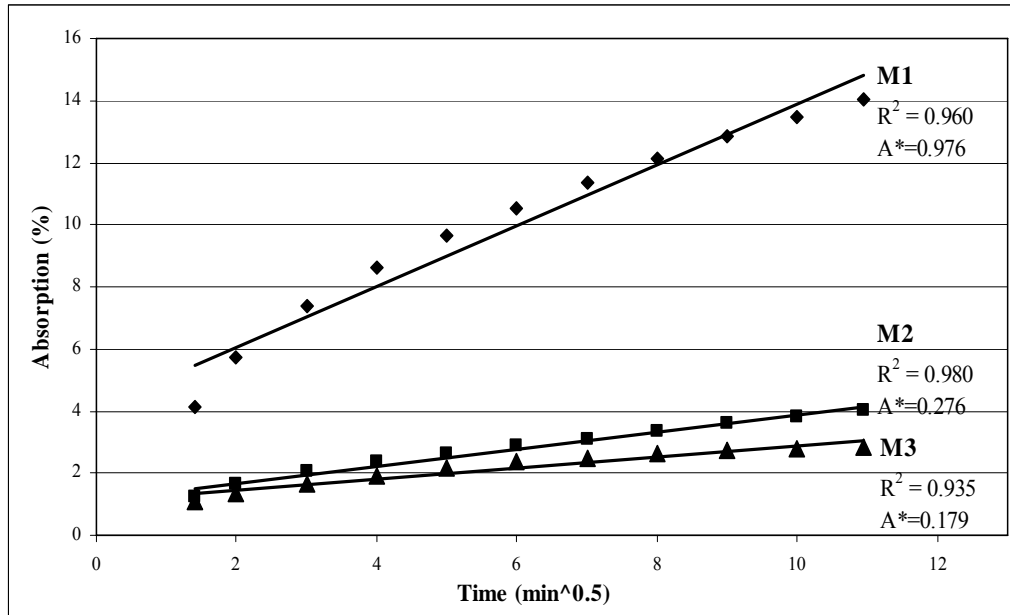


Figure 4.19: Absorption indices for M1, M2 and M3

4.3.2 Absorption of SIFCON

In the following sections, results of water absorption test conducted on different SIFCON specimens are presented and discussed. The discussions are focused on the effects of steel fiber content, mix constituents and fiber type.

4.3.2.1 Effect of fiber content

The results of water absorption test of the slurry and mortar SIFCON mixes are shown in Figures 4.20 and 4.21. The figures included also the results of plain mixes for comparative purposes. In all the cases of slurry SIFCON and mortar SIFCON it is obvious that inclusion of steel fiber reduces the absorption of the plain mixes.

In slurry SIFCON, Figure 4.20, the absorption after 48 hours ranged from 12 to 15 %, depending on fiber content. The absorption of the unreinforced slurry

(M1) was 20.4 %. Therefore, unfortunately, the presence of steel fibers with such relatively high volume fractions (7 %, 9.5 %, and 12 %) did not help much in reducing the very high absorption of the plain slurry. Such high levels of absorption are usually not acceptable for conventional concrete. Most good concretes have absorption well below 10 % by mass [55].

For the effect of fiber content itself, Figure 4.20 shows that the higher fiber volume fraction in the mix, the less the absorption. However, increasing fiber content from 7 % to 12 % had slight impact on reducing the absorption.

Being a non-absorbent material, including steel fiber in the matrix simply reduces the volume available for water flow inside the SIFCON composite. This is believed to be the most important reason behind the role of steel fibers in reducing absorption. In addition, it can be assumed that the fibers act as physical barriers that intersect the capillary pores and channels, and form obstacles that prevent, to a certain extent, flow from moving freely through the matrix. Therefore, the higher is the content of steel fibers in the mix, the more difficult the water can flow through it.

The same trends were observed in mortar SIFCON mixes as can be seen in Figure 4.21. Here, adding steel fiber reduced the absorption from 9 % for the plain mortar to the level of 4 % to 7 %. Unlike slurry SIFCON, reduction in absorption was sensitive to the increase in fiber content.

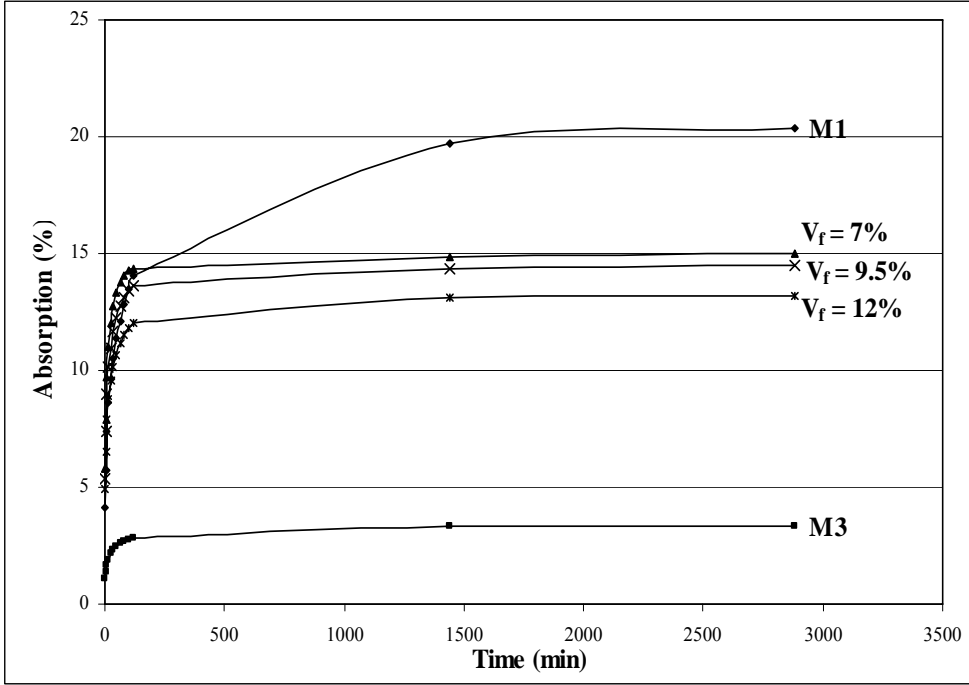
Comparing to slurry SIFCON, the levels of absorption in mortar SIFCON are quite low, especially in the case of V_f of 12 % which showed absorption values close to the values recorded usually in low permeability normal concrete (4 % to 5 %) [82]. Nevertheless, the absorption of mortar SIFCON is still higher than that for concrete used as a control mix (M3). This concrete showed only 3.4 % absorption after 48 hours, thanks to its low W/C ratio and the low absorption of coarse aggregate used in it.

The previously mentioned explanation on the effect of increasing fiber content on absorption of slurry SIFCON applies also to mortar SIFCON. According to ASTM C 642, the absorption is usually calculated with respect to the total dry weight of the sample as a whole (including all its ingredients) [60]. Table 4.5 shows the absorption results of different SIFCON mixes, but based on the mass of slurry or mortar only. The calculations are made here by excluding the weight of steel fiber from the total weight of the specimens.

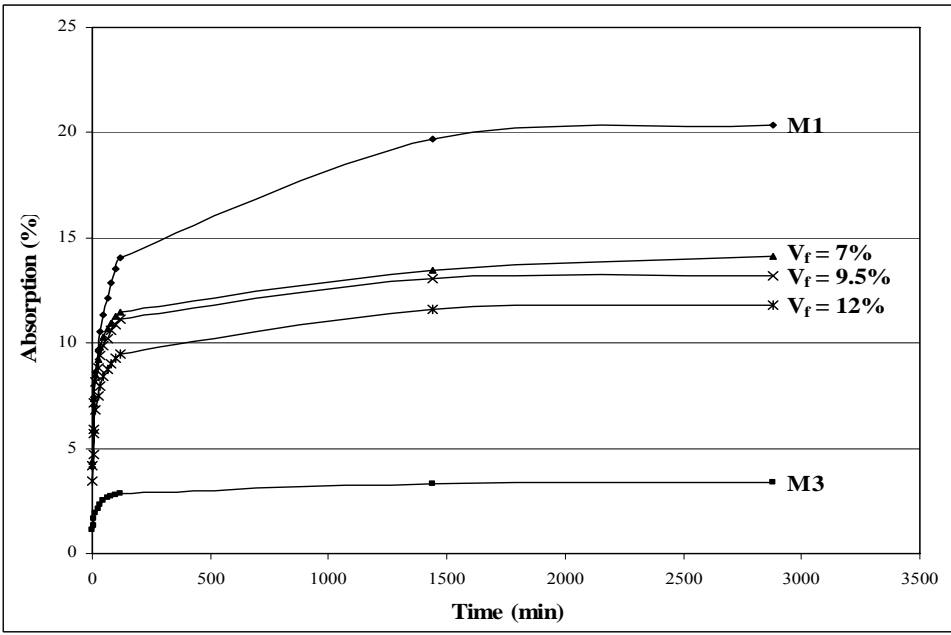
Interpretation of the results presented in the table leads to the fact that absorption capacity of both the cement paste and mortar remained almost the same after adding steel fibers. Actually, there is a very small increase in slurry and 1 mm sand mortar absorption after including the fibers. The finer mortar showed negligible decrease in absorption upon adding the fibers. This may prove the assumption mentioned earlier about why including fibers reduces the absorption of the specimen as a whole. Therefore, depending on the results of Table 4.4, it can be said that the steel fibers do not reduce the absorption of the plain matrix itself (the phases of paste or mortar), but they reduce the absorption of the material as a whole by simply decreasing the volume subjected to absorption. Fibers themselves do not absorb any water.

It seems also that the effect of having several transition zones between the fibers and the matrix on the absorption of SIFCON was not important in this case. Anyway, the very small increase in matrix absorption after adding the fibers in most of the mixes can be attributed to the presence of more transition zones as fiber content increases.

Table 4.4 presents also the coefficients of variation (COV) for all the measured results which were all less than 10 % which indicates low variation in the testing method. The COV values for the absorption ranged from 1.6 % to 7.4 %.

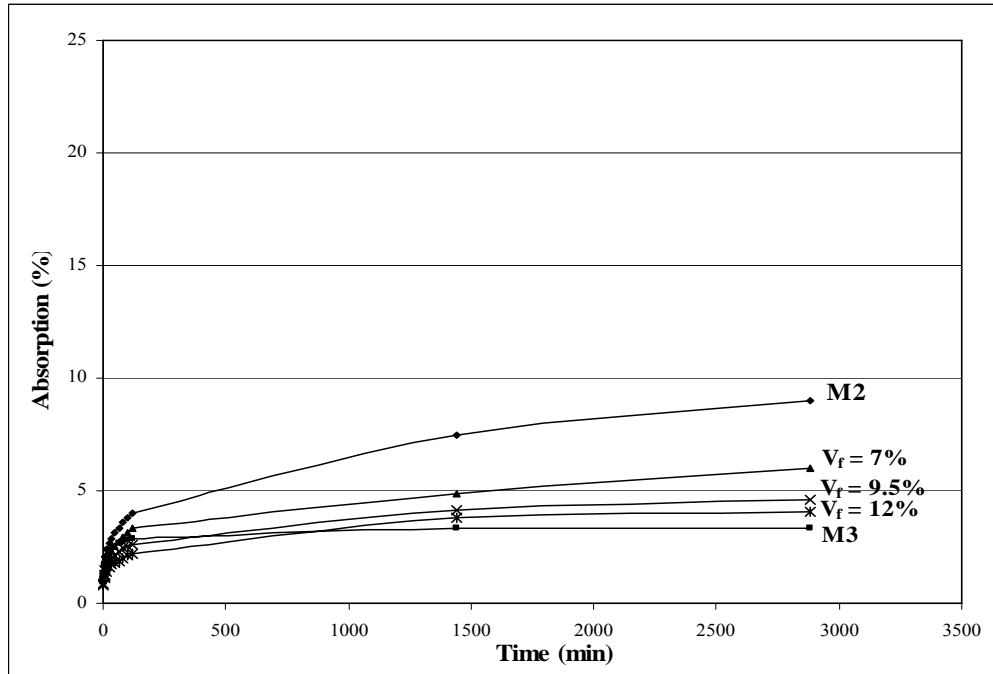


(a) With hooked fibers

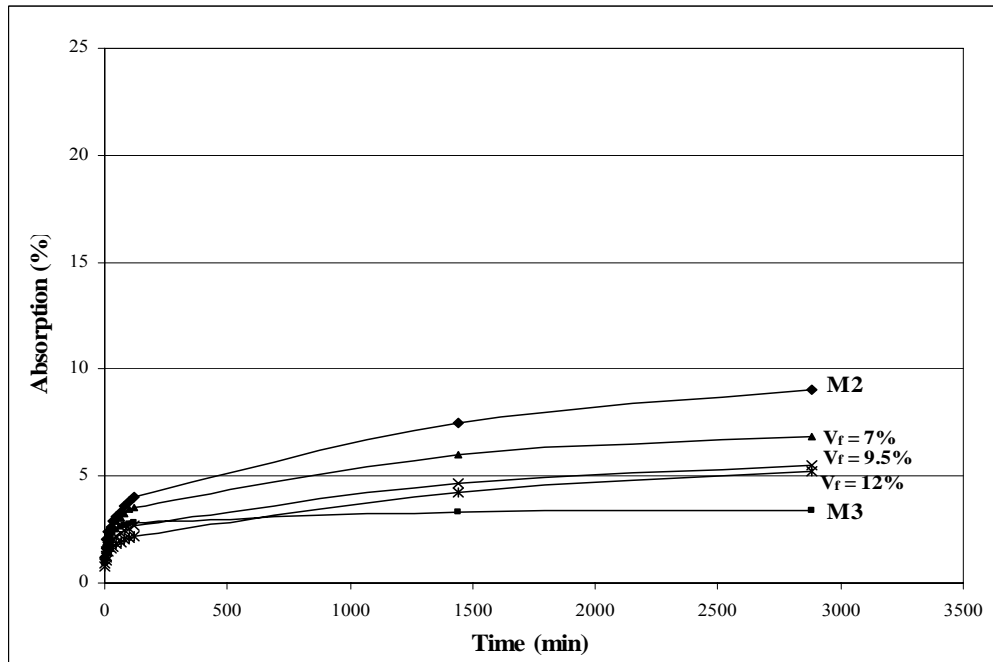


(b) With crimped fibers

Figure 4.20: Absorption vs. time in 48 hrs for slurry SIFCON, M1 and M3



(a) With hooked fibers



(b) With crimped fibers

Figure 4.21: Absorption vs. time in 48 hrs for mortar SIFCON with 1.0 mm sand, M2 and M3

Table 4.4: Absorption of SIFCON mixes by weight of slurry or mortar

Matrix type	Matrix ID	Absorption by weight of slurry or mortar (%)
Plain slurry	M1	20.35 (2.7) ^(*)
Slurry SIFCON (hooked fibers)	M1F1 - 7	20.83 (2.2)
	M1F1 - 9.5	21.53 (2.5)
	M1F1 - 12	21.20 (4.0)
Slurry SIFCON (crimped fibers)	M1F2 - 7	20.38 (7.2)
	M1F2 - 9.5	21.44 (6.3)
	M1F2 - 12	21.21 (2.3)
Plain mortar (1mm sand)	M2	9.03 (1.8)
Mortar SIFCON (hooked fibers, 1mm sand)	M2F1 - 7	9.11 (1.6)
	M2F1 - 9.5	9.60 (4.0)
	M2F1 - 12	9.54 (6.7)
Mortar SIFCON (crimped fibers, 1mm sand)	M2F2 - 7	9.20 (6.1)
	M1F2 - 9.5	9.23 (5.3)
	M1F2 - 12	9.68 (7.4)
Plain mortar (0.6mm sand)	M2(F)	12.75 (2.4)
Mortar SIFCON (hooked fibers, 0.6mm sand)	M2F1(F) - 7	12.44 (5.36)
	M2F1(F) - 9.5	12.12 (1.8)
	M2F1(F) - 12	12.57 (6.8)
Mortar SIFCON (crimped fibers, 0.6mm sand)	M2F2(F) - 7	12.28 (7.0)
	M2F2(F) - 9.5	12.37 (3.2)
	M2F2(F) - 12	12.28 (1.3)

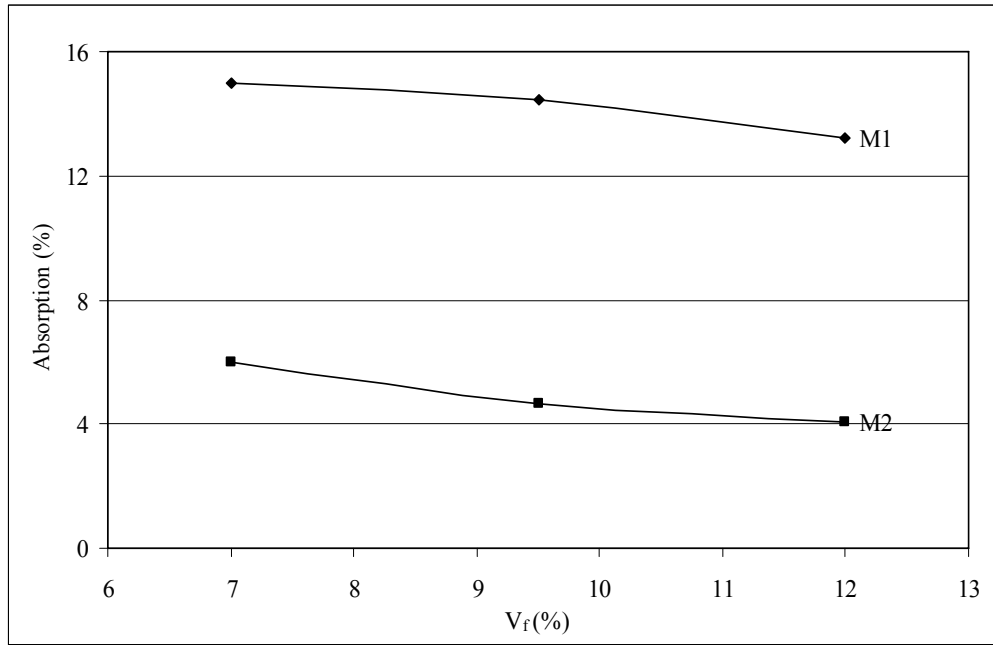
(*) Number in parentheses represents the coefficients of variation (%)

4.3.2.2 Effect of mix composition

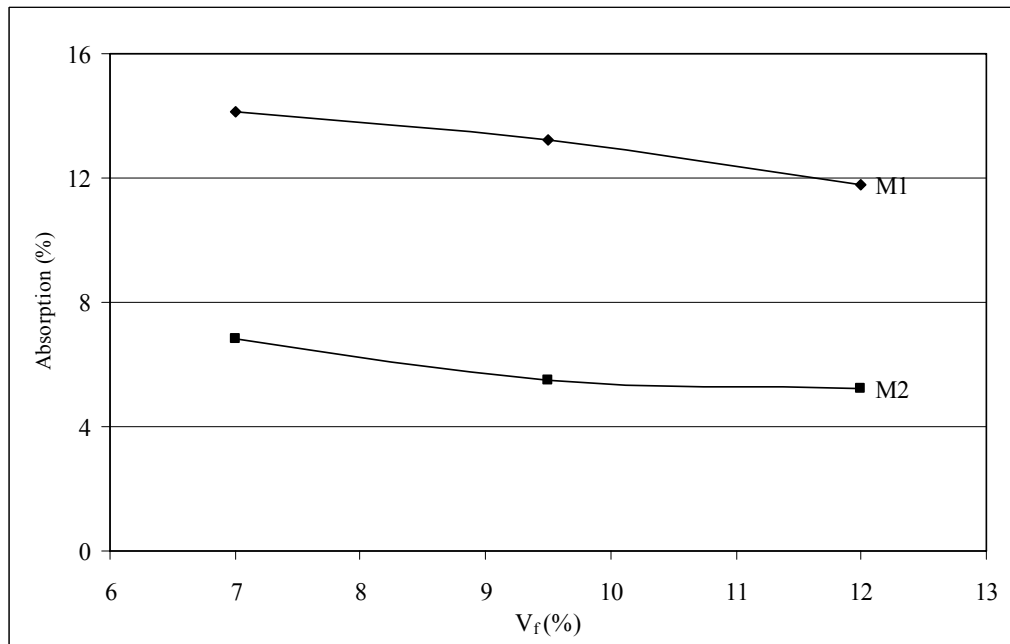
The differences in absorption percentage between slurry SIFCON and mortar SIFCON can be examined through Figure 4.22. Figure 4.22(a) presents the absorption results of slurry SIFCON and mortar SIFCON made with hooked fibers (F1), while Figure 4.22(b) shows the results when crimped fibers (F2) are used.

The trends are the same for the both types of fibers. The advantages of mortar SIFCON over slurry SIFCON concerning water absorptions are very clear in the figures. The difference in absorption between the two mixes is about 9 % when (F1) are used, and 7 % in the case of (F2). Such observations are coherent with the results of absorption test conducted on the plain matrices (M1) and (M2). The high absorption of slurry SIFCON when compared with mortar SIFCON is most probably related to the following points:

- (a) The presence of aggregate, sand in this case, usually reduces the absorption as discussed earlier in Section 4.3.1.
- (a) The high water content in slurry SIFCON increases the permeability.
- (b) The cracking phenomenon in slurry SIFCON, because of drying, makes it more permeable by providing more channels for the water to flow through the cracks. These cracks were noticed also in the drying shrinkage test as discussed previously. Actually, the problem here was expected to be more severe because of the high drying temperature in the oven to obtain the dry weights. All specimens were kept at 100 °C temperature until the complete drying is reached before starting the test. This was in accordance with the requirements of the standard absorption test method ASTM C 642 [60].



(a) With hooked fibers



(b) With crimped fibers

Figure 4.22: Effect of SIFCON mix type on total water absorption

As mentioned earlier, there are no standard methods to test SIFCON, and adopting the method of testing conventional concrete as it is to test SIFCON can affect the reliability of results sometimes. For example, probably it would be more appropriate to dry the SIFCON specimens at a lower temperature, say 50 °C, to reduce the possibility of the development of drying cracks, especially in slurry SIFCON. Anyway, such cracks cannot be prevented completely because they happened even in the room temperature (20 – 25 °C) as noticed in the drying shrinkage test.

In addition to the comparison made between slurry SIFCON and mortar SIFCON, an investigation was also made on the effect of the maximum size of sand used in mortar SIFCON on the water absorption. The sand used in making all mortar SIFCON specimens in this research was of maximum aggregate size (MAS) of 1.0 mm. Sand of the same origin but with smaller MAS of 0.6 mm was used to prepare comparison absorption specimens. The grading of both sand sizes presented earlier in Chapter 3, Figure 3.2.

The plain mix made with the finer sand of 0.6 mm size was given the designation M2(F). The absorption of this mix, made with the two types of fibers, versus the plain mix of M2(F) and M3 is shown in Figure 4.23. The figure shows the same behavior recorded in mortar SIFCON made with the coarser sand of 1.0 mm size. The positive impact of introducing steel fiber on reducing the absorption is observed here too. The absorption of this mix of mortar SIFCON was well lower than the absorption of the plain matrix, but still higher than the results of the control concrete and the mixes made with 1.0 mm sand.

Expected findings were recorded when the two sizes of sand were compared with each other in terms of the absorption of SIFCON prepared using them. The results can be examined in the Figure 4.24. The mixes made with finer

sand showed higher absorption. This agrees with the assumption that absorption decreases with increasing the size of aggregate. Another explanation can be related to cracking. Although mortar SIFCON showed few cracks due to drying, it is expected that mortar SIFCON prepared with the coarser sand will show better volume stability, and thus less cracking. The influence of cracks on absorption has been mentioned previously. Another possible reason can be related to the assumption that coarser sand reduces the volume of permeable pores in the matrix.

4.3.2.3 Effect of fiber type

For every one of the SIFCON mixes used in this study, the comparison was made between the absorption of the mixes made with hooked fibers and the ones prepared using crimped fibers. To make the comparison easier, it was made only on the basis of the 48 hours absorption. The results are shown in Figure 4.26. In every one of the three relations contained in this figure, there was a clear trend without any overlapping in the results.

In the case of slurry SIFCON, Figure 4.25 (a), it can be seen that the specimens made with hooked fibers showed slightly higher absorption than the specimens made using crimped fibers. This behavior may be attributed to the higher spread of surface cracks that occurred due to the high drying temperature in the case of mixes made with hooked fibers. This was noticed also in the drying shrinkage test. As discussed previously in Section 4.2.4, the cracking was more in hooked fiber specimens because of the stronger restraining effect of the hooked-end fibers due to its geometrical shapes.

On the contrary, it was found that hooked fibers showed better results in the case of mortar SIFCON made with the two sizes of sand, 0.6 mm and 1.0 mm as can be seen in Figure 4.25 (b) and (c). Here the cracking effect is excluded,

because mortar SIFCON specimens were almost free of visible cracks. Therefore, there is a strong possibility that the geometrical shape itself of hooked fibers with their abrupt ends plays some role in reducing the absorption. For some reason, it seems that water infiltrates mortar SIFCON more easily when crimped fibers are present. After all, this point may require further investigation to establish a cut relation, if any, between the fiber geometry and the absorption of SIFCON.

4.3.3 Summary of water absorption results

Table 4.5 summarizes the results of water absorption tests carried out in this study. The table shows the average values of absorption after 48 hours and absorptivity, in addition to the values of the coefficients of correlation (R^2) for the linear regression between absorption and ($t^{1/2}$).

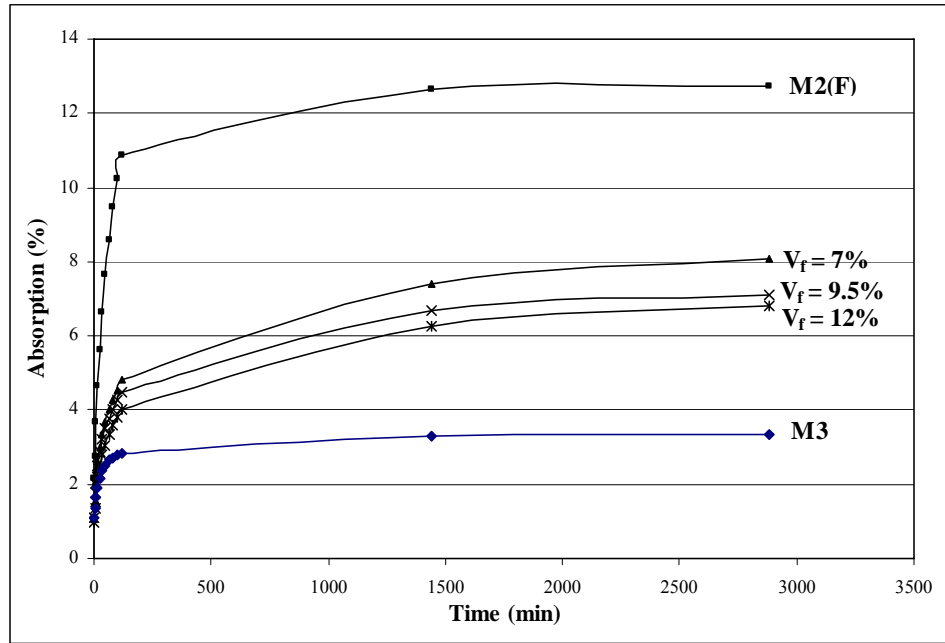
The findings can be listed in the following points:

- (a) SIFCON, in general, has very high absorption capacities that range from 2 to 5 times of the control concrete absorption, depending on the matrix composition.
- (b) Inclusion of steel fibers reduces the absorption. The higher is the fiber content, the lesser is the absorption.
- (c) The coarser matrices showed lesser absorption.
- (d) The using of crimped fibers resulted in lesser slurry SIFCON absorption. On the contrary, hooked fibers were better for mortar SIFCON.

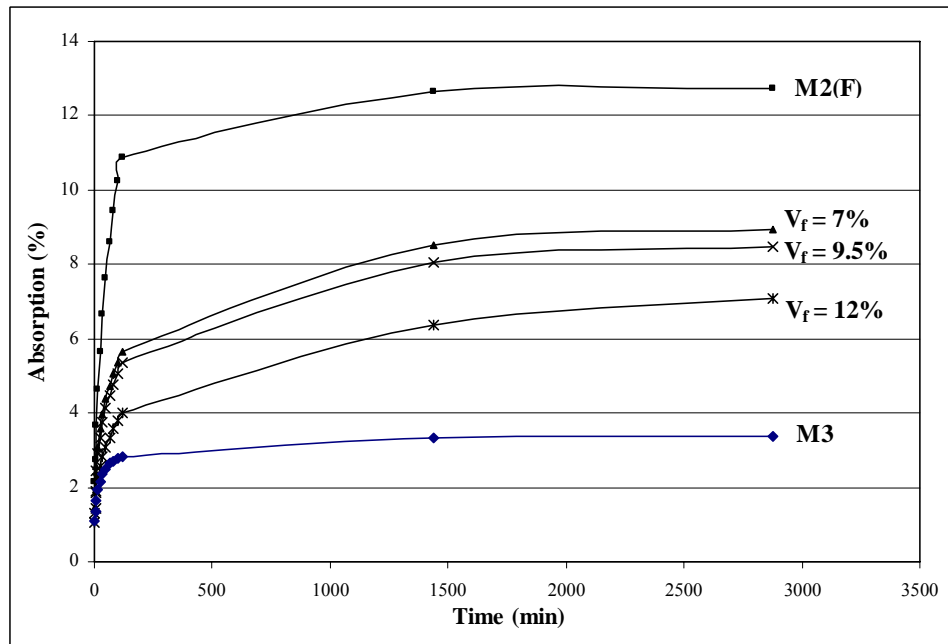
The possible reasons for those observations were discussed already.

Concerning absorptivity and coefficients of correlation, the following remarks may be stated:

- (a) In general, for most of the mixes, the values of (R^2) were higher than 0.9 which indicates strong enough linear relationships. The linearity was much clear in mortar SIFCON specimens when compared with slurry SIFCON.
- (b) Generally, high values of (A^*) refer to high absorption. Table 4.5 shows how adding steel fibers results in decreasing (A^*) values significantly. Some previous studies concluded the validity of using (A^*) to evaluate the total absorption of normal concrete [81, 82]. In the case of SIFCON, the results shown in Table 4.5 indicate that this can be true only in the case of slurry SIFCON.
- (c) For mortar SIFCON, it seems that relying only on (A^*) to appraise the water flow through the pores is not enough. Mortar mixes of high fiber volume fraction (9.5 % and 12 %) showed (A^*) values less than that of control concrete, although the final absorption of mortar SIFCON after 48 hours was well higher than concrete absorption. This is due to the fact that the rate of absorption of mortar SIFCON in the first two hours of immersion is less than that of concrete. After the first two hours, the absorption rate decreases sharply in concrete, unlike in the case of mortar SIFCON. Figure 4.21(b) represents a typical example of this behavior,
- (d) There is also a strong correlation between (A^*) and SIFCON mix type. A direct proportionality is found between (A^*) values and the fineness of the matrix. For example, the absorptivity values of plain slurry and plain 1.0 mm sand mortar were 0.976 and 0.276 respectively. On the other hand, this value was as low as 0.179 in conventional control concrete.

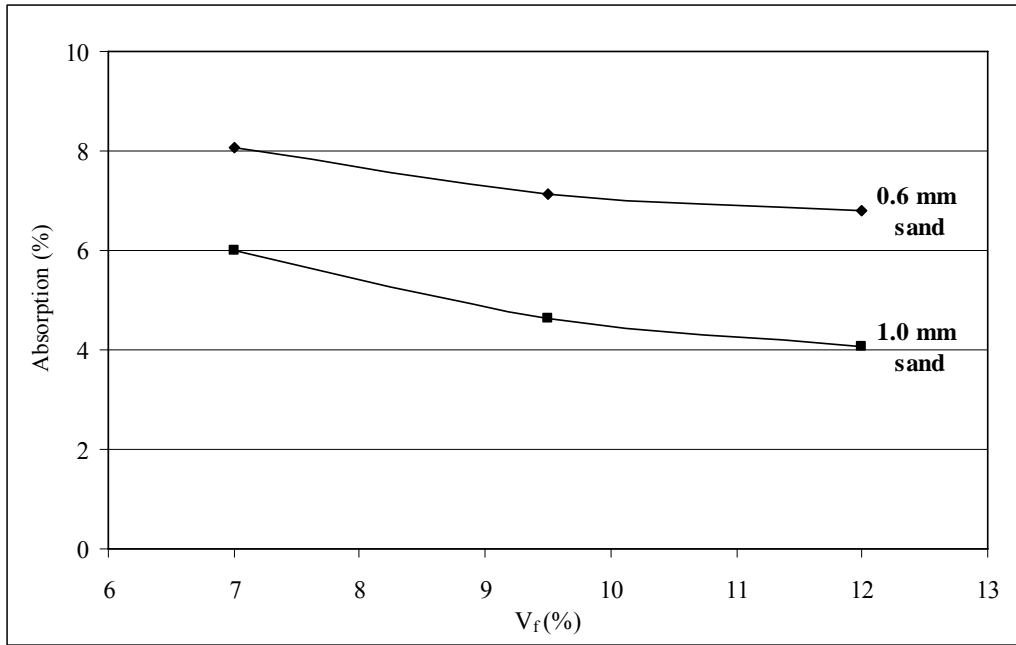


(a) With hooked fibers

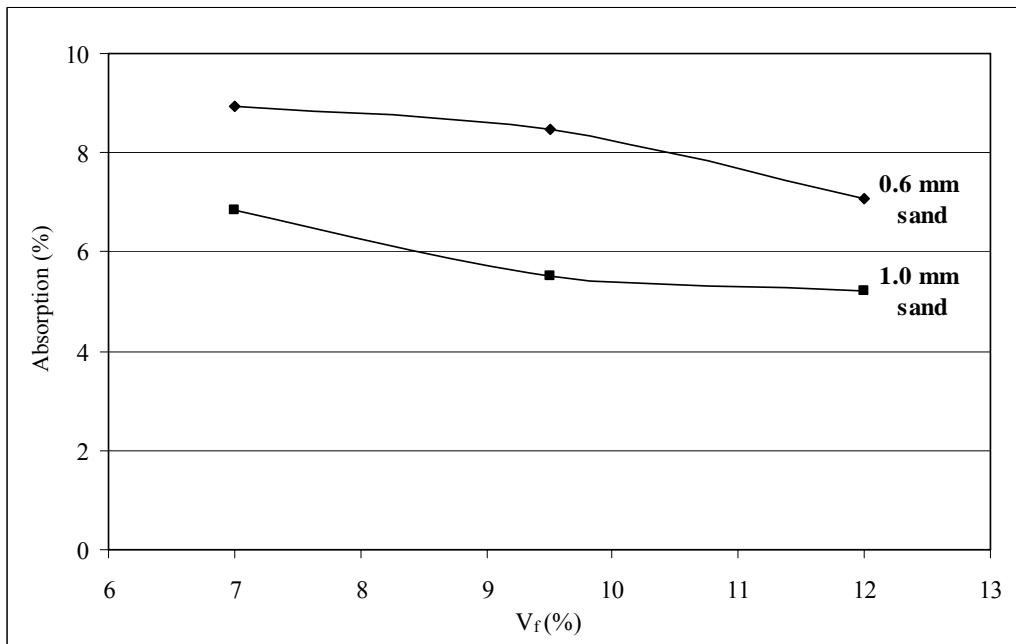


(b) With crimped fibers

Figure 4.23: Absorption vs. time in 48 hrs for mortar SIFCON with 0.6 mm sand, M2(F) and M3

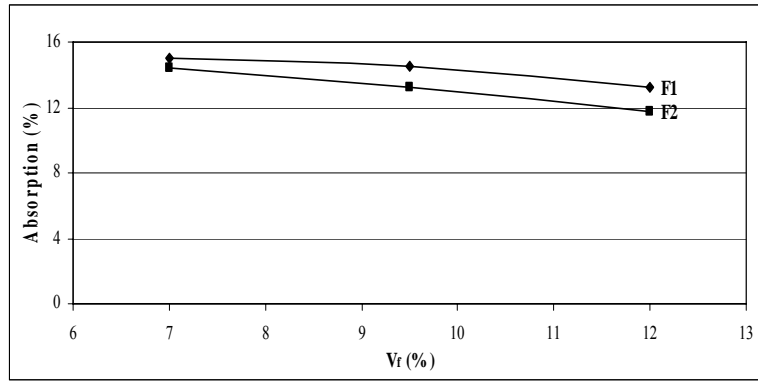


(a) With hooked fibers

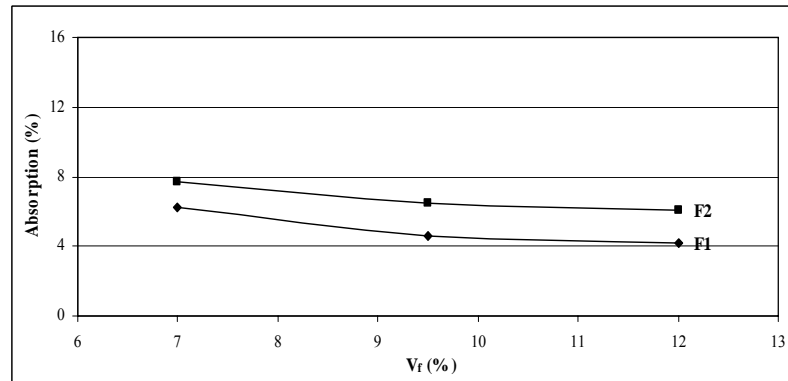


(b) With crimped fibers

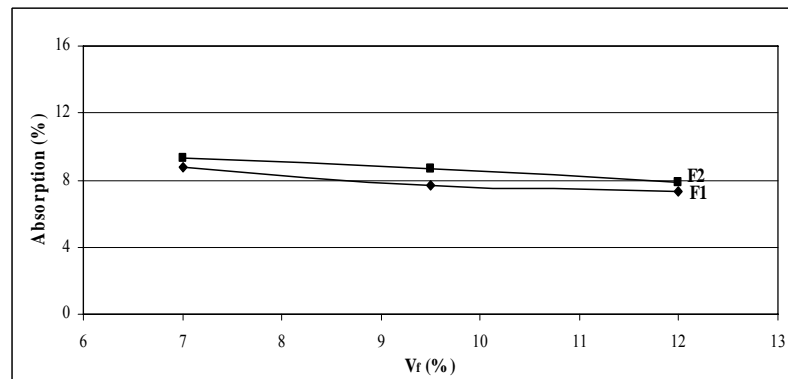
Figure 4.24: Effect of sand size on total absorption of mortar SIFCON



(a) Slurry SIFCON



(b) Mortar SIFCON with 1mm size sand



(c) Mortar SIFCON with 0.6 mm size sand

Figure 4.25: Effect of fiber type on the absorption of several SIFCON mixes

Table 4.5: Summary of water absorption results

Matrix type	Matrix ID	Absorption by total weight of specimen (%)	Absorptivity (A*)	Coef. of correlation (R²)
Plain slurry	M1	20.35 (2.7) ^(*)	0.976 (1.1)	0.960
Slurry SIFCON (hooked fibers)	M1F1 - 7	14.97 (2.5)	0.677 (1.6)	0.887
	M1F1 - 9.5	14.47 (1.8)	0.655 (1.4)	0.923
	M1F1 - 12	13.22 (3.2)	0.583 (3.4)	0.941
Slurry SIFCON (crimped fibers)	M1F2 - 7	14.13 (1.2)	0.572 (1.6)	0.915
	M1F2 - 9.5	13.22 (2.4)	0.556 (0.6)	0.925
	M1F2 - 12	11.80 (3.2)	0.500 (4.6)	0.923
Plain mortar (1.0 mm sand)	M2	9.03 (1.8)	0.276 (4.0)	0.980
Mortar SIFCON (hooked fibers, 1.0 mm sand)	M2F1 - 7	6.01 (0.8)	0.208 (1.3)	0.990
	M2F1 - 9.5	4.63 (3.9)	0.151 (4.7)	0.979
	M2F1 - 12	4.06 (1.9)	0.117 (2.1)	0.994
Mortar SIFCON (crimped fibers, 1.0 mm sand)	M2F2 - 7	6.85 (6.5)	0.223 (2.3)	0.975
	M2F2 - 9.5	5.50 (4.3)	0.156 (5.6)	0.980
	M2F2 - 12	5.22 (3.3)	0.123 (2.7)	0.979
Plain mortar (0.6 mm sand)	M2(F)	12.75 (2.4)	0.936 (3.1)	0.998
Mortar SIFCON (hooked fibers, 0.6 mm sand)	M2F1(F) - 7	8.08 (2.8)	0.355 (5.1)	0.984
	M2F1(F) - 9.5	7.12 (1.3)	0.322 (2.7)	0.981
	M2F1(F) - 12	6.79 (4.2)	0.290 (5.2)	0.987
Mortar SIFCON (crimped fibers, 0.6 mm sand)	M2F2(F) - 7	8.93 (4.8)	0.406 (4.0)	0.986
	M2F2(F) - 9.5	8.46 (3.5)	0.383 (4.6)	0.988
	M2F2(F) - 12	7.07 (4.0)	0.278 (2.2)	0.988
Control concrete	M3	3.36 (3.2)	0.179 (3.4)	0.935

(*) Numbers in parentheses represent the coefficients of variation (%).

4.4 Chloride penetration test

Corrosion of steel reinforcement, caused primarily by chloride attack, is one of the major causes of deterioration of reinforced concrete structures. SIFCON should be more susceptible to problems related to chloride penetration because, when compared to concrete, it has almost no protecting cover and it includes high quantities of steel fibers distributed throughout the SIFCON element. Accordingly, studying chloride penetration resistance was one of the main objectives of this research.

The problem of chloride attack arises usually when chloride ions ingress from outside. This can be caused by de-icing salt or sea water in contact with concrete or SIFCON. Chlorides can also deposit on the surfaces in the form of air-borne dust which subsequently becomes wetted by dew [55].

As stated earlier in Section 3.4.4, the test procedures were carried out in accordance with the standard test method AASHTO T 259 [61]. Chemical analysis of dust samples resulted in finding the total chloride contents by total weight for SIFCON specimens and control concrete. To construct chloride penetration profiles with depth, chloride contents were found at five different depths. In conventional concrete, if the amount of penetrated chloride at the steel reinforcement reaches the limiting threshold value for corrosion, the reinforcing bars start to corrode. The procedures for finding total chloride ion contents were carried out in accordance with the standard test method AASHTO T 260 [63].

Standards generally prescribe strict limits on the chloride content of the concrete from all sources. For example, BS 8110: Part 1 limits the *total* chloride ion content in reinforced concrete to 0.40 % by mass of cement [83]. The same limit is prescribed by the European Standard ENV 206 [84]. The approach of ACI 318 is to consider *water-soluble* chloride ions only. On that

basis, the chloride ion content of reinforced concrete is limited to 0.15 % by mass of cement [85]. The two values are not substantially different from one another because water-soluble chlorides are only a part of the total chloride content, namely, the free chlorides in pore water [55]. On the other hand, there are no specified limits yet related to chloride contents of SIFCON.

It can be noticed that all standards deal with chloride contents on the basis of percentage by mass of cement not by total mass of the tested dust sample. This is because the resistance of concrete to corrosion, caused by chloride penetration is related mainly to its cement content. Generally, the higher is the cement percentage of total weight, the better is the resistance to corrosion. Simply, the higher cement contents results in more CH products, and hence higher pH values. It is assumed that there is a direct proportionality between pH value and protection to reinforcement against corrosion.

In view of the above, the results will be discussed in the following sections, mainly, on the basis of chloride content by mass of cement. The cement contents of different mixtures tested in this investigation, Table 4.6, are expected to play an important role in evaluating threshold contents of chloride ions in SIFCON.

Table 4.6: Cement contents by total weight in mixtures under study

Mixture	Cement percentage in total weight (%)
Slurry (M1)	71.43
Mortar (M2)	41.45
Control concrete (M3)	20.14

Based on the fact that steel fiber pieces were removed from dust samples using a magnetic plate, all samples were chemically analyzed in the form of plain cement paste, mortar or concrete.

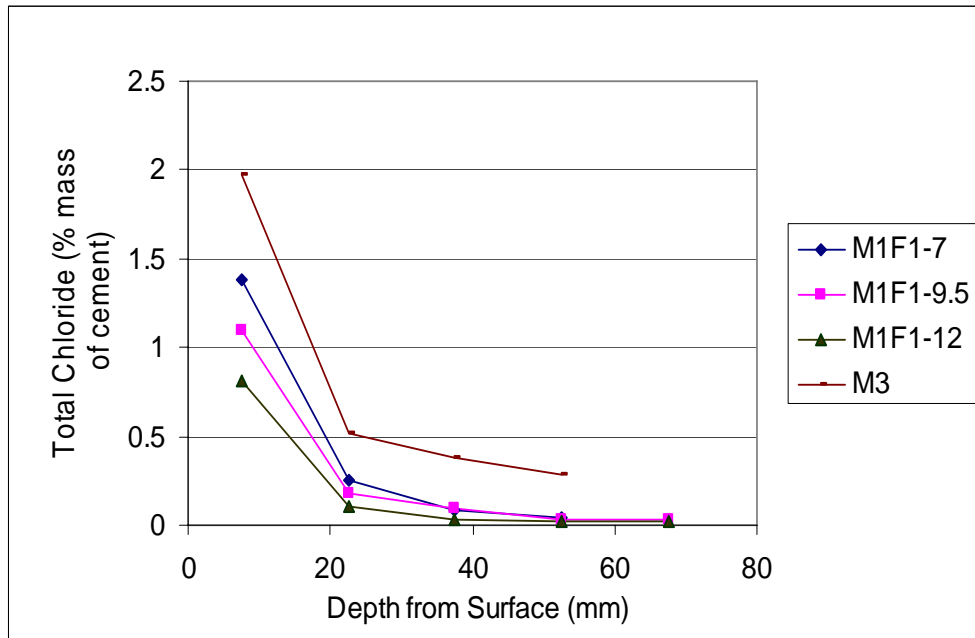
4.4.1 Analysis of total chloride contents by weight of cement

The chloride ion profiles of slurry SIFCON and mortar SIFCON are shown in Figures 4.26 and 4.27 respectively. The two figures demonstrate in a clear way that SIFCON, either made with slurry or mortar, has shown less chloride contents by mass of cement when compared with the control concrete. Even when chloride percentages were calculated as a fraction of the total weight, Section 4.4.2, SIFCON showed higher chloride content comparing with control concrete only in the first portion of the depth (0 – 15 mm).

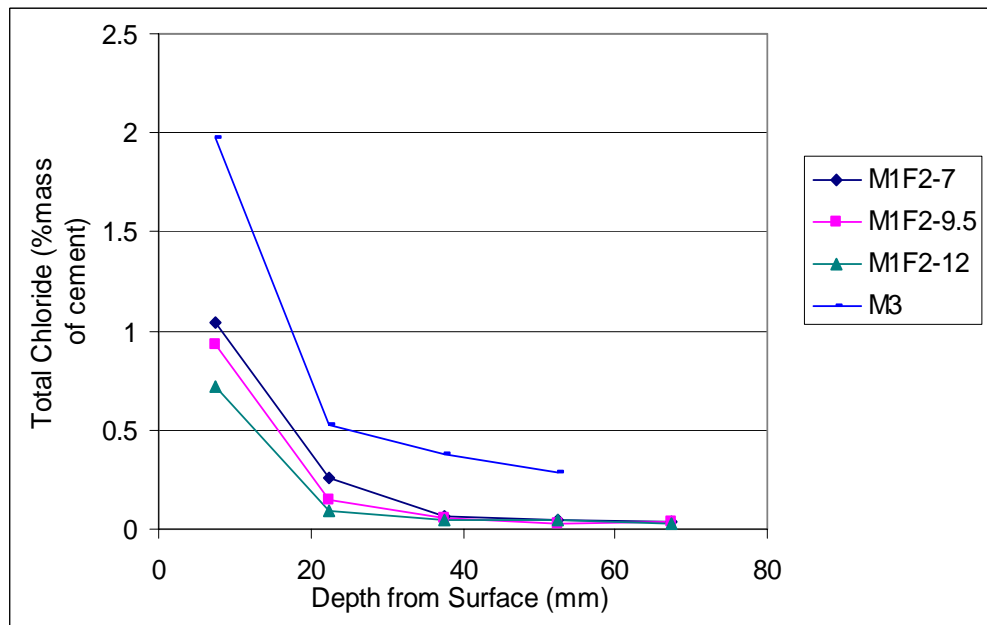
However, what matters is not how much chloride is absorbed and infiltrated through SIFCON matrix, but how much is the percentage of chloride ions with respect to the weight of the cement ingredient. Figures 4.26 and 4.27 show also the already expected behavior of decreasing of chloride contents with depth from surface. The degree of decrease in chloride content with increasing the depth depends mainly on the permeability of the material.

In spite of the fact that the results of water permeability test, Section 4.3, proved that SIFCON has high absorption capacity, its high cement contents, especially in slurry SIFCON, made the chloride content always less than that recorded in control concrete when calculated with respect to cement weight in accordance with the standards mentioned earlier [83-85]. This was true in all mixtures of slurry SIFCON and mortar SIFCON.

Another finding was that the drop in chloride content from the first depth (average 7.5 mm) to the next depth (average 22.5 mm) was more appreciable in SIFCON when compared with concrete, Table 4.7. The lesser percentages in the table indicate that the drop in chloride content after the first portion of the depth (> 15 mm) is higher. The very dense steel fiber network causes a higher drop in the amount of penetrated chloride after the more permeable first depth which corresponds to the surface layer of 15 mm thickness when compared to control concrete.

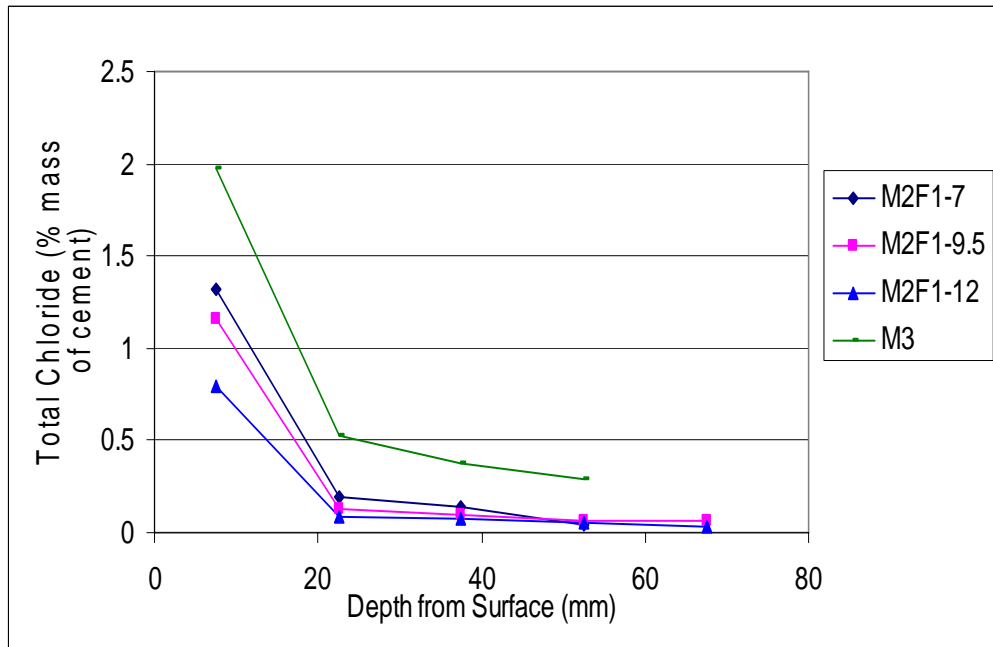


(a) Hooked fibers

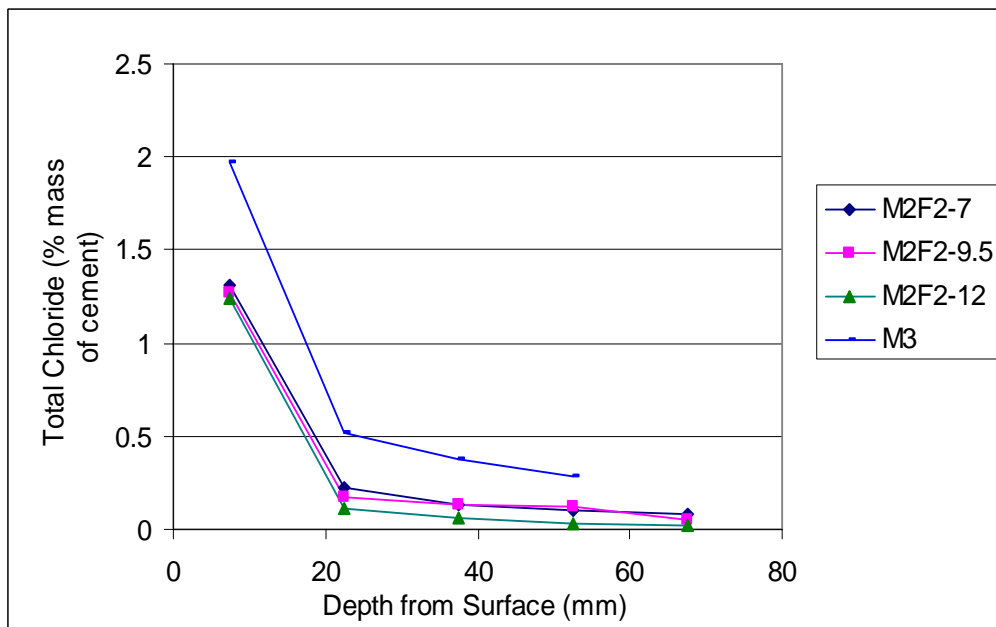


(b) Crimped fibers

Figure 4.26: Chloride ingress profiles for slurry SIFCON vs. control concrete (Based on chloride content by mass of cement)



(a) Hooked fibers



(b) Crimped fibers

Figure 4.27: Chloride ingress profiles for mortar SIFCON vs. control concrete (Based on chloride content by mass of cement)

It can be assumed that the concentration of steel fibers in the core of SIFCON is well higher than that of the outer few millimeters. It can be noticed, as well, that the higher the fiber fraction, the more is the decrease in chloride content in the following depth. To prove this assumption, slices were cut from selected SIFCON samples, and the densities were calculated. The results are shown in Table 4.8.

In all cases, inner layers of SIFCON (15-30 mm) were 12 % to 16 % more dense than the exterior surface layers (Table 4.8). This may explain the reason of the higher reduction in chloride contents in deeper segments when compared to control concrete in which the edge effect is irrelevant. In some SIFCON specimens, chloride contents in the second depth (15 – 30 mm) were as low as 10 % of the chloride concentration found in the outer layer.

Table 4.7: Effect of depth from surface on reduction of chloride ions ingress

Matrix type	Matrix ID	Chloride content at depth of 22.5mm from surface with respect to that at 7.5mm depth (%)
Slurry SIFCON (hooked fibers)	M1F1-7	18.5
	M1F1-9.5	16.7
	M1F1-12	13.0
Slurry SIFCON (crimped fibers)	M1F2-7	25.0
	M1F2-9.5	15.7
	M1F2-12	12.3
Mortar SIFCON (hooked fibers)	M2F1-7	14.6
	M2F1-9.5	11.1
	M2F1-12	10.7
Mortar SIFCON (crimped fibers)	M2F2-7	17.2
	M2F2-9.5	13.6
	M2F2-12	8.6
Control concrete	M3	26.5

This percentage was about 27 % in the control concrete. Accordingly, it can be stated that most of the absorbed water in the water absorption test carried out on SIFCON mixtures was absorbed by the outer layers, because of the surface cracks and the lesser density (Table 4.8). Although water will be absorbed more by the surface portions of SIFCON due to surface cracking, the relatively low density of fibers and the high permeability of plain slurry or mortar in these portions of SIFCON, the absorbed quantity decreases substantially in the core of the SIFCON material. This appreciable reduction can be attributed to higher density of fibers, and the absences of cracking in the deepest portions of SIFCON.

Table 4.8: The influence of edge effect on density of SIFCON

Matrix type	Matrix ID	Density of depth 0-15 mm (ρ_1 , g/mm ³)	Density of depth 15-30 mm (ρ_2 , g/mm ³)	$\rho_2/\rho_1 \times 100$ (%)
Slurry SIFCON (hooked fibers)	M1F1-7	0.002263	0.002621	116
	M1F1-9.5	0.002349	0.002674	114
	M1F1-12	0.002522	0.002816	112
Mortar SIFCON (hooked fibers)	M2F1-7	0.002552	0.002902	114
	M2F1-9.5	0.002597	0.002937	113
	M2F1-12	0.002689	0.003020	112

The surface cracking occurs due to the drying shrinkage that took place in the 28 days period of drying the specimens in the lab environment. This relatively long period of drying, after curing, was in accordance with the requirements of the related standard test method [61], but it caused the development of shrinkage cracks before starting the test, especially in slurry SIFCON specimens.

In the case of concrete, because there are no visible cracks caused by drying on the surfaces, the absorption of the surface layer was less comparing to SIFCON. On the other hand, the degree of decrease in absorption in deeper depths of concrete was not as high as the case of SIFCON because of the absence of the effects of surface cracks and steel fibers.

In short, the high permeability of SIFCON realized by water absorption test does not necessarily lead to high chloride penetration in deeper portions. It was found that about 80 % of the cumulative chloride contents in all depths of SIFCON existed in the outer 15 mm of SIFCON specimens. This percentage was only 60 % in the case of the reference concrete.

However, although the total chloride contents by mass of cement in all SIFCON matrices were well lower than that of the low permeability control concrete, these contents in the outer layers were higher than the limit accepted by the standards mentioned earlier, which is limited to 0.40 % by mass of cement [83, 84]. This is expected to result in corrosion problems in SIFCON if its surface is not protected with some appropriate protective overlays with enough thickness. These overlays can be made of low permeability plain concrete. Different from traditional reinforced concrete, where steel reinforcement is protected from the environment by the cover, the steel fibers in SIFCON are exposed to the surface with very thin cover, or practically without any cover at all.

4.4.1.1 Effect of fiber volume fraction

As expected, generally, the increase in steel fiber content in SIFCON matrix leads to reduction in chloride penetration. This finding is in conformance with the results of water absorption test, and the same reasoning of the influence of fiber volume fraction on water absorption is applicable in the case of interpreting the results of chloride penetration test. This can be seen in the

Figures 4.26 and 4.27. The effects of fiber volume fractions are more pronounced in the first depth (0 – 15 mm). The chloride contents in the deeper depths become less affected by the fiber content.

4.4.1.2 Effect of SIFCON matrix type

It was found previously that slurry SIFCON had higher absorptivity than mortar SIFCON when the absorption is calculated with respect to the total weight of the matrix, Section 4.3.2.2. Anyhow, finding chloride contents in SIFCON as percentage by weight of cement, not the total weight, resulted in the following:

- a) When hooked fibers are used, Figure 4.28, the chloride profiles of both slurry SIFCON and mortar SIFCON nearly coincide with each other.

- b) When crimped fibers are used, Figure 4.29, slurry SIFCON showed better performance than mortar SIFCON when it comes to penetrated chloride contents by weight of cement. The reason for this, which was observed only in the case of crimped fibers, can be related to the low chloride concentrations in slurry SIFCON made with crimped fibers which when presented as percentages by weight of cement were even lower than the chloride concentrations of mortar SIFCON presented in the same way. Nevertheless, the differences were clear only in the first depth representing the surface layer.

4.4.1.3 Effect of fiber type

In this case, dealing with either chloride percentages with respect to total weight or to cement weight will not affect the findings related to the influence of fiber shape on chloride penetration.

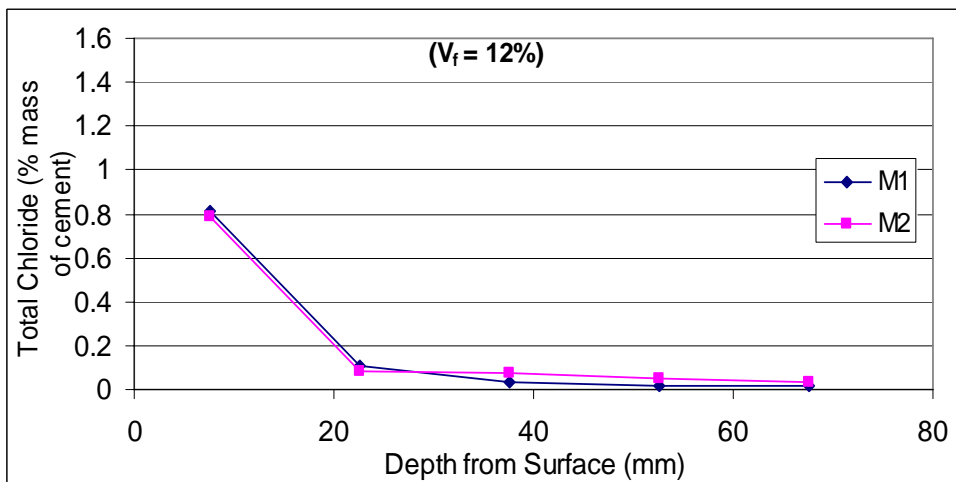
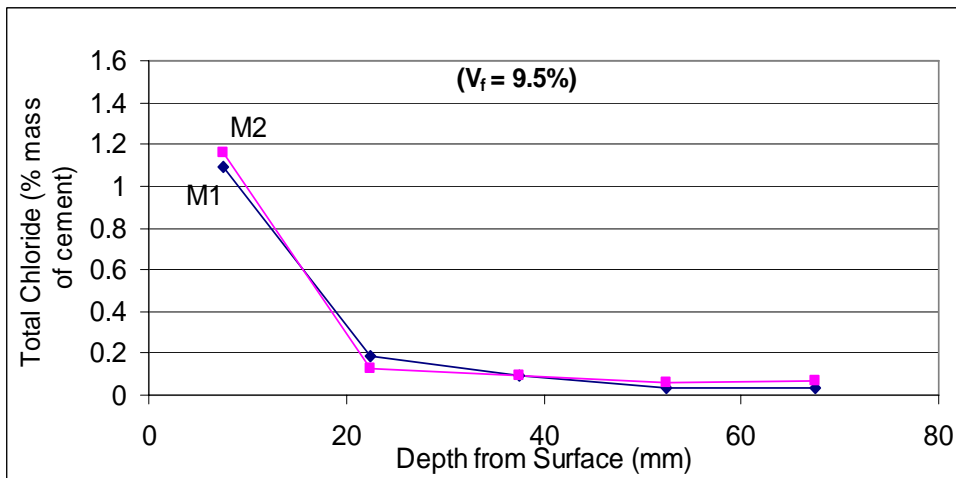
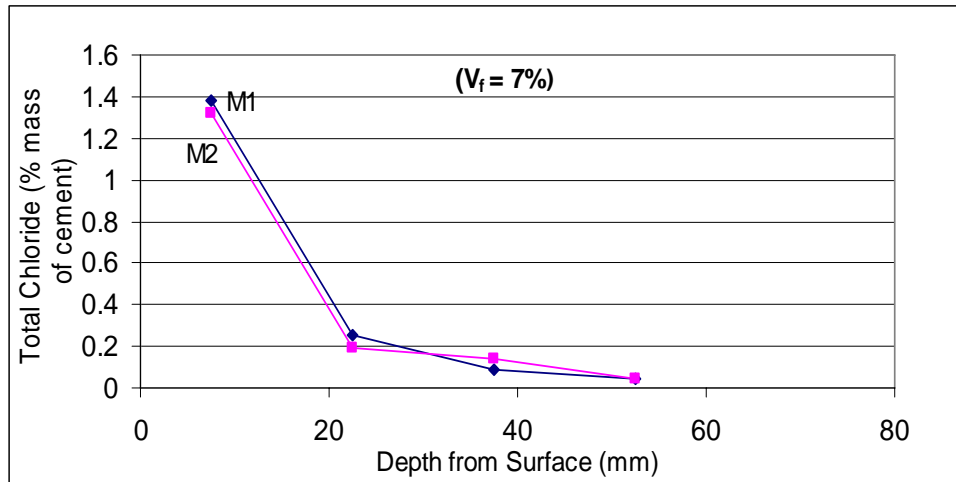


Figure 4.28: Effect of mix type on chloride penetration when hooked fibers (F1) are used (Based on chloride content by mass of cement)

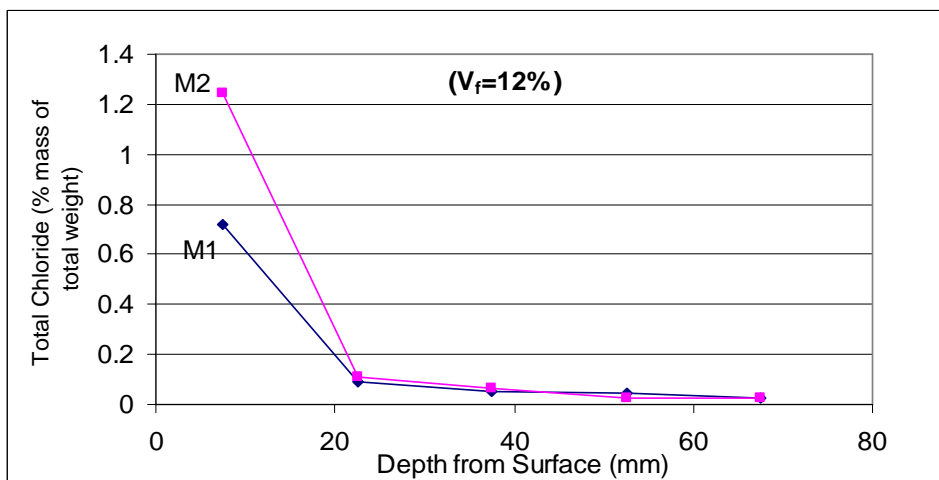
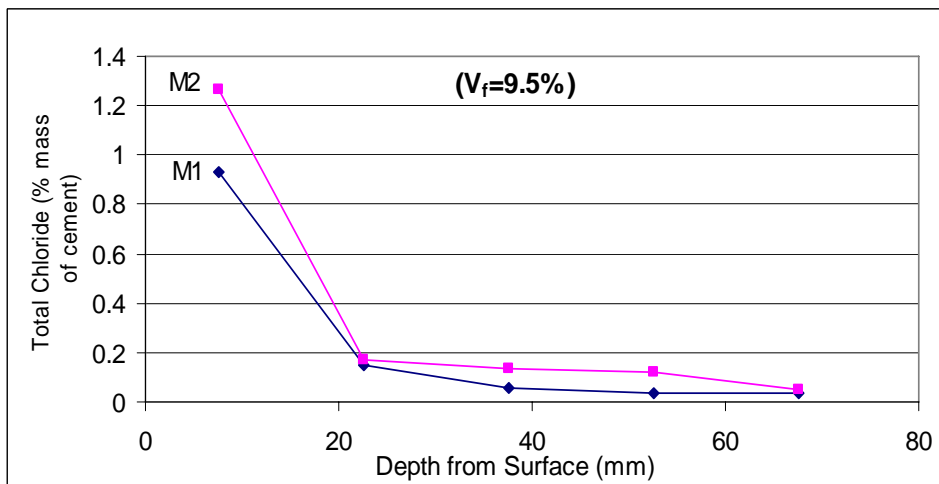
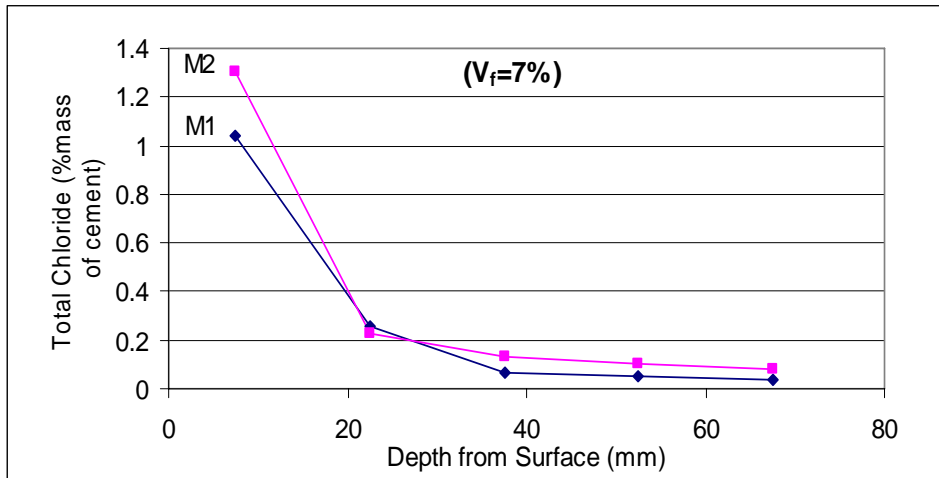


Figure 4.29: Effect of mix type on chloride penetration when crimped fibers (F2) are used (Based on chloride content by mass of cement)

In the case of slurry SIFCON, Figure 4.30, crimped fibers have reduced chloride penetration in the surface layers slightly better than hooked fibers did. As previously mentioned in Section 4.3.2.3, this finding is in conformance with the results of water absorption test also. On the other hand, for mortar SIFCON, Figure 4.31, it was found that changing fiber type was not effective except for the case of V_f of 12 % where specimens made with hooked fibers showed less chloride penetration. Again, the same behavior was also noticed in the water absorption test.

4.4.2 Total chloride contents by total weight

As stated in Section 4.4, all related standards limit chloride contents in concrete to certain values as a percentage of cement used, not as a percentage of total mass of concrete (or SIFCON). Therefore, the chloride profiles constructed with respect to the total weight are given only for comparative purposes in Appendix C.

4.4.3 Chloride diffusion coefficients (D_a)

Chloride diffusion coefficient is a value which describes numerically the diffusivity of concrete. The diffusion coefficient can be used for service-life prediction calculations of concrete structures. When the diffusion coefficient and the depth of reinforcement are known, simple diffusion equations can be used to calculate an estimate for the time necessary for a critical chloride level to reach the reinforcement [86, 87].

The use of diffusion coefficients to describe the ingress of chloride ions into concrete dates back to 1972 [88]. The chloride ingress could be approximated by Fick's second law of diffusion for non-stationary flow into a semi-infinite medium.

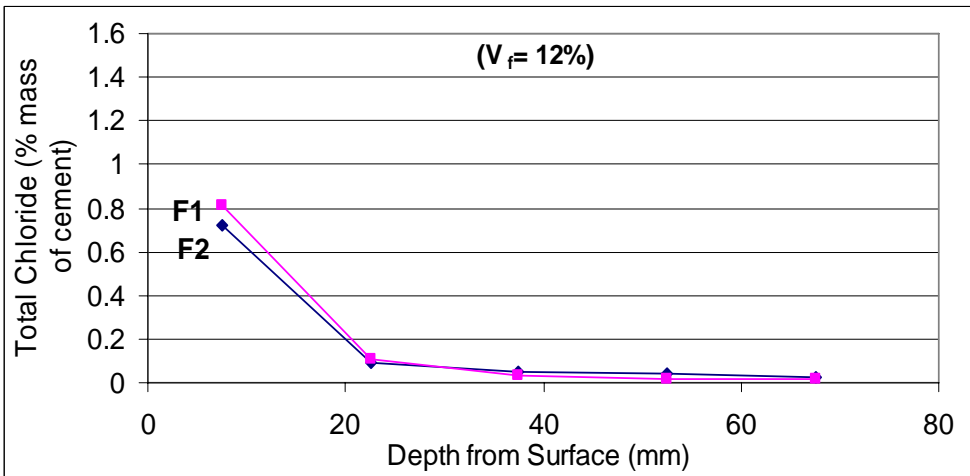
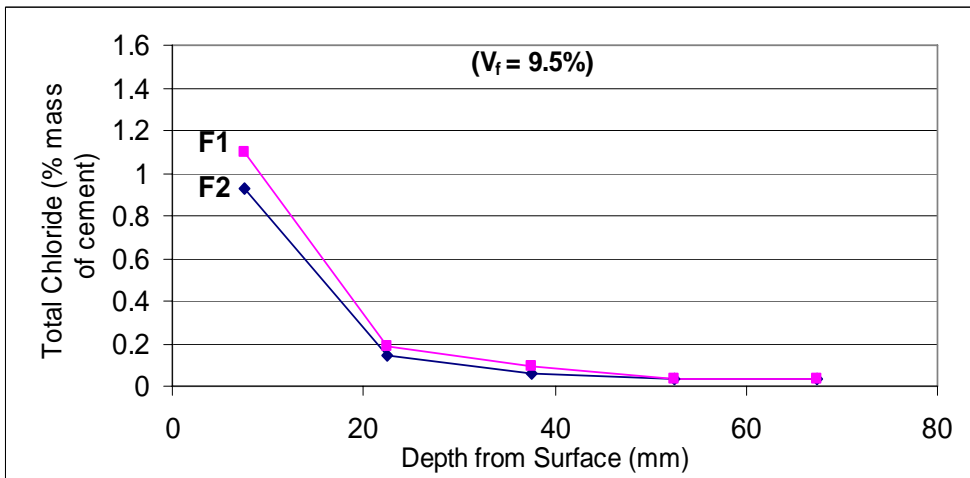
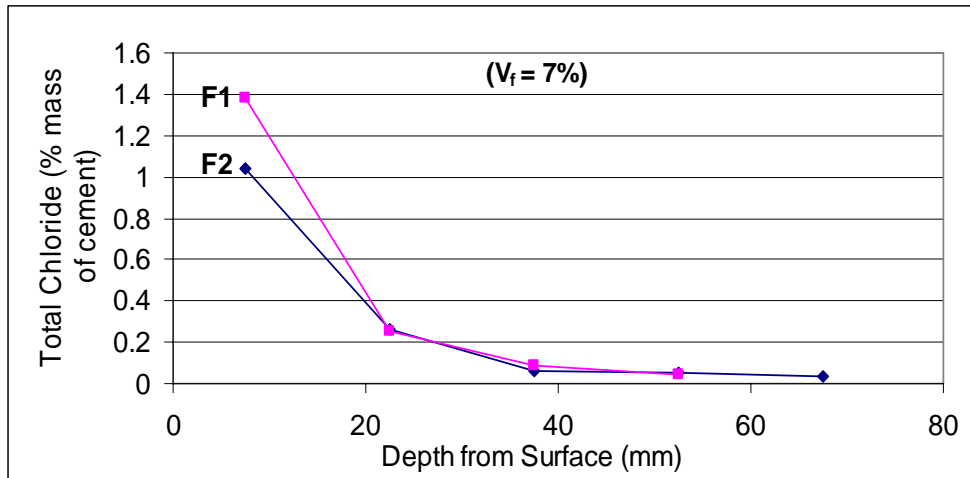


Figure 4.30: Effect of fiber type on chloride penetration of slurry SIFCON (Based on chloride content by mass of cement)

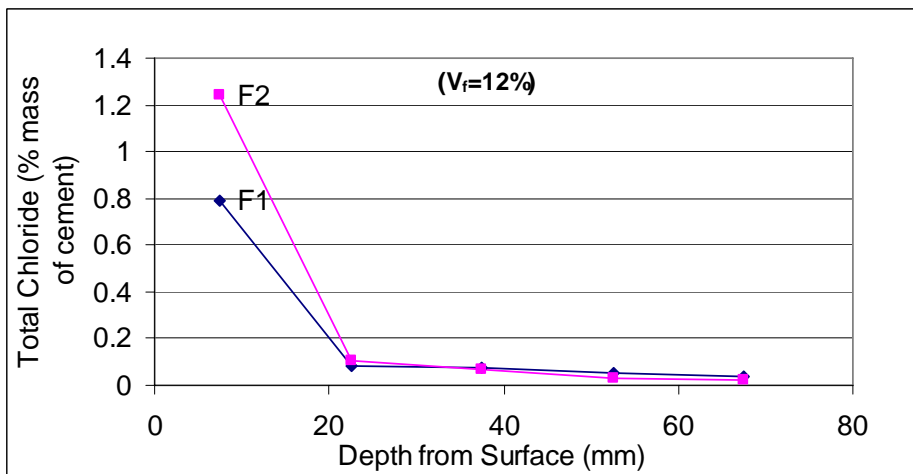
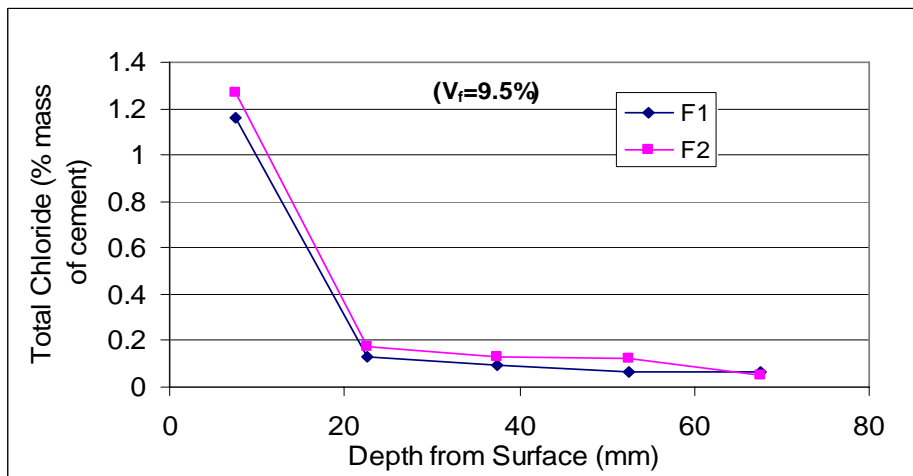
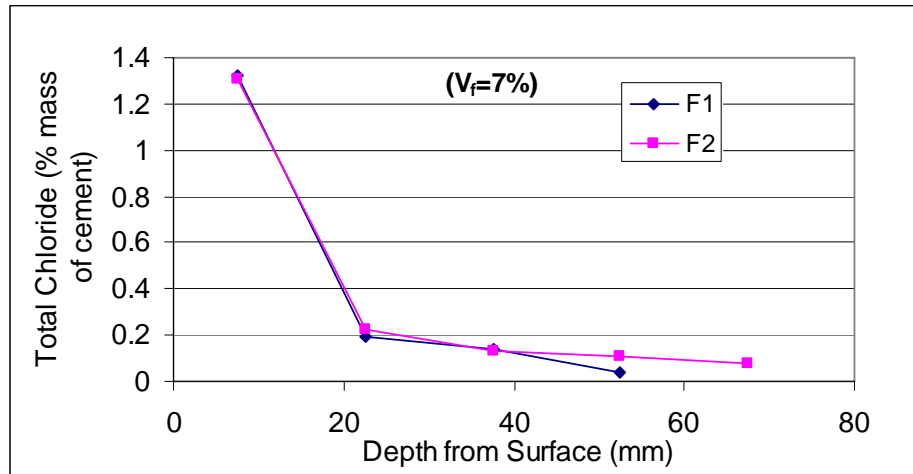


Figure 4.31: Effect of fiber type on chloride penetration of mortar SIFCON (Based on chloride content by mass of cement)

The analytical solution to Fick's second law is given by:

$$C_{x,t} = C_s \left(1 - \operatorname{erf} \left(\frac{x}{2\sqrt{D_a t}} \right) \right) \quad (4.1)$$

where: $C_{x,t}$ = Chloride concentration at depth x and time t ,

C_s = Chloride content at the surface (%),

x = depth (m),

t = time (s),

erf = error function,

D_a = apparent chloride diffusion coefficient (m^2/s)

Values of C_s and D_a are found by iteration to produce the best fit by least squares approximation. In fact, the process of obtaining a diffusion coefficient depends on some assumptions without proper statements on the exact procedure. Therefore, it is not surprising if two people obtain different values of D_a from the same data due to the influence of the methodology employed on the results [86].

Consequently, D_a values for SIFCON used in this research were calculated and compared with that of control concrete. It was found that the values of D_a are more sensitive to chloride contents in the deeper depths. Using the chloride concentration value either on the basis of mass of cement or total weight will not affect the results of D_a . The procedure of obtaining D_a values was carried out using a Microsoft Excel software. The results are given in Table 4.9, whereas the comparisons between the models and the experimental data are given in Appendix C.

The results shown in Table 4.10 demonstrate that D_a values of SIFCON, in general, range from 8×10^{-12} to 17×10^{-12} m^2/s approximately. This range is 1.5 to 3 times lower than the D_a value recorded for concrete which was 25×10^{-12}

m^2/s . The low chloride contents of SIFCON in deeper depths ($> 20 \text{ mm}$) compared with concrete, made the D_a values of SIFCON less than that of concrete, although, as a whole, concrete was found to be less permeable than SIFCON in the water absorption test. This means that the diffusivity of chlorides in SIFCON is even less than the diffusivity of low permeability concrete due to the effects of dense steel fiber network included in SIFCON. However, this should not be considered as an advantage of SIFCON over concrete if steel fibers are not protected by some sort of suitable overlays.

Table 4.10: Best-fit diffusion coefficients for SIFCON and concrete

Matrix type	Matrix ID	$D_a (\times 10^{-12} \text{ m}^2/\text{s})$
Slurry SIFCON (hooked fibers)	M1F1-7	13.35
	M1F1-9.5	12.60
	M1F1-12	10.17
Slurry SIFCON (crimped fibers)	M1F2-7	17.22
	M1F2-9.5	11.76
	M1F2-12	9.97
Mortar SIFCON (hooked fibers)	M2F1-7	11.49
	M2F1-9.5	9.45
	M2F1-12	9.27
Mortar SIFCON (crimped fibers)	M2F2-7	13.10
	M2F2-9.5	10.98
	M2F2-12	8.08
Control concrete	M3	25.00

Most of the observations related to the effects of fiber content, fiber type, and SIFCON matrix type on chloride penetration and absorptivity were noticed here also. For example, increasing fiber content resulted in reduced D_a values for all SIFCON types. In addition, mortar SIFCON had smaller D_a values when compared to slurry SIFCON.

4.5 Freezing and thawing test

There is no doubt that the deterioration in concrete structures due to freezing and thawing is one of the major durability problems of the concrete industry in cold climates. Freezing and thawing may damage concrete structures seriously. Therefore, one of the purposes of this study was to determine the behavior of various SIFCON matrices exposed to freezing and thawing, and to compare it with the performance of control concrete of low permeability tested under the same conditions.

The details of the test method were presented earlier in Section 3.4.5. The results of the test are presented and discussed below. The method used to assess SIFCON and concrete deterioration due to freezing and thawing was to measure the change in the dynamic modulus of elasticity (DME) and weight. In addition, visual inspection of the specimens throughout the different stages of the test helped in assessing the deterioration.

4.5.1 Change in dynamic modulus of elasticity

Initial measurements of DME were taken before starting the test. Afterwards, at the end of every 100 cycles of freezing and thawing, measurements of DME were taken again, and the relative dynamic modulus of elasticity (RDME) with respect to the initial value was considered. According to ASTM C 666, the specimens are considered to have failed when DME reaches 60 % of the initial modulus [65].

The values of DME were calculated based on the following approximate theoretical relationship:

$$\text{DME} = \rho \cdot v^2 \quad (4.2)$$

where: $v =$ The ultrasonic pulse velocity (UPV) in m/s

$\rho =$ The density in kg/m^3
 $DME =$ The dynamic modulus of elasticity in N/m^2

4.5.1.1 Drop in RDME in plain mixes

Figure 4.32 presents the results of drop in RDME for plain slurry, mortar and concrete. The big drop in RDME for plain slurry can be noticed. This drop after 300 cycles was close to the failure limit of 60 % as specified by ASTM C 666 [65]. This observation can be related to the high absorption of slurry when compared with concrete or mortar. The more ingress of NaCl solution in slurry caused more internal pressures due to freezing and thawing. This pressure caused internal damage in the form of cracks, which in turn caused some decrease in UPV, and consequently lower DME, and more drop in RDME.

On the other hand, plain mortar and concrete performed much better with a drop in RDME of only 10 % approximately.

4.5.1.2 Effect of steel fibers on RDME drop in SIFCON

In general, it is found that incorporating steel fibers in SIFCON had shown positive effects on decreasing internal damage that may happen due to freezing and thawing. The drop in values of RDME is a good indicator to assess the damage that can occur inside SIFCON specimens. The higher is the V_f , the lesser is the drop in RDME, and hence the less the deterioration. This was true for both slurry SIFCON and mortar SIFCON as can be seen in Figures 4.33 and 4.34. The positive effect of fibers on reducing the drop in RDME compared with plain mixes is more pronounced in slurry SIFCON. In all cases, the drop was less than 10 %.

This behavior is expected to be a direct result of the role of steel fibers in reducing absorption which was found also in the water absorption and chloride penetration tests. In addition, fibers aid in arresting the microcracks induced in the matrix by the internal pressure that built up as a result of frost action. Some previous studies mentioned also the positive effect of using steel fibers in restraining the decline of DME, and then improving frost resistance, even when included in small fractions in normal fiber reinforced concrete, paste and mortar [66, 67, 89-91].

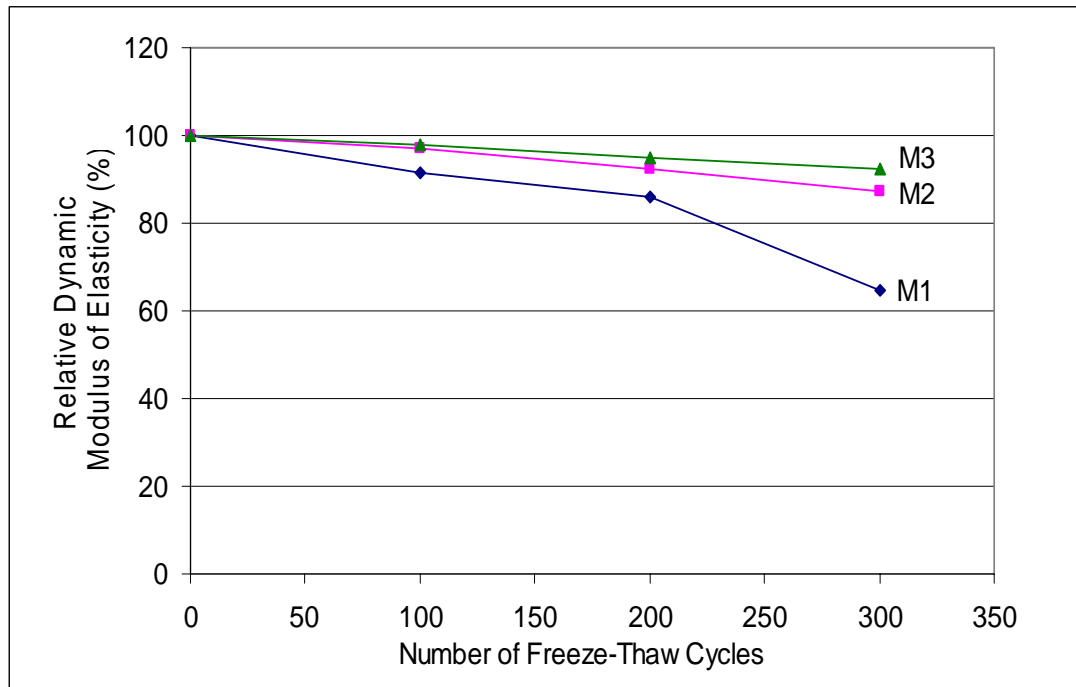


Figure 4.32: Drop in RDME for plain mixes

4.5.1.3 Influence of matrix type on drop in RDME

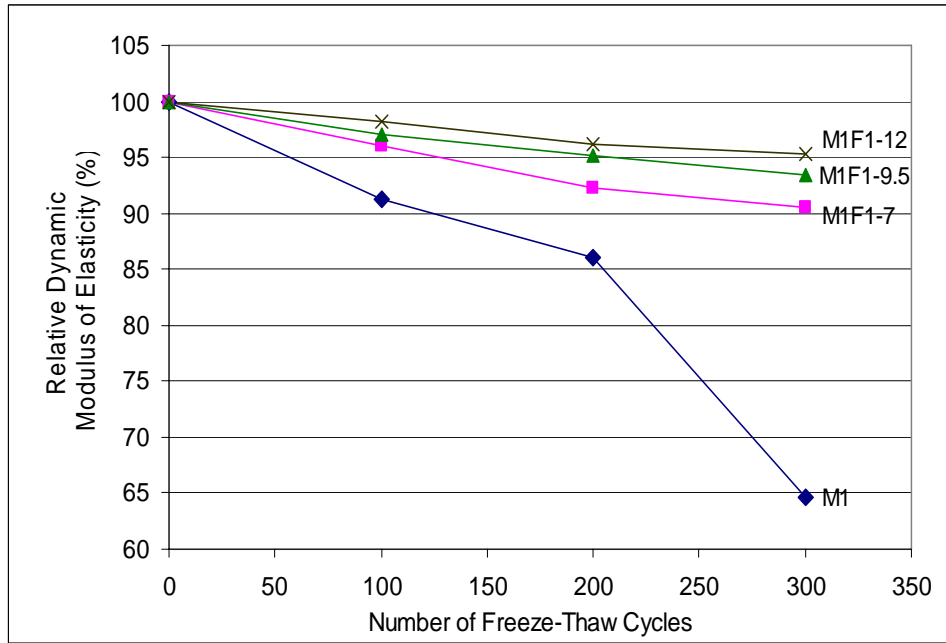
Figure 4.35 presents the results of reduction in DME with respect to the initial values as a result of freeze-thaw cycles. It can be concluded that the results of

the two SIFCON mix types were very close to each other, with only very slightly better performance recorded in mortar SIFCON over slurry SIFCON. This observation is again in conformance with the results of water absorption and chloride penetration tests, and it was applicable for mixes made with both hooked and crimped fibers.

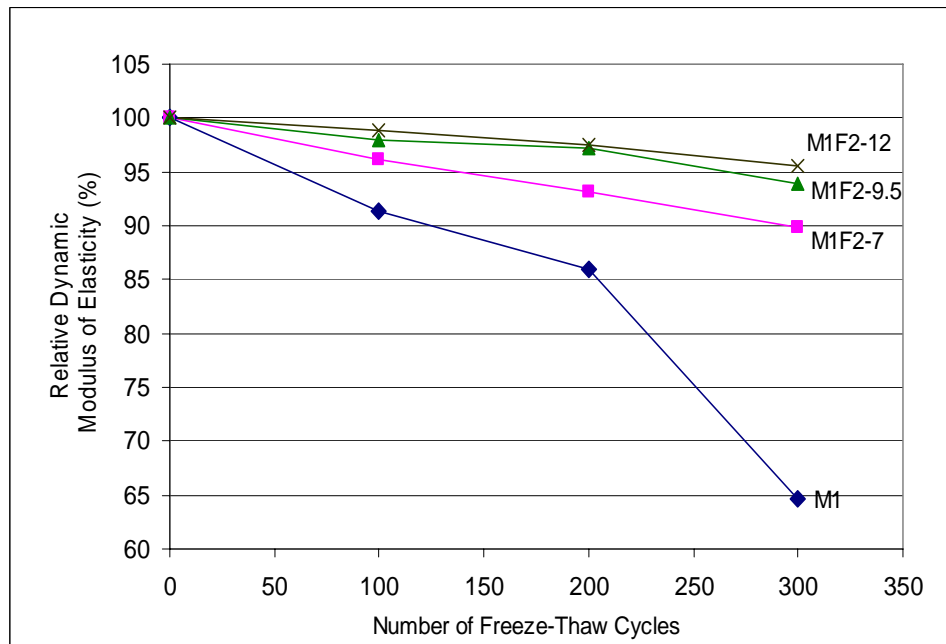
The only difference in this case, is that mortar SIFCON was not noticeably better than slurry SIFCON. The reason is that also slurry SIFCON showed substantially less drop of DME when compared with plain slurry. This restraining effect was very similar and close to what was observed in mortar SIFCON.

4.5.1.4 Effect of fiber type on RDME drop

As mentioned above, both hooked and crimped fibers have shown good effects on decreasing the drop in RDME. The differences between the results of the two types were practically negligible, with very slightly better behavior of hooked fibers over crimped ones in the case of mortar SIFCON as can be examined from Figure 4.36.

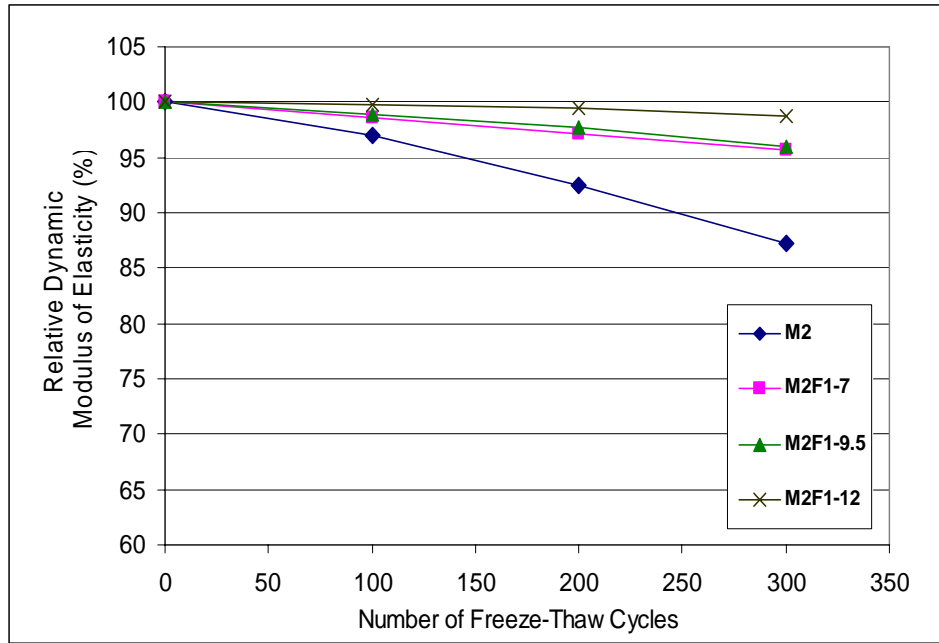


(a) With hooked fibers

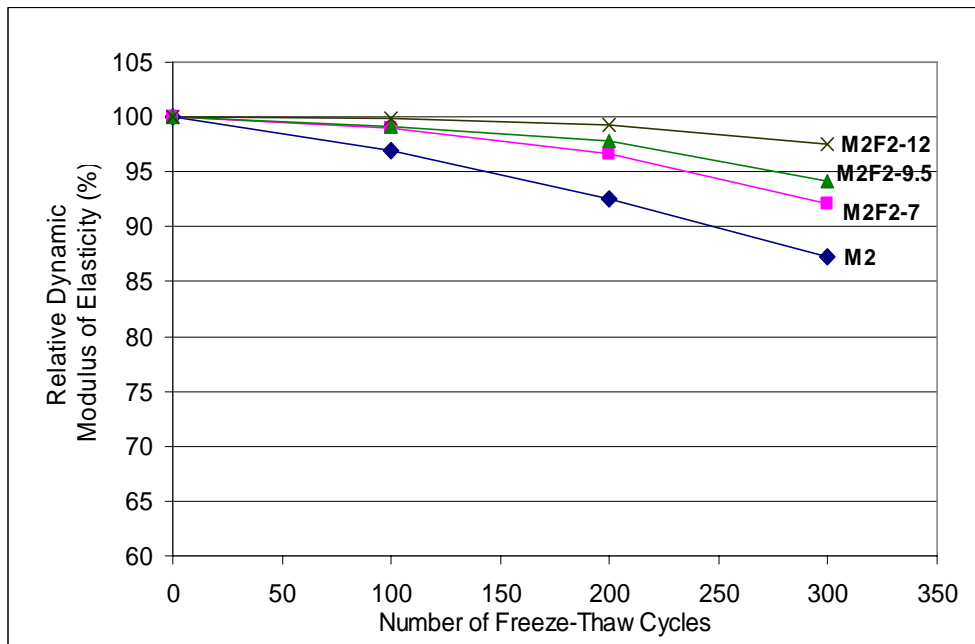


(b) With crimped fibers

Figure 4.33: Drop in RDME for slurry SIFCON vs. plain slurry

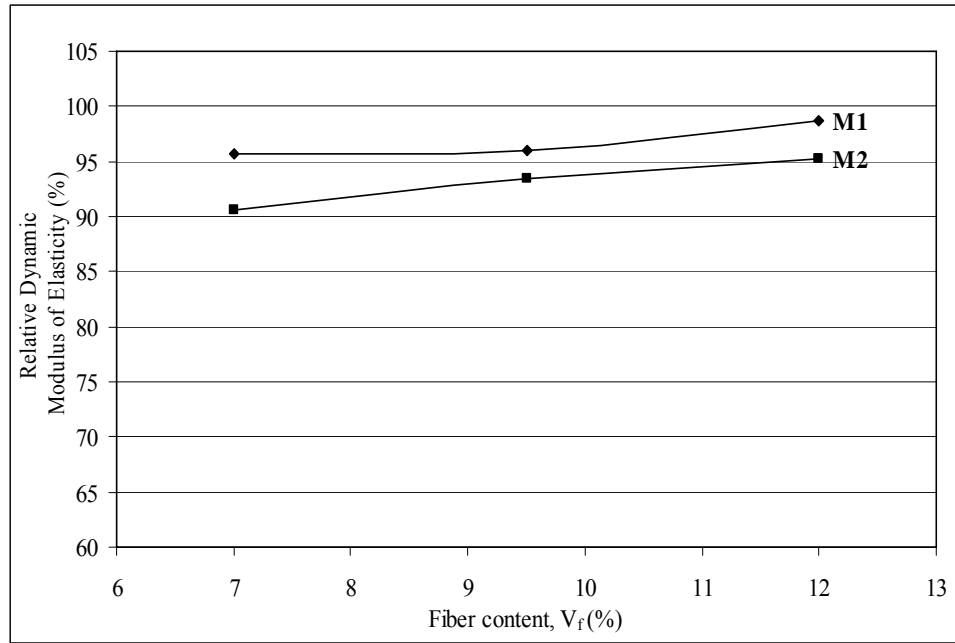


(a) With hooked fibers

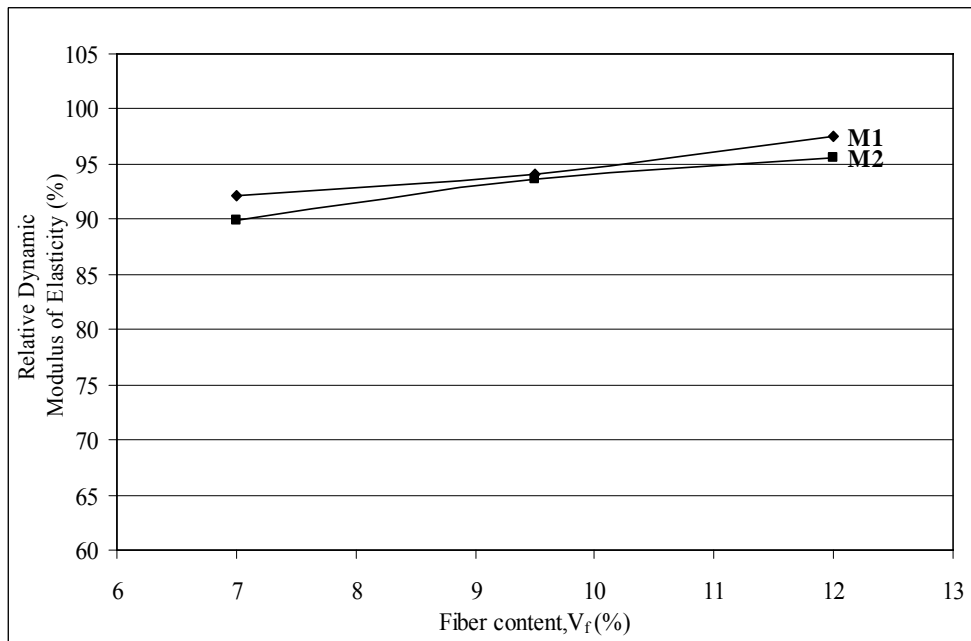


(b) With crimped fibers

Figure 4.34: Drop in RDME for mortar SIFCON vs. plain mortar

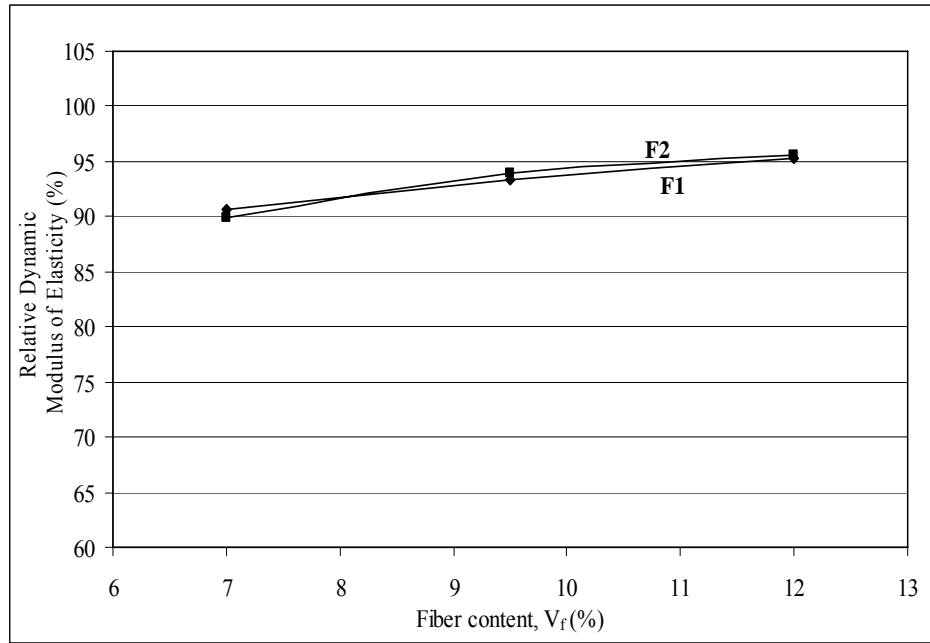


(a) With hooked fibers

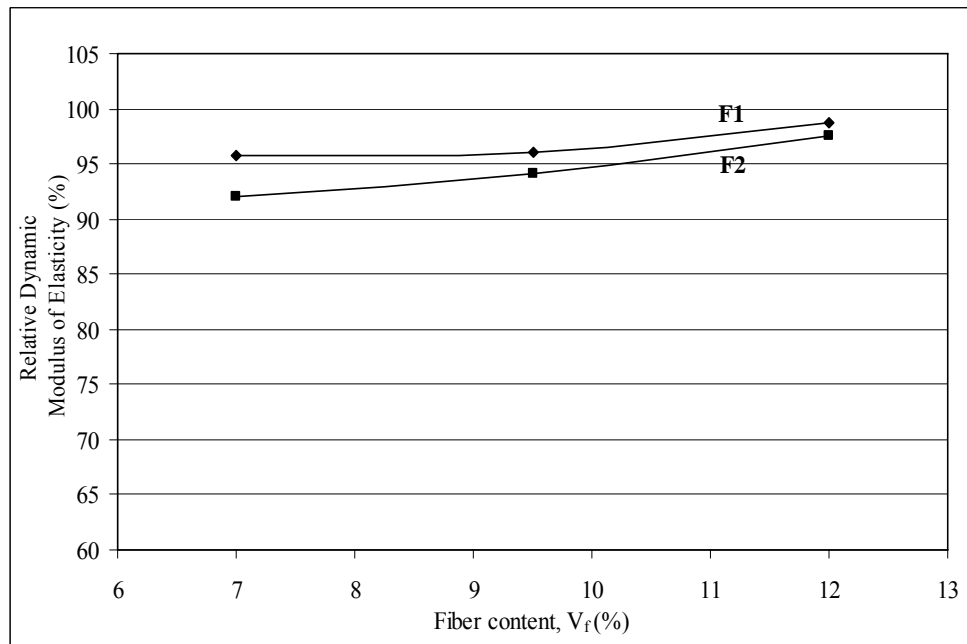


(b) With crimped fibers

Figure 4.35: Effect of mix type on drop in RDME after 300 freeze-thaw cycles



(a) Slurry SIFCON



(b) Mortar SIFCON

Figure 4.36: Effect of fiber type on RDME drop after 300 freeze-thaw cycles

4.5.2 Weight loss

Another important concept to assess the damage caused by freeze-thaw cycles is to weigh the specimens after specified number of cycles, and to measure the weight losses with respect to the initial weight before starting the test. The weight loss, if any, is due to surface scaling in specimens as a result of the deterioration effect caused by repetitive freezing and thawing. According to the test procedure, the specimen is considered to have failed if its weight loss exceeded 5.0 % [65].

4.5.2.1 Weight loss in plain mixes

The plain slurry specimens showed excessive and progressive deterioration during the test, responding to the effects of freeze-thaw cycles. As a result, the weight loss after terminating the test was very close to the failure limit of 5.0 %. On the other hand, plain mortar and concrete experienced quite small weight loss of less than 0.4 %.

Figure 4.37 illustrates the weight loss results of the plain matrices, while Figure 4.38 shows the severe deterioration of slurry when compared to mortar and concrete. This behavior can be attributed to the higher absorption of plain slurry, which was proven already by the water absorption test.

4.5.2.2 Effect of steel fiber content on weight loss

Adding steel fibers to slurry mixes had a great effect on reducing the weight loss (deterioration) of the plain matrices as illustrated in Figure 4.39. The weight loss was reduced from about 5 % to less than 1 %. The effects of fiber content itself was very limited where the weight loss results after 300 freeze-thaw cycles were all close to each other.

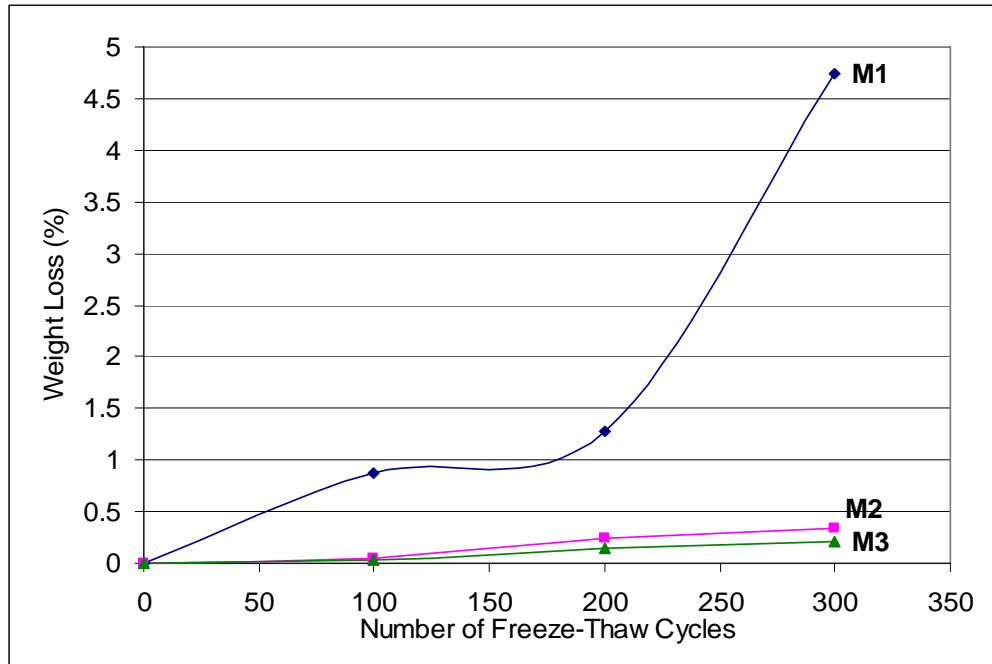
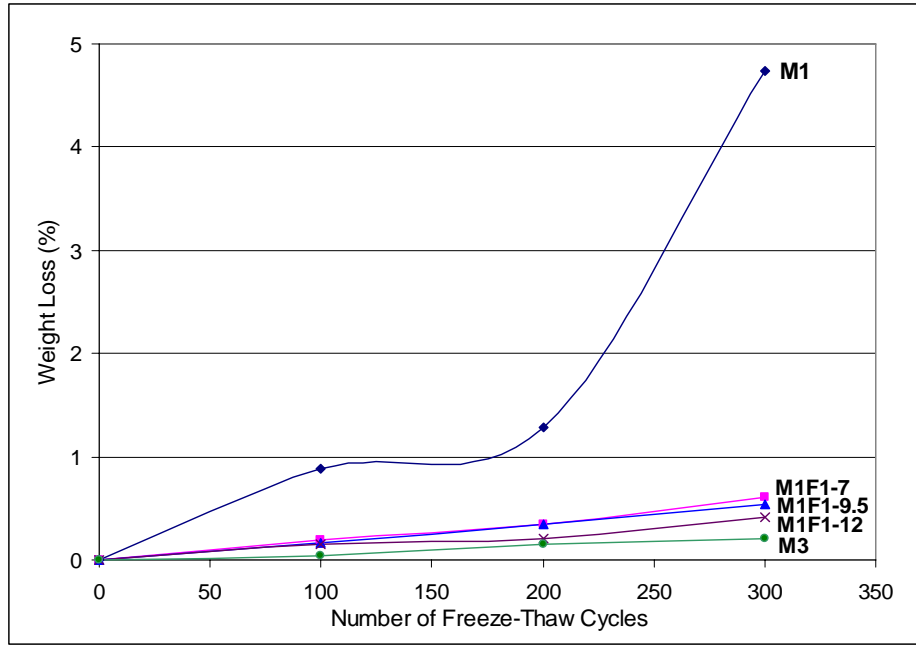


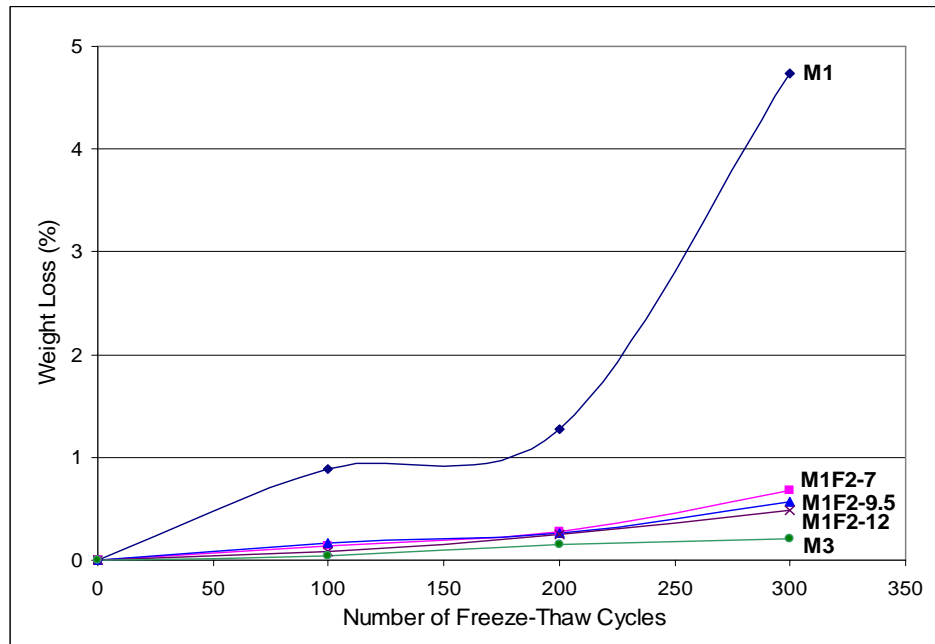
Figure 4.37: Weight loss of plain mixes due to freeze-thaw



Figure 4.38: Plain specimens after 300 cycles of freezing and thawing
Only plain slurry (M1) suffered severe deterioration



(a) With hooked fibers



(b) With crimped fibers

Figure 4.39: Weight loss in slurry SIFCON due to freeze-thaw cycles

On the other hand, it was observed that specimens made with the highest fiber volume fraction showed relatively more scaling than the other specimens, as can be seen in Figure 4.40. This result was due to the fact that the quantity of steel fibers in the surface layers is directly proportional to V_f , therefore, higher quantities of fibers will be present near the surfaces.

Being susceptible to corrosion by the effects of NaCl, the steel fibers will have corrosion products formed on their surfaces. This will result in some increase in the initial volume of fibers, and hence creating internal pressures on the matrix, which leads to more scaling at the end.

Although it seems, visually, that more scaling occurs as fiber contents increase, the weight loss results of the specimens with the highest V_f showed the smaller value. The initial weight of specimens containing more fibers is higher, of course, and it seems that the loss occurred because the surface scaling did not affect much with respect to the initial total weight. In addition, some small parts of specimens with the smaller V_f were broken away because of the deterioration as can be seen in Figure 4.40. The weight of these parts, which are usually free of fibers, affected the final results of weight loss. The 12 % V_f specimens did not experience such fractures due to its high content of fibers.

Almost similar observations are recorded in mortar SIFCON, Figure 4.41. The scale of the chart was selected as to show the small differences between the curves clearly. Here, as well, including steel fibers resulted in reducing the weight loss, but not to the degree noticed in case of slurry SIFCON, because even plain mortar specimens showed low levels of weight loss. In this case also, the scaling was more noticeable in the 12 % V_f specimens, Figure 4.42. In spite of this, the weight loss of these specimens was even lower than that of the low permeability reference concrete (M3).

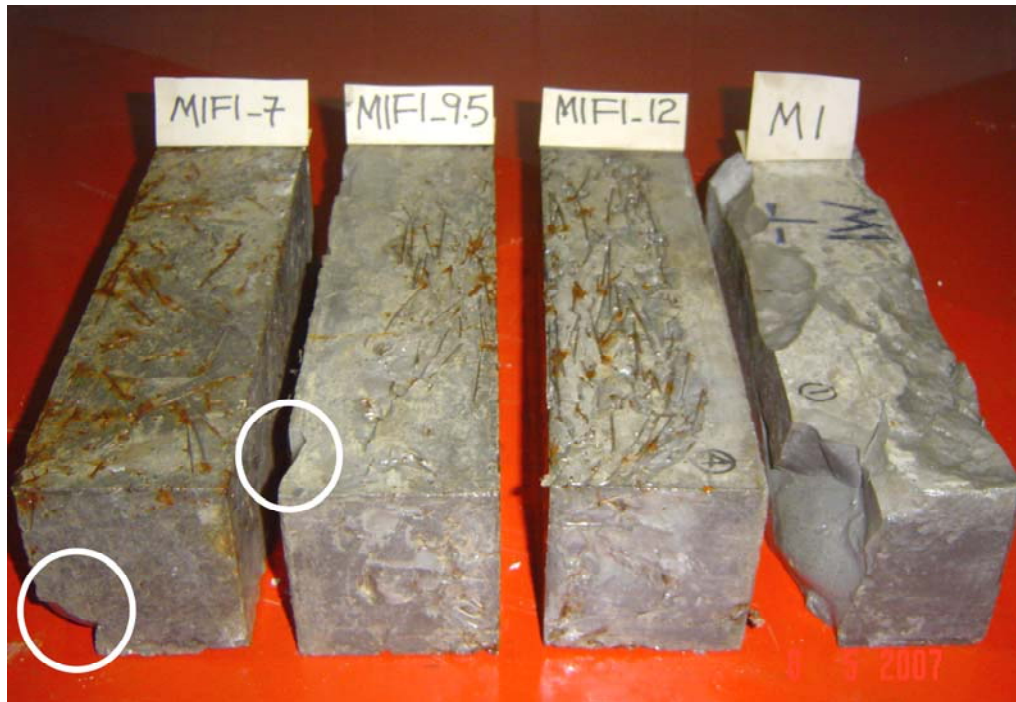
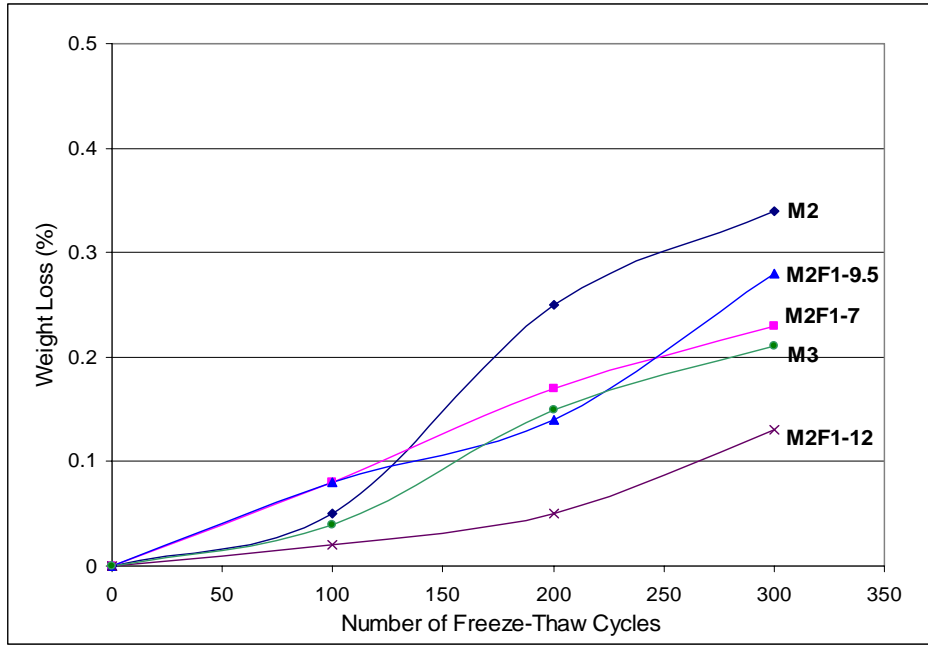


Figure 4.40: The surface scaling in slurry SIFCON made using hooked fibers

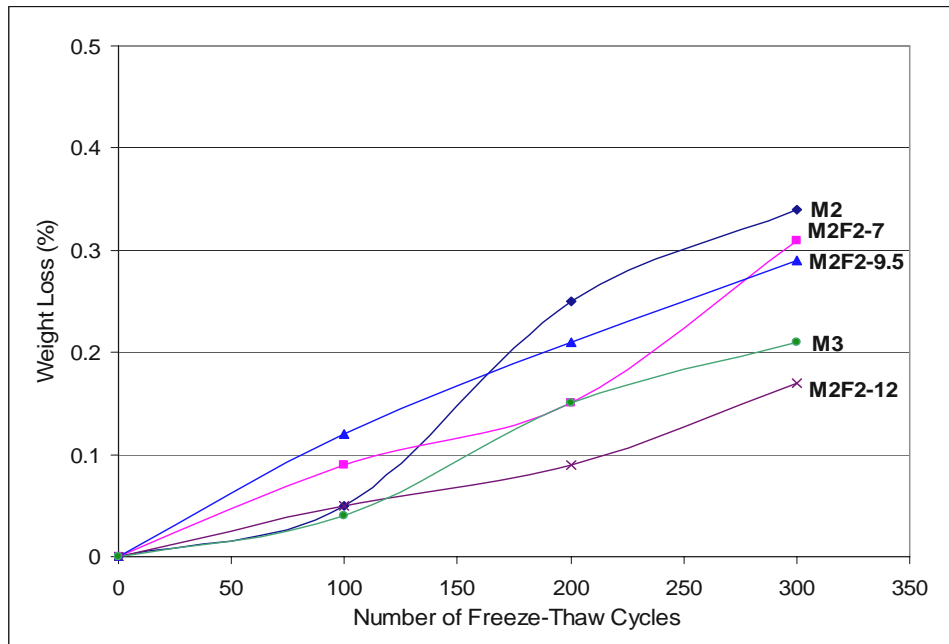
The circles refer to the broken parts in SIFCON due to the deterioration effects

4.5.2.3 Effect of matrix type on weight loss

Regardless the fiber type, all slurry SIFCON specimens experienced more weight loss due to surface scaling when compared with mortar SIFCON. Figure 4.43 illustrates this behavior. The reasons are related to permeability. Once slurry is more permeable than mortar, the deleterious effects of freezing and thawing of NaCl infiltrated in the SIFCON specimens will be much clear in slurry SIFCON.



(a) With hooked fibers



(b) With crimped fibers

Figure 4.41: Weight loss in mortar SIFCON due to freeze-thaw cycles



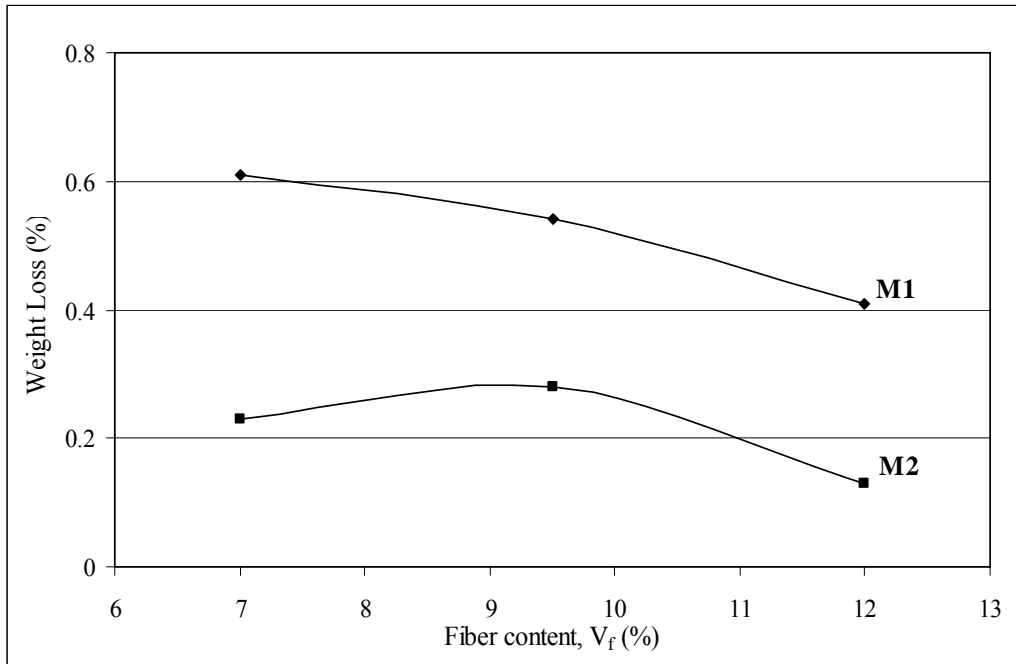
Figure 4.42: Representative samples of mortar SIFCON after 300 cycles of freezing and thawing

The 12 % V_f specimens showed more scaling and corrosion stains

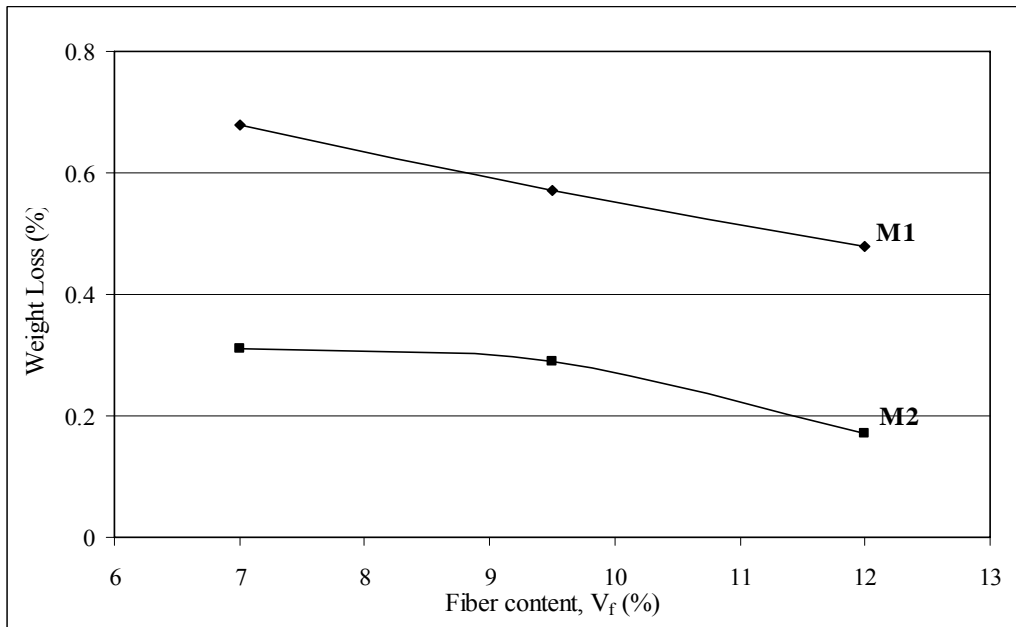
4.5.2.4 Influence of fiber type on weight loss

Such as in the case of investigating the drop in RDME, the behavior of the two steel fiber types regarding scaling and weight loss was not so different from each other. In all slurry and mortar matrices, using of hooked fibers (F1) resulted in slightly less scaling and weight loss when compared with the other type. This is shown in Figure 4.44.

It is supposed that specimens made with hooked fibers absorbed less quantities of NaCl, possibly due to the characteristics of their fibers geometric shape. The same reasoning that discussed earlier in Section 4.3.2.3 may be applicable here too.

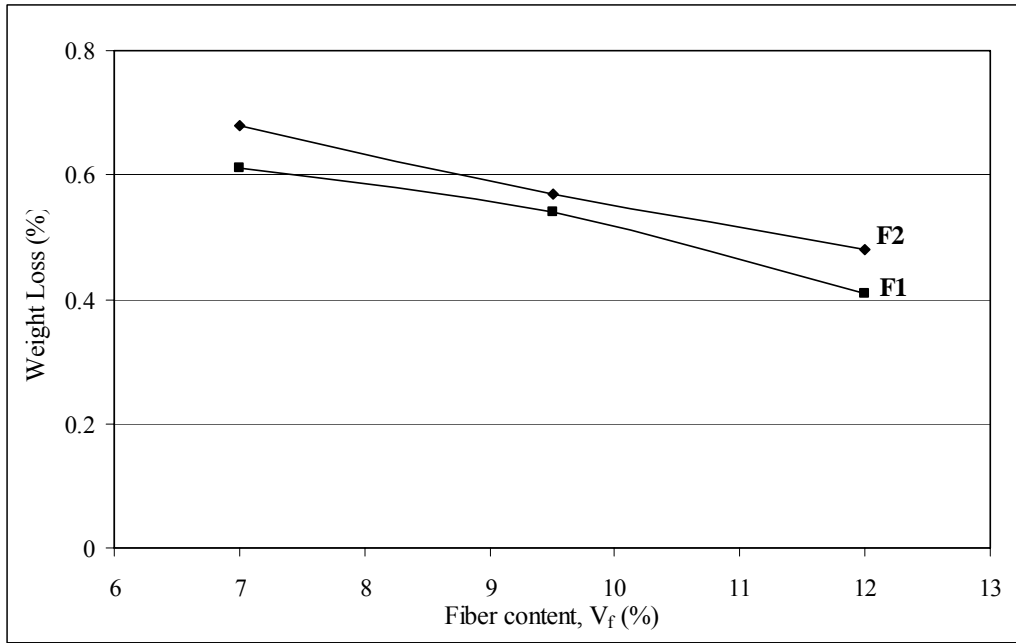


(a) With hooked fibers

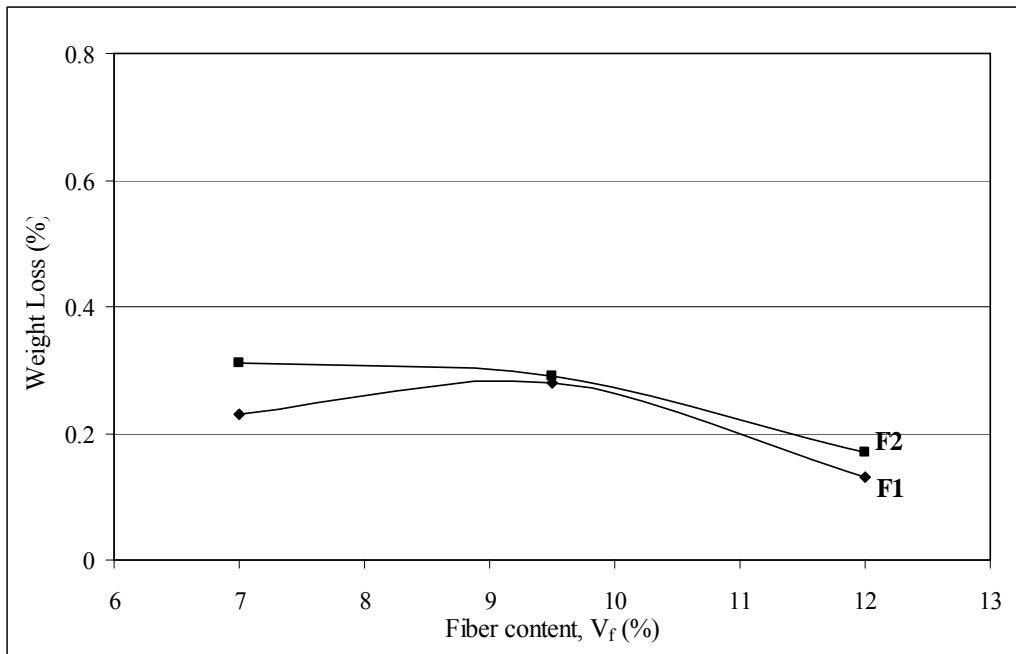


(b) With crimped fibers

Figure 4.43: Effect of mix type on weight loss of SIFCON due to 300 freeze-thaw cycles



(a) Slurry SIFCON



(b) Mortar SIFCON

Figure 4.44: Effect of fiber type on weight loss after 300 freeze-thaw cycles

4.5.3 Summary of the results of freezing and thawing test

This investigation showed that the resistance of different SIFCON matrices to rapid freezing and thawing when compared to the low permeability control concrete was, in general, quite promising in spite of the relatively high absorption of SIFCON, and in spite of not using air-entraining admixtures. It is expected that the relatively low W/C ratio of 0.4 participated in the good performance of concrete and SIFCON specimens subjected to this test. After 300 cycles of freezing at -10 °C and thawing at 50 °C, the weight losses were well below 1 % in all specimens, and the drop in RDME did not exceed 10 % of the initial values. Mortar SIFCON showed better performance, similar to what found in all the other investigations carried out in the study.

The only problem regarding freezing and thawing of SIFCON seems to be the occurrence of some surface scaling especially when the material is prepared with the highest fiber volume fraction. This, once again, raises the issue of the necessity of protecting the surfaces of SIFCON with some suitable overlays or impermeable coatings to prevent the emergence of the problems related to ongoing scaling and corrosion, and to preserve the aesthetic features of the surfaces.

CHAPTER 5

CONCLUSIONS AND RECOMMENDATIONS

5.1 Conclusions

This study deals with an experimental research carried out to investigate various durability aspects of slurry infiltrated fiber concrete (SIFCON). It was composed of investigating the resistance of SIFCON to drying shrinkage, water absorption, chloride penetration, and freezing-thawing cycles. Two types of steel fibers, hooked and crimped, were incorporated in three different volume percentages, and two types of matrices, slurry and mortar, were investigated. The following conclusions were derived based on the obtained results.

- a) Incorporating steel fibers in high quantities resulted in reduced free shrinkage when compared with plain matrices. The drying shrinkage of all SIFCON matrices, measured after 224 days, was lower than that exhibited by the conventional control concrete except for SIFCON made with relatively low fiber volume fraction (7 %). It was found that the higher is the fiber content the lower is the shrinkage.

Moreover, the multiple microcracks developed on the surfaces of slurry SIFCON were found to affect the shrinkage. Consequently, slurry SIFCON specimens experienced 50 % to 100 % less shrinkage than mortar SIFCON. For the effect of fiber shape on the drying shrinkage, it

was found that specimens made with hooked fibers showed less shrinkage when compared to those made using crimped fibers.

- b) Slurry SIFCON showed quite high water absorption capacities that ranged from 12 % to 15 % depending on the fiber type and content. The absorption range was 4 % to 7 % in the case of mortar SIFCON, which is relatively close to the 3.5 % absorption recorded in the low permeability reference concrete.

It was found that as the steel fiber volume fraction increases the absorption capacity of SIFCON reduces. The use of crimped fibers was more effective in reducing the absorption in slurry SIFCON. On the contrary, hooked fibers performed better in mortar SIFCON specimens. However, the results of other tests related to permeability, led to the conclusion that water absorption test alone is not enough to evaluate the permeability, hence the durability, of SIFCON.

- c) In spite of their relatively higher absorption, all investigated SIFCON matrices showed lower total chloride ion contents by mass of cement when compared with the control concrete. This resulted from the combined effect of the high concentrations of steel fibers, and the high cement contents (40 % to 70 % compared with only 20 % in concrete).

However, although the total chloride contents by mass of cement were well lower than that of concrete, those in the outer layers were higher than the limit accepted by the related standards for concrete. Containing high amounts of steel fibers without having any protective cover, SIFCON is more susceptible to corrosion problems caused primarily by chloride ions ingress, if the surfaces are not properly protected.

Chloride diffusion coefficients (D_a) were also found for all the matrices investigated. The results demonstrated that D_a values for SIFCON, in general, ranged from 8×10^{-12} to 17×10^{-12} m²/s. Comparing this range with the D_a value of concrete (25×10^{-12} m²/s) led to the conclusion that the diffusivity of chloride ions into SIFCON material is even less than that of low permeability concrete. This indicates that although the surfaces of SIFCONs may be prone to the chloride ions ingress, their further movement into the rest of the material is 1.5 to 3 times more difficult when compared with even a low-permeability control concrete.

- d) Both slurry and mortar SIFCONs showed relatively good resistance to the deterioration mechanisms caused by repetitive freezing and thawing. The weight loss due to surface scaling was less than 0.7 % in all SIFCON specimens, while the dynamic modulus of elasticity (DME) values after the freeze-thaw cycles were all higher than 90 % of the initial values in all cases. Mortar SIFCON showed relatively better performance than slurry SIFCON regarding freezing and thawing resistance.

Still however, steel fibers did not prevent the deterioration completely. Some surface scaling is inevitable, especially in SIFCON specimens made with the highest possible steel fiber content. The high steel fiber concentrations close to the exposed surfaces will cause the formation of more corrosion products due to NaCl penetration. This leads to creating internal stresses, and hence to more surface scaling.

- e) Generally speaking, SIFCON, especially mortar SIFCON, had shown good durability characteristics in spite of its apparent high absorption. For the effects of fiber content, it was found that increasing it will result in improved durability. On the other hand, there were no definite relationships between the fiber shape and the durability aspects studied. In

some aspects, hooked fibers have shown better results, while in some others the use of crimped fibers was proven to be slightly more successful.

5.2 Recommendations

The recommendations made below are proposed based on the findings of this experimental study. These recommendations are divided into two parts, as those for practical use and those for future research.

5.2.1 Recommendations for practice

- a) SIFCON is a material with many differences from both conventional concrete and fiber reinforced concrete, especially regarding its composition. Therefore, special standard test methods and compliance criteria should be prepared for this material.

- b) To ensure better performance of SIFCON, fine aggregate with maximum size of 1.0 mm should be included in the mix. It is recommended not to use slurry SIFCON that is made only of cement paste because of its relatively high absorption, more surface cracking problems, and weaker mechanical properties when compared with mortar SIFCON.

- c) In corrosive environments, covering the exposed surfaces of SIFCON with appropriate impervious or low permeability protective overlays may be beneficial to protect the almost exposed steel fibers close to the surfaces against corrosion that can be caused as a result of chloride penetration. In addition, such treatments may also be necessary to minimize surface scaling of SIFCON in cold areas due to frost damage.

- d) Using maximum possible steel fiber volume fraction is always recommended to achieve a better performance, provided that the necessary precautions mentioned in the previous point are taken into consideration.

5.2.2 Recommendations for future research

The following topics can be recommended for further research:

- a) Investigating the effects of permeability reducing admixtures on SIFCON absorption, and studying the bleeding of SIFCON.
- b) Investigating the effect of expansive cements, which are used for making shrinkage-compensating concrete, on reducing the risk of cracking of SIFCON due to drying shrinkage, especially slurry SIFCON.
- c) The effects of different mix compositions on the durability aspects of SIFCON can be also investigated. For example, mixes with W/C ratio less than 0.4, or with different cement types and mineral admixtures (fly ash or silica fume).
- d) For freezing and thawing test, it is recommended to subject SIFCON to more than the limit of 300 cycles, and to investigate the influences of air-entraining admixtures in this respect, in addition to preloading the specimens to certain stress ratios. Furthermore, it is proposed to investigate the mechanical behavior of SIFCON after being subjected to the freeze-thaw cycles, and to correlate it with the performance of virgin control specimen by measuring flexural strength and toughness.
- e) Conducting a comparative study on SIFCON durability using shorter steel fibers which will make it possible to approximately double the fiber

volume fractions. It is recommended also to investigate the effects of changing fiber aspect ratio (l/d).

- f) Studying the simultaneous effects of fiber length and specimen size on the deviations of the results of stress-strain relationships.

REFERENCES

- [1] Lankard, D.R., "Preparation, Properties and Applications of Concrete-Based Composites Containing 5 % to 20 % Steel Fiber", Steel Fiber Concrete, US-Sweden Joint Seminar, June 1985, pp. 199-217.
- [2] Balaguru, P.M., and Shah, S.P., "Fiber Reinforced Concrete Composites", McGraw-Hill Inc., New York, 1992.
- [3] Lee, M.K., Lark, R.J. and Barr, B.I.G., "A State of the Art Review on HPRCC", Report for Sub-Task 15, Sustainable Advanced Materials for Road Infrastructure (SAMARIS), 2003.
- [4] Lankard, D.R., "Preparation, Applications: Slurry Infiltrated Fiber Concrete (SIFCON)", Concrete International, V.6, No.12, Dec. 1984, pp. 44-47.
- [5] Homrich, J.R. and Naaman, A.E., "Stress-Strain Properties of SIFCON in Compression", Fiber Reinforced Concrete - Properties and Applications, ACI SP-105, American Concrete Institute, Detroit, Michigan, 1987, pp. 283-304.
- [6] Balaguru, P.M., and Kendzulak, J., "Mechanical Properties of Slurry Infiltrated Fiber Concrete (SIFCON)," Fiber Reinforced Concrete Properties and Applications, SP-105, American Concrete Institute, Detroit, Michigan, 1987, pp.247-268.
- [7] Mondragon, R., "SIFCON in Compression", Fiber Reinforced Concrete Properties and Applications, SP-105, American Concrete Institute, Detroit, Michigan, 1987, pp. 269-282.
- [8] Reinhardt, H.N., and Fritz, C., "Optimization of SIFCON Mix", Fiber Reinforced Cements and Concretes - Recent Developments, Elsevier, 1989, pp. 11-20.

- [9] Naaman, A.E., “Engineered Steel Fibers with Optimal Properties for Reinforcement of Cement Composites”, *Journal of Advanced Concrete Technology*, V.1, No.3, Nov. 2003, pp. 241-252.
- [10] Sonebi, M., Svermova, L., and Batros, P.J.M., “Statistical Modeling of Cement Slurries for Self-Compacting SIFCON Containing Silica Fume”, *Materials and Structures Journal*, 38, Jan.–Feb. 2005, pp. 79-86.
- [11] Naaman, A.E., Wight, J.K., and Abdou, H., “SIFCON Connections for Seismic Resistant Frames”, *Steel Reinforced Concrete, Compilation 27*, American Concrete Institute, Detroit, Michigan, 1991, pp. 62-67.
- [12] Kosa, K., Naaman, A.E., and Hansen, W., “Durability of Fiber Reinforced Mortar”, *ACI Materials Journal*, V.88, No. 3, May-June 1991, pp. 310-319.
- [13] Naaman, A.E., Otter, D., and Najm, H., “Elastic Modulus of SIFCON in Tension and Compression”, *ACI Materials Journal*, V. 88, No.6, Nov.-Dec. 1991, pp. 603-612.
- [14] Naaman, A.E., and Baccouche, M.R., “Shear Response of Dowel Reinforced SIFCON”, *ACI Structural Journal*, V.92, No.5, Sep.-Oct. 1995, pp. 587-569.
- [15] Naaman, A.E., Reinhardt, H.W., and Fritz, C., “Reinforced Concrete Beams with a SIFCON Matrix”, *ACI Structural Journal*, V.89, No.1, Jan.-Feb. 1992, pp. 79-88.
- [16] Naaman, A.E., and Homrich, J.R., “Tensile Stress-Strain Properties of SIFCON”, *ACI Materials Journal*, V.86, No.3, May-June 1989, pp. 244-251.
- [17] Hamza, A.M., “Bond Strength Characteristics of Deformed Reinforced Steel Bars Embedded in SIFCON”, Ph.D. Thesis, Civil and Environmental Engineering Department, University of Michigan, Ann Arbor, 1992, 202 pp.

- [18] Doğan, E., “Retrofit of Non-Ductile Reinforced Concrete Frames Using High Performance Fiber Reinforced Composites”, Ph.D. Thesis, Civil Engineering Department, North Carolina State University, Raleigh, 1998, 227 pp.
- [19] Wood., B.T., “Use of Slurry Infiltrated Fiber Concrete (SIFCON) in High Regions of Earthquakes Resistant Structures”, Ph.D. Thesis, Civil Engineering Department, North Carolina State University, Raleigh, 2000, 265 pp.
- [20] Mehta, P.K., and Monteiro, P.J.M., “Concrete - Microstructure, Properties, and Materials”, Indian Concrete Institute, Indian Edition, 1999.
- [21] Balaguru, P.M., and Kendzulak, J., “Flexural Behavior of Slurry Infiltrated Fiber Concrete (SIFCON) Made Using Condensed Silica Fume”, Fly Ash, Silica Fume, Slag, and Natural Pozzolans in Concrete, ACI SP-91, American Concrete Institute, Detroit, Michigan, 1986, pp.1215-1230.
- [22] Naaman, A.E., “SIFCON: Tailored Properties for Structural Performance”, High-Performance Fiber Reinforced Cement Composites, E&FN Spon, 1992, pp. 18-38.
- [23] Wang, M.L., and Maji, A.K., “Shear Properties of Slurry Infiltrated Fiber Concrete (SIFCON)”, High Performance Reinforced Cement Composites, RILEM, France, Ed. by Naaman, A.E., and Reinhardt, H.N., 1992, pp. 203-212.
- [24] Van Mier, J.G.M., and Timmers, G., “Shear Fracture in Slurry Infiltrated Fiber Concrete (SIFCON)”, Proceedings of RILEM International Workshop on High Performance Fiber Reinforced Cement Composites, Mainz, Germany, 1991.
- [25] Hamza, A.M., and Naaman, A.E., “Bond Characteristics of Deformed Reinforcing Steel Bars Embedded in SIFCON”, ACI Materials Journal, V.93, No.6, Nov.-Dec. 1996, pp. 578-588.

- [26] Bentur, A., and Mindess, S., "Fiber Reinforced Cementitious Composites", Elsevier Science Publishers Ltd., England, 1990.
- [27] Kendzulak, J., "Engineering Properties of Slurry Infiltrated Fiber Concrete (SIFCON)", M.S. Thesis, The State University of New Jersey, Rutgers, May 1986, 115 pp.
- [28] Lankard, D.R., "Use of SIFCON for Concrete Pavement Overlays", Lankard Materials Laboratories, Inc., Ohio, Dec. 1983.
- [29] Mondragon, R., "SIFCON Bridge Repairs", Task Report for the New Mexico State Highway Department, NMERI-42, New Mexico Research Institute, Albuquerque, July 1984.
- [30] Schneider, B., "Development of SIFCON through Applications", High-Performance Fiber Reinforced Cement Composites, E & FN Spon, 1992, pp. 177-194.
- [31] Lankard, D.R., and Newell, J.K., "Preparation of Highly Reinforced Concrete Composites", Fiber Reinforced Concrete, SP-81, American Concrete Institute, ACI, Detroit, Michigan, 1984, pp. 287-306.
- [32] Krstulovic-Opara, N., Haghayeghi, A.R., Haidar, N., and Krauss, P.D., "Use of Conventional and High-Performance Steel-Fiber Reinforced Concrete for Bridge Deck Overlays", ACI Materials Journal, V.92, No.6, Nov.-Dec. 1995, pp. 669-677.
- [33] Lankard, D.R., "Slurry Infiltrated Fiber Concrete (SIFCON): Properties and Applications", Proceedings of Material Research Society, Fall Meeting, V.42, Potential for Very High Strength Cement-Based Materials, 1984.
- [34] Schneider, B., Mondragon, R., and Kirst, J., "Task Report NMERI, TA8-69 (8.36/01)", New Mexico Research Institute, June 1984, 83pp.

- [35] Lankard, D.R., and Lease, D.H., “Highly Reinforced Precast Monolithic Refractories”, American Ceramic Society Bulletin, V.61, No.7, 1982, pp. 728-732.
- [36] Lankard, D.R., “Factors Affecting the Selection and Performance of Steel Fiber Reinforced Monolithic Refractories”, American Ceramic Society Bulletin, V.63, No.7, 1984, pp. 919-925.
- [37] American Society for Testing and Materials, “ASTM C 150, Standard Specification for Portland Cement”, 2002.
- [38] American Society for Testing and Materials, “ASTM C 188, Standard Test Method for Density of Hydraulic Cement”, 1995.
- [39] American Society for Testing and Materials, “ASTM C 204, Standard Test Method for Fineness of Hydraulic Cement by Air- Permeability Apparatus”, 2000.
- [40] American Society for Testing and Materials, “ASTM C 187, Standard Test Method for Normal Consistency of Hydraulic Cement”, 1998.
- [41] British Standard Institution, “BS EN 196-3, Methods of Testing Cement: Determination of Setting Time and Soundness”, 1995.
- [42] American Society for Testing and Materials, “ASTM C 191, Standard Test Method for Time of Setting of Hydraulic Cement by Vicat Needle”, 2001.
- [43] American Society for Testing and Materials, “ASTM C 109, Standard Test Method for Compressive Strength of Hydraulic Cement Mortars”, 2001.
- [44] American Society for Testing and Materials, “ASTM C 114, Standard Test Methods for Chemical Analysis of Hydraulic Cement”, 2000.

- [45] American Society for Testing and Materials, “ASTM C 127, Standard Test Method for Density, Relative Density (Specific Gravity), and Absorption of Coarse Aggregate”, 2001.
- [46] American Society for Testing and Materials, “ASTM C 128, Standard Test Method for Density, Relative Density (Specific Gravity), and Absorption of Fine Aggregate”, 2001.
- [47] American Society for Testing and Materials, “ASTM C 136, Standard Test Method for Sieve Analysis of Fine and Coarse Aggregate”, 2001.
- [48] American Society for Testing and Materials, “ASTM C 33, Standard Specification for Concrete Aggregates”, 1999.
- [49] American Society for Testing and Materials, “ASTM C 494, Standard Specification for Chemical Admixtures for Concrete”, 1999.
- [50] Degussa Construction Chemicals - Rheobuild 1000, www.degussacc.com.au/admix/rbuild4.htm, Last access date Apr. 2006.
- [51] ACI Committee 544, “State of the Art Report on Fiber Reinforced Concrete”, Concrete International, V.4, No. 5, 1982, pp. 10.
- [52] American Society for Testing and Materials, “ASTM C 305, Standard Practice for Mechanical Mixing of Hydraulic Cement Pastes and Mortars of Plastic Consistency”, 1999.
- [53] Mindess, S., Young, J.F., and Drawin, D., “Concrete”, 2nd ed., Pearson Education Ltd., New Jersey, 2003.
- [54] McHenry, D., and Shideler, J.J., “Review of Data on Effect of Speed on Mechanical Testing of Concrete”, Symposium on Speed of Testing of Nonmetallic Materials, ASTM STP 185, pp.72-82, 1955.

- [55] Neville, A.M., "Properties of Concrete", 4th ed., Pearson Education Ltd, Essex, England, 1995.
- [56] Ghambir, M.L., "Concrete Technology", 2nd ed., Tata McGraw-Hill Publishing Co. Ltd., New Delhi, 1995.
- [57] American Society for Testing and Materials, "ASTM C 157, Standard Test Method for Length Change of Hardened Hydraulic-Cement Mortar and Concrete", 1999.
- [58] Goodspeed, C.H., Vanikar, S., and Cook, R.A., "High Performance Concrete Defined for Highway Structures", FHWA-SA-98-082, 1998.
- [59] Mehta, P.K., "Durability of Concrete - Fifty Years of Progress?", Second International Conferences on Durability of Concrete, ACI SP-126, V.1, Montreal, Canada, Aug., 1991, pp. 1-31.
- [60] American Society for Testing and Materials, "ASTM C 642, Standard Test Method for Density, Absorption, and Voids in Hardened Concrete", 1997.
- [61] American Association of State Highway and Transportation Officials, "AASHTO T 259-80, Standard Method of Test for Resistance of Concrete to Chloride Ion Penetration", 1993.
- [62] Stanish, K.D., Hooton, R.D., and Thomas, M.D.A., "Testing the Chloride Penetration Resistance of Concrete: A Literature Review", FHWA Contract DTFH 61-97-R-00022, University of Toronto, Canada, 1997.
- [63] American Association of State Highway and Transportation Officials, "AASHTO T 260-94, Standard Method of Test for Sampling and Testing for Total Chloride Ion in Concrete and Concrete Raw Materials", 1994.

- [64] Pigeon, M., Zuber, B., and Marchand, J., “Freeze – Thaw Resistance”, *Advanced Concrete Technology: Concrete properties*, Edited by Newman, J., and Choo, B.S. V.2, Elsevier Ltd. Oxford, 2003.
- [65] American Society for Testing and Materials, “ASTM C 666, Standard Test Method for Resistance of Concrete to Rapid Freezing and Thawing”, 1997.
- [66] Mu, R., Miao, C., Luo, X., and Sun, W., “Interaction between Loading, Freeze-Thaw Cycles, and Chloride Salt Attack of Cement With and Without Steel Fiber Reinforcement”, *Cement and Concrete Research*, V. 32, 2002, pp. 1061-1066.
- [67] Sun, W., Mu, R., Luo, X., and Miao, C., “Effect of Chloride Salt, Freeze-Thaw Cycling and Externally Applied Load on the Performance of the Concrete”, *Cement and Concrete Research*, V. 32, 2002, pp. 1859-1864.
- [68] Eglinton, M., “Resistance of Concrete to Destructive Agencies”, *Lea’s Chemistry of Cement and Concrete*, 4th ed., Edited by Hewlett, P.C., Elsevier Ltd., Oxford, 1998, pp. 299-342.
- [69] Ronning, T.F., “Freeze-Thaw Resistance of Concrete: Effect of Curing Conditions, Moisture Exchange and Materials”, Ph.D. Thesis, Division of Structural Engineering, The Norwegian Institute of Technology, Trondheim, 2001, 416 pp.
- [70] Ministry of Environment and Forestry, General Directorate of Meteorological Works, Turkey, www.meteoroloji.gov.tr/2006/arastirma/files/maxsic.pdf and www.meteoroloji.gov.tr/2006/arastirma/files/minsic.pdf, Last access date: July 2007.
- [71] American Society for Testing and Materials, “ASTM C 597, Standard Test Method for Pulse Velocity through Concrete”, 1997.

- [72] Matsumoto, T., and Mihashi, H., “DFRCC Terminology and Application Concepts”, *Journal of Advanced Concrete Technology*, V. 1, No. 35, Nov. 2003, pp. 335-340.
- [73] Jastrzebski, Z.D., “The Nature and Properties of Engineering materials”, 3rd Ed., John Wiley & Sons, Inc., Canada, 1987.
- [74] Erdoğan, T. Y., “Materials of Construction”, Middle East Technical University Press, Ankara, 2002.
- [75] Mangat, P. S., and Azari, M. M., “Shrinkage of Steel Fiber Reinforced Composites”, *Journal of Materials and Structures*, V. 21, 1988, pp. 163-171.
- [76] Zhang, J., and Li, V.C., “Influences of Fibers on Drying Shrinkage of Fiber-reinforced Cementitious Composites”, *ASCE Journal of Engineering Mechanics*, V. 127, No. 1, 2001, pp. 37-44.
- [77] L’hermite, R., “Volume Changes of Concrete”, *Proceedings of the 4th International Symposium on the Chemistry of Cement*, Washington, 1960, pp. 659-694.
- [78] Powers, T.C., “Causes and Control of Volume Change”, *Journal of Portland Cement Association*, V. 1, No. 1, Jan. 1959, pp. 29-39.
- [79] Federal Highway Association, USA,
www.fhwa.dot.gov/pavement/pccp/thermal.cfm, Last access date: May 2007.
- [80] Lafhaj, Z., Goueygou, M., Djerbi, A., and Kaczmarek, M., “Correlation between Porosity and Ultrasonic Parameters of Mortar with Variable Water/Cement Ratio and Water Content”, *Cement and Concrete Research*, V.36, 2006, pp. 625-633.

- [81] Bin Ahmad, R., "Characterization of Concrete Quality by Absorption and Permeability Tests", M.S. Thesis, Department of Civil Engineering, University of Toronto, 1991.
- [82] El-Dieb, A.S., "Permeation of Fluid through High Performance Concrete", Ph.D. Thesis, Department of Civil Engineering, University of Toronto, 1994, pp. 420.
- [83] British Standards Institution, "BS 8110: Part 1, Structural Use of Concrete, Code of Practice for Design and Construction", 1985.
- [84] European Standards Organizations, "ENV 206, Concrete: Performance, Protection, Placing, and Compliance Criteria", 1990.
- [85] American Concrete Institute, "ACI 318, Building Code Requirements for Structural Concrete Practice, Part 3: Use of Concrete in Building-Design, Specifications and Related Topics", 1996.
- [86] De Rooij, M.R., and Polder, R.B., "What Diffusion Coefficient is Used for Chloride Diffusion Modeling?", International Symposium on Advances in Concrete through Science and Engineering, The RILEM Spring Meeting, Evanston, USA, March 2004.
- [87] Thomas, M.D.A., and Bamforth, P.B., "Modeling Chloride Diffusion in Concrete; Effect of Fly Ash and Slag", Cement and Concrete Research, V.29, 1999, pp. 487-495.
- [88] Collepardi, M., Marcialis, A., and Turriziani, R., "Penetration of Chloride Ions into Cement Pastes and Concrete", Journal of the American Ceramic Society, V.55, No. 10, 1972, pp. 534-535.
- [89] Miao, C., Mu, R., Tian, Q., and Sun, W., "Effect of Sulfate Solution on the Frost Resistance of Concrete with and without Steel Fiber Reinforcement", Cement and Concrete Research, V.32, 2002, pp. 31-34.

[90] Pigeon, M., Pleau, R., Azzabi, M., and Banthia, N., “Durability of Microfiber Reinforced Mortars”, Cement and Concrete Research, V.26, 1996, pp.601-609.

[91] Pigeon, M., Azzabi, M., and Pleau, R., “Can Microfibers Prevent Frost Damage?”, Cement and Concrete Research, V.26, 1996, pp. 1163-1170.

**APPENDIX A: RESULTS OF STRESS-STRAIN TEST IN UNIAXIAL
COMPRESSION**

Table A.1: A part of the data of a typical stress-strain test

Specimen: M1F1-9.5-3									
T(sec)	LVDT1	LVDT2	$\Delta L1$ (mm)	$\Delta L2$ (mm)	ΔL avg (mm)	Load Cell (volts)	Load (tons)	Strain	Stress (MPa)
0	2.965	3.005	0	0	0	0.006	0.114	0	0.142
1.1	3.105	3.15	0.14	0.145	0.1425	0.013	0.148	0.0007	0.185
2	3.175	3.22	0.21	0.215	0.2125	0.024	0.201	0.0011	0.251
3	3.31	3.35	0.345	0.345	0.345	0.059	0.371	0.0017	0.464
4	3.365	3.39	0.4	0.385	0.3925	0.184	0.978	0.0020	1.221
5	3.445	3.46	0.48	0.455	0.4675	0.331	1.691	0.0023	2.112
6.1	3.51	3.52	0.545	0.515	0.53	0.411	2.079	0.0027	2.596
7	3.54	3.545	0.575	0.54	0.5575	0.546	2.734	0.0028	3.414
8	3.585	3.585	0.62	0.58	0.6	0.598	2.986	0.0030	3.730
9	3.6	3.59	0.635	0.585	0.61	0.665	3.311	0.0031	4.136
10	3.62	3.61	0.655	0.605	0.63	0.69	3.432	0.0032	4.287
11	3.625	3.615	0.66	0.61	0.635	0.738	3.665	0.0032	4.578
12.1	3.64	3.63	0.675	0.625	0.65	0.786	3.898	0.0033	4.869
12.9	3.655	3.635	0.69	0.63	0.66	0.81	4.014	0.0033	5.014
14	3.66	3.655	0.695	0.65	0.6725	0.857	4.242	0.0034	5.299
15	3.68	3.67	0.715	0.665	0.69	0.882	4.364	0.0035	5.450
15.9	3.685	3.675	0.72	0.67	0.695	0.927	4.582	0.0035	5.723
17	3.695	3.69	0.73	0.685	0.7075	0.951	4.698	0.0035	5.869
18	3.705	3.695	0.74	0.69	0.715	0.999	4.931	0.0036	6.159
19	3.715	3.705	0.75	0.7	0.725	1.022	5.043	0.0036	6.299
20	3.725	3.71	0.76	0.705	0.7325	1.068	5.266	0.0037	6.577
20.9	3.73	3.715	0.765	0.71	0.7375	1.09	5.373	0.0037	6.711
22.1	3.745	3.735	0.78	0.73	0.755	1.135	5.591	0.0038	6.983
23	3.75	3.74	0.785	0.735	0.76	1.179	5.804	0.0038	7.250
24	3.76	3.75	0.795	0.745	0.77	1.2	5.906	0.0039	7.377
25	3.77	3.75	0.805	0.745	0.775	1.243	6.115	0.0039	7.638
26.1	3.775	3.765	0.81	0.76	0.785	1.287	6.328	0.0039	7.904
27	3.78	3.77	0.815	0.765	0.79	1.309	6.435	0.0040	8.038
27.9	3.78	3.77	0.815	0.765	0.79	1.331	6.542	0.0040	8.171
28.7	3.78	3.77	0.815	0.765	0.79	1.373	6.746	0.0040	8.426
30.5	3.78	3.77	0.815	0.765	0.79	1.414	6.944	0.0040	8.674
31	3.78	3.77	0.815	0.765	0.79	1.434	7.042	0.0040	8.795
32	3.78	3.77	0.815	0.765	0.79	1.47	7.216	0.0040	9.013
33.3	3.83	3.82	0.865	0.815	0.84	1.501	7.367	0.0042	9.201
34.3	3.835	3.825	0.87	0.82	0.845	1.518	7.449	0.0042	9.304
35.3	3.84	3.83	0.875	0.825	0.85	1.541	7.561	0.0043	9.444
36.4	3.84	3.83	0.875	0.825	0.85	1.564	7.672	0.0043	9.583
36.8	3.84	3.83	0.875	0.825	0.85	1.564	7.672	0.0043	9.583
38.2	3.855	3.85	0.89	0.845	0.8675	1.597	7.832	0.0043	9.783
39	3.855	3.85	0.89	0.845	0.8675	1.608	7.886	0.0043	9.850
40.1	3.86	3.86	0.895	0.855	0.875	1.629	7.988	0.0044	9.977
41	3.86	3.86	0.895	0.855	0.875	1.639	8.036	0.0044	10.037
42.2	3.865	3.865	0.9	0.86	0.88	1.66	8.138	0.0044	10.165

Table A.2: An example of toughness calculations

MIF1-7 (Three Specimens)								
Strain1	Stress1 (MPa)	Toughness 1 (KJ/m ³)	Strain2	Stress2 (MPa)	Toughness 2 (KJ/m ³)	Strain3	Stress3 (MPa)	Toughness 3 (KJ/m ³)
0.0000	0.0	0	0.0000	0.0	0	0.0000	0.0	0
0.0017	6.5	5.534	0.0014	7.4	5.292	0.0013	8.1	5.102
0.0018	6.8	6.380	0.0016	7.7	6.272	0.0013	8.4	5.636
0.0019	7.1	6.830	0.0016	8.0	6.272	0.0014	8.7	6.191
0.0020	7.3	7.280	0.0017	8.3	7.314	0.0014	9.1	6.191
0.0020	7.7	7.768	0.0018	8.7	7.867	0.0015	9.4	7.366
0.0022	7.9	8.781	0.0018	9.0	8.440	0.0015	9.7	7.366
0.0022	8.2	9.306	0.0019	9.3	9.033	0.0017	10.1	8.625
0.0023	8.5	9.829	0.0019	9.6	9.033	0.0017	10.4	8.625
0.0024	8.8	10.954	0.0020	9.9	9.668	0.0017	10.7	8.625
0.0024	9.1	10.954	0.0020	10.3	10.324	0.0018	11.0	10.035
0.0025	9.4	12.154	0.0021	10.6	10.975	0.0018	11.4	10.035
0.0025	9.7	12.154	0.0021	10.9	11.673	0.0019	11.7	11.505
0.0027	10.0	13.408	0.0022	11.2	12.391	0.0019	12.0	11.505
0.0027	10.3	14.065	0.0023	11.5	13.130	0.0020	12.3	12.296
0.0028	10.5	14.741	0.0023	11.8	13.889	0.0020	12.7	13.108
0.0029	10.8	15.435	0.0024	12.2	14.640	0.0020	13.0	13.108
0.0029	11.1	16.146	0.0025	12.5	15.410	0.0021	13.3	13.963
0.0030	11.4	16.877	0.0025	12.8	15.410	0.0022	13.6	14.839
0.0031	11.7	17.628	0.0025	13.1	16.252	0.0022	13.9	15.735
0.0031	12.0	18.367	0.0027	13.4	17.978	0.0022	14.3	15.735
0.0032	12.2	19.941	0.0027	13.7	17.978	0.0023	14.6	16.675
0.0032	12.5	19.941	0.0027	14.0	18.880	0.0024	14.9	17.635
0.0034	12.8	21.587	0.0028	14.3	19.802	0.0024	15.2	17.635
0.0034	13.1	21.587	0.0029	14.7	20.744	0.0025	15.6	19.598
0.0035	13.4	23.239	0.0029	14.9	20.744	0.0025	15.8	19.598
0.0035	13.6	23.239	0.0029	15.2	21.725	0.0025	16.1	19.598
0.0036	13.9	25.028	0.0030	15.5	22.686	0.0026	16.5	21.718
0.0036	14.1	25.028	0.0030	15.8	23.705	0.0026	16.8	21.718
0.0038	14.5	26.887	0.0031	16.1	24.743	0.0027	17.1	22.819
0.0038	14.8	27.804	0.0031	16.3	24.743	0.0028	17.4	23.939
0.0039	15.1	28.776	0.0032	16.7	26.886	0.0028	17.7	23.939
0.0040	15.4	29.765	0.0032	17.0	26.886	0.0028	18.0	25.098
0.0040	15.6	30.771	0.0034	17.3	29.068	0.0029	18.3	26.232
0.0041	15.9	31.794	0.0034	17.5	29.068	0.0029	18.6	27.384
0.0042	16.1	32.835	0.0034	17.8	30.216	0.0029	18.8	27.384
0.0042	16.4	33.893	0.0036	18.1	32.548	0.0031	19.2	29.852
0.0043	16.7	34.969	0.0036	18.4	32.548	0.0031	19.5	29.852
0.0043	16.9	36.018	0.0036	18.6	33.750	0.0031	19.7	29.852
0.0044	17.2	37.127	0.0037	18.9	34.970	0.0032	20.0	32.438
0.0045	17.4	39.377	0.0038	19.2	36.208	0.0032	20.3	32.438
0.0045	17.7	39.377	0.0038	19.5	37.415	0.0032	20.6	32.438
0.0047	18.0	41.697	0.0039	19.7	39.911	0.0033	20.9	35.133
0.0047	18.2	41.697	0.0039	20.0	39.911	0.0033	21.2	35.133
0.0048	18.4	44.032	0.0040	20.2	41.217	0.0034	21.4	36.517
0.0048	18.7	44.032	0.0041	20.5	42.539	0.0035	21.7	37.865
0.0049	18.9	46.432	0.0041	20.7	42.539	0.0035	22.0	37.865
0.0050	19.2	47.671	0.0042	21.0	45.250	0.0035	22.3	39.302

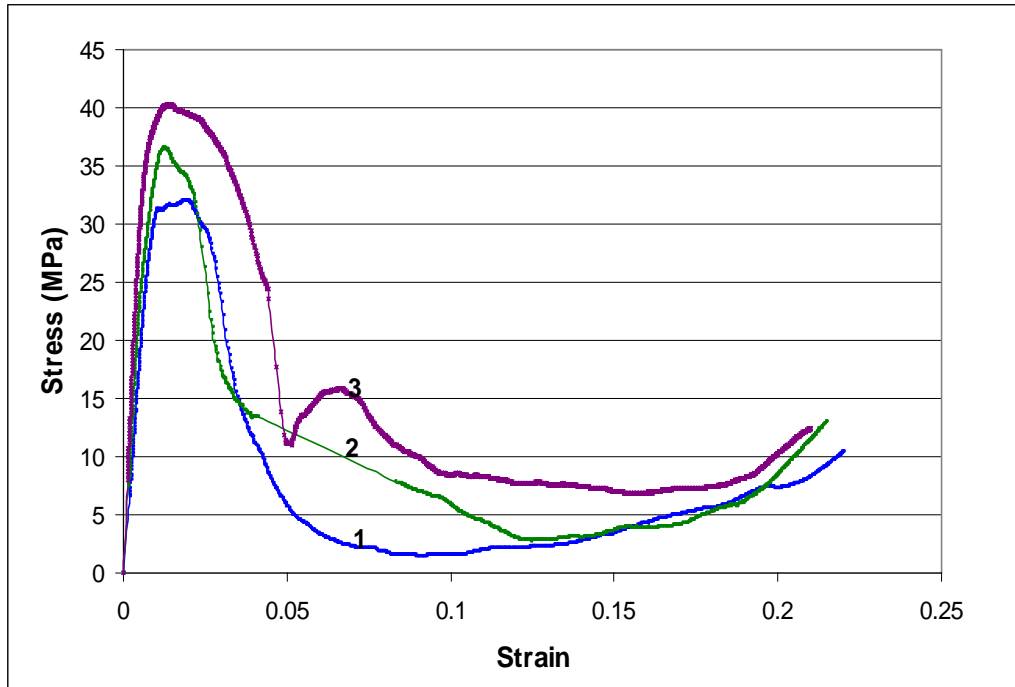


Figure A.1: Stress-strain results of M1F1-7 (three specimens)

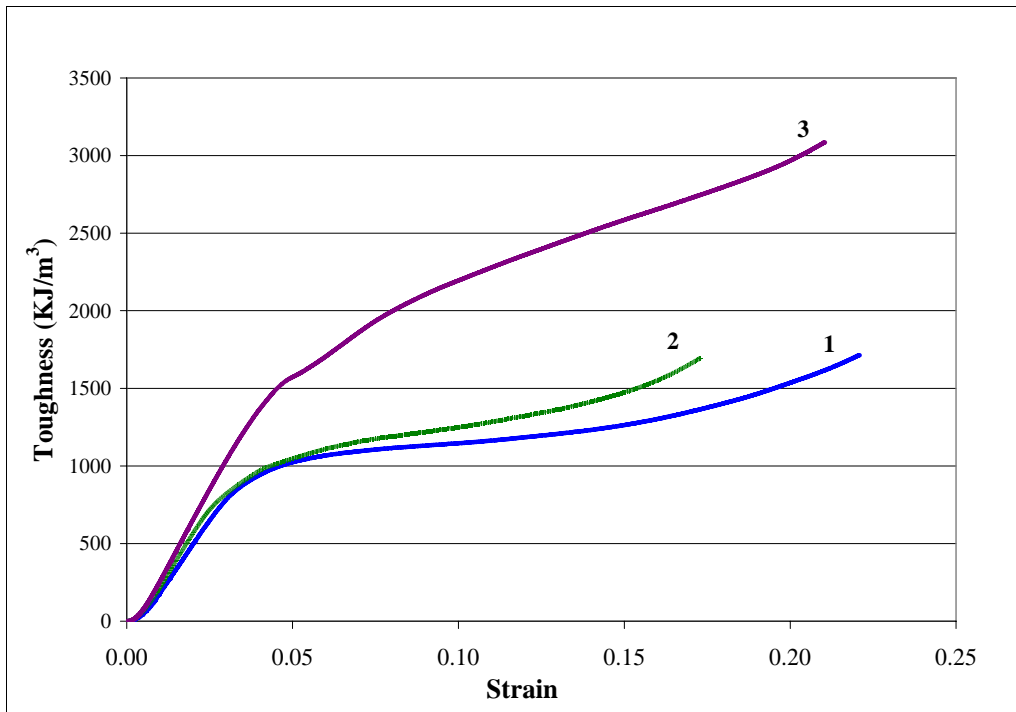


Figure A.2: Toughness-strain results of M1F1-7 (three specimens)

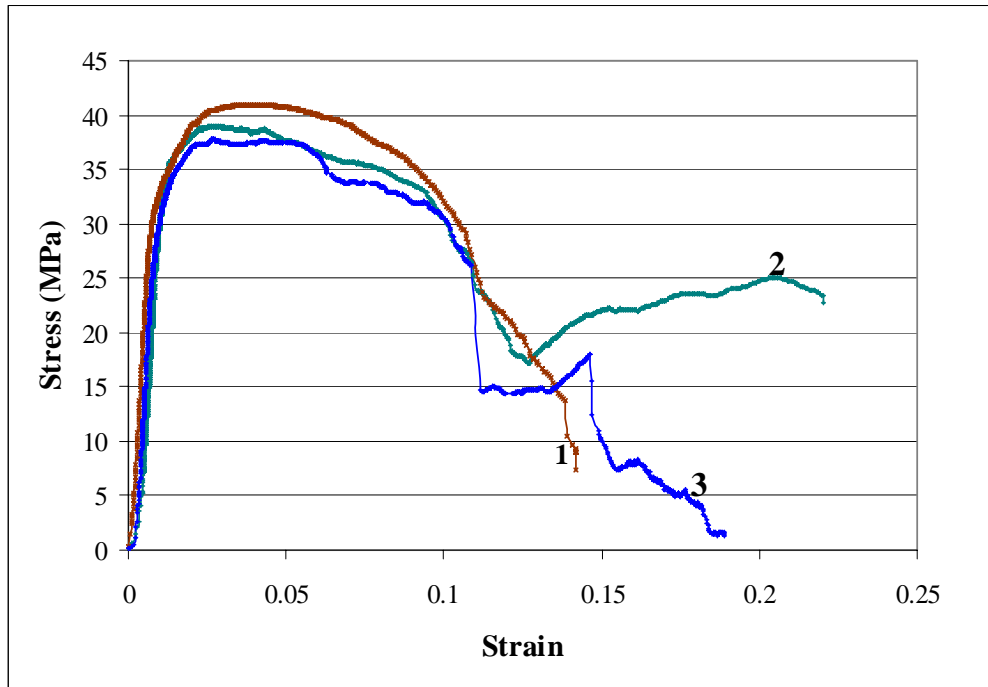


Figure A.3: Stress-strain results of M1F1-9.5 (three specimens)

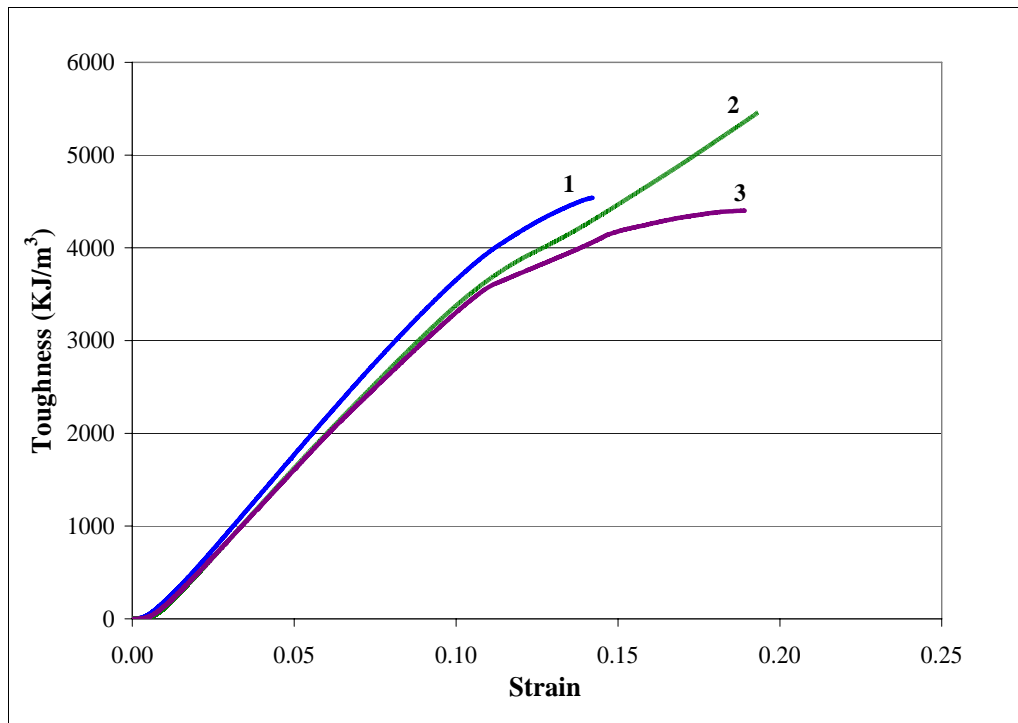


Figure A.4: Toughness-strain results of M1F1-9.5 (three specimens)

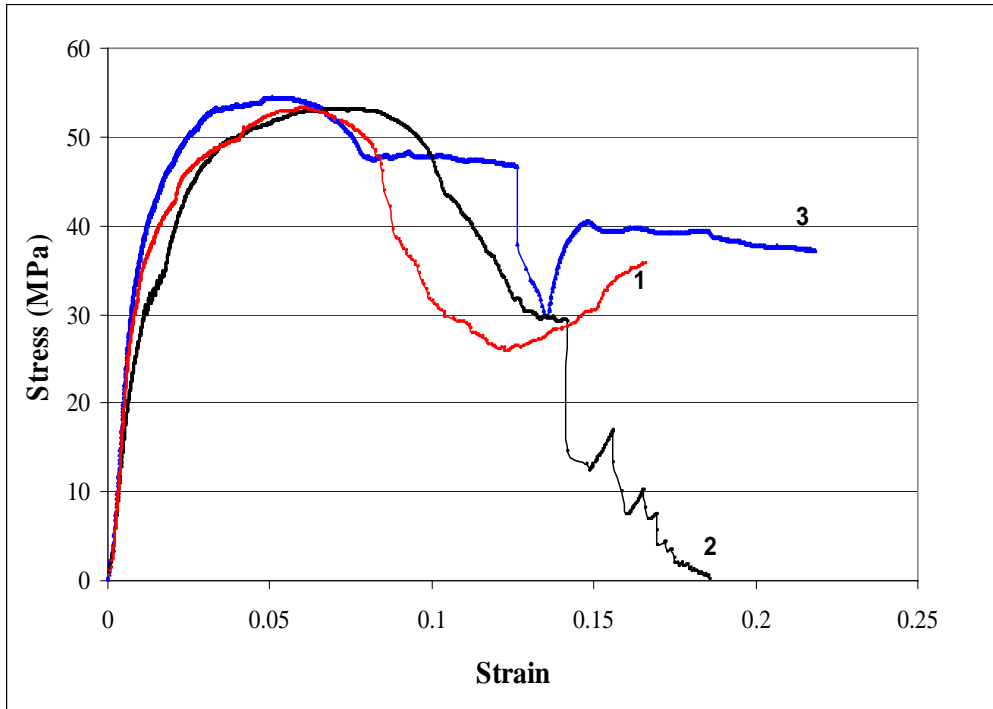


Figure A.5: Stress-strain results of M1F1-12 (three specimens)

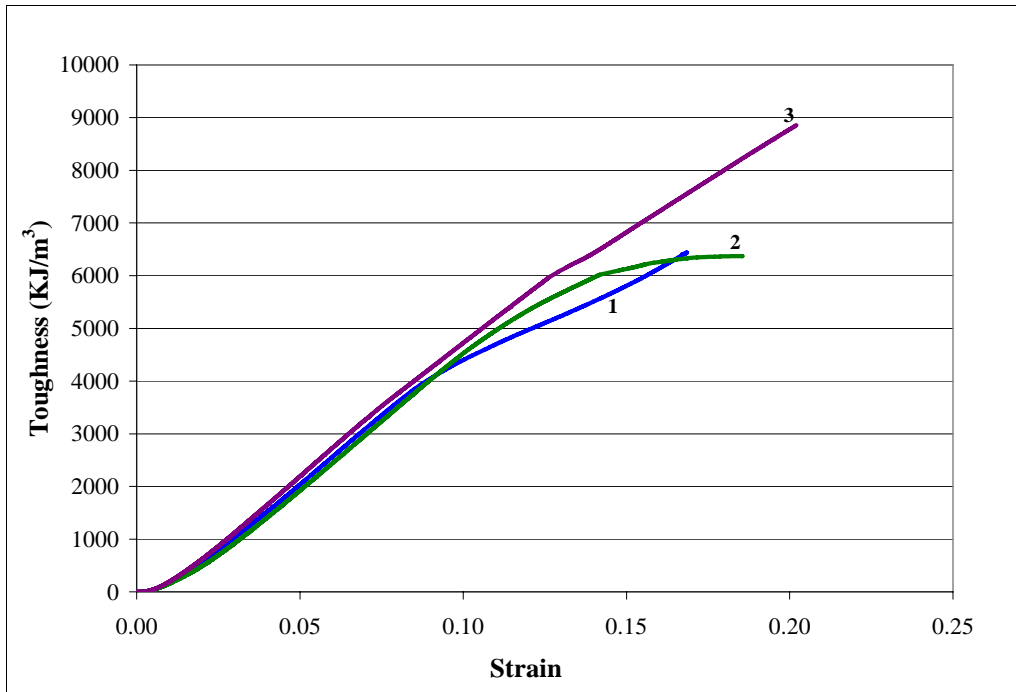


Figure A.6: Toughness-strain results of M1F1-12 (three specimens)

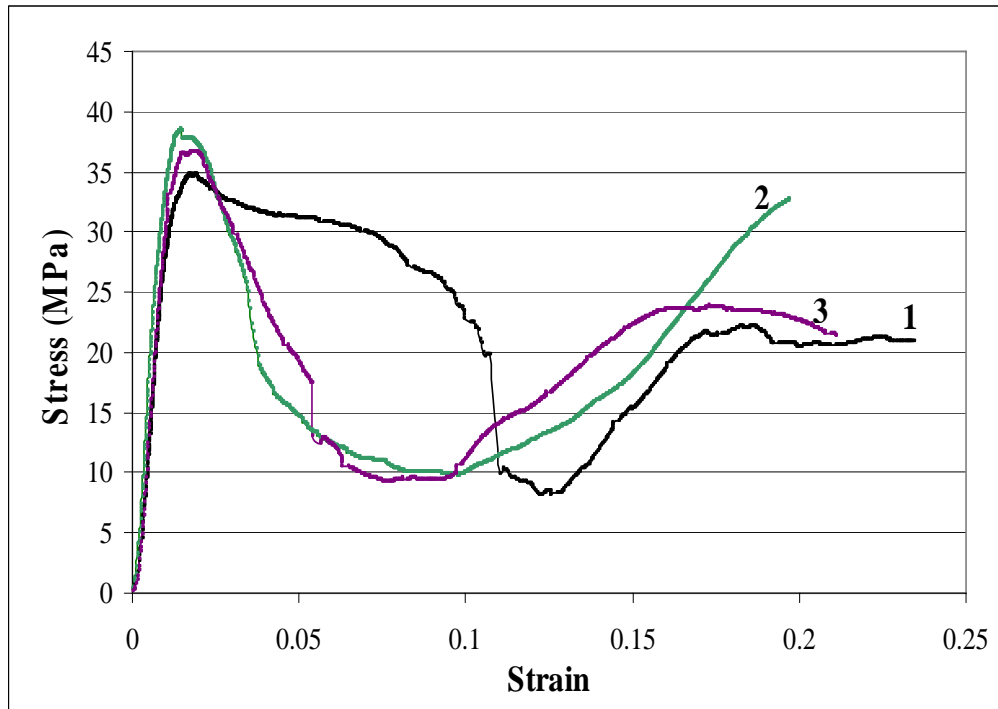


Figure A.7: Stress-strain results of M1F2-7 (three specimens)

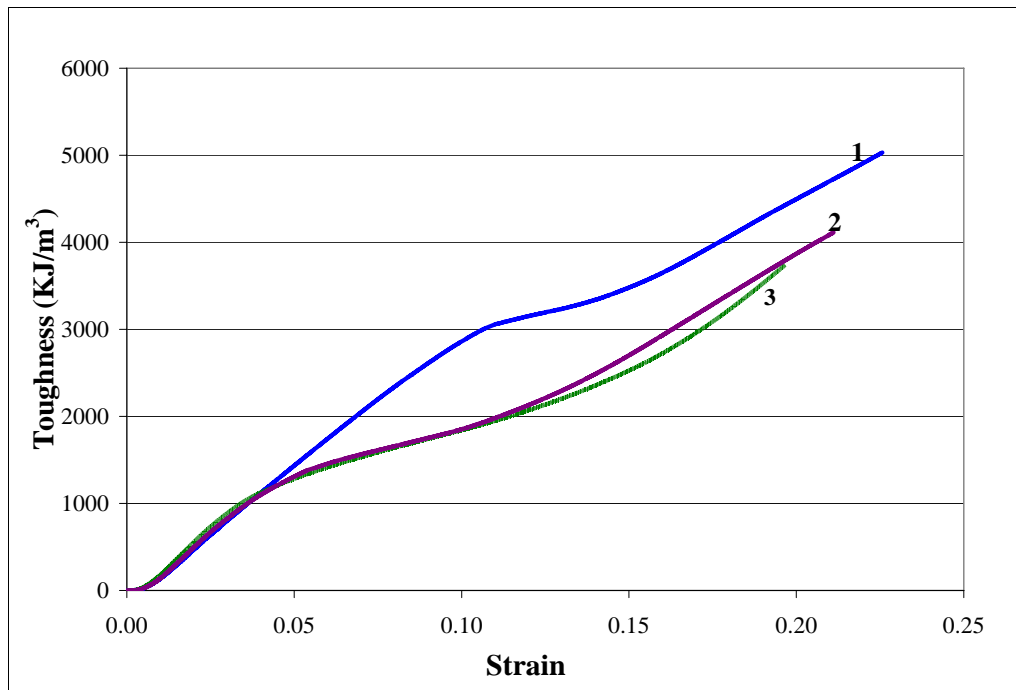


Figure A.8: Toughness-strain results of M1F2-7 (three specimens)

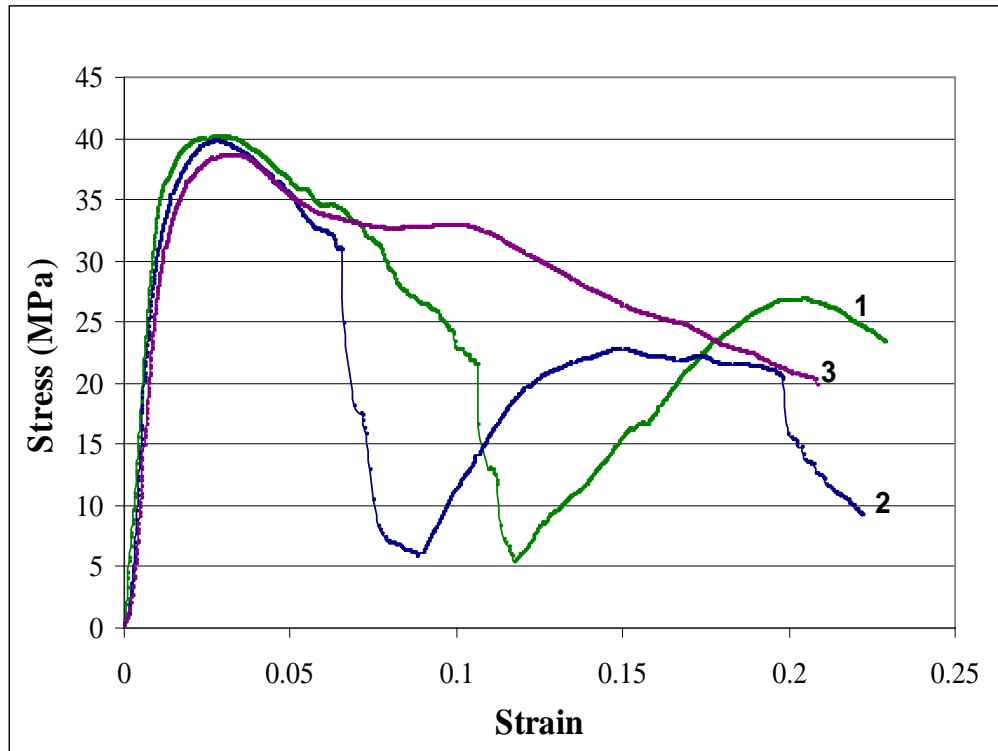


Figure A.9: Stress-strain results of M1F2-9.5 (three specimens)

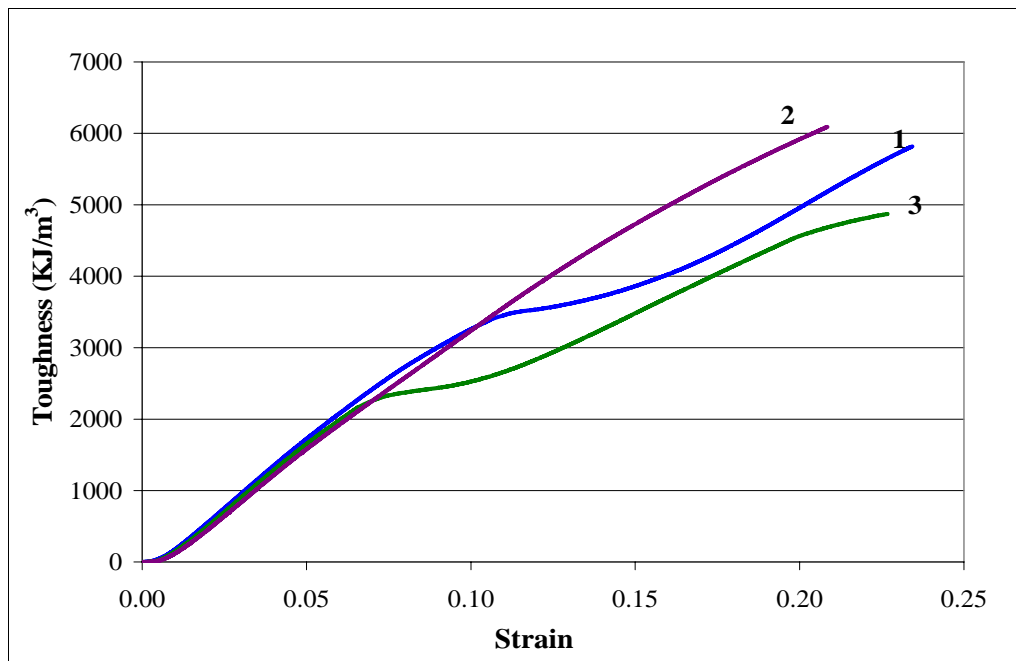


Figure A.10: Toughness-strain results of M1F2-9.5 (three specimens)

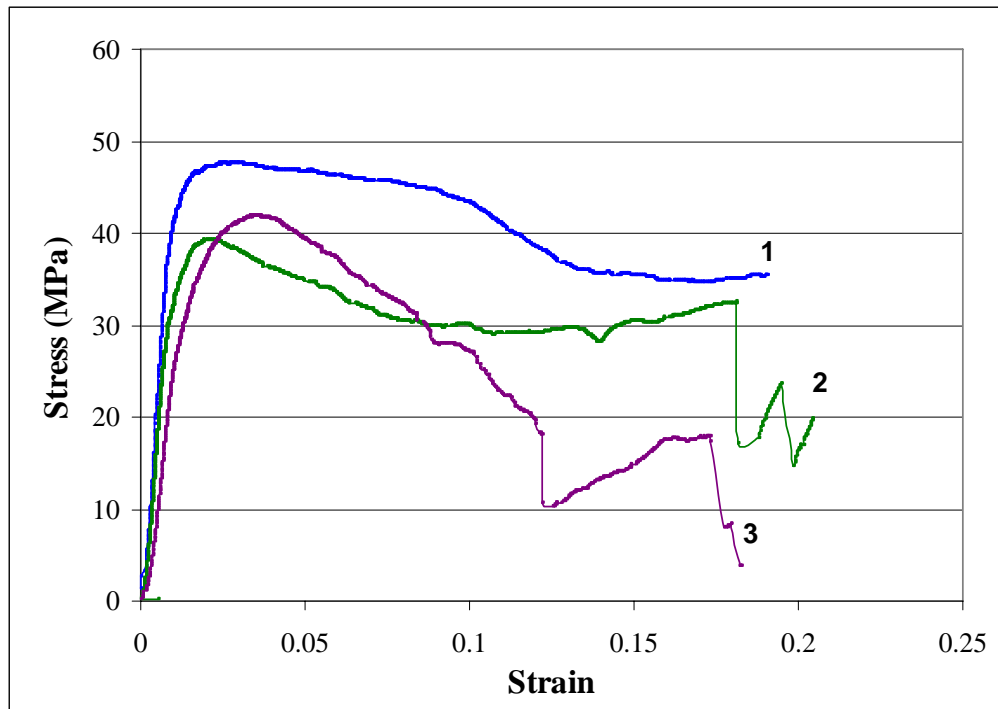


Figure A.11: Stress-strain results of M1F2-12 (three specimens)

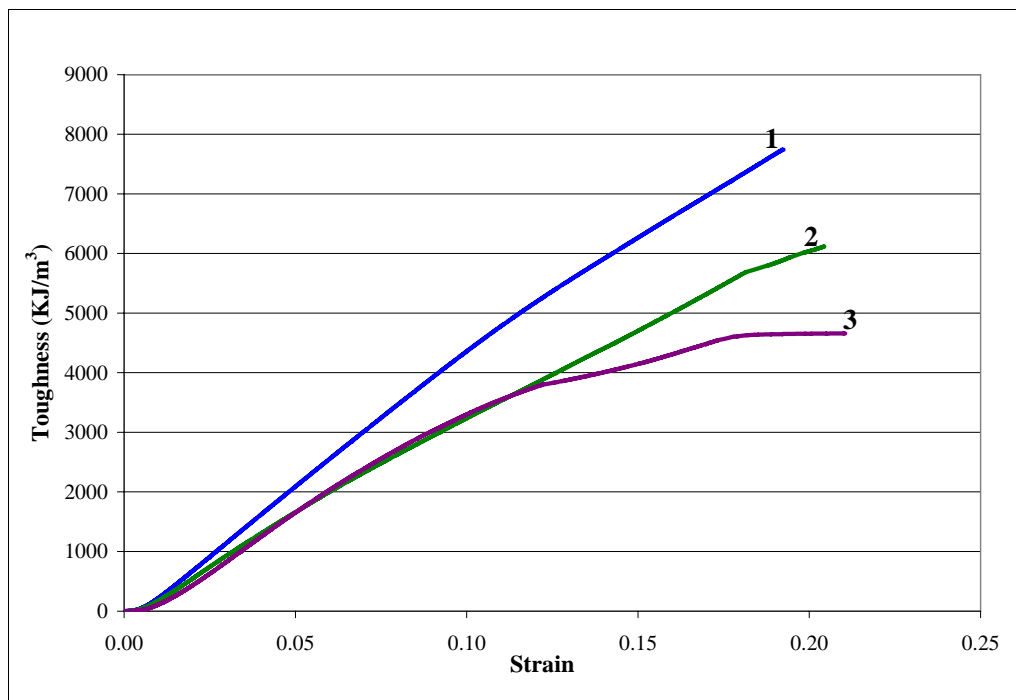


Figure A.12: Toughness-strain results of M1F2-12 (three specimens)

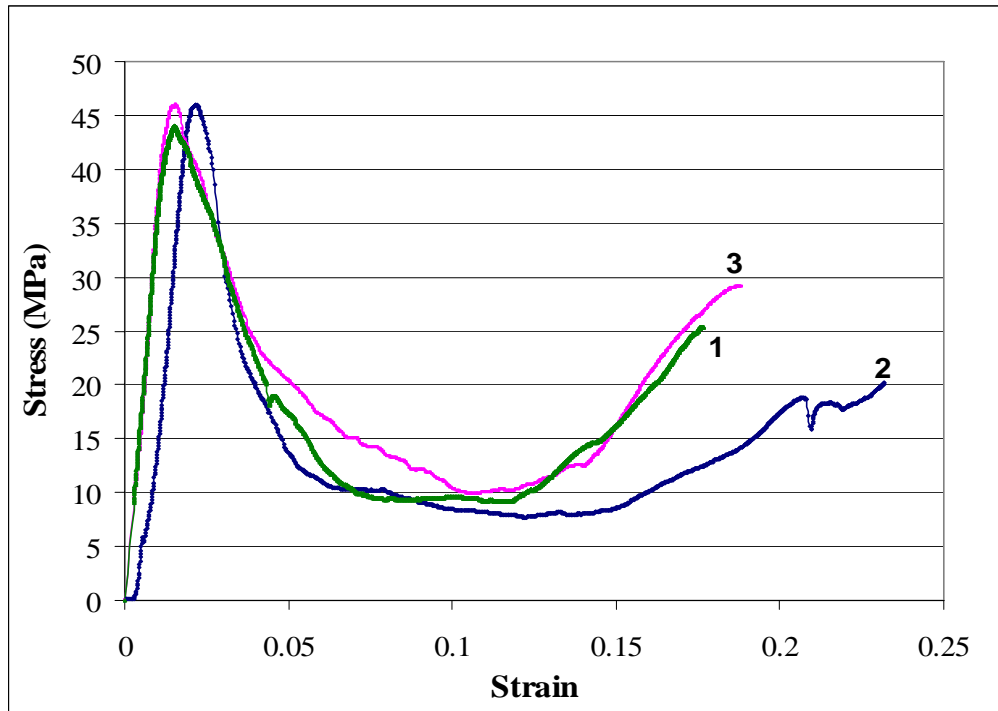


Figure A.13: Stress-strain results of M2F1-7 (three specimens)

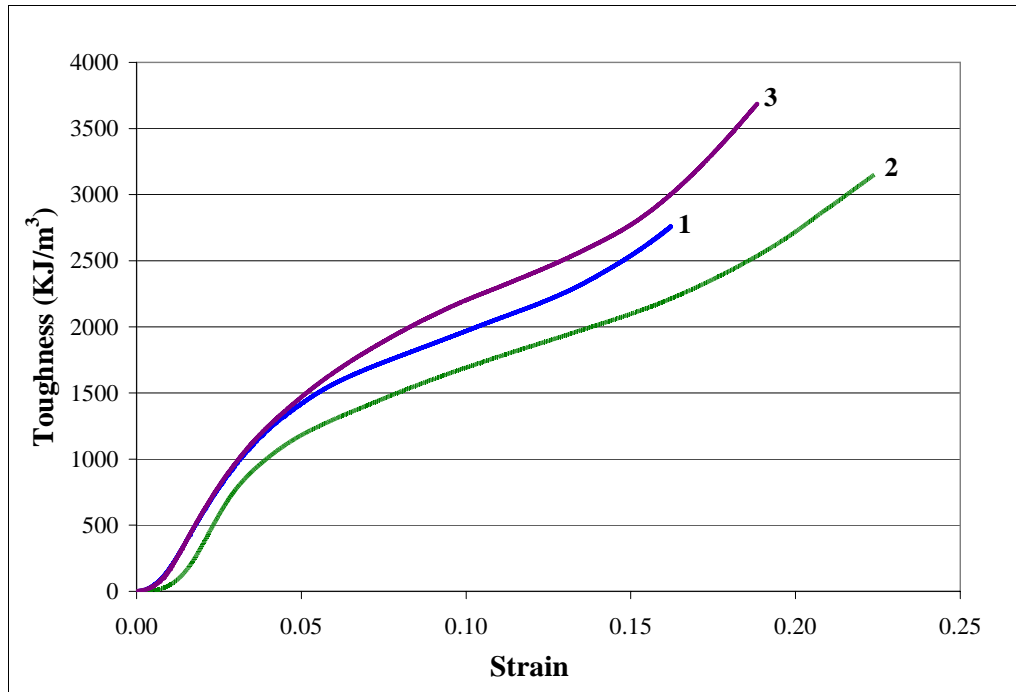


Figure A.14: Toughness-strain results of M2F1-7 (three specimens)

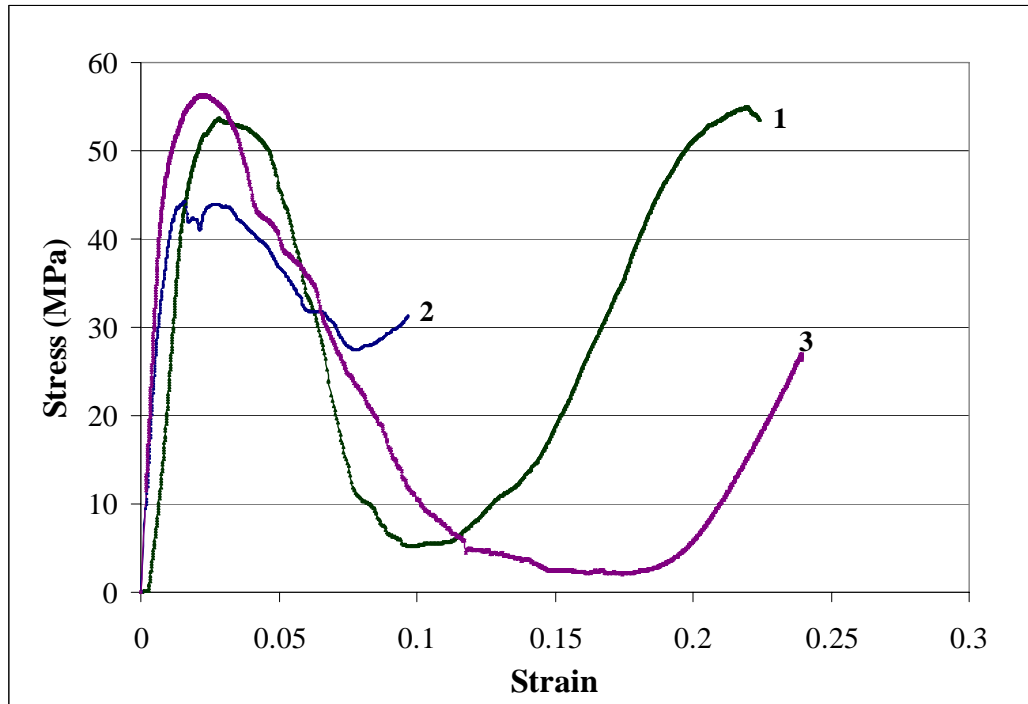


Figure A.15: Stress-strain results of M2F1-9.5 (three specimens)

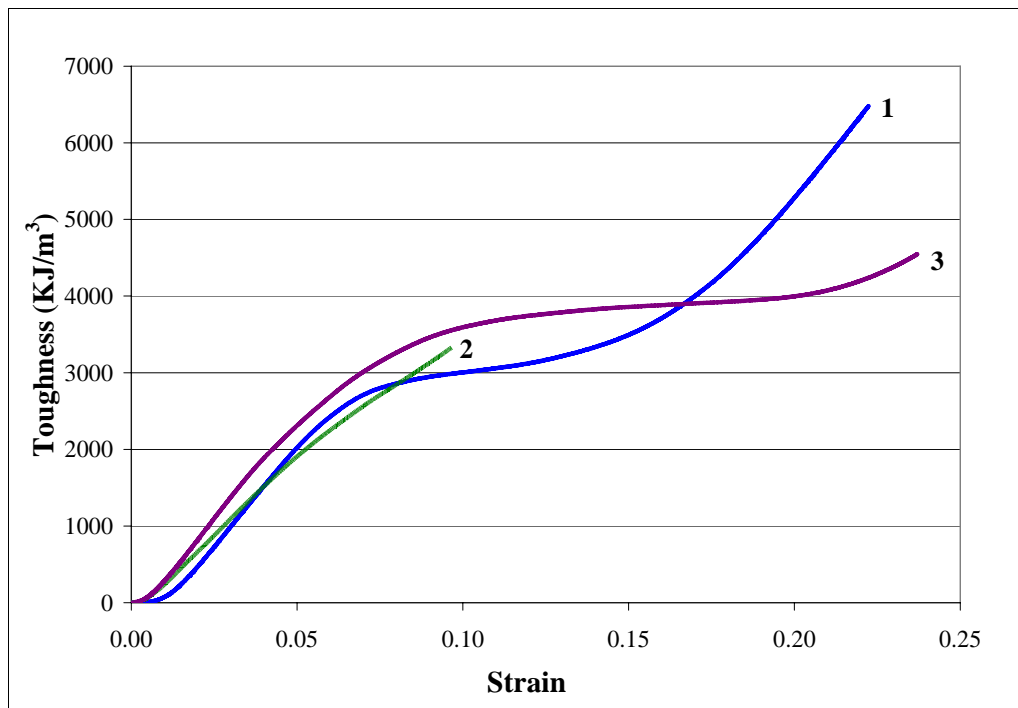


Figure A.16: Toughness-strain results of M2F1-9.5 (three specimens)

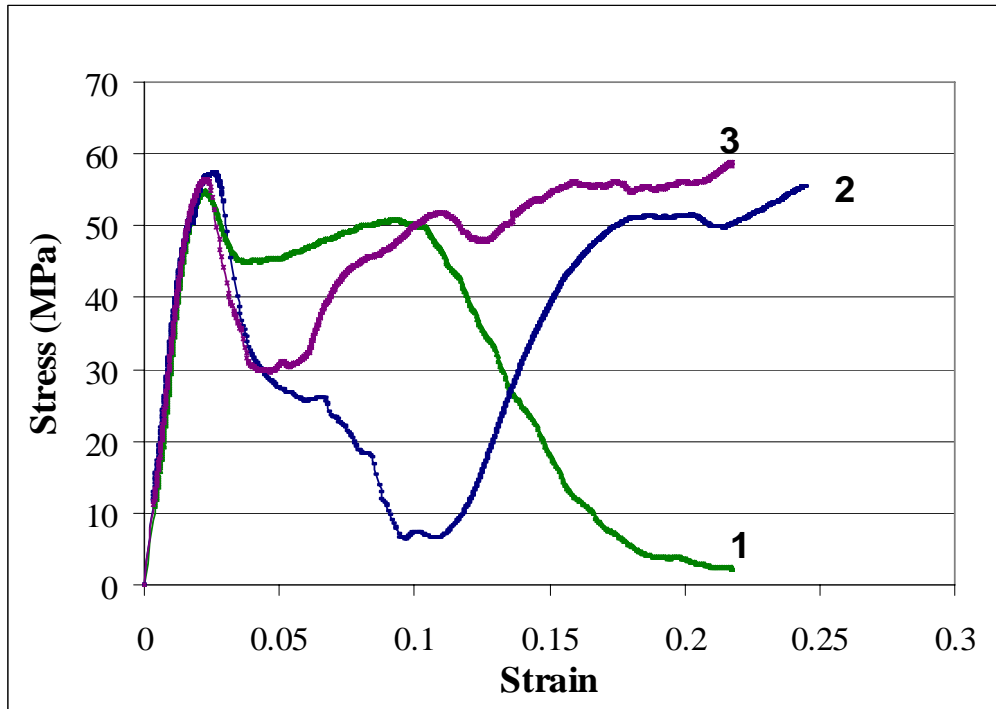


Figure A.17: Stress-strain results of M2F1-12 (three specimens)

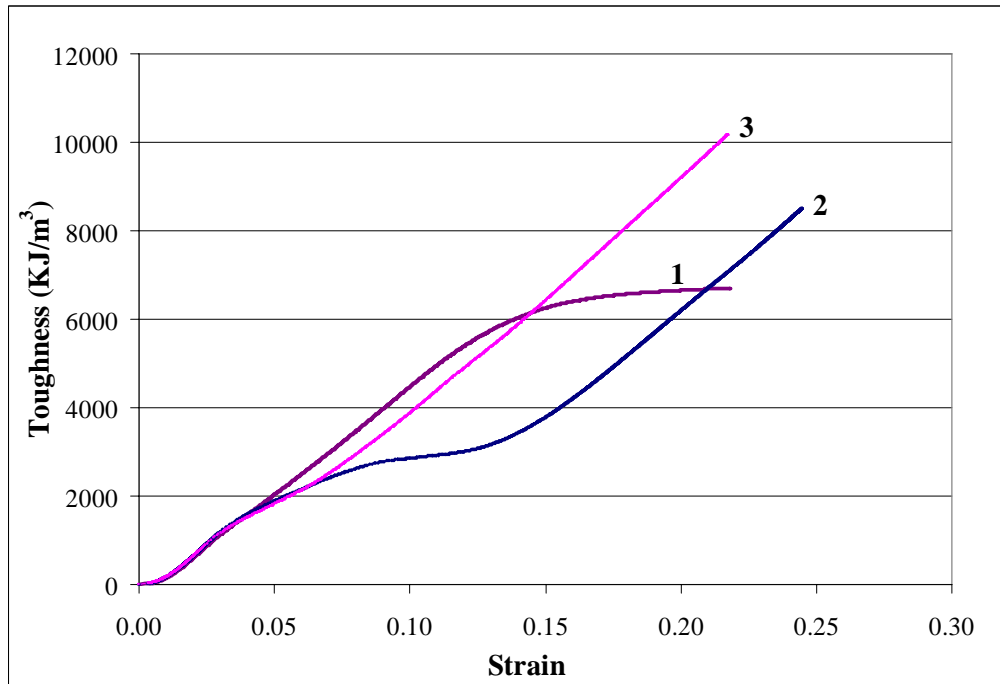


Figure A.18: Toughness-strain results of M2F1-12 (three specimens)

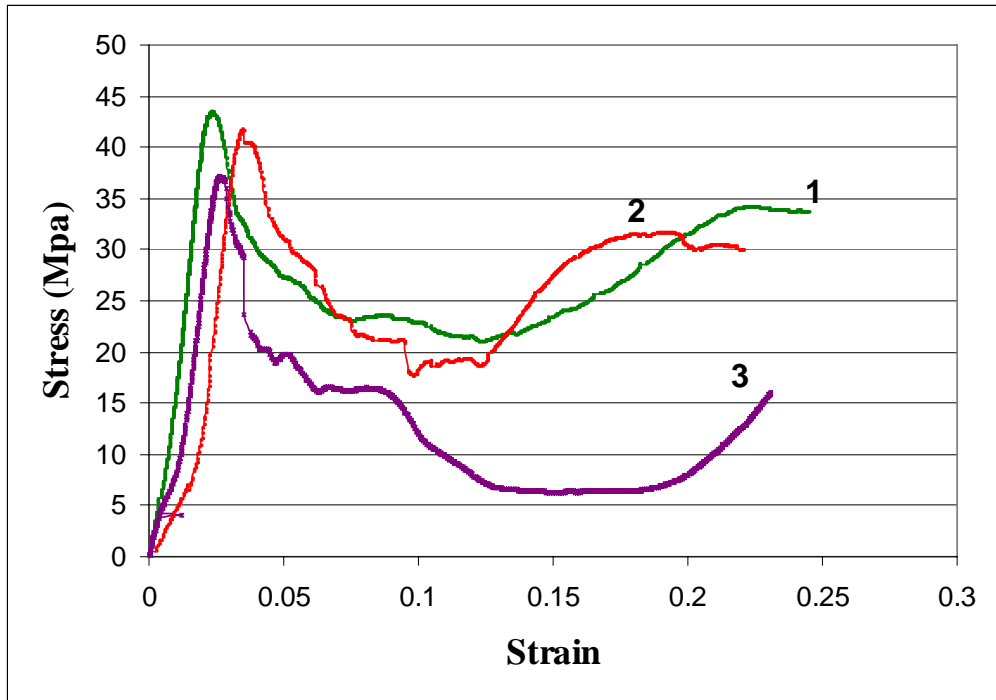


Figure A.19: Stress-strain results of M2F2-7 (three specimens)

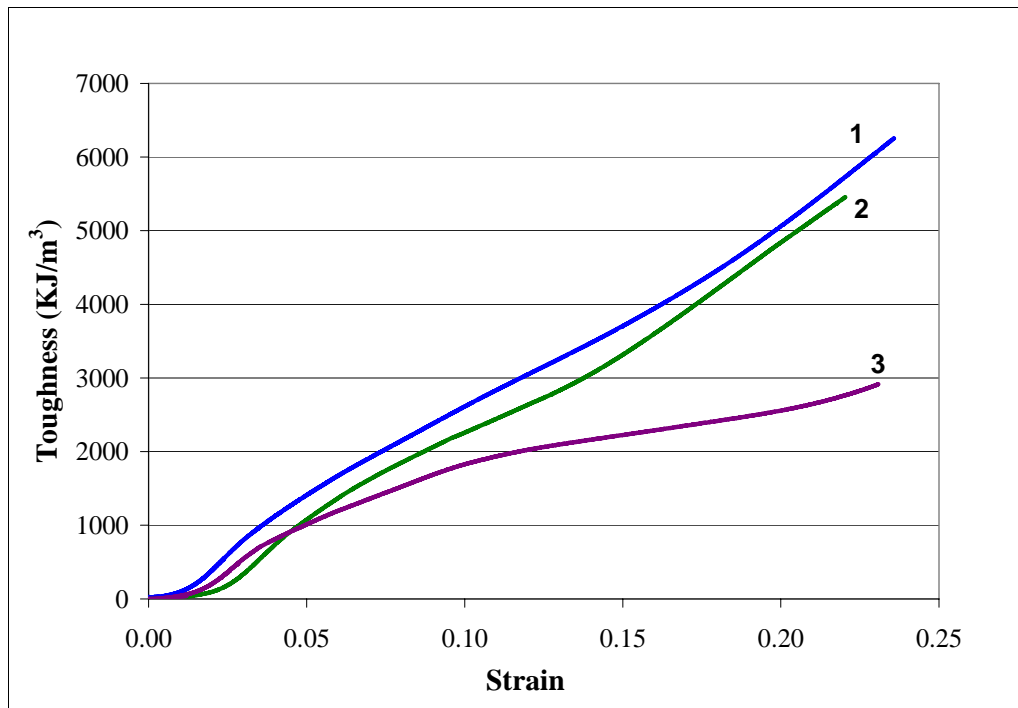


Figure A.20: Toughness-strain results of M2F2-7 (three specimens)

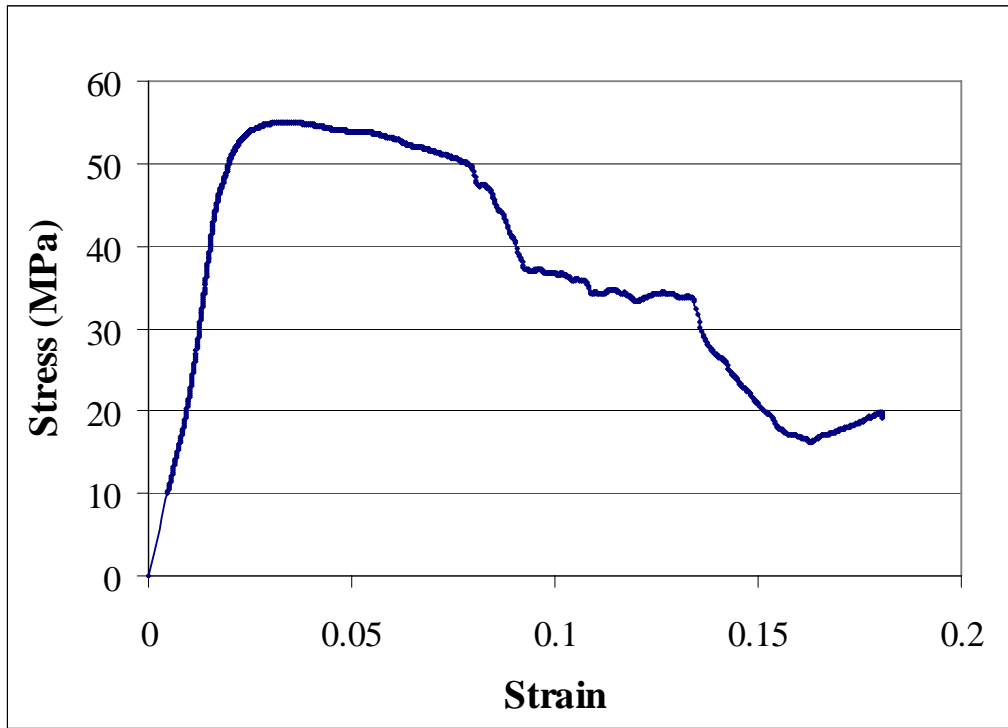


Figure A.21: Stress-strain results of M2F2-9.5 (only one specimen)

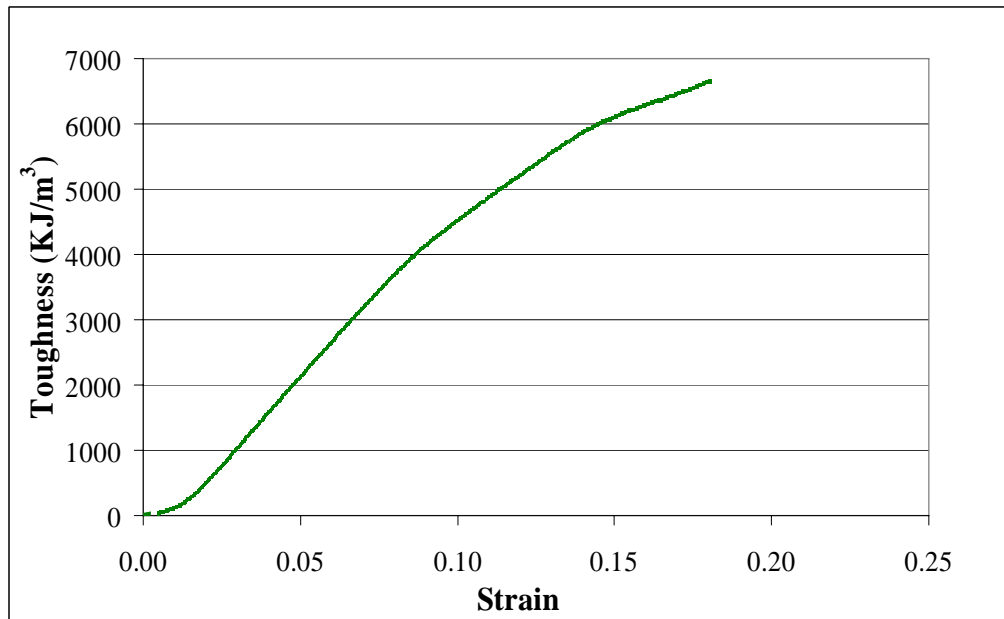


Figure A.22: Toughness-strain results of M2F2-9.5 (only one specimen)

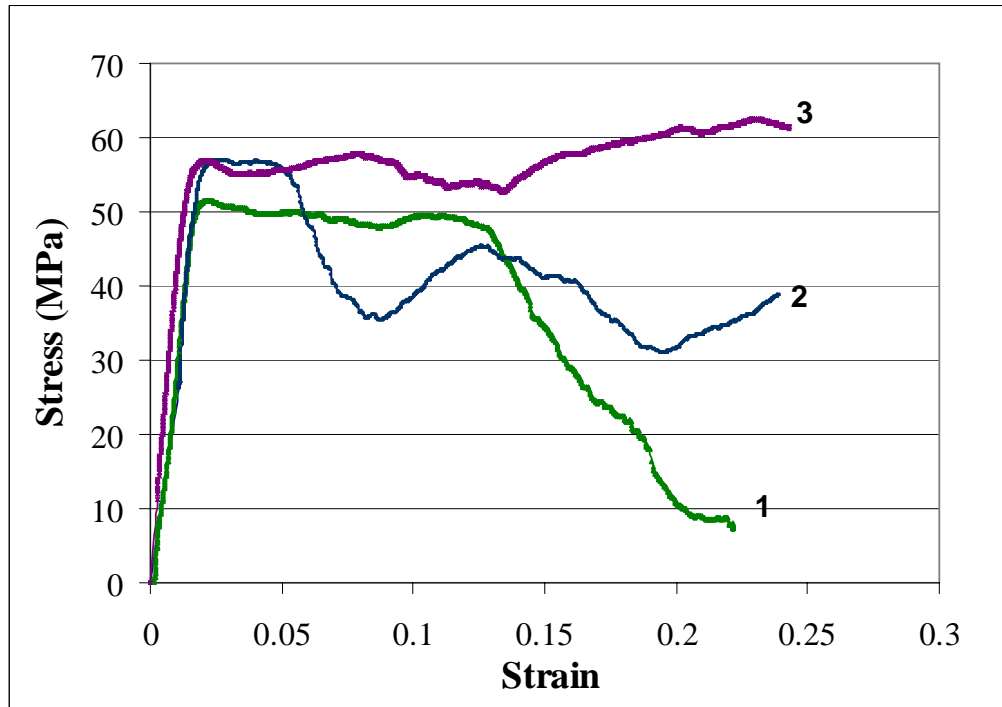


Figure A.23: Stress-strain results of M2F2-12 (three specimens)

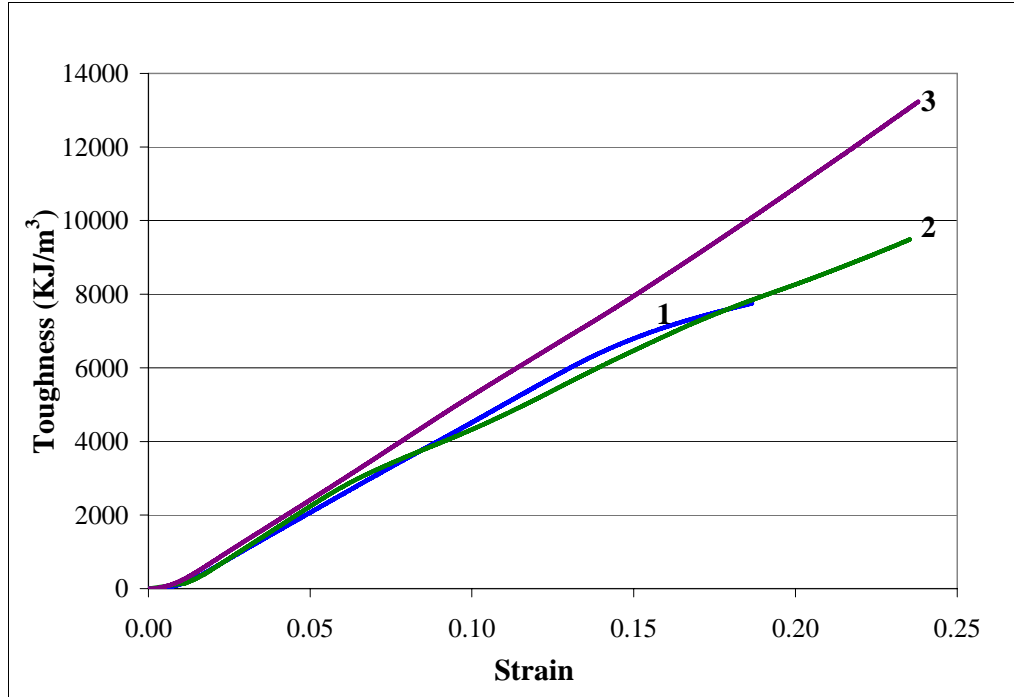


Figure A.24: Toughness-strain results of M2F2-12 (three specimens)

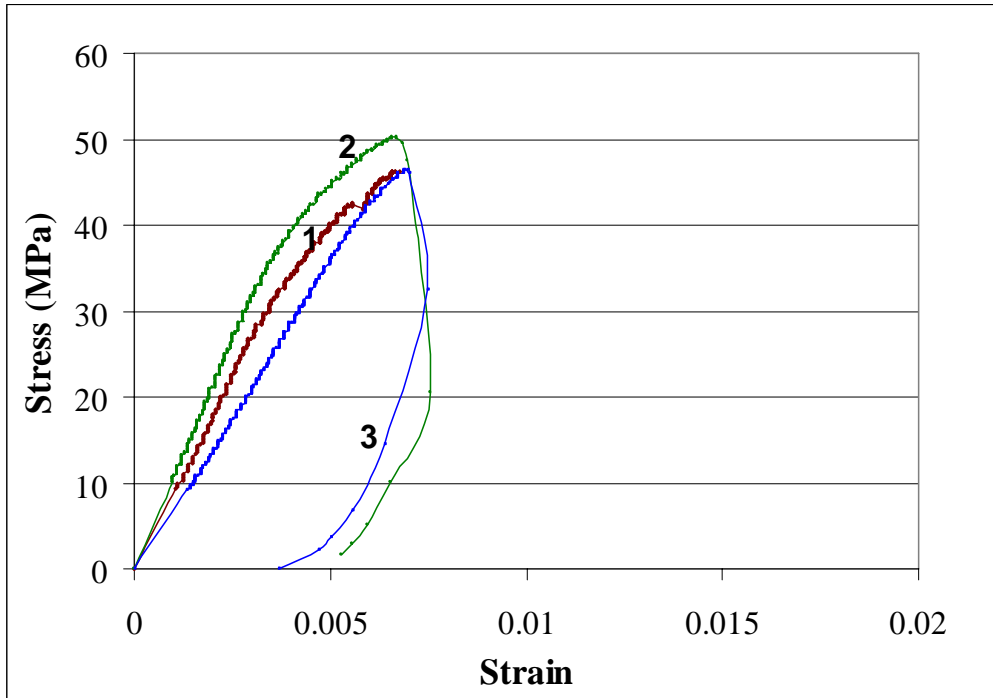


Figure A.25: Stress-strain results of M3 (three specimens)

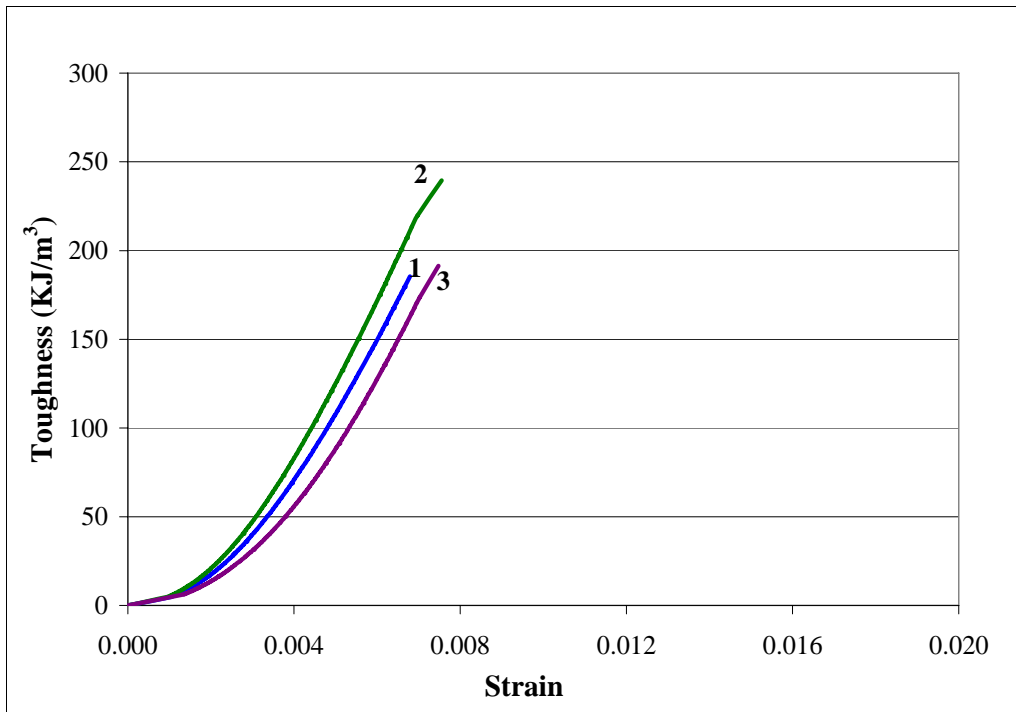


Figure A.26: Toughness-strain results of M3 (three specimens)

APPENDIX B: RESULTS OF WATER ABSORPTION TEST

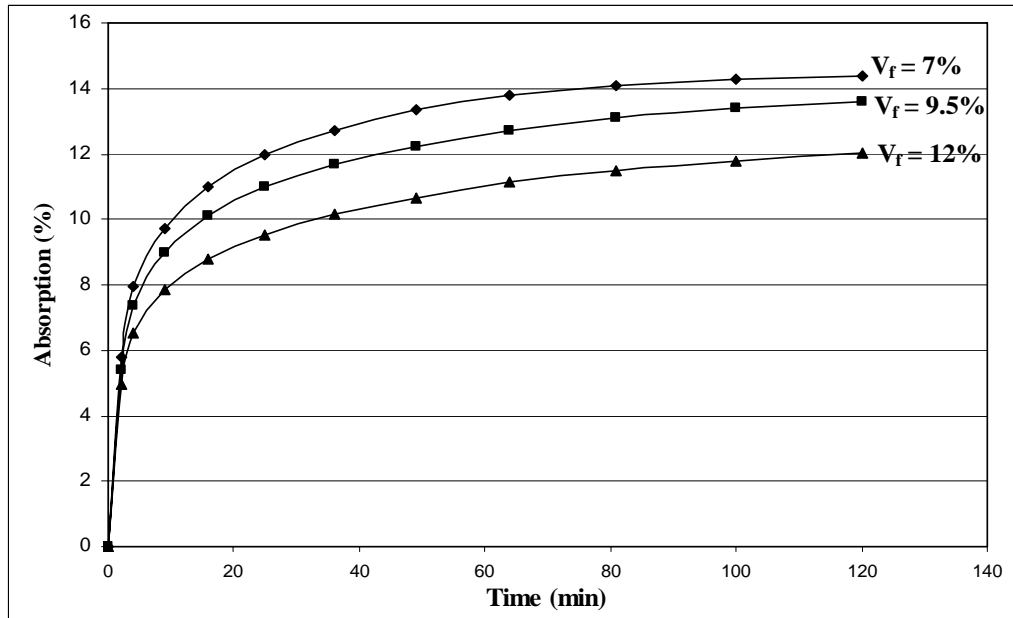


Figure B.1: Absorption vs. time during the first 2 hrs for M1F1

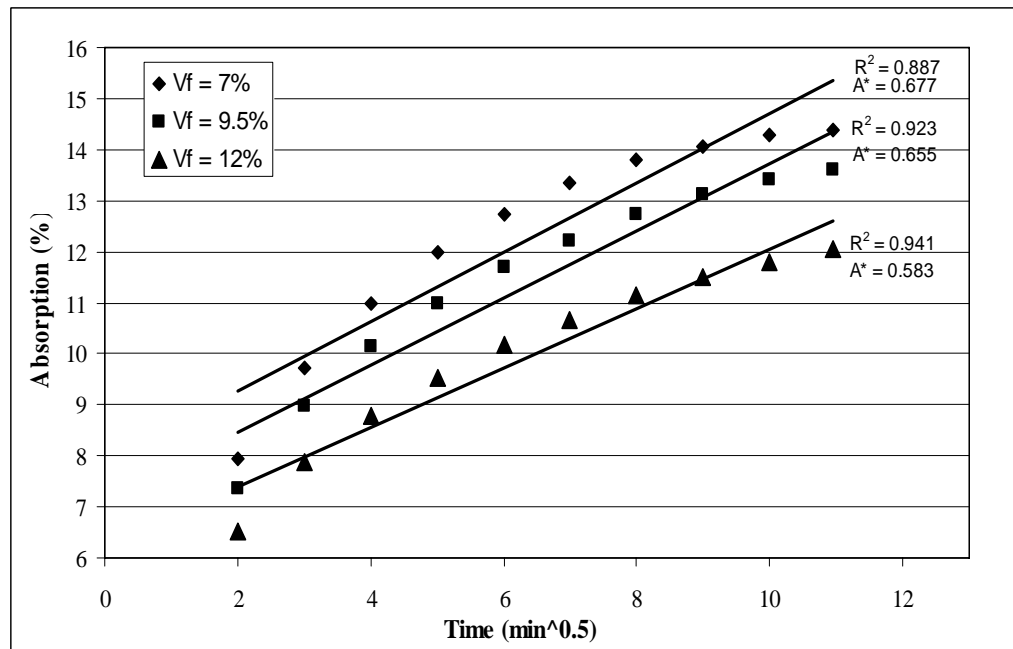


Figure B.2: Absorption indices for M1F1

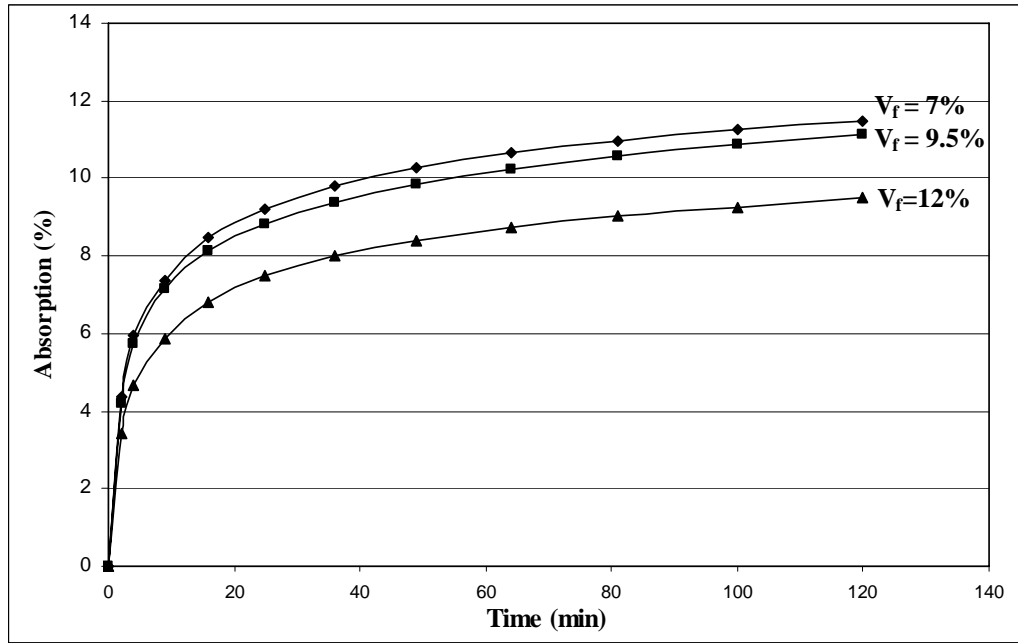


Figure B.3: Absorption vs. time during the first 2 hrs for M1F2

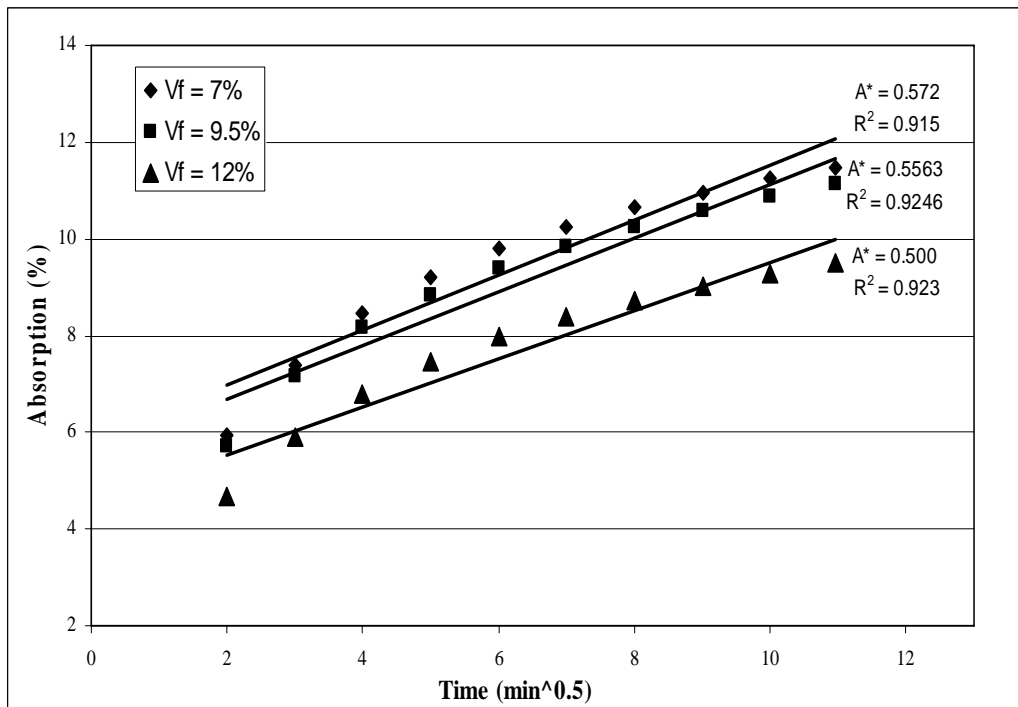


Figure B.4: Absorption indices for M1F2

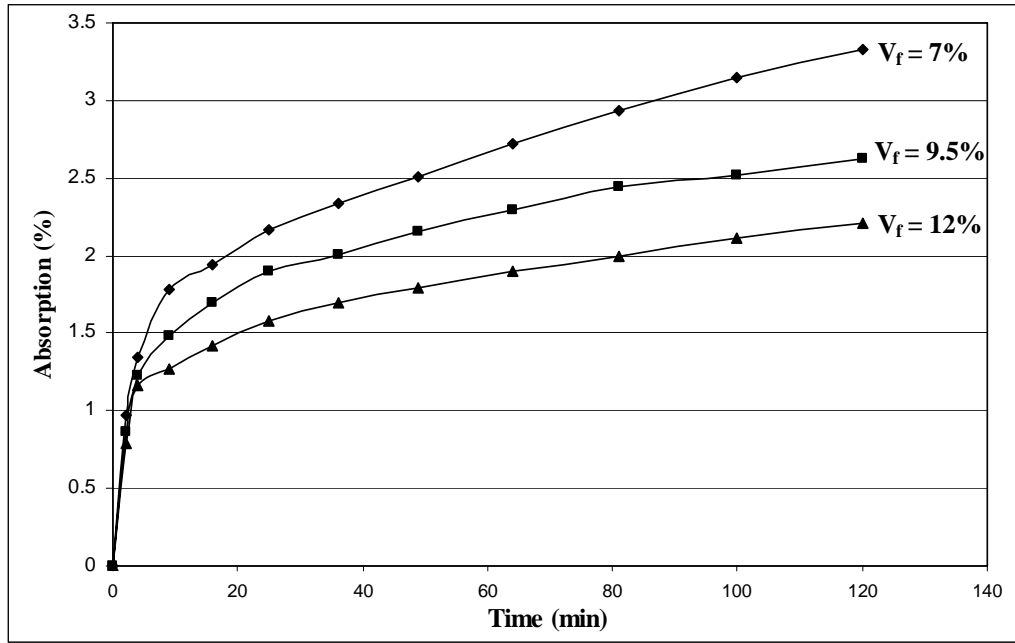


Figure B.5: Absorption vs. time during the first 2 hrs for M2F1

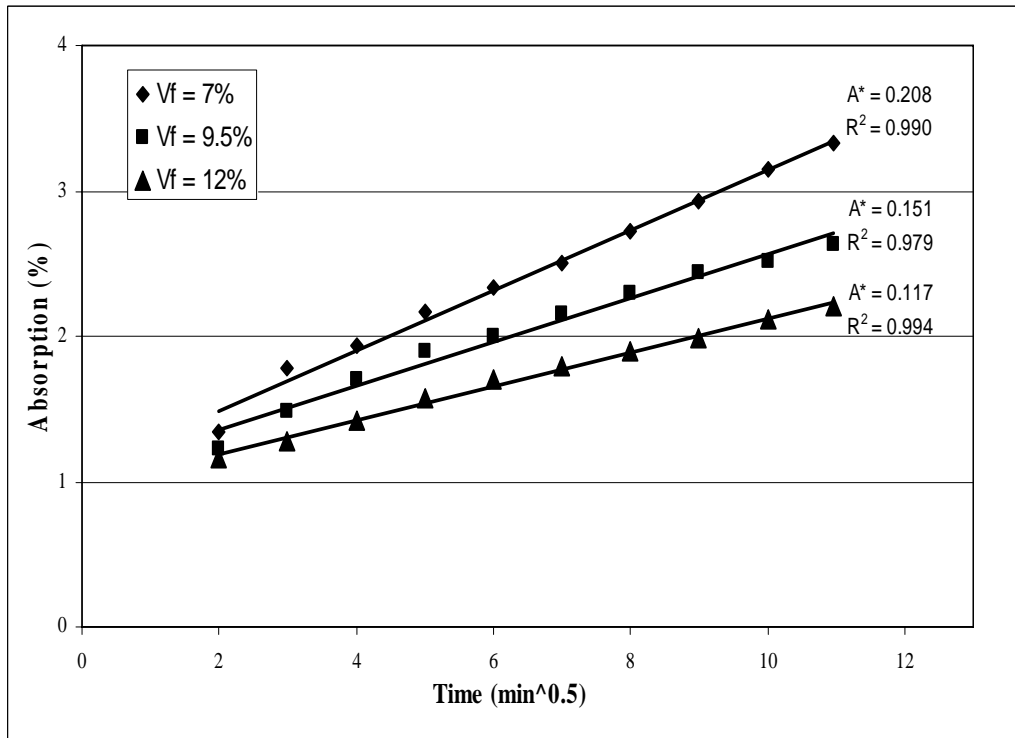


Figure B.6: Absorption indices for M2F1

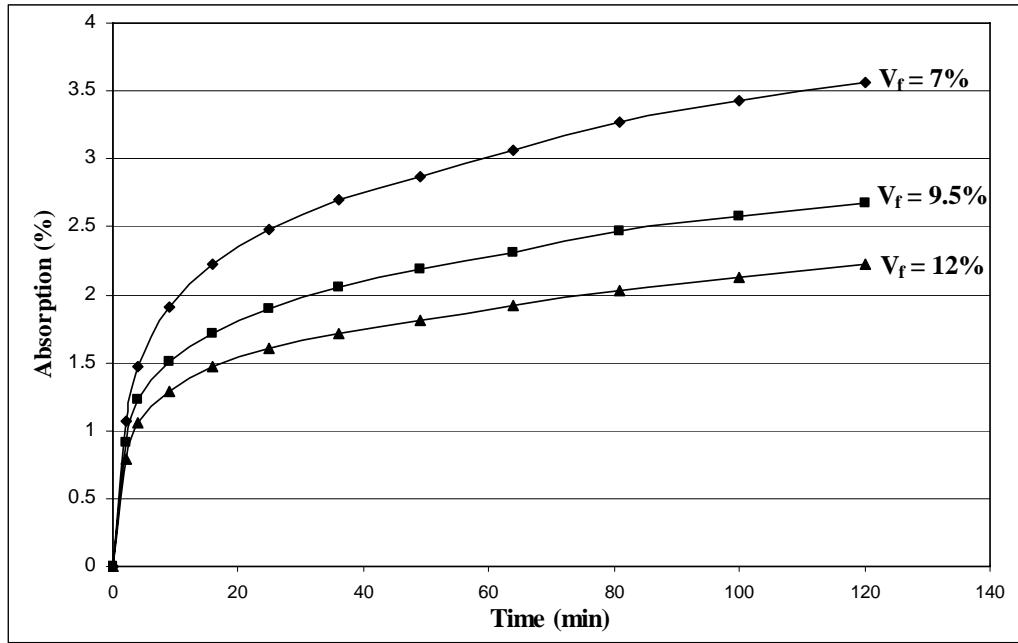


Figure B.7: Absorption vs. time during the first 2 hrs for M2F2

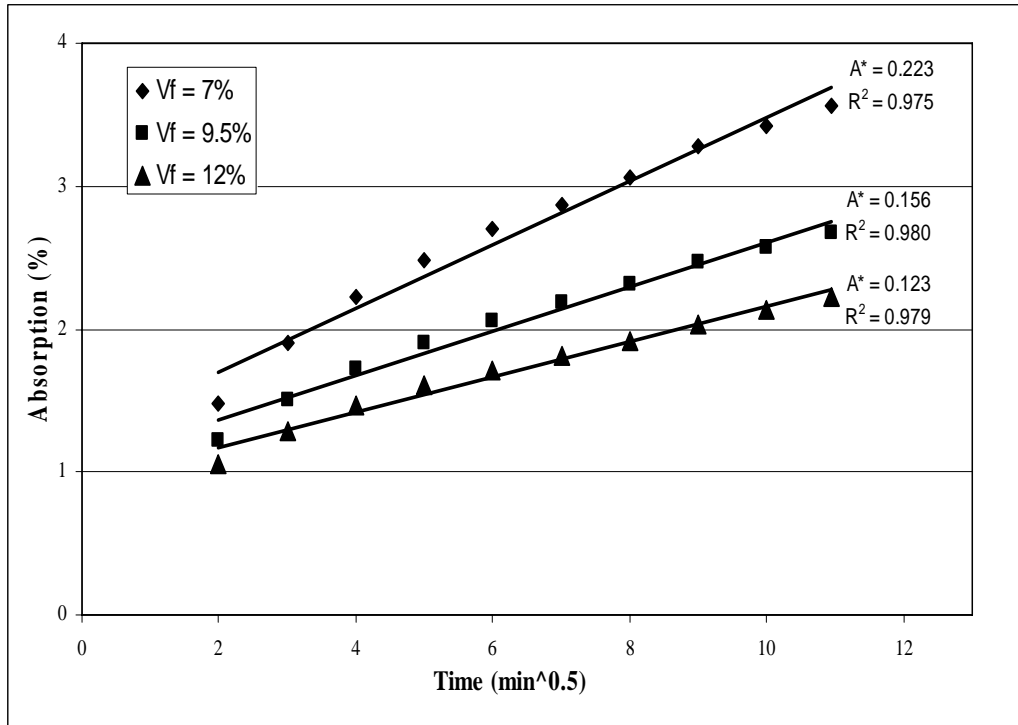


Figure B.8 Absorption indices for M2F2

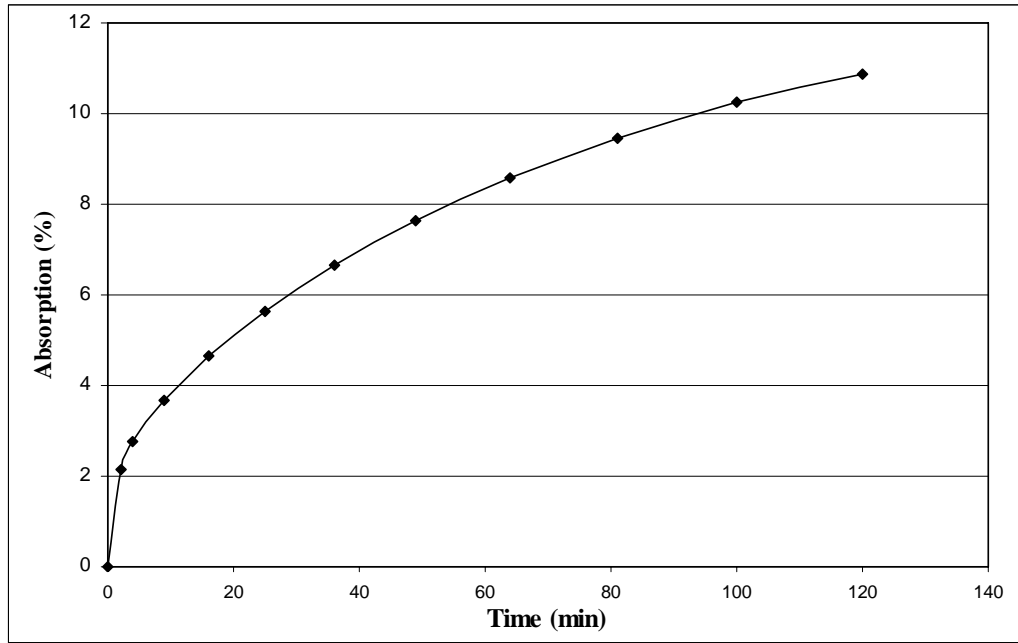


Figure B.9: Absorption vs. time during the first 2 hrs for M2(F)

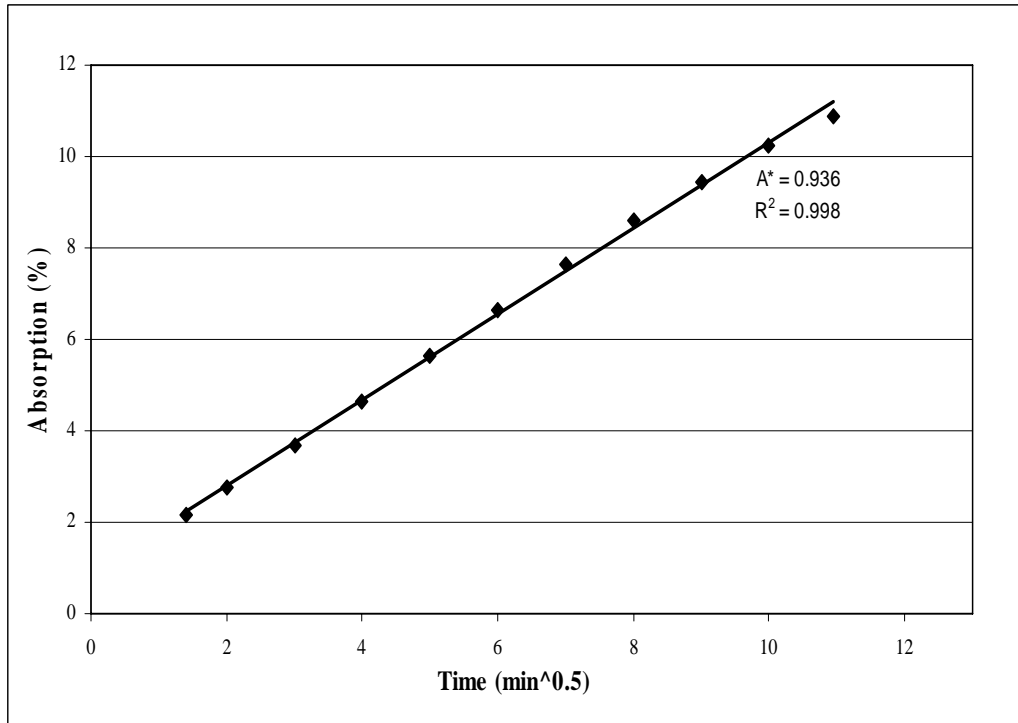


Figure B.10: Absorption index for M2(F)

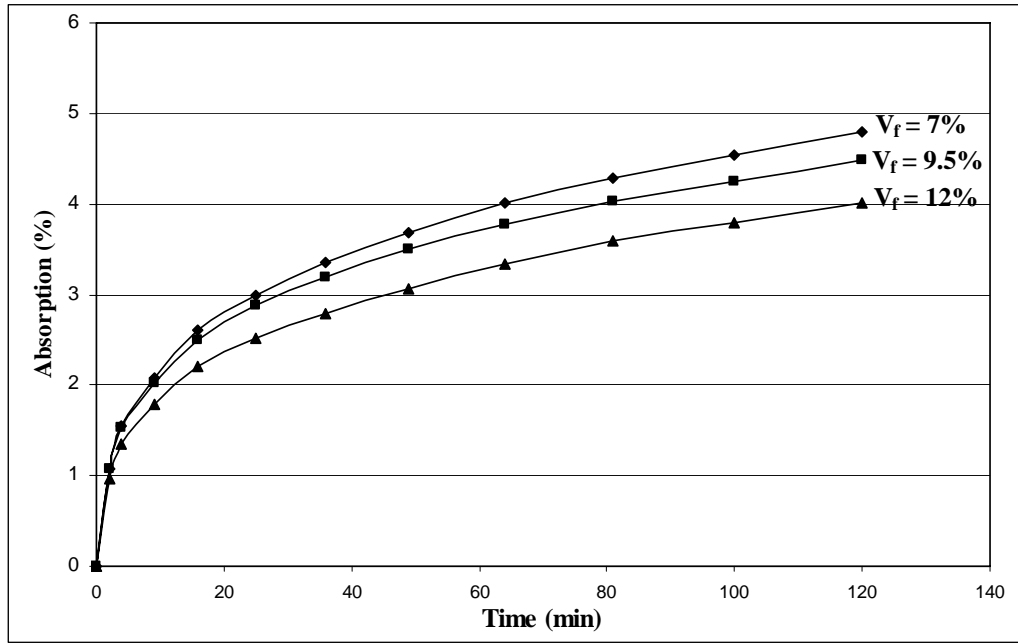


Figure B.11: Absorption vs. time during the first 2 hrs for M2F1(F)

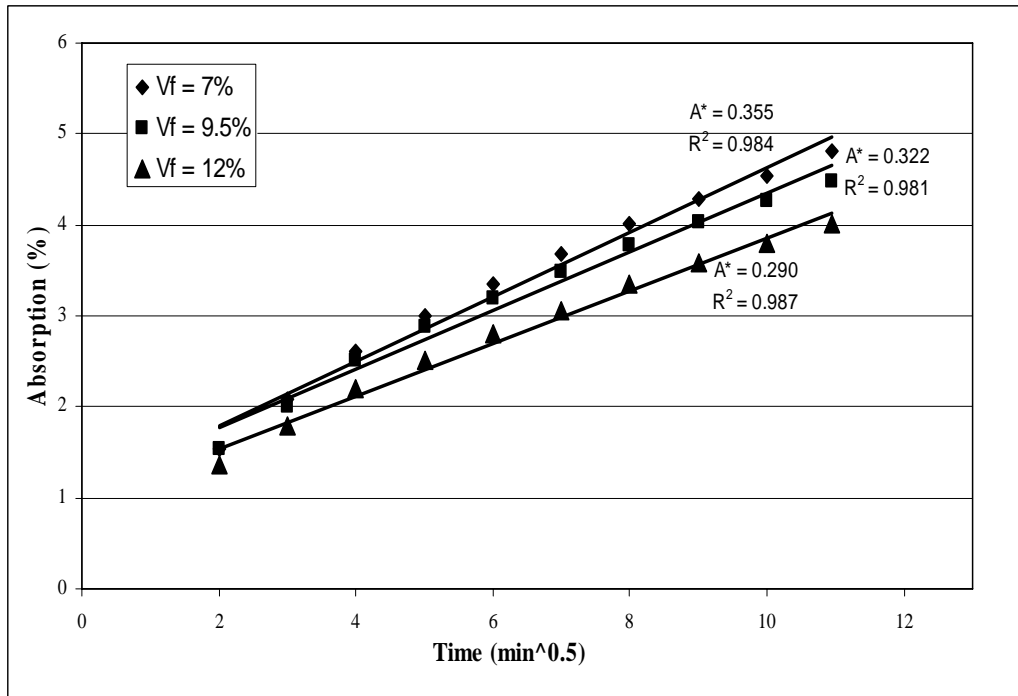


Figure B.12: Absorption indices for M2F1(F)

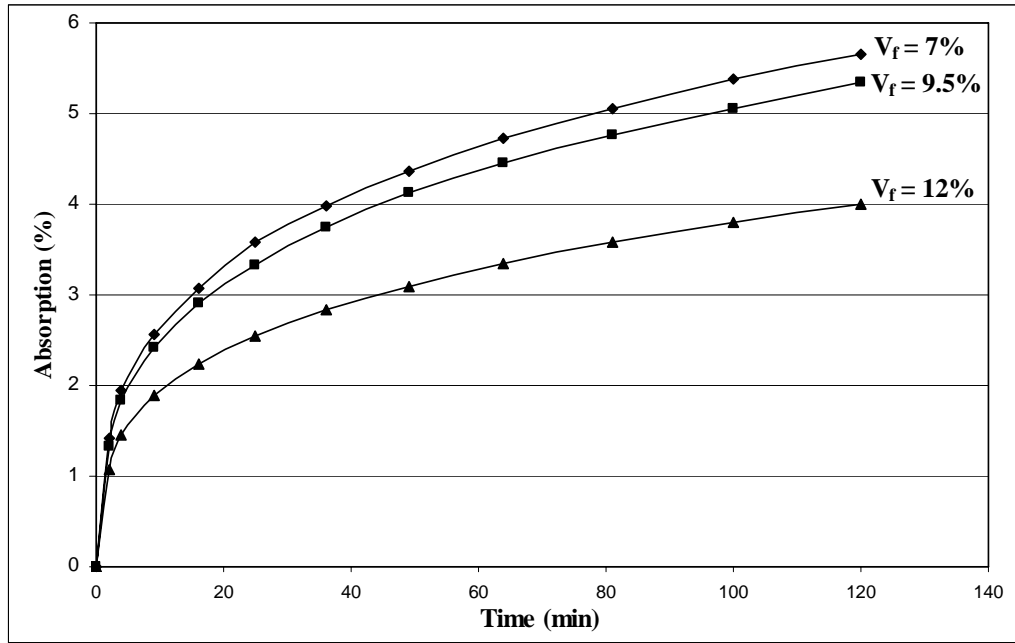


Figure B.13: Absorption vs. time during the first 2 hrs for M2F2(F)

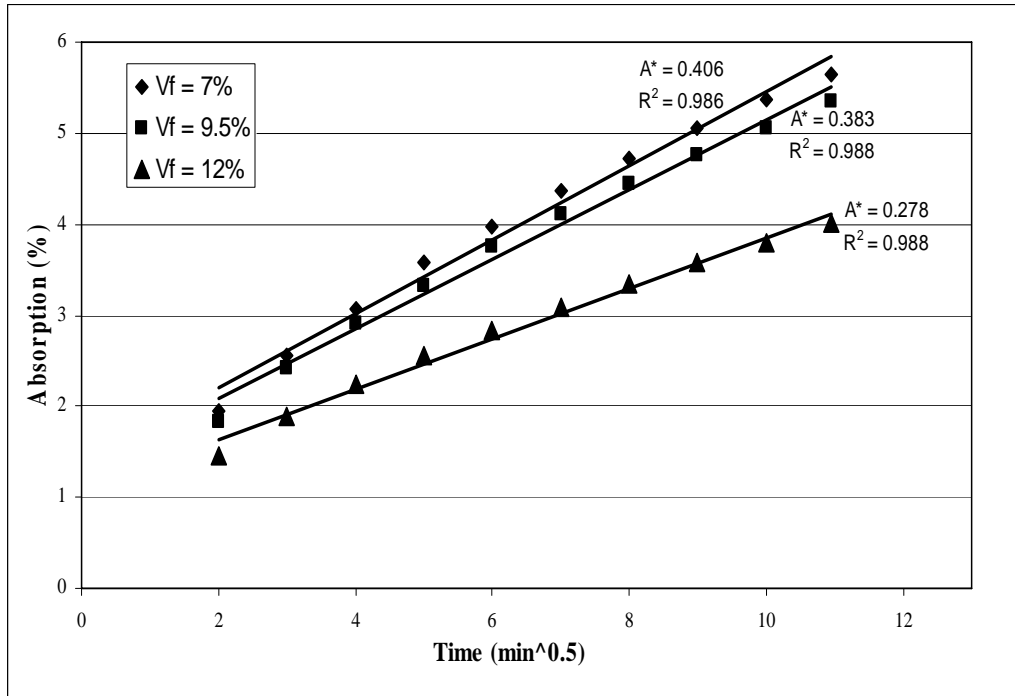
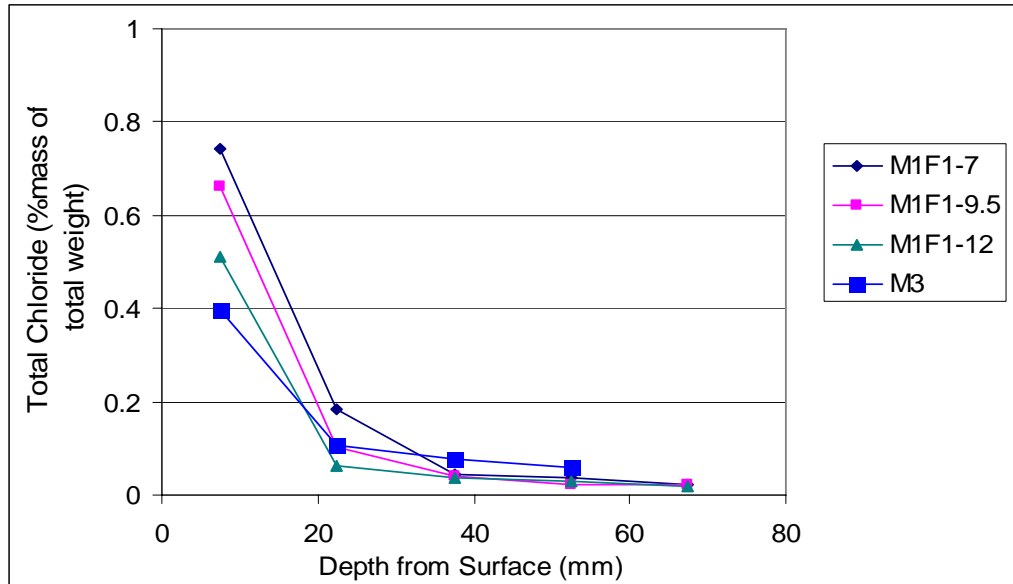


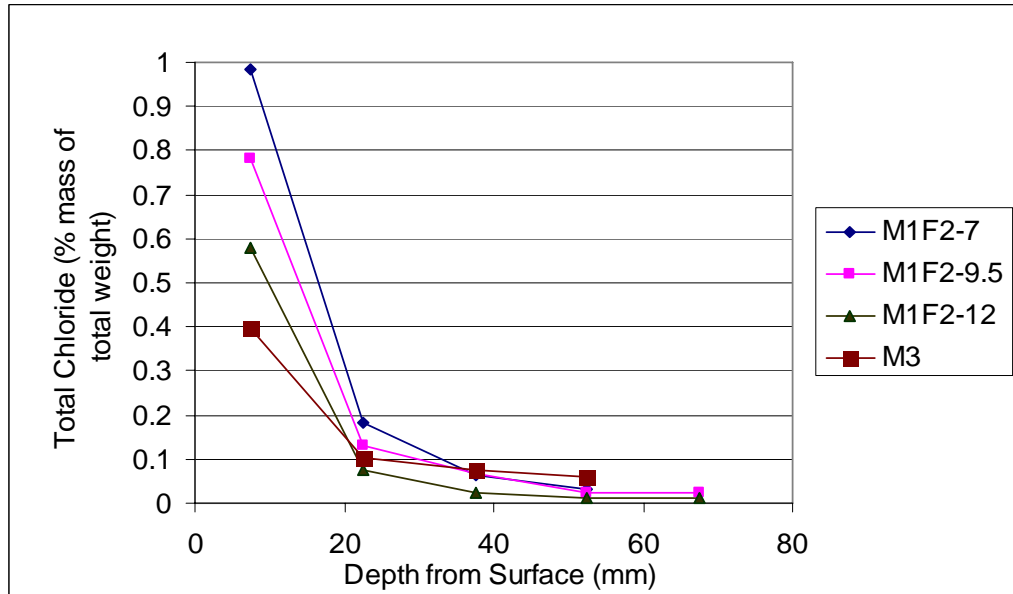
Figure B.14: Absorption indices for M2F2(F)

APPENDIX C: RESULTS OF CHLORIDE PENETRATION TEST

C.1) Total Chloride Content Profiles with respect to Total Weight

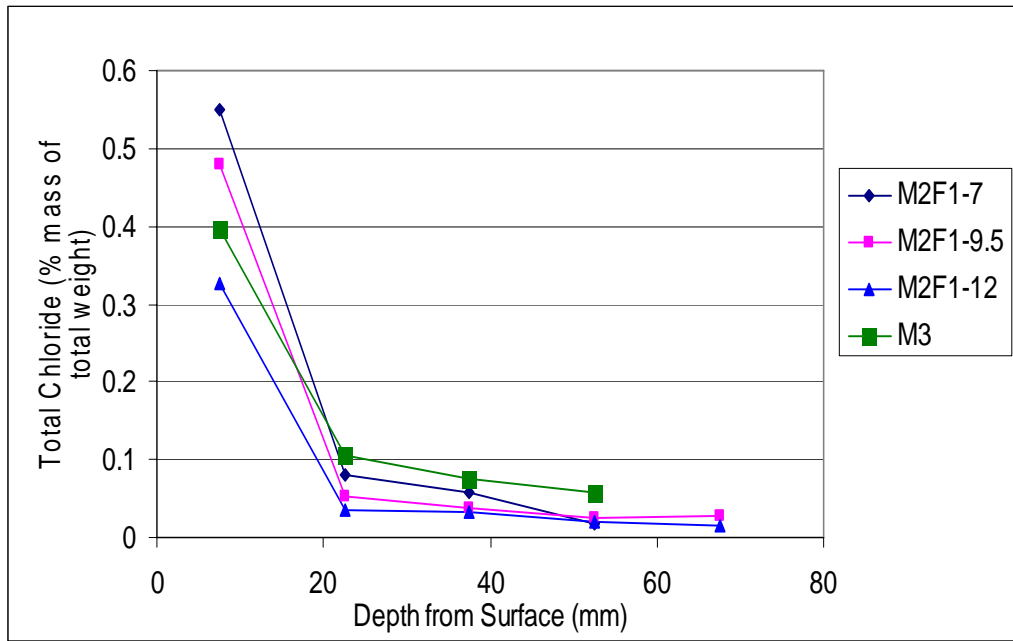


(a) With hooked fibers

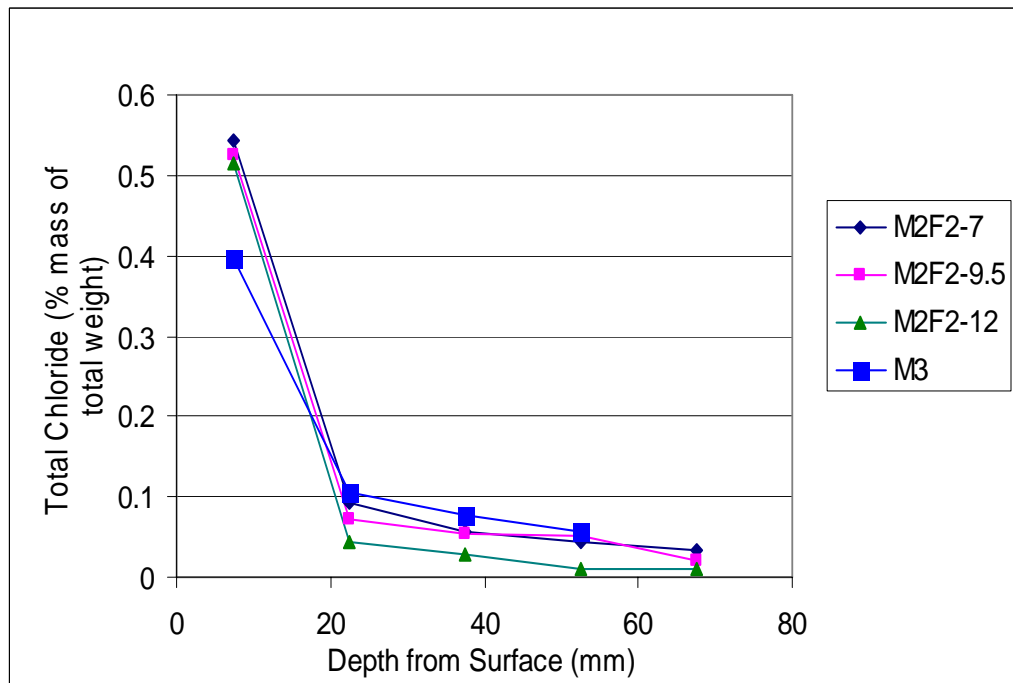


(b) With crimped fibers

Figure C.1: Chloride ingress profiles for slurry SIFCON vs. control concrete (Based on chloride content by total weight)



(a) With hooked fibers



(b) With crimped fibers

Figure C.2: Chloride ingress profiles for mortar SIFCON vs. control concrete (Based on chloride content by total weight)

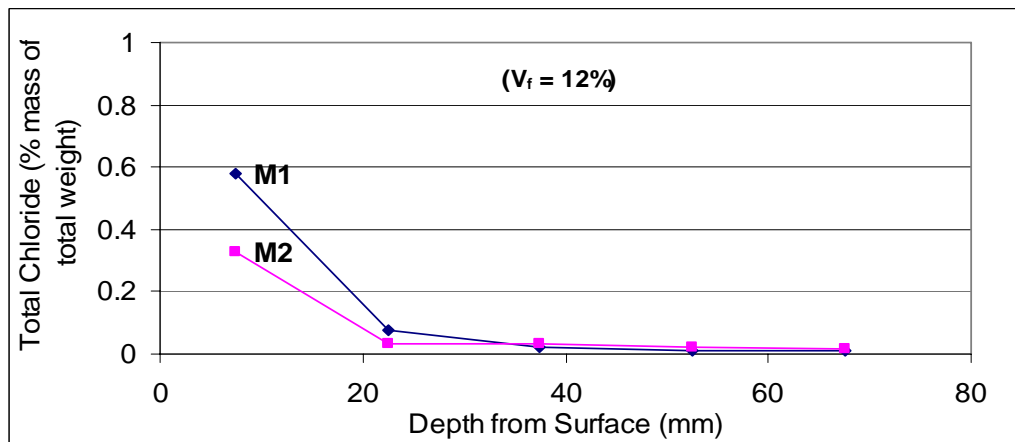
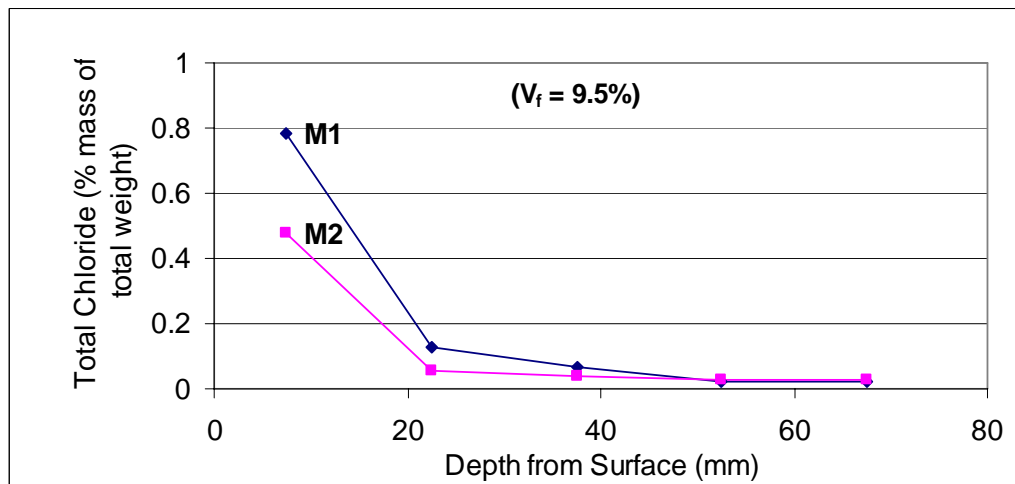
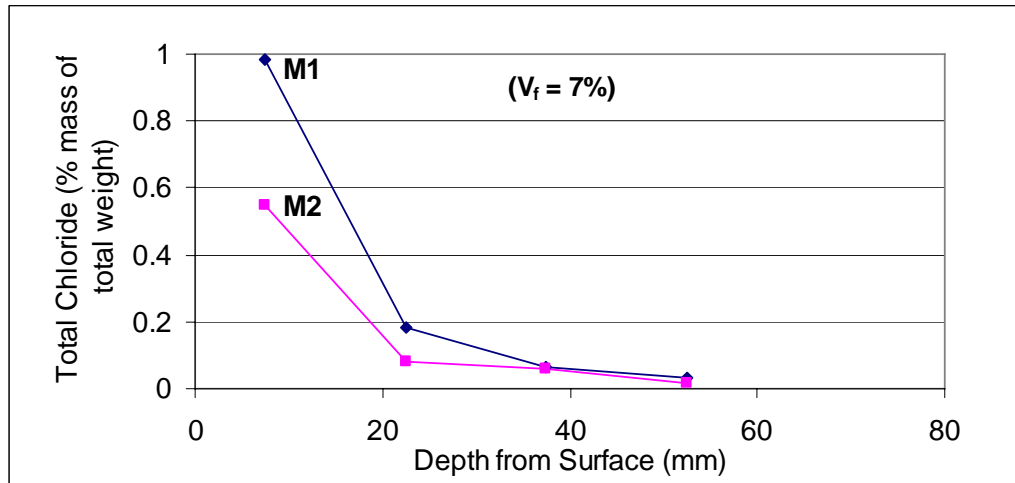


Figure C.3: Effect of mix type on chloride penetration when hooked fibers (F1) are used (Based on chloride content by total weight)

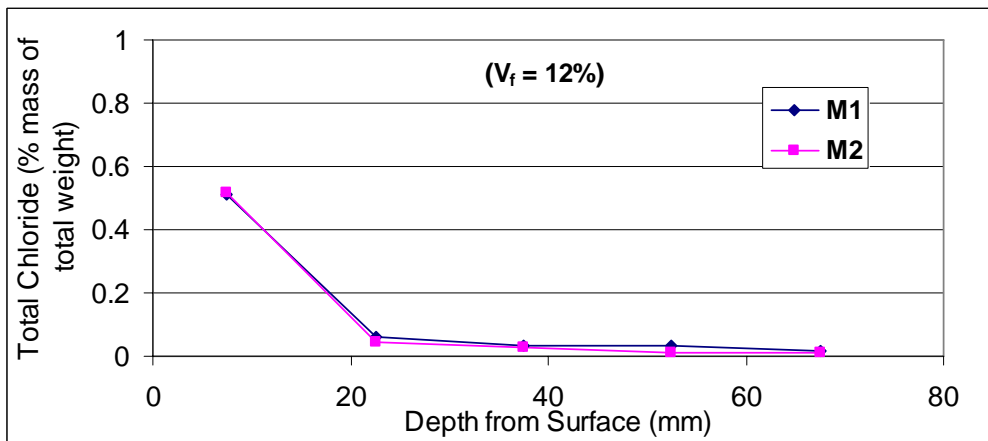
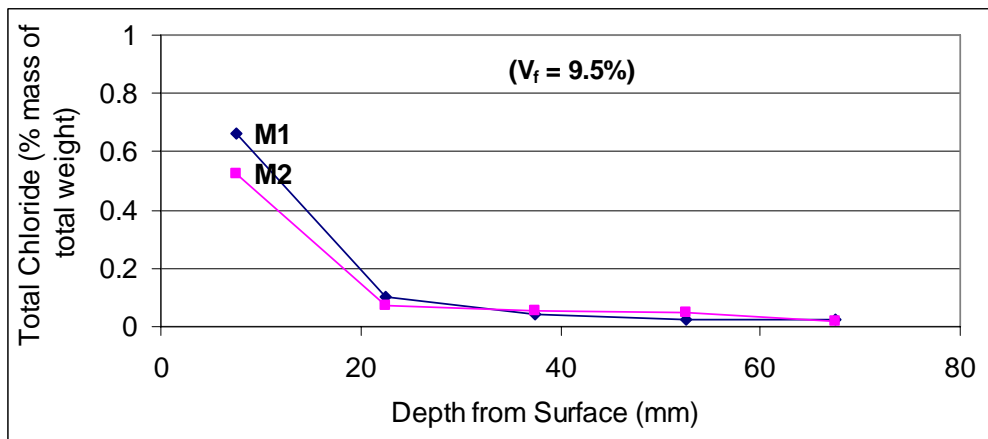
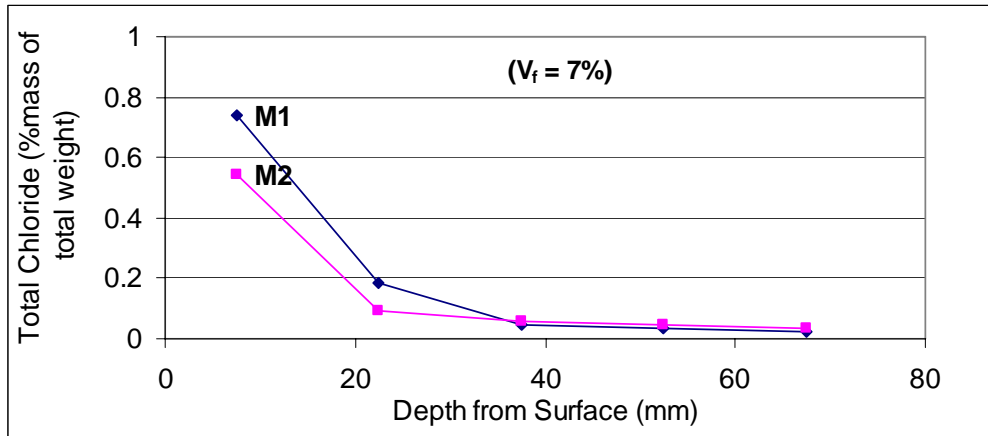


Figure C.4: Effect of mix type on chloride penetration when crimped fibers (F2) are used (Based on chloride content by total weight)

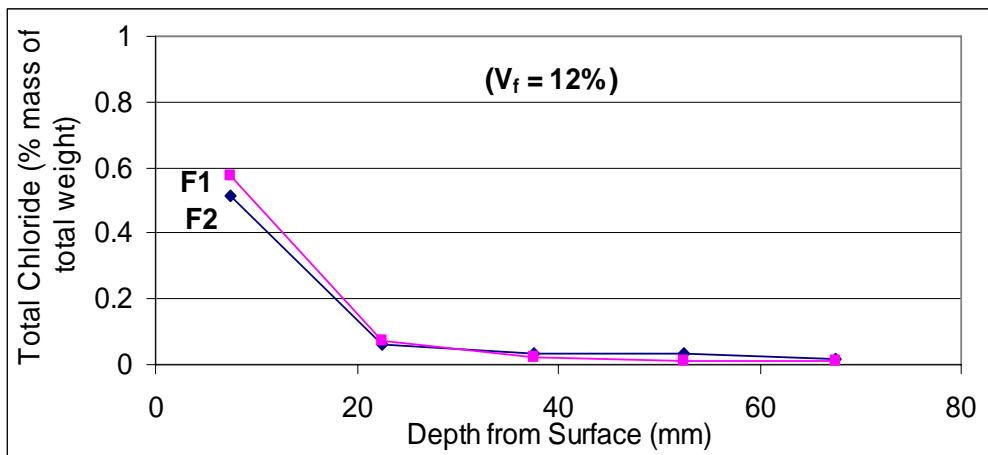
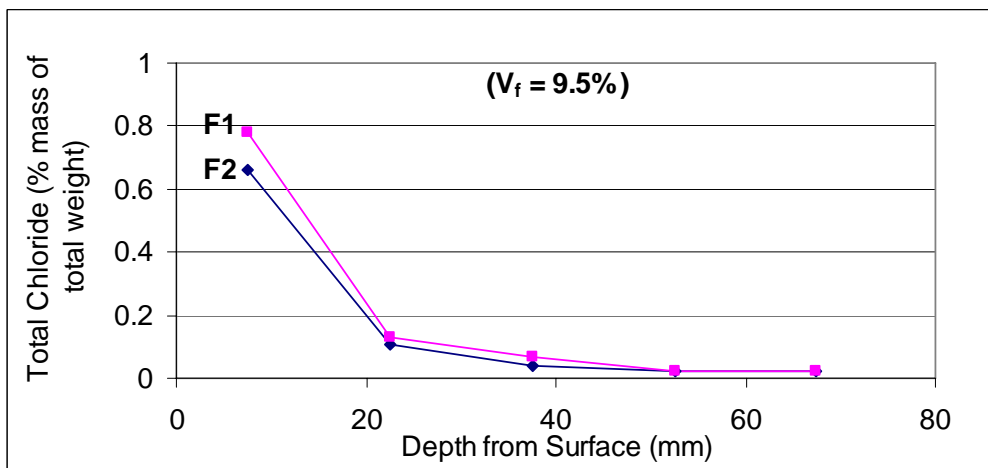
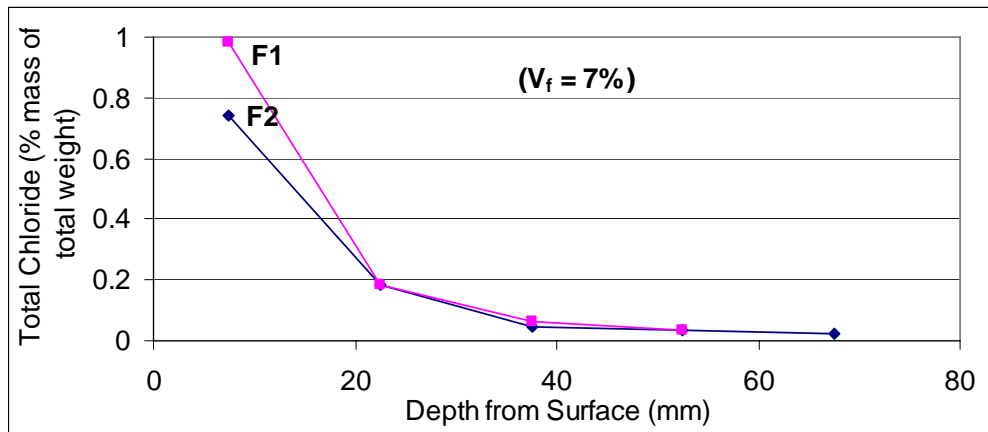


Figure C.5: Effect of fiber type on chloride penetration of slurry SIFCON (Based on chloride content by total weight)

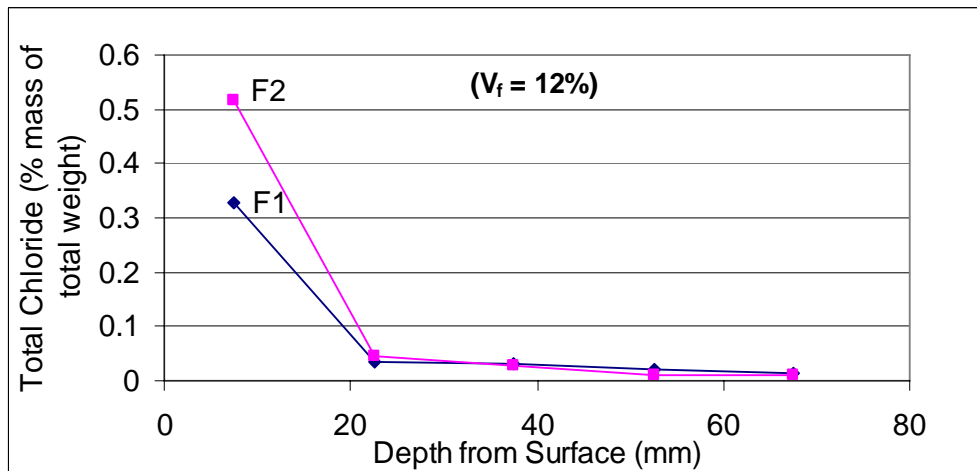
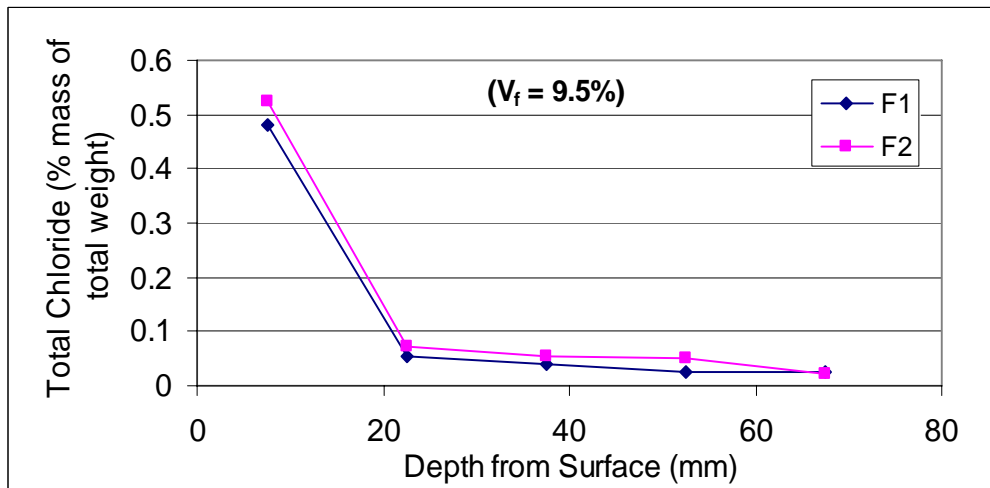
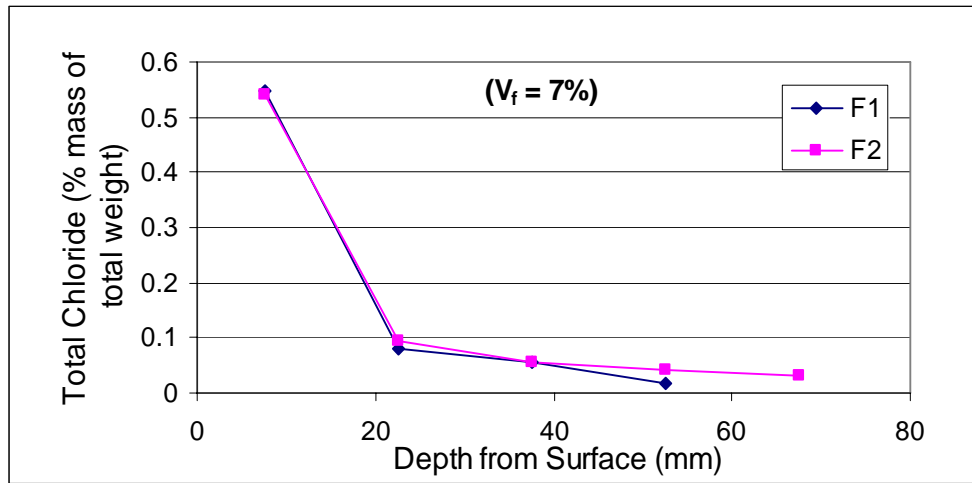


Figure C.6: Effect of fiber type on chloride penetration of mortar SIFCON (Based on chloride content by total weight)

**C.2) Comparisons between model and experimental data in calculations
of chloride diffusion coefficients**

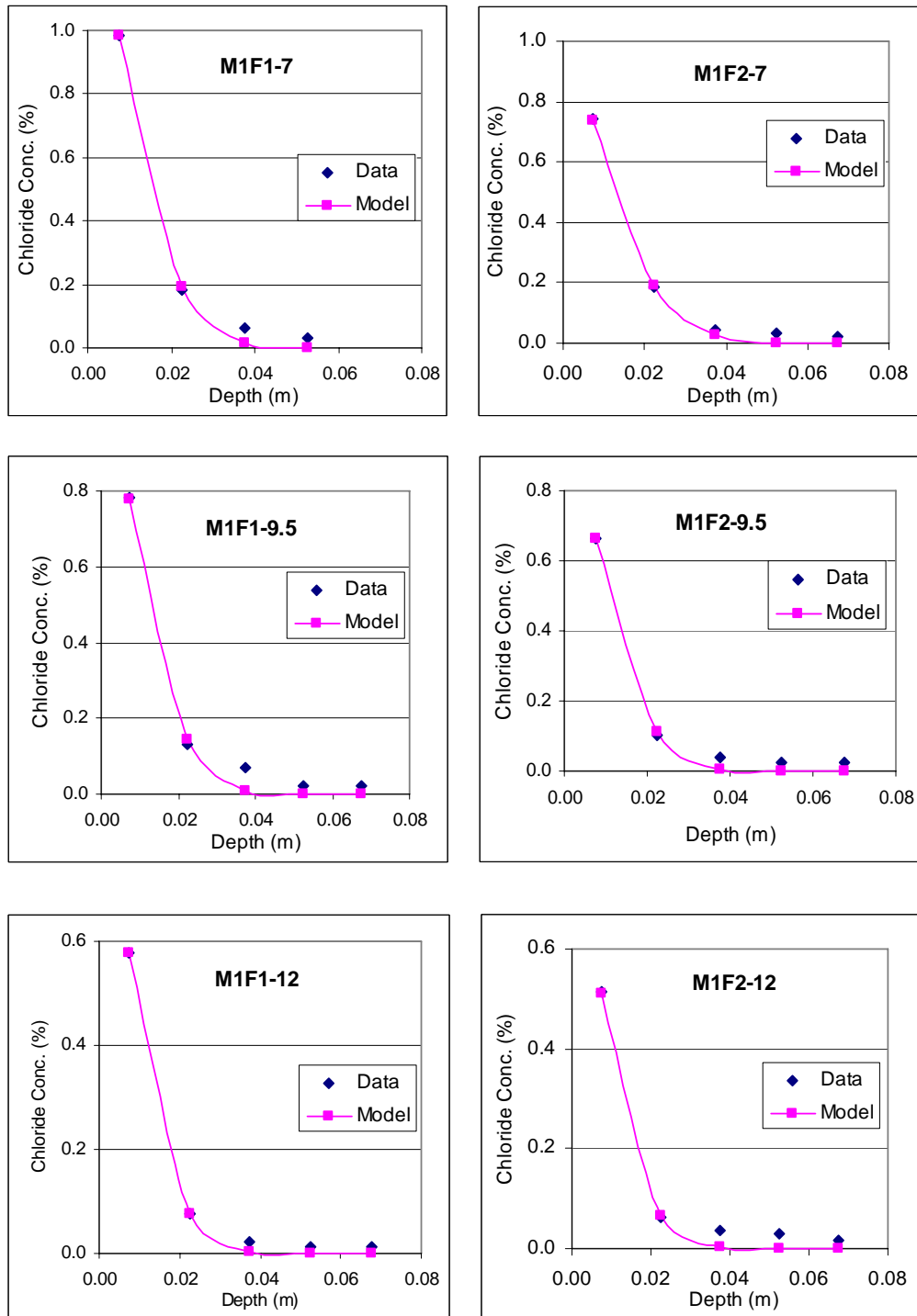


Figure C.7: Comparison of model and experimental data for slurry SIFCON

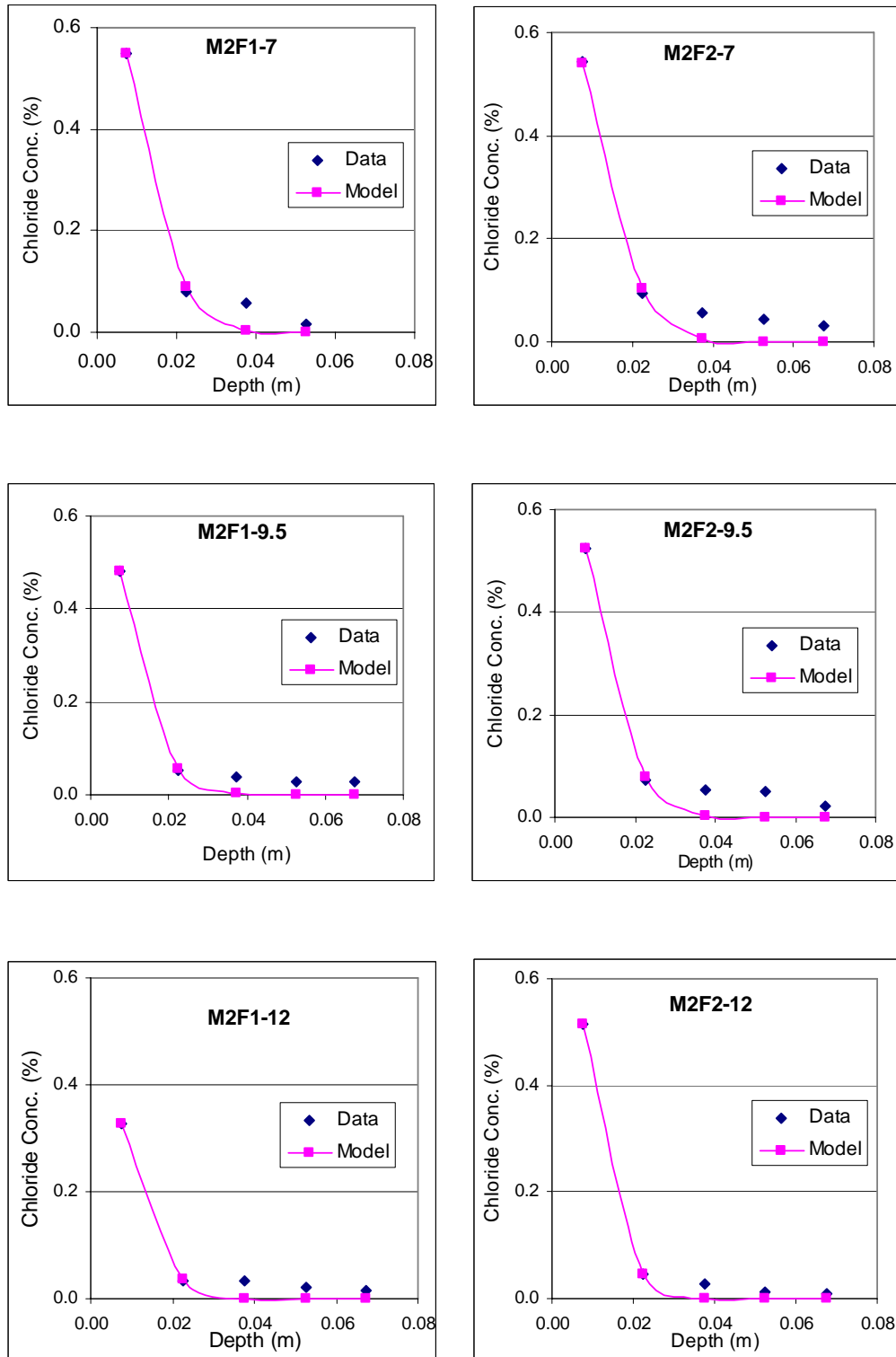


Figure C.8: Comparison of model and experimental data for mortar SIFCON

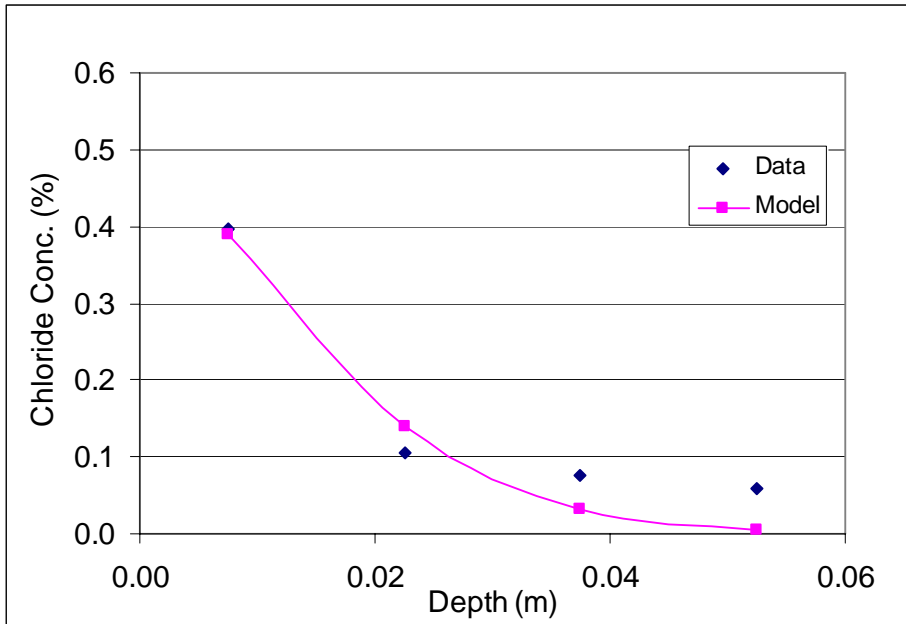


Figure C.9: Comparison of model and experimental data for control concrete

CURRICULUM VITAE

Personal Information

Name: Adel M. Gilani
Nationality: Libyan
Date of Birth: July 8, 1970
Place of Birth: London, U.K.
Marital Status: Married
e-mail: gilani@bonyan-ce.com

Education

Degree	Institution	Graduation Year	GPA
M.S.	Civil Eng. Dept., Al-Fateh University, Tripoli, Libya	1998	3.42/4.00
B.S.	Civil Eng. Dept., Al-Fateh University, Tripoli, Libya	1993	72.28 % (Rank 4 in 46 students)

Academic Experience

1996 to 1998:
Teaching assistant, Civil Engineering Department, Al-Fateh University, Tripoli, Libya.

1999 to 2001:
Assistant lecturer, Civil Engineering Department, Al-Fateh University, Tripoli, Libya.

The academic duties included teaching the following courses:

1996 to 1998:
CE264 – Construction Materials, Lab.

1998 to 2000:
CE342 – Soil Mechanics I, Lab.

2000 to 2001:
CE203 – Structural Analysis I.

In addition to co-supervising several B.S. graduation projects, and participating in giving training courses on laboratory and field tests in the area of construction materials and soil mechanics to the technicians of several public agencies.

Professional Experience

1993 to 2001:

Bonyan consulting engineers (BCE), Tripoli, Libya. Participated in the following projects and jobs:

- 1) Investigation and repair of honeycombing in the concrete elements of some buildings in Khaled Juma housing Complex, Janzour, Tripoli, 1994.
- 2) Investigation and repair of cracks in foundation concrete of Surman waste water treatment station, 1994.
- 3) Preparing bills of quantities and specifications of repair of corrosion deteriorated R.C. elements of Medical and Synthetical Alcohol Factory building, Bab Ben Ghashier, Tripoli, 1994.
- 4) Investigation of R.C. deteriorations of Al-Ahram Hotel Complex buildings, Tripoli, 1996.
- 5) Investigation and repair of a 220 KV transmission line tower R.C. foundations, El-Fjej – Ubari, South of Libya, 1996.
- 6) Structural design of administration and conference hall buildings of Abu-Kammash chemical complex, 1997
- 7) Investigation and repair of deteriorated basement slabs in some buildings of South Soug Ettlat project, Tripoli, 1997.
- 8) Supervising of pile foundation construction, North Soug Ettlat housing project, Tripoli, 1997 to 1999.
- 9) Study of the suitability of Bughilan - El Guasem quarry sands for concrete works, 1998.
- 10) Investigation and repair of honeycombed R.C. elements of Tripoli harbour passenger station quay wall, 1998.
- 11) Assessment, diagnosis and repair of structural concrete of a school building project, El Garabulli, 1998 to 1999.
- 12) Investigation of concrete cracking of R.C. water tanks, Gharyan, 1999.
- 13) Supervision of the construction of Tripoli Corinthia hotel, Soug Ettlat El-Gdeem, Tripoli, 1999 to 2001.
- 14) Investigation and repair of deteriorated structural concrete and steel elements of The Great Man Made River Stadium in the sport city of Tripoli, 2000.
- 15) Investigation of the structural safety of the slabs of several residential and educational buildings in Tajura, Zaiwa and Tripoli, 1993 to 2001.

1995 to 2000:

Expertise house for engineering works, Tripoli, Libya. The projects involved mainly appraisal works of damaged buildings, and specifying required remediation. Furthermore, field testing have been carried out extensively for quality control of the earth works of a major railways project, Ein Zara, Tripoli.

2001:

The Libyan Arab Domestic Investment Company (LADICO), Tripoli, Libya.

The duties included:

- 1) Supervision of various phases of construction in Hay Al-Zuhour major housing project, Tripoli.
- 2) Adminstrating of concrete quality assurance works (Batching plants an lab testing).
- 3) Supervision of soil works, including field testing to control the backfilling compaction.

Committees

1993 to 1994:

The organizing committee of the 5th Arab structural engineering conference.

2000 to 2001:

The technical committee of the Libyan standard specification for “Aggregates for Concrete”, The national center for specifications and standardization, Tajura, Libya.

Publications

- 1) Adel Gilani, and Adel Elwefati, “Quality Control Systems for Construction Materials Laboratories in Libya – Appraisal and Accreditation”, A Seminar on Conformity and Assessment, The national center for specifications and standardization, Tajura, Libya, 1997 (In Arabic).
- 2) Adel Gilani, and Adel Elwefati, “Towards A National System for Laboratory Accreditation in Libya”, The 1st National Conference for Engineers, Misurata, Libya, 1998 (In Arabic).

Unions:

2003 to 2004, and 2006 to 2007:

The general secretary of the Libyan Students Union in Turkey.

Languages:

Arabic (Native), English (Advanced), Turkish (Intermediate), Italian (Basic).